STUDIES OF MOLECULAR INTERACTIONS
USING
PHYSICAL TECHNIQUES

A thesis

presented to the University of Aston in Birmingham

for the degree of Doctor of Philosophy

by

Padungkiart Polanun B.Sc.

The Chemistry Department

University of Aston in Birmingham

March, 1974.

SUMMARY

The investigations described in this thesis concern the molecular interactions between polar solute molecules and various aromatic compounds in solution. Three different physical methods were employed. Nuclear magnetic resonance (n.m.r.) spectroscopy was used to determine the nature and strength of the interactions and the geometry of the transient complexes formed. Cryoscopic studies were used to provide information on the stoichiometry of the complexes. Dielectric constant studies were conducted in an attempt to confirm and supplement the spectroscopic investigations. The systems studied were those between nitromethane, chloroform, acetonitrile (solutes) and various methyl substituted benzenes.

In the n.m.r. work the dependence of the solute chemical shift upon the compositions of the solutions was determined. From this the equilibrium quotients (K) for the formation of each complex and the shift induced in the solute proton by the aromatic in the complex were evaluated. The thermodynamic parameters for the interactions were obtained from the determination of K at several temperatures.

The stoichiometries of the complexes obtained from cryoscopic studies were found to agree with those deduced from spectroscopic investigations. For most systems it is suggested that only one type of complex, of 1:1 stiochiometry, predominates except that for the acetonitrile-benzene system a 1:2 complex is formed.

Two sets of dielectric studies were conducted, the first to show that the nature of the interaction is dipole-induced dipole and the second to calculate K. The equilibrium quotients obtained from spectroscopic

and dielectric studies are compared. Time-averaged geometries of the complexes are proposed. The orientation of solute, with respect to the aromatic for the 1:1 complexes, appears to be the one in which the solute lies symmetrically about the aromatic six-fold axis whereas for the 1:2 complex, a sandwich structure is proposed. It is suggested that the complexes are formed through a dipole-induced dipole interaction and steric factors play some part in the complex formation.

CONTENTS

CHAPTER 2

General and Theoretical Aspects of Various Experimental Methods Employed in the Investigations

CHAPTER 3

Experimental Principles of The Various Physical Techniques Employed in the Studies of Molecular Interactions

ILLUSTRATIONS

CHAPTER 1

GENERAL CONSIDERATIONS OF MOLECULAR COMPLEXES FORMED IN SOLUTION

1.2 INTRODUCTION TO THE STUDY OF MOLECULAR COMPLEXES

Many studies have been made of molecular complexes formed in solution[1]. The majority of methods employed to study these reactions regard the complexes as being formed in a fast reaction typified by

$$A + B \rightleftharpoons A \ldots\ldots B \qquad (1.1)$$

In general the concentration of the various solute species (A and B) in the solvent (S) is assumed to be sufficiently low for the systems to be treated as dilute solutions, so that the activity coefficients of the interacting species can be neglected. In most cases the purpose of the investigations is to determine the position of equilibrium, i.e. the equilibrium constant (quotient) K, which provides values of the free energies and the corresponding enthalpy and entropy changes for complex formations. Usually a single experimental technique is employed and the information that can be obtained from such studies is limited.

The present series of investigations employs the nuclear magnetic resonance (n.m.r.) method to evaluate the K values and thermodynamic parameters for several systems of the type (1.1) studied, and also involves the use of dipole moment and cryoscopic studies to throw light on the structures, stoichiometries and nature of the interactions, thereby achieving more information relating to the complexes. The present chapter will be devoted to the properties of molecular interactions in general, but particular reference will be given to the type of reactions studied later and the methods employed in so doing.

1.3 CLASSIFICATION OF INTERACTIONS

The nature of attractive forces, holding molecules together in solution,

is electronic in origin. In practice intermolecular forces constitute a series of interactions, which for historical and practical reasons has been divided into a spectrum of interaction types as follows. For polar molecules there are two types of electrostatic interaction (neglecting quadrupole and higher interactions), namely dipole-dipole and dipole-induced dipole, whereas for neutral molecules the forces are dispersive in nature. For some molecular interactions the transfer of electrons is involved, and complexes are formed which are called charge-transfer complexes. The associations which depend on the acidic or basic characteristics of the molecules are termed hydrogen-bonded interactions. These interactions will now be considered in greater detail.

1.3.a DIPOLE-DIPOLE INTERACTION

The molecules, taking part in this type of interaction, possess an overall electrical dissymmetry, in other words electric dipole moments. Even though a molecule may be electrically neutral the electrons in it, on average, spend more of their time around one nucleus than others, leading to positive and negative characteristics within the molecule, i.e. electrical dissymmetry.

When molecules possess a permanent dipole moment, the oppositely charged ends of molecules can be attracted to each other and the portions with like charge repelled. The resulting force between molecules, either attractive or repulsive, depends on the mutual orientation of molecules and if all the arrangements are equally probable the repulsion will cancel the attraction and no association will occur. In general, molecules tend to orientate themselves in such a way that the attraction between them is favoured. The extent of molecular association due to

this type of interaction is reduced by thermal agitation and therefore a high degree of association exists only at low temperatures. The average energy of a dipole-dipole interaction is given[2] by

$$E = -\frac{2}{3}\frac{\mu^4}{r^6 kT} \qquad (1.2)$$

where μ is the dipole moment, r the distance between the centres of the dipoles, k the Boltzmann's constant and T the absolute temperature.

1.3.b DIPOLE-INDUCED DIPOLE INTERACTION

This interaction may be termed an induction interaction. It is due to the polarisation of one molecule by the dipole of a second molecule, or by the total electric field due to surrounding polar molecules. The induced polarisation has the effect of increasing the dipole moment of the subject molecule and so increases the energy of attraction with other polar molecules. The induction energy is given[2] as

$$E = -2\mu^2\alpha / r^6 \qquad (1.3)$$

where α is the polarisability of the polarised molecule and μ the dipole moment of the polar molecule. In the case of dipolar molecules each polarises another to give a reciprocal effect. However, this type of interaction also occurs when a polar molecule with a permanent dipole moment approaches another molecule which is nonpolar. The former molecule will induce a temporary dipole in the latter in such a way that the interaction can occur. It is complexes, the formation of which is governed primarily by this mechanism, which are the subject of the studies reported in this thesis.

1.3.c VAN DER WAALS (DISPERSION) INTERACTION

For a neutral molecule, even one with a spherically-symmetrical charge distribution, there will be no permanent dipole moment and therefore no permanent inductive contributions to intermolecular forces. However, such a molecule may possess an instantaneous dipole moment, according to the positions of electrons and nuclei within the molecule[3] even though the average moment, taken over a period of time, is zero. These dipoles interact with each other in the same way as permanent dipoles. The instantaneous dipoles will set up a field which polarises the neighbouring molecules or atoms and the induced moments tend to keep in phase with the oscillation of the original dipoles. These interactions lead to an attractive energy which is independent of the presence of a permanent dipole. The dispersion energy between two molecules A and B can be given[2] as

$$E = -\frac{3}{2}\frac{I_A I_B}{(I_A+I_B)} \cdot \frac{\alpha_A \alpha_B}{r^6} \qquad (1.4)$$

where I is the ionisation potential and α the average polarisability. It will be seen from (1.3) and (1.4) that the induction energy is proportional to the polarisability of the polarised molecule whereas the dispersion energy varies as the product of the polarisabilities of the two interacting molecules.

1.3.d CHARGE-TRANSFER INTERACTION

The interaction of this type involves weak interactions between an electron donor and an electron acceptor, including those in which a "covalent" bond is formed. An electron donor is a molecule which has weakly bound electrons and a low ionisation potential whereas an electron acceptor has a low lying vacant orbital and a high electron affinity. The interaction occurs when the two molecules come close together in such a way

that their electron clouds overlap and this, is followed by the transfer of electrons. The enthalpy of formation is usually small, but the rates of formation and decomposition into the components are so high that the interaction, in the time period of normal observation techniques, appears to be instantaneous. Mulliken[4] has divided the donor and acceptor species into various groups, depending on the orbitals from which the transferred electrons come. In some cases a single species may behave both as a donor and as an acceptor[5] in the formation of complexes.

1.3.e HYDROGEN BOND INTERACTION

The interaction generally occurs for molecules which have hydrogen attached to electronegative atoms such as fluorine, oxygen or nitrogen, and originates from the bonding of hydrogen to an electronegative atom. Thus in general one component acts as an acidic or proton-donating group and the other behaves as a basic or proton-accepting group. The actual strength of a hydrogen bond depends upon the geometry of the molecular combination, the nature of neighbouring atoms and the acid-base character of the molecules. Steric effects also play an important part in the interaction since the active portions of the molecules may not be able to approach each other so closely, and the energy of association between the solute and solvent will be reduced. Hydrogen bonding may depend on whether the relevant molecule is in solution or not as this affects the position of the equilibrium governing the bonding. The extent of intermolecular hydrogen bonding is governed by the concentration in solution. This behaviour is closely related to the solubility of the solute. Any compounds possessing an intermolecular hydrogen-bonded structure will retain the structure only in aprotic solvents such as carbon tetrachloride and the solubility may be less than that of similar compounds, lacking the structure. However, in polar solvents, which can take part in hydrogen bond formation among themselves, the bond may be destroyed in favour of a

hydrogen-bonded structure forming between the solute and solvent, resulting in an increase in solubility. In the case of intramolecular hydrogen bonding the effects of solvents on this are usually extremely small.

The discussion so far has been devoted to the origin and formation of molecular complexes. The methods of studying them will now be discussed in more detail.

1.4 GENERAL METHODS EMPLOYED IN THE STUDIES OF THE INTERACTIONS

1.4.a INTRODUCTION

Several methods are employed in the studies of molecular interactions in solutions, and the parameter required in most investigations is the equilibrium constant K. Although the interactions may give rise to more than one species of complex in solutions, most methods of evaluating K have been based, at least initially, on the assumption that a single complex species with a definite stoichiometry is formed. If a complex species of 1:1 stoichiometry exists in an equilibrium between two molecules of different species (A and B), which can be represented by

$$A + B \rightleftharpoons A.....B \qquad (1.1)$$

then the equilibrium constant for the system is given as

$$K = \frac{[AB]}{[A][B]} \cdot \frac{\gamma_{AB}}{\gamma_A \gamma_B} \qquad (1.5)$$

where $[AB]$, $[A]$, $[B]$ are the equilibrium concentrations of AB, A, B respectively and can be defined in terms of molarities, mole fractions or molalities; γ refers to the relevant activity coefficients.

When the activity coefficients of all species are neglected (assumed all

equal to unity), (1.5) can be written as

$$K = [AB] / [A][B] \qquad (1.6)$$

and K is normally referred to as the equilibrium quotient.

The present section is devoted to brief discussions of various methods which are generally applicable to the studies of molecular interactions and capable of yielding values for K.

1.4.b OPTICAL METHODS

Electronic spectroscopy has been widely used in the study of molecular interactions, especially those resulting in charge-transfer complexes. In general the solutions which contain both the donor (B) and acceptor (A) species show not only the bands corresponding to the absorptions of B and A, but also new bands arising from the intermolecular charge-transfer transitions of the complex as a whole. The intensity of these bands have been used to measure the concentrations of complexes in solutions.

The interacting species (A and B) normally show bands at well defined frequencies. The determinations of K are then usually based upon intensity measurements of these bands and also on that due to the complex AB. Assumptions have to be made that the concentrations of A and B are proportional to absorptions at their own frequencies, and that the complex species formed will not produce an absorption band at those frequencies.

1.4.c HEAT OF MIXING STUDIES

This method has been widely applied to the study of hydrogen-bonded complexes. The existence of complexes in solutions can be confirmed from

the observation that large heats of mixing are evolved when the solutions are prepared. The heat produced can be related linearly with K (determined from another method) for the system[6]. In general, this method is employed in conjunction with optical studies to obtain full understanding of the system under consideration. Moreover, it proves to be useful in the determination of the stoichiometry of the reaction. The plots of heats of mixing per mole of solution against solution compositions provide the reaction stoichiometry, in particular for the case of complexes with 1:1 stoichiometry, whereby these plots show a symmetrical structure with a maximum at a point where the ratio between concentrations of interacting species is 1:1[7]

1.4.d PARTITION METHODS

The equilibrium properties of interacting species can be determined by studying the change in partition of one component of a complex between two immiscible liquids when the initially absent second component, soluble in only one of the two phases, is added to the system. Any interaction between solute and solvent will bring about an increase in the distribution ratio between the two phases. The method has been applied in the study of interaction between acetone and benzene[8], in which water was employed as the first phase and cyclohexane as the second phase. Although this approach was only developed by other workers in this laboratory during the period in which the work described herein was being conducted, it is interesting to comment on one significant finding of the partition work. If the concentration of solute (acetone) was kept constant, but that of benzene varied, it was found that K decreases as the concentration of the latter increases, which shows that K depends upon the initial concentrations of the reacting species.

One of the advantages of employing the partition method in the study of molecular interactions is that it allows a quantitative analysis of the reaction in so much that the concentration of transiently formed complexes can be determined directly.

1.4.e OTHER METHODS

These include, for example, n.m.r., cryoscopy and dielectric constant studies. Since these methods are employed in the present work, they will be discussed in detail in the next chapter.

From previous studies of molecular interactions in solution by the various methods mentioned above it is possible to summarise the general characteristics of intermolecular complexes. These characteristics will prove to be useful in the interpretation of results obtained from the three techniques used in the current investigations. They will now be discussed in greater detail.

1.5 GENERAL CHARACTERISTICS OF MOLECULAR COMPLEXES

1.5.a INTRODUCTION

Molecular complexes do possess some characteristics of their own which depend on the nature of the interacting species, the sizes, physical properties, structures and environment of molecules taking part in the interactions. In some cases it is possible to predict some characteristics of the complexes whereas in others this is difficult even in simple terms. Since the interaction (usually dipole-induced dipole) resulting in complex formation is weak and occurs in a fast reaction, i.e. the breakdown and formation of complexes are occurring rapidly,

the distribution of complexes is averaged and so are their characteristics so far as the techniques used for their study are concerned. This section will be restricted to a general discussion of interactions between solutes and aromatic molecules, acting as solvents, since these systems are of interest in the present work.

1.5.b THE NATURE OF MOLECULAR COMPLEX

The π - electron system in aromatic molecules represents a relatively exposed region of electronic charge directed normal to the molecular plane. When a solute species interacts with an aromatic molecule, the interaction will be primarily through the π-electrons, and the interacting molecules in complex tend to have a preferred set of mutual orientations. The types of complex formed may arise from several types of interaction. For example a polar solute, having a large dipole moment, tends to induce a dipole within an aromatic molecule and gives rise to a dipole-induced dipole complex, such as in the case of vinyl compounds[9]. Alternatively, an aromatic molecule may act as an electron donor in the formation of a charge-transfer complex. In this case electrons will be transferred to the solute molecule possessing an electron-deficient region, for example p-nitrobenzaldehyde[10]. The site of association is then governed by the electron distribution in the solute molecule. Polar substituents on the aromatic molecule will affect the stability of the complex of this type. The substituents with electron-releasing property, such as methyl groups, provide an increasing tendency for the aromatic molecule to donate electrons, thereby increasing the stability of the complex. Electron-withdrawing substituents such as the nitro-groups reduce the donating property of aromatic molecule, leading to a reduction in complex stability.

The present investigations involve interactions between polar solutes with large dipole moments and various non-polar aromatic molecules. It is expected that the complexes formed will arise from dipole-induced dipole interactions as described above, and further evidence in later chapters will clarify this for the systems under study.

1.5.c STRENGTH OF THE COMPLEX

Generally the strength of a complex is measured either in terms of the standard heat (ΔH°) or free energy (ΔG°) of formation. When the activity coefficients of the interacting species are taken to be unity, or self cancelling, the Gibbs standard free energy change for such a reaction is related to K at temperature T by

$$\Delta G^{\circ} = - RT \ln K \qquad (1.8)$$

where R is the gas constant.

(1.8) assumes negligible pressure dependence in the condensed phase. If K in (1.8) is expressed in mole fractions, ΔG° then represents the free energy change when one mole of each of the reacting species combine to produce one mole of complex.

The temperature dependence of ΔG° is given by the Gibbs-Helmholtz equation in the form of

$$\frac{\left[\partial(\Delta G/T)\right]}{\left[\partial(1/T)\right]} = \Delta H \qquad (1.9)$$

Combination of (1.8) and (1.9) gives

$$\frac{\partial \ln k}{\partial (1/T)} = \frac{-\Delta H}{R} \qquad (1.10)$$

Therefore a plot of ln K against 1/T should give a slope of $-\Delta H/R$ at any temperature. A linear plot[11] indicates the constancy of ΔH with temperature which, in turn, demonstrates the presence of a single complex. It has been found from experimental results that[12,13] ΔH° for the interactions are of the order of a few KJ mol^{-1}, showing the weak nature of the complexes.

In the past ΔH° has been assumed to be a measure of the strength of interaction between solute and aromatic molecules. Jackson[14] has critically examined the possibility that ΔG°, rather than ΔH°, should be used for this purpose. It was also found from experimental work that[15,16] the interaction energies of complexes vary with temperature (since the interaction distance is temperature dependent), so their strengths should be compared directly with ΔG° and not with ΔH° which is invariant.

1.5.d STOICHIOMETRY OF THE COMPLEX

It is often assumed initially that the stoichiometry of the complex formed between solutes and aromatic molecules is 1:1 and this is found to be true in many cases. However, this is just an assumption and may be wrong in some cases. Generally the stoichiometry of a complex can be confirmed cryoscopically whereby solutions of various concentrations of a solute in an aromatic solvent are cooled down and their freezing points obtained. Any complex formation will be shown by the presence of one maximum (or more) on a plot of concentrations against freezing points, and the position of the maximum will be the same as the

stoichiometry of the complex. Using this technique the interactions of acetonitrile and various aromatic molecules have been studied and the presence of a complex of 1:2 stoichiometry was observed[17]. Similar studies have been made on chloroform with various π-donors including aromatic and olefinic solvents[18], and the results have been interpreted in terms of 1:1 complex formation through weak hydrogen bonds in most cases. However, in the latter case, some corrections have to be made for the self-association of liquid chloroform.

The presence of more than one complex species in a system can sometimes occur. When this situation arises the calculation of K for each complex species becomes more complicated[19]. The system in which small amounts of 1:2 complex are present together with the 1:1 complex has been studied[20], and K for each complex formation computed. Generally in this case, each complex will have a different value of ΔH°. It then follows that the plot of ln K, calculated on the basis of 1:1 stoichiometry, versus 1/T, as described in section 1.5.3, should not be linear since temperature will affect the different values of K to different extents. This approach provides a valuable aid in deciding the stoichiometry of the complexes. The most commonly occurring complexes, in solutions, are bimolecular. Complexes of stoichiometries higher than 1:2 are rarely found, which may be due to factors such as steric effects, sizes of interacting molecules and the nature of interactions.

1.5.e. GEOMETRY OF THE COMPLEX

Molecular complexes, formed between solutes and aromatic molecules, are generally found to do so with reasonably well defined configurations. In those complexes involving aromatic compounds the six-fold symmetry axis of the aromatic can be taken as a reference axis, and the arrangement

of polar solute molecules characterised by the relation of their dipolar axes relative to this. The geometry of the dipole(aromatic) induced dipole complexes which are expected to exist in systems under the present investigations can be classified into two main groups as follows:

(a) The solute molecule may lie close to the aromatic ring, with its dipolar axis parallel to the plane of the ring, i.e. at right angles to the aromatic six-fold axis, giving rise to a planar configuration of the complex[21,9]. It was suggested that, if the solute contains electrical dissymmetry within itself, its positively charged end will be close to the ring whereas the other end moves away from the centre of the ring.

(b) Solute molecule may arrange itself such that its dipolar axis is coincident (or near) with the six-fold symmetry axis[18,22]. However, Homer and Cooke[16] have shown theoretically that (b) should be favoured normally.

A method has been employed to study the geometry of some complexes by making use of the screening induced in nuclei of the solute, by aromatic molecules, at various points surrounding the aromatic molecule[23,24]. The co-ordinates of any point relative to the aromatic ring are defined by reference to two axes, one of which is in the plane of the ring and the other along the six-fold symmetry axis. It is then possible to fix the positions of the solute relative to the ring and thus the geometry of complex. The method has been applied to the interactions between polar solutes and aromatic molecules from which it is found that the resultant dipole direction of solutes lies along the aromatic six-fold

axis. In some cases when the solute molecules are symmetrical, they "wobble" about the six-fold axis.

1.5.f STERIC EFFECTS ON COMPLEX FORMATION

The effect of steric hindrance can play some part in the formation of complexes. Solutes containing side-chain branching groups or, for aromatic solutes, groups in ortho position to active protons, will prevent aromatic solvent molecules from approaching the influenced protons of the solutes. The K values of these complexes will be smaller when compared with similar systems without steric hindrance[1].

Alkyl substitutions on benzene can exhibit steric effect upon complex formations in two ways[25]; they can increase K value of a system by trapping as well as reduce it by blocking the approach of solute molecule towards the aromatic solvent molecule.

The present investigations involve studies on interactions between polar solutes, such as acetonitrile and nitromethane, and various methyl-substituted benzenes by employing measurements of the n.m.r. chemical shifts, dielectric constants and freezing points. The n.m.r. and dielectric studies will be focussed on dilute solutions of solutes in aromatic solvents, from which it is expected that information on the nature, strength, geometry of complexes will be obtained, whereas cryoscopic studies will give information on the stoichiometry of complexes. The next chapter will be devoted to the discussion on various experimental methods employed in the present work.

CHAPTER 2

GENERAL AND THEORETICAL ASPECTS OF VARIOUS EXPERIMENTAL METHODS EMPLOYED IN THE INVESTIGATIONS

INTRODUCTION

The methods employed in the present investigations are nuclear magnetic resonance (n.m.r.) spectroscopy, dipole moment and cryoscopic studies. It is expected that n.m.r. studies will provide information on the nature, stereochemistry, stoichiometry and strength of the interactions.[1] It is also hoped that the other two approaches will selectively elucidate some of these points for the complexes formed. Taken together these studies should allow the characteristics of the complexes under investigations to be elucidated more precisely than possible by using only one technique as is done normally. It is necessary, before going any further, to discuss in detail the general theories and principles of each particular method employed. The present chapter fulfils this purpose and, for a matter of convenient discussion, is classified into three separate sections. Section A deals with the general principles of n.m.r. spectroscopy whereas section B and C with those of dipole moment and cryoscopic studies respectively.

SECTION A

N.M.R. SPECTROSCOPY

2.A.1 INTRODUCTION

Some atomic nuclei possess magnetic moments in addition to possessing electric charges. The magnetic characteristics were first inferred from a study of the hyperfine structure occurring in atomic spectra detected using optical spectrographs[26]. Pauli[27] suggested from the presence of this structure that certain nuclei possess angular momentum and thus a magnetic moment which interacts with the electrons in the atomic orbitals.

If an external magnetic field is applied to a system containing nuclei of this type, the nuclear magnets experience torques so that only certain orientations, each with different energy, relative to the applied field direction are allowed. It is then possible, by subjecting the system to radiation, having a magnetic field component oscillating at a suitable frequency and appropriate energy, to observe transitions occuring between the nuclear energy levels associated with these orientations. The nuclei, absorbing energy from the magnetic field, give rise to what are called n.m.r. spectra.

The first successful application of n.m.r. techniques was performed by Ramsey[28], developing the method of Stern and Gerlach[29], in connection with the molecular-beam experiments. In this method a molecular beam was passed through two oppositely inclined magnetic fields of similar gradients. The molecules were thus diffused and brought to focus on a detector by the fields. A uniform magnetic field and a coil energised by a radiofrequency (r.f.) signal, being placed in such a way that the oscillating magnetic component of the r.f. signal was at right angles to the main field, was positioned between the first two fields. Whenever the frequency of the oscillating field was equal to that required to induce transitions between nuclear energy levels, a reduction in the density of the molecules reaching the detector was observed. The first actual n.m.r. spectra were observed by Bloch et al[30] in water and by Purcell et al[31] in paraffin wax.

To develop n.m.r. theory, it is convenient first to consider the properties of an isolated nucleus, then move on to an assembly of nuclei and finally nuclei in molecules.

2.A.2 AN ISOLATED NUCLEUS IN A MAGNETIC FIELD

A nucleus may be considered to behave as a spinning spherical (or ellipsoidal) body so possessing an angular momentum. Nuclear angular momentum is quantised and a nucleus has $(2I + 1)$ distinct energy states, where I is the spin quantum number. The corresponding components of angular momentum, along any particular direction, have values I, $(I - 1)$, $(-I + 1)$, $-I$ in terms of $\hbar$ units, where $\hbar$ is the reduced Planck's constant ($= h/2\pi$). The magnitude of the angular momentum for a system with spin I is given by [32]

$$\hbar \sqrt{I(I + 1)}$$

The spinning charged nucleus gives rise to a magnetic field, the axis of which is coincident with the axis of spin. Thus, the magnetic moment and angular momentum behave as parallel vectors (Fig. 2.1) that can be related by [33]

$$\vec{\mu} = \gamma \vec{I} \hbar \qquad (2.1)$$

where μ is the magnetic moment and γ is a characteristic property of a particle, known as the magnetogyric ratio. If $I = 0$, then $\mu = 0$, and no magnetic moments are observed, but if I is non-zero, μ will have a finite value and is parallel to $I\hbar$. Since the values of $I\hbar$ are quantised, this restriction will affect μ which thus can possess only discrete components, each of which has specific orientation relative to the reference axis. This axis is taken as the direction of the applied magnetic field B_o (- z direction). In the case of a particular orientation of μ to the B_o direction, represented by an angle θ (Fig 2.1), the energy of the nucleus will be

$$E = E_o - E_z \tag{2.2}$$

where E_o is the energy in the absence of a field and

$$E_z = \vec{\mu}_z B_o \tag{2.3}$$

where $\vec{\mu}_z$ is the component of μ in the z direction.

The change in energy due to the imposition of B_o is thus

$$E_z = -\mu \cos\theta \, B_o \tag{2.4}$$

and this is governed by the allowed values of I which are described by the nuclear magnetic quantum number (m). m can have the values

$$m = I, I-1, \ldots , -I + 1, -I \tag{2.5}$$

Therefore $\cos\theta = m/I$ and

$$\mu_z = m\mu /I \tag{2.6}$$

Thus

$$E_z = - m\mu B_o/I \tag{2.7}$$

In the absence of B_o, the different energy levels are degenerate, but when B_o is present they will separate in a similar manner to the Zeeman splitting of electronic levels. The energies of the allowed levels are given as

$$-\mu B_o, -\frac{(I-1)}{I} \mu B_o, \ldots , \frac{(I-1)}{I} \mu B_o, \mu B_o$$

In order to obtain the n.m.r. spectra one has to induce transitions of nuclei between the various energy levels to provide the necessary absorption or emission of energy. However, the selection rule[34]

$$\Delta m = \pm 1$$

governs the nuclear transitions, so the transitions can only occur between successive energy levels.

Consequently the energy difference between two adjacent levels is

$$\Delta E = \mu B_o / I \qquad (2.8)$$

For the case when $I = \frac{1}{2}$, as for a proton, the splitting can be represented as

$$\Delta E = \mu B_o / I = 2 \mu B_o \qquad (2.9)$$

or illustrated as

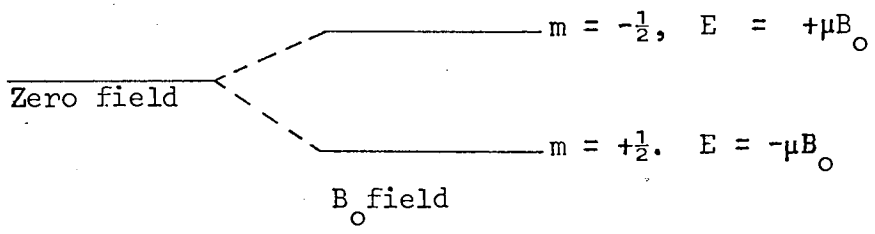

From the Bohr frequency condition $\Delta E = h\nu$, the frequency of the radiation required to induce a transition is given by

$$\nu = \Delta E / h = \mu B_o / Ih \qquad (2.10)$$

Equation (2.10) may be expressed alternatively in terms of γ by

$$\nu = \gamma B_o / 2\pi \qquad (2.11)$$

Since a particular nuclear species has constant values of μ and I, ν depends directly on B_o so, unlike most other spectroscopic techniques, the magnetic resonance spectrum can occur under a variety of conditions. For example, for a proton two typical conditions where resonance occurs are

$B_o = 1.4092$ tesla ; $\nu = 60.004$ MHz

$B_o = 2.3490$ tesla ; $\nu = 100.000$ MHz

2.A.3 CLASSICAL TREATMENT OF NUCLEAR RESONANCE CONDITION

If a spinning charged particle or nucleus is placed in a magnetic field B_o with its magnetic moment making an angle θ to the direction of this field, it will experience a torque $\vec{L}$ tending to constrain it parallel to

the field. Newton's law states that the rate of change of angular momentum p with time is equal to the torque, or

$$dp/dt = \vec{L} \tag{2.12}$$

Because magnetic theory requires that[35]

$$\vec{L} = \vec{\mu} B_o \tag{2.13}$$

It is evident that

$$dp/dt = \vec{\mu} B_o = \gamma \vec{p} B_o \tag{2.14}$$

Equation (2.14) describes the precession of the nuclear magnet about B_o with an angular velocity ω_o defined by

$$dp/dt = \vec{p}\omega_o \tag{2.15}$$

Hence

$$\omega_o = \gamma B_o \tag{2.16}$$

(2.16) is called the Larmor equation which can be written in terms of the precession frequency ν_o as

$$\nu_o = \gamma B_o/2\pi \tag{2.17}$$

If a small rotating magnetic field B_1 is applied at right angles to the main static field B_o in order to change the orientation and thus the magnetic energy of the nucleus (Fig 2.2), B_1 must rotate in synchronisation with the precession of μ about B_o, i.e. the rotation of B_1 must be in resonance with the Larmor precession about B_o. Whenever this condition is fulfilled, B_1 will always have the same disposition to μ throughout the rotation and the angle θ will eventually change. If the frequency of rotation of B_1 is swept through the Larmor frequency, the effect will be greatest at the Larmor frequency and will show up as resonance phenonenon. In practice the effect can be observed by applying a linearly oscillating field since such a field can be regarded as a superimposition of two fields rotating in opposite directions. One field component will be rotating in the opposite sense to the nucleus and will have little effect on it, whereas the other component is used to perturb the precessional motion and induce

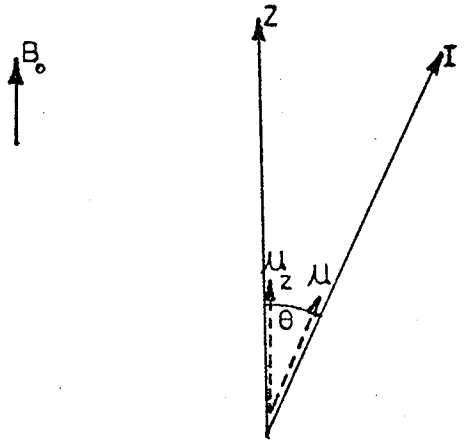

Fig. 2.1 THE RELATIONSHIP BETWEEN THE MAGNETIC MOMENT μ AND THE SPIN ANGULAR MOMENTUM I

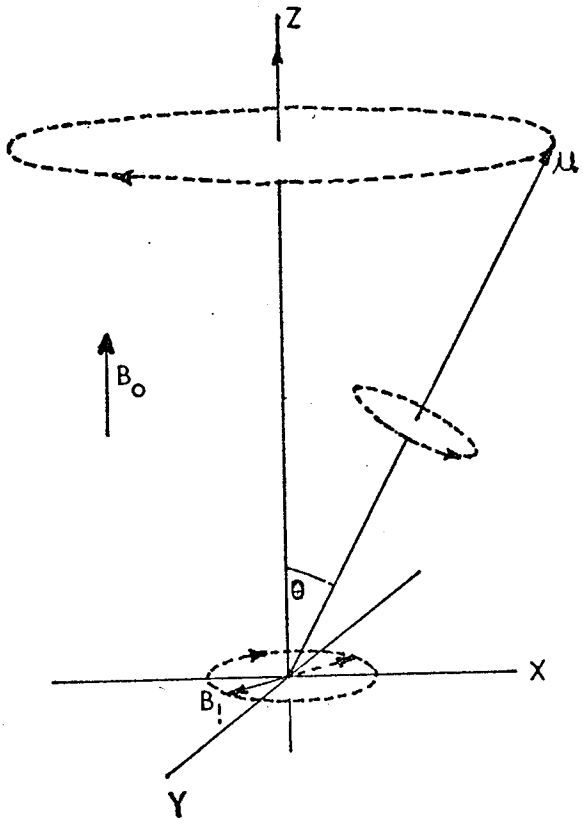

Fig. 2.2 VECTORIAL REPRESENTATION OF THE CLASSICAL LARMOR PRECESSION

energy changes when its frequency corresponds to the Larmor frequency.

2.A.4 THE POPULATION OF SPIN STATES

When a nucleus is at the resonance condition, the transition probabilities occuring by absorption or emission of energy are equal, thus the overall effect will depend on the nuclear distribution between the two energy levels.. When there is thermal equilibrium throughout the assembly, nuclei will distribute themselves among the spin states according to a Boltzmann distribution. For N nuclei at equilibrium at temperature T, the number of nuclei N_i, in a particular level with energy E_i, is given by[36]

$$N_i/N = \exp(-E_i/kT) / \Sigma_i \exp(-E_i/kT) \qquad (2.18)$$

where k is the Boltzmann constant.

Since there are 2I + 1 levels separated by an energy of $\mu B_o/I$ for nuclei with spin I, the probability of any given nucleus occupying a particular level of magnetic quantum number m is given by

$$\frac{1}{2I+1} \exp\left(\frac{m\mu B_o}{IkT}\right) \qquad (2.19)$$

Under operating conditions at room temperature, $\mu B_o/kT$ is small and (2.19) will approximate to

$$\frac{1}{2I+1}\left(1 + \frac{m\mu B_o}{IkT}\right) \qquad (2.20)$$

For a nucleus with $I = \frac{1}{2}$ the probabilities of it being in either the upper or lower states are

$$\tfrac{1}{2}(1 - \mu B_o/kT) \quad \text{and} \quad \tfrac{1}{2}(1 + \mu B_o/kT) \qquad (2.21)$$

respectively.

The above equation shows that normally there is an excess of nuclei in the lower energy state, so that when n.m.r. signals are observed a nett absorption of energy is observed. If the number of nuclei present in the upper and lower states are represented by N_H and N_L respectively, and the probability of an emission or absorption is P, then at the resonance condition the change is[37]

$$P (N_L - N_H) = P.N_{excess} \qquad (2.22)$$

corresponding to the overall absorption of energy.

As N_{excess}, the number of excess nuclei in the lower state, decreases and tends to zero during resonance, the n.m.r. signals can weaken and eventually disappear with increasing intensity of the radiofrequency field. This phenomenon, known as saturation, is discussed in more detail in section 2.A.6.

2.A.5. RELAXATION PROCESSES

The tendency of the nett absorption of energy at the resonance condition, is to reduce the excess population and, in doing so, reduce the extent of further absorption. At the same time there are processes which tend to restore the original energy level distribution, following the absorption of radiofrequency energy, by removing excess energy from an excited spin state. These processes are referred to as relaxation processes of which there are two principal types, namely spin-spin relaxation and spin-lattice relaxation. These processes occur continually and are competitive with the absorption process during resonance condition and, after resonance, the latter restores the system to the pre-resonance equilibrium.

2.A.5.a SPIN-LATTICE RELAXATION

The term lattice refers to the molecular system as a whole, which contains

the nuclei being studied. All molecules in this system undergo translational, rotational and vibrational motion; thus any nuclear magnetic moment which may be present will experience a rapidly fluctuating magnetic field produced by neighbouring magnetic moments. Whenever the field has a component at a frequency which is synchronous with the precessional frequency of a neighbouring nucleus, this field is capable of inducing a nuclear transition. Both emission and absorption transitions can then proceed, but since the probability of the former is greater than the latter, the nett effect is that energy is transferred from the spin system to the surrounding lattice. The relation between the upward and downward transition probabilities P_1 and P_2 (for interaction of a nucleus with other molecular degrees of freedom) is immediately obvious from simple thermodynamics i.e.

$$P_2 \text{ (upper} \longrightarrow \text{lower)} > P_1 \text{ (lower} \longrightarrow \text{upper)}$$

The spin-lattice relaxation is responsible for the initial distribution of spin states when a nuclear system is placedin a magnetic field; this effect can be described as follows. When an assembly of nuclear spins of $I = \frac{1}{2}$ is placed in a steady magnetic field the instantaneous initial population of the two spin states is equal and a finite time is required for the populations of these states to reach their new equilibrium value. If a system is considered in which there are N_1 and N_2 as the number of nuclei per unit volume in the lower and upper states respectively, then at equilibrium (in the presence of a magnetic field)

$$N_1 P_1 = N_2 P_2 \tag{2.23}$$

where

$$N_1 - N_2 = N_{excess} \tag{2.24}$$

From (2.18)

$$P_1/P_2 = \frac{N_2}{N_1} = \exp(-\mu B_o/IkT)$$

$$= \exp(-2\mu B_o/kT) \text{ when } I = \tfrac{1}{2} \qquad (2.25)$$

In other words

$$\frac{N_2}{N_1} = 1 - 2\mu B_o/kT \qquad (2.26)$$

Since an upward transition decreases and a downward transition increases N_{excess} by 2, then the rate of change of N_{excess} is

$$dN_{excess}/dt = 2(N_2P_2 - N_1P_1) \qquad (2.27)$$

If P represents the mean transition probability, then

$$P = (P_1 + P_2)/2 \qquad (2.28)$$

and from (2.25), one obtains

$$P_1 = P \exp(-\mu B_o/kT) \qquad (2.29)$$

and

$$P_2 = P \exp(\mu B_o/kT) \qquad (2.30)$$

From (2.29) and (2.30), expanding the exponential functions and assuming $\mu B_o/kT \ll 1$, it is evident that (2.27) reduces to

$$dN_{excess}/dt = -2P\left[N_{excess} - (N_1 + N_2)\mu B_o/kT\right] \qquad (2.31)$$

If N_{eq}, the equilibrium value of N_{excess}, is given by

$$N_{eq} = \frac{\mu B_o}{kT}(N_1 + N_2) \qquad (2.32)$$

one obtains from (2.31)

$$dN_{excess}/dt = -2P(N_{excess} - N_{eq}) \qquad (2.33)$$

Integration of (2.33) gives

$$N_{excess} - N_{eq} = (N_o - N_{eq}) \exp(-2Pt) \qquad (2.34)$$

Where N_o is the initial value of N_{excess} (per unit volume). The spin-lattice relaxation time T_1 is given by[33]

$$T_1 = \frac{1}{2P} \qquad (2.35)$$

Therefore, from (2.34)

$$N_{excess} - N_{eq} = (N_o - N_{eq}) \exp(-t/T_1) \qquad (2.36)$$

T_1 can thus be seen to be a measure of the rate at which the spin system moves into thermal equilibrium with the other degrees of freedom.

2.A.5.b. SPIN-SPIN RELAXATION

Apart from interacting with the lattice, magnetic nuclei also interact among themselves. Not only does the steady magnetic field B_o act upon each nuclear magnet but also the small local magnetic field, B_{loc}, produced by other surrounding nuclear magnets contributes to give the total field. The neighbouring nuclear magnets precess about the direction of B_o, and B_{loc} then can be resolved into the oscillating (B_{osc}) and static (B_{stat}) components. B_{stat} will be (anti)parallel to the direction of B_o whereas B_{osc} is at right angles to it. Hence a nucleus j, producing an oscillating magnetic field with the Larmor frequency, may induce a transition in the other nucleus k in a manner similar to that induced by an applied oscillating field. Nucleus j provides the energy for the process and the interchange of energy proceeds while the total energy of the pair is conserved. A time interval will be required for spin exchange since the nuclei, which are precessing in phase at one instant of time, get out of phase in the time T_2, the spin-spin relaxation time.

Only identical nuclei undergo spin exchange whereas unlike nuclei will contribute to B_{loc}.

The spin-spin relaxation time, T_2, can be defined as the lifetime or phase memory time of a nuclear spin state. It is also known as the transverse relaxation time.

2.A.6 SATURATION

If the strength of the oscillating field, B_1, is too high, the intensity of the absorption spectrum decreases, owing to the reduction in the excess population in the lower energy state, i.e. the number of nuclei capable of absorbing energy. The absorption will decrease until an equilibrium is reached and saturation occurs since the rate of absorption is comparable to, or greater than, the rate of relaxation between the energy states. Saturation is usually characterised by Z_o, the saturation factor[33], where

$$Z_o = (1 + \gamma^2 B_1^2 T_1 T_2)^{-1} \qquad (2.37)$$

As B_1 increases the resonance lines get broader. The magnitude of the broadening increases linearly with B_1 for low values of B_1, but tends to a constant value at high values of B_1. Since the values of T_1 and T_2 may vary for different nuclei within one molecule, differing saturation effects for different lines[38] in the same spectrum can be observed.

2.A.7 FACTORS AFFECTING THE LINE SHAPES

An important characteristic of any resonance line is its width, which is usually defined as the width at half height and expressed either in terms of the applied field or frequency. The widths will vary from being rather

small in liquids to large in solids. For single lines in liquids the shape is found to be Lorentzian[39,40]. The line width is normally governed by several factors but is chiefly affected by T_1 and T_2. These factors will now be considered.

2.A.7.a SPIN-LATTICE RELAXATION

The environment of a particular nucleus produces a fluctuating magnetic field from which transitions of that nucleus are induced. This phenomenon places some uncertainty on the lifetime of the nucleus in a particular energy state which is of the order of $2T_1$. Since the uncertainty principle requires that

$$\Delta E.\ \Delta t = h/2\pi \tag{2.38}$$

and

$$\Delta E = h\Delta\nu \tag{2.39}$$

It is evident that

$$\Delta\nu = \frac{1}{2\pi\ \Delta t} \tag{2.40}$$

But

$$\Delta t = 2T_1 \tag{2.41}$$

and so

$$\Delta\nu = \frac{1}{4\pi T_1} \tag{2.42}$$

i.e., small values of T_1 will lead to line broadening, because of the spread in the values of ν at which resonance may occur.

2.A.7.b SPIN-SPIN RELAXATION

This relaxation process produces an uncertainty in the lifetime of any particular nuclear state in a similar manner to that of spin-lattice relaxation, i.e. a broadened absorption signal can be observed over a small range of frequencies.

2.A.7.c ELECTRIC QUADRUPOLE EFFECTS

Nuclei with spin $I > \frac{1}{2}$ possess electric quadrupole moments due to their asymmetric charge distribution. These nuclear quadrupoles will interact with the electric field gradients produced across the nuclei by the environment of an atom possessing those nuclei. The interaction provides another mechanism for spin-lattice relaxation and therefore leads to smaller values of T_1[41] which will increase the resonance line width. The distribution of field gradients in solids can also lead to the line broadening and smaller value of T_2.

2.A.7.d MAGNETIC DIPOLAR BROADENING

In some cases the interaction of magnetic dipoles can produce a greater broadening than the spin-lattice relaxation. This happens in solids and highly viscous liquids since nuclei stay in fixed positions for a long time whereas in normal liquids and gases the effect is negligible. The broadening is induced by the static component (B_{stat}) of the local magnetic field (B_{loc}) (see section 2.A.5.b) which is given[39] by

$$B_{stat} = \frac{\mu}{r^3} (3 \cos^2\theta - 1) \qquad (2.43)$$

at a point distance r from the dipole and lying on a line inclined to the dipolar axis at an angle θ. In solids B_{loc} can have any value in the range $\mp 2\mu/r^3$ and resonance occurs over a range of frequencies and the lines are broadened. In liquids and gases because molecules undergo rapid random motion $\cos^2\theta$ averages to 1/3 and $B_{stat} = 0$. and the magnetic fields average out. The molecular motions necessary to produce such averaging are of shorter time than that required to observe a nuclear resonance signal, and the effect of magnetic dipoles on line width is negligible in liquid and gaseous samples.

2.A.7.e MAGNETIC FIELD INHOMOGENEITY

The variation of the static magnetic field B_o over the dimensions of the sample can cause line broadening due to resonance occuring not at a particular field strength, but over a range of field as different portions of the sample experience the resonance condition at slightly different times. This contribution to the line width can be partially overcome by rapid spinning of the sample.

2.A.8 THE CHEMICAL SHIFT

It has been assumed so far that the resonance frequency of a nucleus is just a function of the applied r.f. field and the magnetogyric ratio of the nucleus. However, it was discovered at an early stage[42,43,44] that the resonance frequency is also, to some extent, dependent upon the chemical environment of the nucleus. The phenomenon was a general one for all magnetic nuclei and was called "the chemical shift". It is observed whenever two or more nuclei of the same isotopic species are in different environments and a separate resonance is observed for each distinct group with an intensity proportional to the number of nuclei in the group.

The chemical shift is directly proportional to the applied field strength. It arises from small intramolecular and intermolecular contributions to the field applied to a particular nucleus. These contributions have their origin in the various circulations of electrons in the molecule, together with effects associated either with individual atoms or with the whole medium. These effects will alter the strength of the local field produced at the nucleus by a factor σ, the shielding (screening) coefficient or constant. If B_o is the applied field, then the actual field experienced by the nucleus is given by

$$B_{loc} = B_o (1 - \sigma) \qquad (2.44)$$

where σ is dimensionless and commonly positive. The reduction of B_o will reduce the Zeeman splittings and for the case of $I=\frac{1}{2}$ this can be shown as:

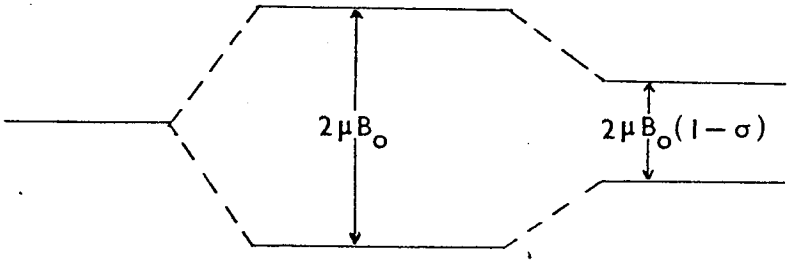

Therefore the energy required for a transition between the energy states is smaller and resonance occurs at a lower frequency. In other words, if the experiment is performed by varying the field B_o until resonance is obtained at a fixed frequency, the applied field will have to be of a value higher than that for an unscreened nucleus.

If two nuclei of the same isotopic species in environments i and j have shielding constants of σ_i and σ_j respectively at the same value of B_o, then the chemical shift difference δ_{ij} is given as

$$\delta_{ij} = \sigma_i - \sigma_j \qquad (2.45)$$

Since it is not possible to measure the resonance position of a nucleus stripped of all its electrons, absolute chemical shifts cannot be determined. Thus reference compounds giving single sharp lines are generally chosen to overcome the problem and the chemical shift of the nucleus is measured relative to the reference compound in terms of a dimensionless number (δ), given for practical reasons by

$$\delta = \frac{(B_c - B_R)}{B_R} \times 10^6 \quad \text{p.p.m.} \qquad (2.46)$$

where B_c is the resonance field for the nucleus under observation and B_R is is that for the reference compound.

Because B is proportional to the frequency ν , δ can also be defined in terms of frequencies as

$$\delta = \frac{(\nu_c - \nu_R) \times 10^6}{\text{oscillator frequency}} \quad \text{p.p.m.} \qquad (2.47)$$

where ν_c and ν_R are the frequencies corresponding to B_c and B_r. The most commonly used reference for proton resonance is tetramethylsilane (T.M.S.),[45] since its resonance is a clear sharp line occuring to high field of most resonances of interest. In this situation the " τ-scale", which is defined in such a way that, for infinite dilution in carbon tetrachloride, the position of the T.M.S. line will be at the τ value of 10, is often used. The τ values of other resonance lines are then expressed as

$$\tau = \delta + 10 \qquad (2.48)$$

Since the work reported in this thesis concerns the study of chemical shifts it is necessary to discuss this parameter in more detail. This will be done in the following sections.

2.A.9 ORIGINS OF THE CHEMICAL SHIFT

For large molecules, the shielding of nuclei can be divided into several individual contributions, the sum of which will represent the total screening of the nuclei. It was first proposed[46] that the screening of a nucleus can be divided into three atomic contributions which are

1. The diamagnetic contribution for the atom
2. The paramagnetic contribution for the atom
3. The contribution for other atoms

However, this approach does not take into account the possible magnetic effects of interatomic currents in which electrons move from one atom to another.

The shielding of any nucleus A can be divided more usefully into two main

terms, representing the intramolecular and intermolecular screenings, such that

$$\sigma_A = \sigma_A^{intra} + \sigma_A^{inter} \text{ (or } \sigma^{sol}) \qquad (2.49)$$

These two terms may be divided further into nine contributions represented by[33,47]

$$\sigma_A^{intra} = \sigma_{AA}^{dia} + \sigma_{AA}^{para} + \sum_{B \neq A} \sigma_{AB}^{mag} + \sigma^{del} \qquad (2.50)$$

and

$$\sigma^{sol} = \sigma_w + \sigma_E + \sigma_b + \sigma_a + \sigma_c \qquad (2.51)$$

An effective difference in the magnitude of any of these terms for two nuclei contributes to the chemical shift between them. However, for the present work, where the chemical shift of a common solute in various aromatic solvents is required, it may be assumed that σ^{intra} of such a solute in those solvents are identical, and it is only necessary to consider σ^{sol}. Each of the terms in (2.50) and(2.51) will now be discussed in more detail with the emphasis on those of σ^{sol}.

2.A.9.a DIAMAGNETIC TERM σ_{AA}^{dia}

This term is proportional to the applied field and is produced at the nucleus by the moment induced through rotation of the electrons about the nucleus. When an atom with a spherically symmetric electron distribution is placed in a uniform magnetic field, the field will induce a motion of the electrons about the nucleus such that a secondary magnetic field, opposing the primary field at the nucleus, is produced (a diamagnetic effect). The nucleus then experiences the effect of both the applied and induced fields and the resultant field is therefore less than the applied field. The magnitude of σ_{AA}^{dia} depends upon the electron density around the nucleus and hence upon the electronegativity of the groups attached to the nucleus.

2.A.9.b PARAMAGNETIC TERM σ_{AA}^{para}

This term arises from the mixing, induced by the applied field B_o, of ground and excited electronic states of an atom[48,49]. The screening arises from local fields induced at the resonant nucleus. When these fields are axially symmetric, with respect to the applied field, there is no paramagnetic screening, but if they are not axially symmetric there is a hindrance to the precession of electrons about the resonant nucleus, resulting in a σ_{AA}^{para} screening. σ_{AA}^{para} should vanish for s electrons since these are spherically symmetrical with no orbital angular momentum. Evaluation of this term requires detailed knowledge of both ground and excited state wave functions which are rarely available[50]. Both σ_{AA}^{para} and σ_{AA}^{dia} will differ for different nuclei of the same type in the same molecule owing to the uneven distribution of electron density, and also depend on the orientation of the molecule relative to the magnetic field.

2.A.9.c INTERATOMIC SHIELDING σ_{AB}^{mag}

This term originates from induced currents in adjacent anisotropic electron groups and may have diamagnetic or paramagnetic characteristics[46]. When a molecule is placed in a strong magnetic field, different magnetic moments may be considered to be induced along the principal axes of the bonds, and these induced dipoles produce secondary fields at a nucleus (neighbour anisotropy effect). The magnitude of σ_{AB}^{mag} depends on the nature of the atom or group in which the secondary field originates and also on the molecular geometry.

2.A.9.d DELOCALISED ELECTRON SHIELDING σ^{del}

This arises from electron circulation, induced by the static magnetic field in fully conjugated π-orbitals such as in benzene[51]. When the magnetic field B_o is applied perpendicular to the plane of the aromatic ring, the delocalised π electrons give rise to a ring current. This ring

current induces a secondary field at the centre of the ring which is in opposition to B_o, but will reinforce B_o at the positions of the aromatic protons. The induced field at the aromatic protons is parallel to the main field and thus these protons are deshielded by the ring current whereas any, which may be on or near the six-fold axis of the ring, experience the diamagnetic part of the induced field and will be shielded due to this effect.

2.A.9.e INTERMOLECULAR SCREENING EFFECTS σ^{sol}

These effects are also called "Solvent effects" since they are contributed either directly or indirectly by the solvent molecules. Generally solvent molecules can affect the resonance positions of a solute nucleus by the same type of mechanisms as the previously discussed intramolecular effects[52] σ^{sol} can be resolved into a number of components according to various types of origins[47] as given by (2.51)

$$\sigma^{sol} = \sigma_w + \sigma_E + \sigma_b + \sigma_a + \sigma_c \qquad (2.51)$$

where σ_b arises from the medium bulk susceptibility, σ_E is the contribution produced by intermolecular electric fields created by permanent or induced electric moments in the solute and solvent molecules, σ_w is that due to van der Waals forces between solute and solvent, σ_a arises from the anisotropy in the molecular magnetic susceptibility of the solvent molecule and σ_c represents the screening arising from specific interactions between solute and solvent molecules.

Both the solute and reference molecules will be subjected to these terms and, if they are affected differently, a correction has to be made to provide a shift value devoid of these effects. The reference compound, when being used externally, has to be contained in a small capillary tube

inserting inside the main sample tube or, if used internally, is mixed with the sample directly. In the latter case some of the effects referred to above may be largely eliminated. These medium effects will now be discussed more fully.

2.A.9.f VAN DER WAALS OR DISPERSION SCREENING σ_w

This effect stems from van der Waals or dispersion interaction forces acting whenever any two molecules come together. When two molecules approach each other the time varying electric dipoles in each produce electric fields which will polarise one another, resulting in a modification of the original electron distributions[53,54] and lead to a change in the nuclear screening constants in these molecules. σ_w may have contributions from two effects which are the:

(a) interaction between the solute and solvent, in their equilibrium configurations, causing a distortion of electronic environment of the nuclei of the solute, leading to a paramagnetic shift. The shift should increase as the charges on the solvent nuclei rise. This effect is expected to be temperature independent.

(b) departures from the equilibrium solvent configurations which affect the solute by leading to a time-dependent distortion of the electronic structure. It also leads to a paramagnetic shift and is temperature dependent.

Marshall and Pople[55] have made a quantum mechanical calculation of the effect of σ_w on the shielding constant of a hydrogent atom separated from another neighbouring hydrogen atom, by distances large compared with the equilibrium separation in the hydrogen molecule , and concluded that van der Waals forces tend to reduce the value of shielding constant.

For systems of the type studies here σ_W is found to be small, not exceeding 0.002 ppm and can be considered negligible[56] when compared to the accuracy of the shift measurements. For those systems investigated in this work the σ_W contribution will thus be considered negligible.

2.A.9.g REACTION FIELD OR ELECTRIC FIELD SCREENING σ_E

In the general case of an X-H bond in solute that does not possess spherical symmetry, if the electric field E is at an angle to the X-H bond it will destroy the axial symmetry of the bond leading to a low field shift proportional to E^2. If E is along the bond direction it will draw electrons away from the proton, thus decreasing the shielding. The total magnitude of the electrical effect has been given by[33]

$$\sigma_E = 2 \times 10^{-5} - 2 \times 10^{-12} E_z - 10^{-18} E^2 \qquad (2.52)$$

where E_z is the component of E along the axis of X-H bond.

A polar molecule, when present in solution, can polarise the surrounding medium and give rise to an electric field, the reaction field (R) at the solute nuclei. Using the Onsager model[57] Buckingham[58] has developed a theory for the effect of R on the chemical shifts. In this model the solute molecule is regarded as a sphere of radius r with a point dipole μ (of the gas phase) at the centre, and the solvent is considered as a continuous medium of dielectric constant ε. R is then given by

$$R = \frac{2(\varepsilon - 1)}{(2\varepsilon + 1)} \cdot \frac{m}{r^3} \qquad (2.53)$$

$$= \frac{2(\varepsilon - 1)(n^2 + 1)}{3(2\varepsilon + n^2)a} \cdot \mu \qquad (2.54)$$

where $m = \mu + aE$, the total dipole moment of the solute in the medium; a is the polarisability of the sphere and is equal to $\frac{n^2 - 1}{n^2 + 2} \cdot r^3$,

and n is refractive index of the pure solute. The value obtained for R may be used in (2.52), vice E, to deduce the reaction field screening effect.

For non-spherical molecules an equation has been derived[59] for R whereby the polarisable dipole is considered to be at the centre of an ellipsoidal cavity, which can be represented by

$$R = \frac{3\mu}{abc} \cdot \xi_a \left[1 + (n^2-1)\xi_a\right] \left[\frac{(\varepsilon - 1)}{\varepsilon + \frac{n^2 \xi_a}{1 - \xi_a}}\right] \cdot \quad (2.55)$$

where a,b,c are the axes of the solute ellipsoid and ξ_a is a shape factor for the solute which can be determined[60]. It has been shown that in case of certain three component systems of the type studied here that the shieldings of the solute due to aromatic and cyclohexane differ slightly and no correction for σ_E is necessary for the observed shifts.[22]

2.A.9.h BULK MAGNETIC SUSCEPTIBILITY TERM σ_b

This arises if the geometry of the sample differs from that of the hypothetical spherical cavity occupied by a molecule within the sample. The molecule is considered to be in a diamagnetic medium and is enclosed within a sphere, small in dimensions compared with the size of the sample, but large when compared with the molecular dimensions. When the sample is placed in a uniform magnetic field B_o, the medium will be polarised and the effective field experienced by a nucleus at the centre of the sphere will depend upon

(a) the external field B_o

(b) the field due to induced magnetism in the inner sphere

(c) the field due to the induced magnetism in the region between the small sphere and the sample boundary.

The medium outside the sphere can be regarded as continuous with a volume diamagnetic susceptibility X_v, so that the effective field at the nucleus can be given by [61]

$$B_{eff} = B_o \left[1 + \left(\frac{4\pi}{3} - a \right) X_v \right] \qquad (2.56)$$

where a is a shape factor which is $4\pi/3$ for a sphere and 2π for a cylinder with length large compared with its own radius. Since cylindrical tubes are usually employed for most high resolution measurements, the diamagnetic susceptibility of the medium contributes $(\frac{2\pi}{3})X_v$ to the observed shielding constant when B_o is transverse to the tube. Hence

$$\sigma_{obs} = \sigma_{mol} + \frac{2\pi}{3} X_v \qquad (2.57)$$

The observed chemical shift of a sample S relative to a reference R, δ_{obs}^{S-R}, is related to the corrected chemical shift for the difference in susceptibility, δ_{corr}^{S-R}, by

$$\delta_{corr}^{S-R} = \delta_{obs}^{S-R} + \frac{2\pi}{3} (X_v^R - X_v^S) \qquad (2.58)$$

where X_v^R is the volume susceptibility of reference compound and X_v^S that of the sample. If an internal reference compound is used all nuclei will be equally influenced by the bulk susceptibility of the solution. In such cases, which is employed in the present investigations, σ_b can be neglected.

2.A.9.i SOLVENT ANISOTROPY EFFECTS σ_a

This effect arises from the presence of solvent molecules, exhibiting anisotropy in their magnetic susceptibility, within the sample. It is

predominant when a solute molecule adopts a preferential orientation with respect to the solvent molecule by reason of steric or other specific interactions. The effect is used to explain the large difference between solute chemical shifts observed in aromatic and non-aromatic solvents. These shifts may be explained qualitatively in terms of the large diamagnetic anisotropy of an aromatic molecule, arising from the circulation of the aromatic π-electrons (ring current effect[51]). The distribution of solvent molecules surrounding a solute molecule may be non-random at small distances because of the latter's presence which may result in a time-averaged non-zero susceptibility tensor, leading to screening at the nucleus of the solute molecule[52,62].

Abraham[63] has deducedthe total anisotropic effect of one anisotropic molecule upon a proton in its vicinity as

$$\sigma_a = -10^{30} \cdot \frac{2}{3}\Delta X \cdot \frac{(r - h)}{(r + 2h)(r^2 + h^2)^{3/2}} \qquad (2.59)$$

where the anisotropic molecule is considered to be a cylinder of radius r (Å) and height $2h$ (Å), and ΔX is the difference in magnetic suscpetibilities parallel and perpendicular to the cylinder axis of the anisotropic molecule. An extension of (2.61) has been made by Homer[64] et al and good results are obtained.

2.A.9.j SPECIFIC ASSOCIATION TERM σ_c

Any type of specific interactions between solute and solvent, or between two different solutes in the same solution, will cause changes in their chemical shifts. The shifts due to ansiotropy effects associated with specific interactions are sometimes included in this term. Whilst all bonding interactions can contribute to this effect there are interactions between solute and solvent, giving rise to σ_c, which are generally

referred to as forming "collision complex." This term is meant to imply a short-lived specific orientation of the solute and solvent molecules brought about by weak (any type of) interactions. The term σ_c is the main interest in the present investigation and will be discussed in greater detail at a later stage.

The discussion so far in this section (section A) has been restricted only to various theoretical aspects of n.m.r. spectroscopy, which will be employed in chapter five. The next section (section B) is devoted to the theory of dipole moments.

SECTION B

THEORETICAL ASPECTS OF THE DETERMINATIONS OF DIPOLE MOMENTS

2.B.1 INTRODUCTION

The molecules of a dipolar substance will normally, depending on their relative orientations, exert forces of attraction and repulsion upon one another. Generally the configuration in which attraction is greatest will be favoured. Thus, in the presence of an inert solvent, the polar solute molecules in the solution tend to associate rather than existing separately. The degree of association will be governed largely by the shape of the molecular species under consideration and the magnitude of its dipole moment (section 1-3). Moreover, when an "active" solvent is present, the interaction between solute and solvent molecule has to be taken into account. If the focus is only on the latter interaction, which is the purpose of the present investigation, then the effect of solute self-associations can be largely reduced by employing dilute solutions of solute in the active solvent.

The present section will be devoted to the discussion of the general principles involved in the determination of dipole moments which will be employed later on in chapter 6. It has to be pointed out here that currently SI units are generally accepted, thus all the calculations being made later on in this thesis will be carried out in accordance with this system. However, for simplicity the equations referred to in this section are expressed such that their original classical well known forms and meanings are still maintained (c.g.s unit). To rationalise the matter, table 2.1 shows the relation between both units for the relevant parameters and how

TABLE 2.1 THE RELATIONSHIP BETWEEN SI AND c.g.s. UNITS OF VARIOUS PHYSICAL AND CHEMICAL QUANTITIES EMPLOYED IN THE PRESENT INVESTIGATION[65,66]

Quantity	SI symbol	Name of SI symbol	Symbol of SI unit	c.g.s. symbol	c.g.s. unit	Conversion factor from c.g.s. to SI unit
electric charge	Q	Coulomb	C	Q	esu	3.335×10^{-10}
electric potential	V	Volt	V	V	erg esu^{-1}	299.8
capacitance	C	Farad	F	C	$esu^2 erg^{-1}$	1.112×10^{-12}
Relative permittivity (dielectric constant)	ϵ_r	-	-	ϵ	dimensionless factor	1
electric field strength	E	Volt per metre	Vm^{-1}	E	dyne esu^{-1}	2.998×10^4
electric dipole moment	p_e	Coulomb metre	Cm	μ	esu cm Debye	3.335×10^{-12} 3.335×10^{-30}
mass	m	Kilogramme	kg	m	g	10^{-3}
density	ρ	Kilogramme per cubic metre	kgm^{-3}	ρ(or d)	g cm^{-3}	10^3
refractive index	n	-	-	n	dimensionless factor	1
molar refraction	R_m	cubic metre per mole	$m^3 mol^{-1}$	R	$cm^3 mol^{-1}$	10^{-6}
molar polarisation	P_m	cubic metre per mole	$m^3 mol^{-1}$	P_m	$cm^3 mol^{-1}$	10^{-6}
molec polarisability ular	α	cubic metre	m^3	α	cm^3	10^{-6}
amount of substance	n	mole	mol	n	mol	1
mole fractions	x	-	-	x	dimensionless quantity	1
volume	V	cubic metre	m^3	V	cm^3	10^{-6}
molar volume	V_m	cubic metre per mole	$m^3 mol^{-1}$	V_m	$cm^3 mol^{-1}$	10^{-6}
specific volume	v	cubic metre per kilogramme	$m^3 kg^{-1}$	v	$cm^3 g^{-1}$	10^{-3}

to convert a required quantity from one into another unit.

2.B.2 DEFINITION OF DIELECTRIC CONSTANT

If one considers a parallel-plate condenser, with plates of large area separated by a small gap, placed in a vacuum and a potential difference V is applied across the plates, so that the charge distributions between the two plates are +Q and -Q respectively, the capacitance is given as[67]

$$C_o = Q/V \qquad (2.60)$$

If the space between the plates is now filled with some isotropic non-polar material, of which the charge distribution in molecules is normally symmetrical, the charges on the plates will polarise the molecules, attracting the positive charges to one end and the negative charges to the other, with the result that charges -R, +R appear on the surfaces of the material. The condenser now holds a charge (Q + R) at an applied potential difference V, and the capacitance is increased to

$$C = (Q + R)/V \qquad (2.61)$$

The dielectric constant of the material can be defined as

$$\varepsilon = C/C_o = \frac{(Q + R)}{Q} \qquad (2.62)$$

and it is evidently dimensionless.

2.B.3 THE CLAUSIUS-MOSOTTI EQUATION AND MOLAR POLARISATION

The majority of methods employed in the determination of dipole moments are based originally upon a relation first proposed by Clausius and Mosotti, which is generally referred to as the Clausius-Mosotti equation. Since the methods described later on in this section also adopt the relation

mentioned above, it is of importance to describe the equation in more detail.

Considering the same condenser as described in the previous section, with electric charges +Q and -Q on the plates respectively, and let the corresponding surface charge densities be represented by $+\sigma$ and $-\sigma$. In the presence of vacuum between the plates, the strength of a uniform electric field produced by two charged plates is given by [68]

$$E_o = 4\pi\sigma \qquad (2.63)$$

When the space between the plates is filled with a nonpolar medium of dielectric constant ε, this field induces dipoles within molecules of the medium such that there exists a secondary field, produced by the dipoles acting in opposite direction to E_o, and the resultant field strength is reduced to [68]

$$E = \frac{4\pi\sigma}{\varepsilon} \qquad (2.64)$$

The decrease in field strength is thus

$$E_o - E = 4\pi\sigma\left(1 - \frac{1}{\varepsilon}\right) = 4\pi\sigma\left(\frac{\varepsilon - 1}{\varepsilon}\right) \qquad (2.65)$$

which is considered to be the same as reducing the surface charge density by the amount of $\sigma\left(\frac{\varepsilon-1}{\varepsilon}\right)$. This quantity is referred to as the electric polarisation (P) of the dielectric medium and is produced by the shift of charges throughout the medium.

The displacement of charges, if the surface area of the medium is A, results in the presence of charges +PA on one surface of the medium and -PA on the other surface and thus gives rise to an electric moment of PAr in the medium, where r is the distance between the plates of the condenser. Since Ar = V, the volume of the medium, it follows that

$$\text{total electric moment} = PV \qquad (2.66)$$

i.e. P is the electric dipole moment per unit volume of the medium.

From (2.65) it is evident that

$$E_o - E = 4\pi P \qquad (2.67)$$

or, from (2.63) and (2.64)

$$(\varepsilon - 1)E = 4\pi P \qquad (2.68)$$

The above discussion applies for the whole medium. If, for a single molecule in the medium, the actual field acting upon it is F and m is the electric moment of the induced dipole produced by the field, then

$$m = \alpha F \qquad (2.69)$$

where α is the molecular polarisability and is a measure of the ability of which the molecule can be polarised. It is a constant, characteristic of the substance and may have different values in different directions in a geometrically anisotropic substance; in such case α represents the mean value. The field F is conveniently considered by assuming a unit charge enclosed by a small sphere which is large when compared to molecular dimensions, but small compared to the distance between the plates. In this case F consists of several components as follows:[69]

(a) the field due to the charges on the plates, i.e. $E_o = 4\pi\sigma$

(b) the field arising from the charges induced on the surfaces of the medium acting in opposite direction to E_o which is $-4\pi P$

(c) the field due to the charge induced on the surface of the sphere and is $\frac{4}{3}\pi P$

(d) the field caused by molecules within the sphere. For a liquid (as an approximation) or gas, in which molecules are oriented at random in the absence of an external field, this contribution is zero.

It is thus evident that

$$F = 4\pi\sigma + \frac{4}{3}\pi P - 4\pi P \qquad (2,70)$$

and, from (2.67), this leads to

$$F = E + \frac{4}{3}\pi P \qquad (2.71)$$

If n is the number of molecules per unit volume, then from the definition of P

$$P = nm = n\alpha F = n\alpha(E + \frac{4}{3}\pi P) \qquad (2.72)$$

Combination of (2.68) and (2.72) leads to

$$\frac{(\varepsilon - 1)}{(\varepsilon + 2)} = \frac{4\pi n\alpha}{3} \qquad (2.73)$$

For a pure substance

$$n = N_A P/M \qquad (2.74)$$

where N_A is the Avo gadro constant, ρ and M are the density and molecular weight of the substance respectively. Substitution of (2.74) into (2.73) leads finally to

$$\frac{(\varepsilon - 1)}{(\varepsilon + 2)} \times \frac{M}{\rho} = \frac{4}{3}\pi N_A \alpha = P_m \qquad (2.75)$$

where P_m is the molar polarisation of the substance and (2.75) is called the Clausius-Mosotti equation.

It is found in many cases that P_m obtained from (2.75) is independent of temperature, provided the substance is nonpolar. Maxwell[70] has derived a relation for such substance in the form of

$$\varepsilon = n_\infty^2 \qquad (2.76)$$

where n_∞ is the refractive index of the substance for light of long wavelength (infrared). Thus from (2.75), the Lorentz-Lorenz expression[84]

$$\frac{(n_\infty^2 - 1)}{(n_\infty^2 + 2)} = \frac{4}{3}\pi N_A \alpha = P_m = R \qquad (2.77)$$

can be derived, with R as the molar refraction.

When the molecules are polarised by the fields discussed above , the whole molecular structure will be distorted and for a nonpolar molecule the distortion arises from two effects which are

(a) displacement of the electrons relative to the nucleus in each atom and is represented by the electronic polarisability α_E

(b) displacement of the atomic nuclei relative to one another or atomic polarisability α_A

The total molecular polarisability can then be written as

$$\alpha = \alpha_E + \alpha_A = \alpha_D \tag{2.78}$$

where α_D is called the distortion polarisability. Therefore it can be seen from (2.75) that

$$P_m = P_D = P_E + P_A = \frac{4}{3}\pi N_A \alpha \tag{2.79}$$

where P_D, P_E and P_A are the distortion, electronic and atomic polarisation respectively.

If a polar substance is placed in the condenser, there will be a third contribution to the polarisability, provided the permanent dipoles of the substance are free to orientate. In the absence of an electric field, the dipoles in the molecules are distributed randomly in all directions. Whenever an electric field is applied, the dipoles tend to align themselves parallel to it, but the departure from the random arrangement is small in fields of intensity normally employed in the measurement. This orientation polarisability, α_o, contributes to α so that a polar substance usually has higher α , and hence ε , than a nonpolar compound.

In other words for polar molecules

$$\alpha = \alpha_A + \alpha_E + \alpha_o = \alpha_D + \alpha_o$$

and $$P_m = P_A + P_E + P_o = P_D + P_o = \frac{4}{3}\pi N_A \alpha_D + P_o \qquad (2.80)$$

where P_o is the orientation polarisation.

2.B.4 THE GENERAL METHODS FOR THE DETERMINATION OF DIPOLE MOMENTS

According to the Clausius-Mosotti equation, P_m is found to be temperature independent. However, when molecules possess permenent dipole moments, the orientation of dipoles in the field gives rise to P_o which is a function of temperature and P_m becomes temperature dependent. It is found that [71]

$$\alpha_o = \frac{\mu^2}{3kT} \qquad (2.81)$$

and thus from (2.75)

$$P_o = \frac{4}{3}\pi N_A \alpha_o = \frac{4}{9}\pi \frac{N_A \mu^2}{kT} \qquad (2.82)$$

where k is the Boltzmann's constant and T the absolute temperature. Substitution of (2.82) into (2.80) leads to

$$\frac{(\varepsilon - 1)}{(\varepsilon + 2)} \cdot \frac{M}{\rho} = P_m = \frac{4}{3}\pi N_A \alpha_D + \frac{4}{9}\pi N_A \frac{\mu^2}{Kt} = \frac{4}{3}\pi N_A \left(\alpha_D + \frac{\mu^2}{3kT}\right) \qquad (2.83)$$

which is called the Debye equation [71]. It is based upon a supposition that the only restriction upon the rotation of polar molecules in an electric field is caused by that field. The equation can be applied to both polar and nonpolar molecules, whereby in the latter case μ is zero and (2.83) reduces to (2.75).

The discussion so far has dealt with systems of gases and vapours. In the case of solutions, upon which the work in the present investigation is focussed, the general methods of determining μ of a polar substance in solutions will be those in which the solutions are made up from small concentrations of the substance (solute) in a solvent. In this situation the dissolved solute molecules are so far apart from each other that the only interaction of importance within solutions is that between the solute and the surrounding solvent molecules. There are a few procedures commonly employed for processing the data to obtain μ and these will now be discussed in turn.

If α_1, and α_2 represent the molecular polarisabilities of the solvent and solute respectively and n_1 and n_2 are the corresponding number of molecules present, then from (2.75)[68]

$$\frac{\varepsilon - 1}{\varepsilon + 2} \times \frac{M}{\rho} = \frac{4\pi}{3} (n_1 \alpha_1 + n_2 \alpha_2) \qquad (2.84)$$

The corresponding mole fractions are

$$x_1 = \frac{n_1}{n_1 + n_2} \qquad x_2 = \frac{n_2}{n_1 + n_2} \qquad (2.85)$$

and the molar polarisations are given by

$$P_1 = \frac{4}{3} \pi N_A \alpha_1 \qquad P_2 = \frac{4}{3} \pi N_A \alpha_2 \qquad (2.86)$$

Substitution of (2.85) and (2.86) into (2.84) leads to

$$\frac{(\varepsilon_{12} - 1)}{(\varepsilon_{12} + 2)} \times \frac{M_1 x_1 + M_2 x_2}{\rho_{12}} = P_1 x_1 + P_2 x_2 = P_{12} \qquad (2.82)$$

where M_1 and M_2 are the molecular weights of the solvent and solute respectively, P_{12} the molar polarisation of the mixture and ρ_{12} and ε_{12} are the corresponding density and dielectric constant. The first

procedure employed is to deduce P_1 and P_{12} values[72] from measurements of the dielectric constants and densities of the pure solvent and dilute solutions respectively, and these values are then used in (2.87) to obtain P_2 for each solution. These P_2 values depend upon the concentrations of the solutions and are found to increase as x_2 decreases. By employing this behaviour of P_2, a plot of P_2 against x_2 can be made for a series of solutions and the resultant curve is extrapolated to infinite dilution of solute to obtain the solute polarisation, P_∞, at which the effect arising from the interaction between solute permanent dipoles is approximately eliminated. P_∞ is therefore the molar polarisation of a single solute molecule completely surrounded by solvent molecules and is, according to (2.83), equal to[72]

$$P_\infty = P_{2D} + P_{20} = P_{2D} + \frac{4}{9}\pi N_A \frac{\mu^2}{kT} \qquad (2.88)$$

in which

$$P_{2D} = \frac{(n_2^2 - 1)}{(n_2^2 + 2)} \times \frac{M_2}{\rho_2} \quad = \text{molar refraction} \qquad (2.89)$$

where n_2 and ρ_2 are the refractive index and density of the solute respectively and P_{2D} and P_{20} are the corresponding distortion and orientation polarisation. Since P_{2D} and P_∞ are determined from the above relations, P_{20} and thus μ of the solute molecule can be calculated. However, the procedure is approximate because it does not take into account the fact that P_1, previously assumed to be constant over a range of concentration, is also dependent upon the concentration of solution owing to the solvent effect (section 2.B.5).

It is found in some cases that μ of the solute obtained from the above procedure is subjected to some experimental errors arising from the uncertainty in the extrapolation of the curve (between P_2 and x_2), which

is generally not a straight line, to obtain P_∞ . As a direct consequence of this uncertainty, an alternative procedure for the determination of μ by employing direct extrapolations[73] of dielectric constants and densities has been applied, since it is found in most cases that ε_{12} and the specific volumes $v_{12} = 1/\rho_{12}$ are linear functions[73,74,75] of the weight fractions of the solute (w_2). In other words they can be written as

$$\varepsilon_{12} = \varepsilon_1 + \alpha w_2 \qquad v_{12} = v_1 + \beta w_2 \qquad (2.90)$$

where ε_1 and v_1 are the dielectric constant and specific volume of the solvent and α and β are the slopes of the straight lines obtained by plotting ε_{12} and v_{12} against w_2 respectively. The values of α and β obtained from the plots are then used in the equation[73]

$$P_\infty = \frac{3\alpha v_1 M_2}{(\varepsilon_1 + 2)^2} + M_2(v_1 + \beta)\frac{(\varepsilon_1 + 1)}{(\varepsilon_1 + 2)} \qquad (2.91)$$

to obtain P_∞ , which is then employed in the calculation of μ in the same way as the above procedure. One certain condition has to be adopted in this procedure, that is, whenever the plots of ε_{12} and v_{12} against w_2 do not show linearity throughout the range of concentration studied, the procedure will be abandoned or applied only to the range which conforms to a linear relation.

The above two procedures lead to similar results and also depend on the accurate measurements of solution densities, according to (2.87) and (2.91), which is found to be difficult normally. It is this difficulty that leads to a third procedure proposed by Guggenheim and can be described as follows.

Guggenheim's procedure[76], although including the density of pure solvent

(ρ_1) in the calculation, only requires an accuracy of 0.1% in the measurement of ρ_1. The procedure is based upon the Debye equation and employs a relation given as

$$P_o = \frac{4}{9}\pi N_A \frac{\mu^2}{kT} = \frac{3M_2}{\rho_1(\varepsilon_1+2)^2} \times \lim_{w_2 \to o} \left(\frac{\partial \varepsilon_{12}}{\partial w_2} - \frac{\partial (n_D)^2_{12}}{\partial w_2}\right) \quad (2.92)$$

By plotting ε_{12} against w_2 one would obtain a curve which fits the expression

$$\varepsilon_{12} = \varepsilon_1 + aw_2 + a'w_2^2 \quad (2.93)$$

with a limiting slope of the curve at $w_2 = o$ of

$$\frac{\partial \varepsilon_{12}}{\partial w_2} = a \quad (2.94)$$

Similarly a plot of $(n_D)^2_{12}$ versus w_2 gives a curve to fit the expression

$$(n_D)^2_{12} = (n_D)^2_1 + vw_2 + v'w_2^2 \quad (2.95)$$

and the slope at $w_2 = o$ is

$$\frac{\partial (n_D)^2_{12}}{\partial w_2} = v \quad (2.96)$$

where $(n_D)_{12}$ and $(n_D)_1$ are the refractive indices of the solution and pure solvent respectively. Substitution of (2.94) and (2.96) into (2.92) gives

$$\mu^2 = \frac{10^{36}}{N_A} \times \frac{27kTM_2}{4\pi\rho_1(\varepsilon_1+2)^2} \times (a - v) \quad (2.97)$$

from which μ of the solute can be calculated. The method also employs

an alternative procedure which is based upon an equation

$$D = \frac{\varepsilon_{12} - 1}{\varepsilon_{12} + 2} - \frac{(n_D)^2_{12} - 1}{(n_D)^2_{12} + 2} = \frac{\varepsilon_1 - 1}{\varepsilon_1 + 2} - \frac{(n_D)^2_1 - 1}{(n_D)^2_1 + 2} + \frac{P_o w_2 \rho_1}{M_2} \quad (2.98)$$

Thus if D is plotted against w_2, the slope of the curve is given by

$$S = \frac{P_o \rho_1}{M_2} \quad (2.99)$$

which, from (2.92), it is evident that

$$\mu^2 = \frac{10^{36} S}{N_A} \times \frac{9kTM_2}{4\pi\rho_1} \quad (2.100)$$

It is these two procedures, due to Guggenheim, which are employed in the present investigation to determine the dipole moments of polar solutes in dilute solutions with various non-polar solvents.

2.B.5 THE SOLVENT EFFECTS

It was found[77] that electric moments of solutes obtained from measurements in solutions are liable to vary with the nature of solvents used and can deviate from the true moments found in the gasous state. The behaviour was explained in terms of

(a) the forces which the solute exert upon one another, i.e. the association. This effect is large for solutes with large dipole moments and will depend on the chemical structure and the "position" of dipoles in the molecules.

(b) The effects of the non-polar solvent on the molecules of the polar solute.

The values of solution moments in such cases were calculated from the polarisation values P_∞ , obtained from extrapolation, to infinite dilution (whereby effect (a) can be neglected) of the solute polarisations in the same way as described in the previous section. Any difference observed between the apparent moment, or solution moment, and the moment of solute molecule in the vapour state is then referred to as the solvent effect.

Attempts have been made to explain and calculate the size and magnitude of the solvent effect. When the anisotropy of a molecule was taken into account[78] in order to calculate the inductive effects of polar solute molecules upon the non-polar solvent molecules, it was found that the effects obtained are of the same magnitude as the observed solvent effects. Higasi[79] treated the solvent as a medium of polarisability α , containing n molecules per unit volume, and located the dipole at the centre of the system. The induced moments obtained are in good agreement with the observed values. Frank[80] has successfully explained the effect in terms of another structure. A spherical solute molecule with a dipole at the centre is assumed to be surrounded symmetrically by six spherical solvent molecules of polarisability α , so that the solute molecule is at the centre of a regular octahedron. These solvent molecules are considered to be at distance r from the solute and making an angle θ with the dipole axis of the solute molecule. Therefore, the field produced by the solute at the solvent molecules in the direction of the solute dipole axis will be

$$E = \frac{\mu}{r^3} (3 \cos^2\theta - 1) \qquad (2.101)$$

where μ is the solute permanent moment. For two solvent molecules locating at both ends of the symmetry axis containing the dipole, θ is 0 and π radians respectively and the induced moment, m, in each molecule is

$$m = E\alpha = \frac{\mu}{r^3}(3\cos^2\theta - 1)\alpha = \frac{2\alpha\mu}{r^3} \qquad (2.102)$$

In the case of four other solvent molecules in the plane perpendicular to the dipole axis, $\theta = \pi/2$ radians and m in each case is

$$m = -\frac{\alpha\mu}{r^3} \qquad (2.103)$$

i.e. m in this case will be acting in the direction opposite to the solute permanent moment. It can be seen from (2.102) and (2.103) that the total sum of induced moments is zero, in other words, the solvent effect for a spherical solute molecule with a dipole at the centre should be zero. If the solute molecule is elongated so that the two solvent molecules in the line of the dipole axis are farther from the dipole, r is increased and the induced moments of these two solvent molecules are decreased and become smaller than the sum of the opposing moments produced in the other four molecules, therefore the resultant m is negative, giving a negative solvent effect. If the dipolar axis is shortened, r will be decreased and the induced solvent moments in the direction of the solute dipole axis is increased, giving a positive solvent effect. In most cases the dipoles tend to lie more nearly in the direction of the longest molecular axis than perpendicular to it, therefore the solution moments in most cases are usually lower than the gas moments.

It is also found[81] that the shape of the solvent molecule, apart from that of the solute molecule, also plays some part in the magnitude and size of solvent effects.

2.B.6 THE EFFECTS OF MOLECULAR INTERACTIONS ON DIPOLE MOMENTS

Evidence of a weak interaction between solute and solvent molecules can

sometimes be obtained from the studies of dipole moments in solutions. The presence of molecular complexes results in changes of the apparent moments of a solute measured in solutions, either by an increase or a decrease when compared with the solute moments in the vapour state. The increase in solution moments when, compared with gas moments, of some solutes has been described in terms of[82] association between solute and solvent giving rise to a polar complex, or that the interaction causes the atomic polarisation of the dissolved solute to be greater than that in the gaseous state, producing an increase in μ. However, studies on dilute solutions provide an effective way of studying the interactions since the effect of solute self-association can be discounted.

One of the most useful methods of determining μ induced from molecular interactions (μ_{ind}) is to study μ of a solute in an inert solvent, and then in an interacting solvent. The difference

$$\mu_{ind} = \mu_{sol} - \mu_{inert} \qquad (2.104)$$

where μ_{inert} and μ_{sol} are of the solute in the inert and interacting solvents respectively, can be used in the interpretation of the results. The method has been employed to study the interactions between various amines and carbon tetrachloride[89] in which the result was discussed in terms of charge-transfer interactions whereby the latter compound acts as an electron acceptor, and that the interaction increases the total polarisation of the system, partly by increasing the atomic polarisation of the interacting molecules and partly by a change in dipole moment.

Frank[80] has derived an equation to calculate the distance of the solute dipole centre from the solvent molecule in the formation of a molecular complex, employing μ_{ind} obtained from experimental studies. The method

was applied successfully by Huck[22] for the interactions between polar solutes and various aromatics.

The present investigation on dipole moments involves studies of polar solutes in cyclohexane and various methyl substituted benzenes, acting as inert and interacting solvents respectively, to determine μ_{ind} for each system. These are then used to study the nature of the interactions. It is expected that the results obtained, together with those from n.m.r. studies, will provide a better understanding of the molecular complexes formed in the systems studied. The experimental results on dipole moment studies will be discussed later on in chapter 6.

SECTION C

CRYOSCOPY

2.C.1 DEFINITION OF THE PHASE RULE

The phase rule first stated by Gibbs relates the number of phases, the number of components, and the number of degrees of freedom, or the variance, of a system in heterogeneous equilibrium, in which it is assumed that the only determinable variables are temperature, pressure and composition. It deals with heterogeneous equilibria involved in processes classified either as physical or as chemical, so long as they are reversible in nature. The rule may be stated as follows:[83]
A system, consisting of C components, can exist in C + 2 phases only when the temperature, total pressure of the system, and concentration of each phase have fixed and definite values. If there are C components in C + 1 phases, only one of the factors may be artitrarily fixed, and if there are only C phases, two of the varying factors may be arbitrarily fixed. The rule can be described in terms of the equation.

$$F = C - P + 2 \qquad (2.105)$$

where F is the variance or number of degrees of freedom of the system, C is the number of components and P is the number of phases. It can be seen from the equation that when P increases, the system condition becomes more defined, or less variable.

It is of importance to discuss briefly each term in (2.105) in order to clarify their limitations.

2.C.2 THE PHASES

A heterogeneous system is made up of different portions, each of which is homogeneous but marked off in space and separated from the other portions by bounding surfaces. These portions are called phases. A phase may also be defined as one of the uniform, homogeneous, mechanically separable portions of a system in dynamic, heterogeneous equilibrium.

The number of phases which can exist together will vary in different systems, but with an exception that there can only be one gas or vapour phase since gases are miscible with one another in all proportions. The number of phases formed by any given substance or group of substances generally increases with the number of participating substances.

2.C.3 THE ORDER OR THE NUMBER OF COMPONENTS

The number of components of a system at equilibrium is generally represented by the smallest number of constituents required to define either directly, or in the form of a chemical equation, the composition of each phase taking part in the equilibrium. The components have to be chosen from among the constituents which are present when the system is in a state of true equilibrium and also taking part in the equilibrium themselves. Each component itself may consist of a number of different species, for example in the case of a liquid- gas equilibrium of a system

$$2\,H_2O \rightleftharpoons 2H_2 + O_2 \qquad (2.106)$$

where the system contains a single component. The constituents of water are not regarded as components since they are not present in the system in a state of real equilibrium, and also they are combined in definite proportions to form water, therefore their amounts cannot be

varied independently. For any given system the number of components will be definite, but it may alter when the conditions imposed upon the system are changed.

2.C.4 THE VARIANCE OR NUMBER OF DEGREES OF FREEDOM

The number of degrees of freedom of a system is the number of variable factors such as temperature, pressure and composition, which must be arbitrarily fixed in order that the condition of the system at a particular equilibrium may be completely defined. In a one-component system the only variables governing the system are temperature and pressure, since the single component can only exist as pure substance, no composition variable is required. For a two-component (binary) system all three variables are operative and if one of the variables, for example. pressure, is kept constant, the condition of which is employed in the present investigation, then the temperature will vary according to the compositon of the system at equilibrium.

The discussion so far can be applied generally. Because of the nature of systems of interest in the present study, the focus from the next section on will be upon the behaviour of binary systems. The main concern will be the cooling at constant pressure of solutions in which equilibrium exists only between solid and liquid phases, and the components of which are completely miscible in the liquid state, no matter what their compositions.

2.C.5 CLASSIFICATION OF A BINARY SYSTEM

When a binary system is subjected to a constant pressure, the only variables left to describe the behaviour of the system are temperature and

composition. It is then possible, under such circumstances, to vary the composition of each component within the system and at the same time study the temperatures at which the components, existing in various phases, are in equilibrium with one another. The most convenient time to detect these temperatures is when there are changes of phases and thus in this case the temperatures will depend on the types of phases being in equilibrium. For the present investigation in which the main interest is on equilibrium between solid and liquid phases, the temperatures are represented by the melting points (or freezing points) of the solutions. If a diagram is constructed from a plot of freezing points for a range of compositions, this will represent the equilibrium between various phases and therefore the behaviour of the system over the whole composition range. Such a diagram is called the phase diagram. A binary system can be classified according to its behaviour upon cooling as follows:

(a) A system in which the only solid phases are the pure components, i.e. no compound formation arising from the interactions between both components.

(b) A system in which a compound with a congruent freezing point is formed. The congruent freezing point represents the point at which the compound (solid phase) is in equilibrium and has the same composition as the two-component liquid phase (solution).

(c) A system in which a compound is formed with an incongruent freezing point. The incongruent freezing point, which is also called the peritectic (or meritectic) point, represents the temperature at which the solid form of the compound is in equilibrium with the solution and also with one of solid components and is below the true freezing point of the compound.

(d) A system in which solid solutions or mixed-crystals are formed.

Each particular system will now be discussed in more detail.

2.C.5.a SYSTEM WITHOUT COMPOUND FORMATION

The diagram representing the behaviour of this system is shown in fig. 2.3 If A and B represent the two components and L the liquid substance and the pure components occur as solid (crystalline) phases, the only systems existing in equilibrium are solid A-L, solid B-L and solid A-solid B-L.

The points A and B, on the diagram, represent the freezing points of the pure components. When a small amount of B is dissolved in liquid A, the freezing point of the solution will be below that of the pure A, and the lowering of the freezing point can be calculated from[84]

$$dT/dx_A = -RT^2/L_A x_A \qquad (2.107)$$

where x_A is the mole fraction of A, T is the freezing point of A on absolute scale, R is the gas constant and L_A is the latent heat of A. However, the expression only holds strictly in the case of ideal solutions.

When a liquid solution at the point E (with more A than B) is cooled down, as soon as the temperature of the solution reaches the point G, solid A will crystalise out. The crystallisation of A continues as long as the temperature is still falling, but at the same time the composition of the liquid will change towards the point C. At the point C, solid B starts to crystallise out, i.e. both solid A and B separate out together while the temperature remains constant. Since at this point the composition must remain constant, solid A and B will crystallise out in constant proportions from the solution. However, the solid, coming out

of the solution, will not be a compound but a mixture of two solid phases.

The curves AC and BC represent the compositions of the solution which, at various temperatures, are in equilibrium with solid A and B respectively. Both curves intersect at the point C, where both solid A and B can exist in equilibrium with a liquid solution of definite composition under constant pressure. The point C is called a eutectic point. According to the Clapeyron-Clausius equation[84]

$$\frac{dT}{dP} = T.\Delta V/L_T \qquad (2.108)$$

where L_T is the heat absorbed in the transition of one phase to another, ΔV is the volume change accompanying the transition, it follows that the eutectic temperature varies with the pressure. An equation relating the eutectic temperature, eutectic composition and pressure has been deduced by McKay and Higman[85] for ideal solutions.

At any temperature above the curves AC and BC, the system exists only as a homogeneous, liquid solution. In the same way, all temperatures below the line DD' will restrict the system to exist only as pure or mixtures of solid components. The areas ACD and BCD' represent equilibria in which solid A and B coexist with the solution respectively.

2.C.5.b SYSTEM WITH A CONGRUENT FREEZING-POINT COMPOUND

A congruent freezing-point compound is a stable compound, capable of existing as a solid compound in equilibrium with a liquid of the same composition. The freezing point of the compound will be represented by a maximum point on the equilibrium curve. The diagram showing the

behaviour of this system is represented by Fig. 2.4. The points A,B and D are at the freezing points of the component A, component B and compound A_xB_y respectively. The curves AC and BE represent the equilibria at different temperatures between the liquid solution and solid A, solid B respectively. The curve CDE shows the equilibrium between the solution and solid compound. The eutectic points C and E corresponds to the temperatures at which the solid mixtures of A + A_xB_y and B + A_xB_y coexist with solutions of definite composition. The behaviour upon cooling of the system will be similar to that in section 2.C.5.a.

The position of the point D will usually depend on the system, the nature and stoichiometry of the interaction between the two components present, which will be different for various systems. Therefore, it may lie higher, lower than or at an intermediate position comparing to those of the pure components. If more than one congruent freezing-point compound is formed, a series of curves similar to the curve CDE will be obtained[86]. The maximum point on each curve shows the composition and freezing point of each compound.

The shape of CDE can also show the stability of the compound formed. If CDE is a pronounced curve, the degree of dissociation of compound will be small, i.e. it will be more stable and if the curve is flat, the degree will be large.

2.C.5.c SYSTEM WITH AN INCONGRUENT FREEZING-POINT COMPOUND

In this system one, or more compounds is formed, which undergoes dissociation leading to the formation of another solid phase at a temperature below the congruent freezing point of the compound. The diagram for the system is shown in Fig. 2.5. In the diagram the continuation of

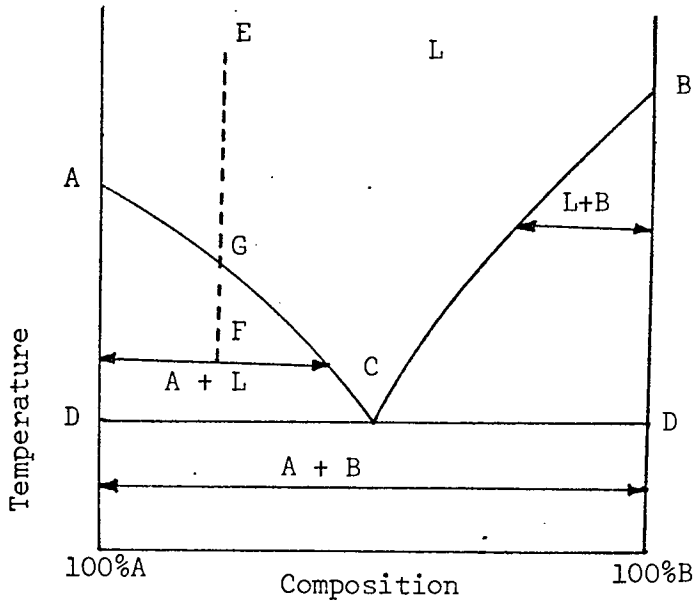

Fig. 2.3 SOLID-LIQUID PHASE DIAGRAM FOR A SYSTEM WITH NO COMPLEX FORMATION

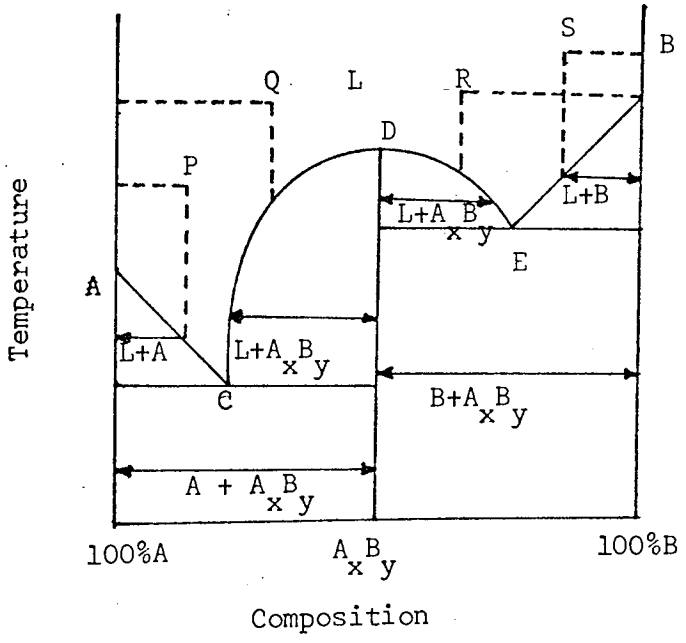

Fig. 2.4 SOLID-LIQUID PHASE DIAGRAM FOR A SYSTEM WITH THE FORMATION OF A COMPLEX WITH A CONGRUENT FREEZING POINT.

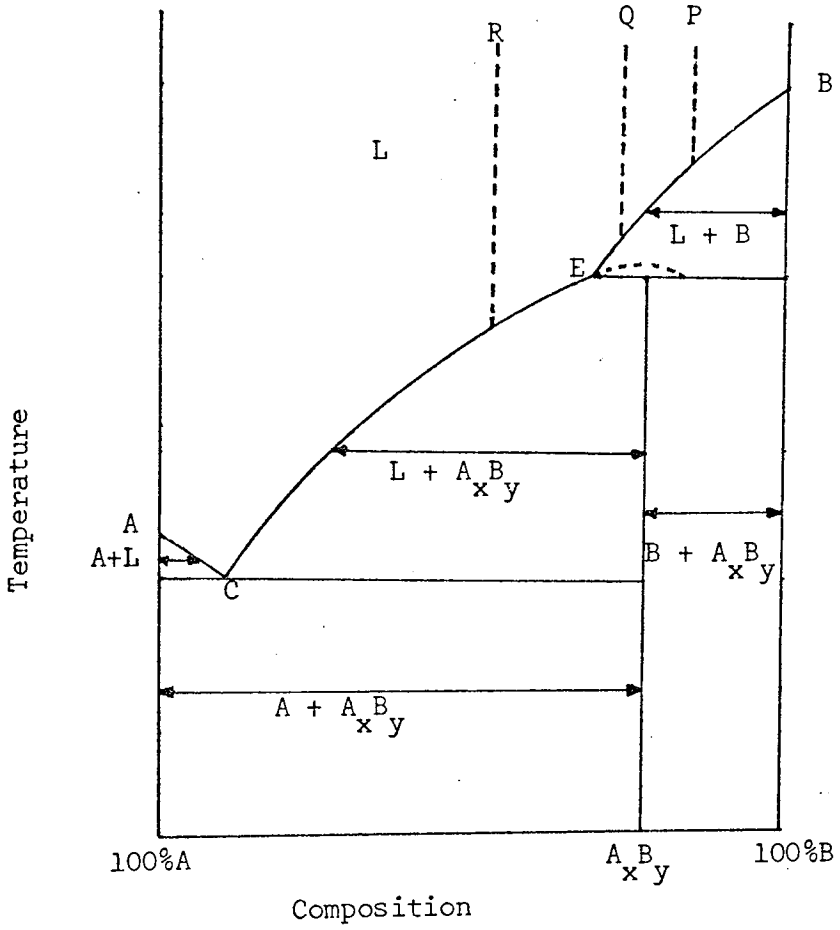

Fig. 2.5 SOLID-LIQUID PHASE DIAGRAM FOR A SYSTEM WITH THE FORMATION OF A COMPLEX WITH AN INCONGRUENT FREEZING POINT

behaviour of the phase curve for the compound is represented by the dotted line, of which the maximum will correspond to the congruent freezing point of the compound, i.e. if the compound did not dissociate previously at a temperature (point E). This maximum can be referred to as the concealed maximum. However, the solid compound in this case will dissociate into another solid phase at the point E before the congruent freezing point is reached. The solid phase obtained from the dissociation may be another compound, or a pure component, the latter case is represented in Fig. 2.5. Since the composition of the compound at this point is not the same as that being formed originally the point E is called an incongruent freezing point or peritectic point. If several incongruent freezing point compounds are formed in a system, then a series of curves will be obtained without any maximum and there will be only one eutectic point.

When a solution at point P which has the amount of B higher than that of the compound, is cooled down, its concentration at the beginning will not change until the temperature reaches curve BE, where solid B starts to separate and the temperature and composition moves along BE towards E. Whenever the condition at E is reached, the separated solid B will react with A in the original solution to form the compound. Since there is not enough A in the original solution to react with all the B present, the solidification results in the formation of a solid mixture of B and A_xB_y. The mixture at Q will behave similarly until it reaches point E, where now there is enough A in the original mixture to change all the separated B into the compound and the whole solid phase after solidification is that of A_xB_y. However, some liquid will still be left at E, therefore the solidification continues along curve EC, after a halt with constant temperature at E, with the further separation of the compound from solution. When the eutectic point C is reached, the separation of

solid A begins, leading to the complete solidification of the solution.

If the mixture at R is cooled down, the peritectic temperature will not be observed since the curve BE is not met. When the temperature reaches curve EC, the compound A_xB_y will be the first to solidify and the behaviour to the finish will follow the same pattern as previously described.

2.C.5.d SYSTEM WITH SOLID SOLUTIONS OR MIX-CRYSTALS

A solid solution is formed when a dissolved substance crystallises out together, in a miscible form, with the solvent. It may behave in some ways similar to a liquid mixture, i.e. if the components are completely miscible in the solid state an unbroken series of solid solutions is formed upon cooling, and if they are partially miscible a broken series will be observed. In the latter case the crystallised solids are that of solid solution and the individual components. Since both liquid and solid solutions are present in the system and the compositions in the two phases are not the same, the system thus possesses two curves, one relating to the liquid and the other to the solid phase. Systems possessing a behaviour of this kind, in general, will be those of inorganic salts and metals. These systems are not of interest in the present investigation and will not be discussed any further.

2.C.6 THE GENERAL METHOD FOR DETERMINING THE PHASE DIAGRAMS OF BINARY MIXTURES

There are several methods available which can be employed to determine the behaviour of any solution when the temperature is varied. The method that proves to be most useful and is employed in the present work will be

that of thermal analysis, which will now be discussed in detail.

In the thermal analysis method the sample is allowed to cool down (or warm up) usually with a constant surrounding temperature for the transfer of heat and a constant rate of temperature change or a constant rate of heat transfer. The freezing, or melting, point of the sample is then plotted against time, e.g. Fig 2.6, and if a series of samples with composition ranging from pure component A to B is conducted, then the phase diagram of the system can be constructed from the corresponding breaks and halts in the cooling or heating curve. No matter what the diagram is, each change in the equilibrium states will generally be accompanied by a break or a sudden change in the rate of cooling or heating. The invariant (eutectic and peritectic) state is represented by a halt or a period of constant temperature. For an ideal or a reference curve, it is assumed that complete equilibrium is retained at every point so that tha actual behaviour of the sample can be followed. However, in practice the equilibrium cannot be retained throughout the experiment, therefore supercooling at phase transitions may be observed. The degree of supercooling will be large if the rate of cooling or heating is increased, thus a slow rate is usually employed so that interpretation of the cooling (or heating) curve can be done more accurately.

If a binary liquid mixture of a simple system yielding pure solids only is cooled down, the rate of cooling will suddently change when a freezing point is reached because of the exothermal crystallisation of a solid. Fig. 2.6 represents the cooling curve for the system where the solid crystallises at the point b. The temperature at this break varies with the composition of the sample. Generally when there is no supercooling, the rate will proceed as the curve bc until it reaches the eutectic temperature at point c. When supercooling is present, no break will be observed

at c but the cooling will proceed to point f, where the solid starts to appear and the temperature of solution moves up along the dotted line to g. The rate of cooling then follows the curve gc. The temperature at c will be constant, and the duration of the halt, for a constant amount of sample, will depend upon the quantity of eutectic liquid present and is maximum if the sample contains the eutectic composition. At point d, where there is no more liquid, the temperature proceeds along de and the cooling is said to be complete.

If the system contains a compound with a congruent freezing point as in Fig. 2.4, the cooling curve will be the same as in Fig 2.6.

For a system with an incongruent freezing-point compound, as in Fig. 2.7, there will be two constant temperature halts on the cooling curve. The first halt (peritectic halt), represented by cd, corresponds to the point E in Fig 2.5, and the duration of the halt will be maximum when the composition of the solution is the same as that of the compound. The second halt, as before, corresponds to the eutectic halt. The dotted curve bhi represents the behaviour on cooling of the solution when there is supercooling.

When there is no supercooling, the freezing point of a solution can be determined directly as the temperature at the break of the cooling curve. In the presence of supercooling, it no longer can be done since the break is not at the real freezing point. A method of finding out the real freezing point in this case, which is also employed in this work, is to extrapolate the curves gc and ic, in Fig. 2.6 and 2.7 respectively, to their intersections with the line ab[32]. The point of intersection represents the real freezing point of the solution. In general the curves gc and ic will be concave downward, except for ideally pure substances, to

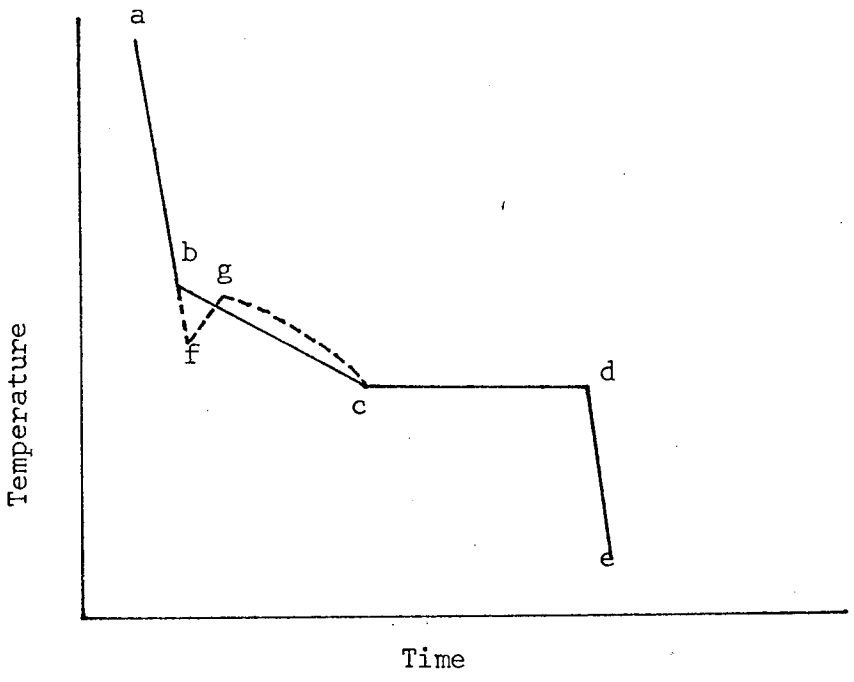

Fig. 2.6 COOLING CURVE OF A SYSTEM WITH NORMAL BEHAVIOUR

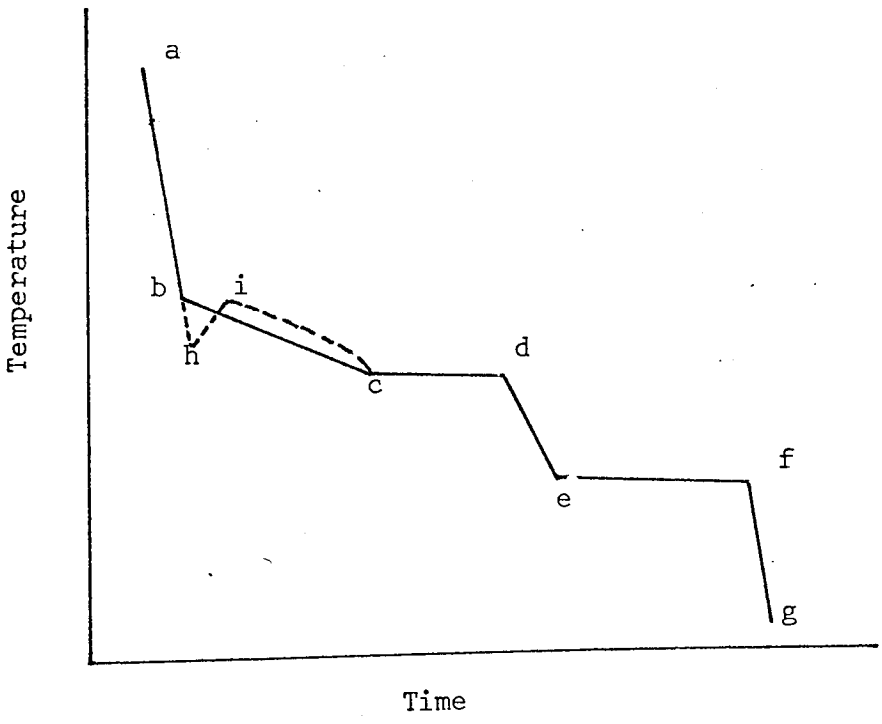

Fig. 2.7 COOLING CURVE FOR A SYSTEM WITH A PERITECTIC POINT

show that equilibrium does exist over these ranges.

Since the duration of both the peritectic and eutectic halts depends on the composition of the solution, i.e. it is maximum when the solution contains the same composition as those of the compound and the eutectic. It follows that the Tammann's method[88] can be employed in finding out the eutectic and compound compositions. In this method, the duration of the halt is plotted against the composition of the solution. The intersection of the two curves (one obtained from samples with compositions "less" than and one "greater" than the complex) gives the maximum halt time and thus the composition. The method will be employed in the present work.

The discussion so far in this section has been devoted mainly to the behaviour of solutions, in which compounds may be formed upon cooling. The reason for this is that cryoscopic studies may provide some information on the stoichiometry of the molecular complexes formed in solution. The technique, when used in conjunection with n.m.r. and dipole moment studies, should help to elucidate the general characteristics of molecular interactions in solution which are the subject of the present investigations. The next chapter will be devoted to the general description of the instruments employed in the present study.

CHAPTER 3

EXPERIMENTAL PRINCIPLES OF THE VARIOUS PHYSICAL TECHNIQUES EMPLOYED IN THE STUDIES OF MOLECULAR INTERACTIONS

INTRODUCTION

The three experimental methods employed in the present investigations are based upon the principles discussed previously in Chapter 2. The experimental aspects of these methods are, for the same purpose as stated earlier in the previous chapter, classified into three separate sections A,B and C, corresponding to those of n.m.r. spectroscopy, dielectric constant and cryoscopy respectively, which will now be discussed in turn.

SECTION A

N.M.R. SPECTROSCOPY

3.A.1 INTRODUCTION

In order to produce high resolution n.m.r. spectra, the apparatus employed should possess the following basic features:

(a) a magnet capable of producing a very strong homogeneous field with high stability.

(b) a sweep unit to allow the main magnetic field and/or frequency to be varied under control over a small range

(c) an r.f. oscillator of high stability

(d) a sample holder or probe which contains the r.f. transmitter/ receiver coil (s) and has provision for sample spinning

(e) an r.f. receiver and amplifier with high gain and low noise

(f) an oscilloscope and/or a pen recorder for presentation of the spectrum.

The basic requirements for the individual components will now be

discussed, and followed by a consideration of the HA 100D Varian NMR spectrometer used in the investigations.

3.A.2 THE MAGNET

Both permanent and electromagnets are employed to provide the main magnetic field B_o for spectrometers. When either type of magnet is used, the resolution corresponding to a field homogeneity of 3 parts in 10^9 can be achieved under optimum conditions. The advantage of the electromagnet is that it enables the field strength to be set anywhere within the range of 0.1-2.5 tesla, so permitting magnetic nuclei to be studied at more than one frequency (section 2.A.2). However, the magnet has a relatively short life-time. The permanent magnet on the other hand lacks this flexibility of operation and additionally its upper limit of field strength is about 2.5 tesla, but it can produce high field resolution stability over a long period of time. Super-conducting magnets are also employed in n.m.r. spectrometers and they can produce a field of the required homogeneity at strengths up to 5 tesla. The latter type of magnets requires elaborate control systems to maintain the temperature of the conducting wire within the region of 10K, which is usually achieved by the use of liquid helium.

The upper limits of the field strengths for conventional magnets quoted above (2.5 tesla) arise from the need for field homogeneity over a volume of $1 \times 10^{-7} m^3$. This requires the pole faces to be parallel, free from machining marks and almost optically flat[90]. The pole cap material must be uniform (metallurgically) and chromium plated to reduce corrosion effects. Improvement to field homogeneity can be made by employing pairs of shim coils, located on or near the pole

faces, such that whenever there are gradients existing in the main field, d.c. currents passed through these coils may be adjusted to produce field gradients that cancel out the natural gradients[91]. As stated earlier in section 2.A.8, the inhomogeneity of the magnetic field experienced by nuclei within the sample results in the broadening of the spectrum lines; the effect can be reduced significantly by employing a cylindrical sample tube and spinning it rapidly about its longitudinal axis, using a small air turbine[92].

In order to obtain accurate measurements of chemical shifts, the field should possess high stability. To achieve this, permanent magnets are often preferred since they are capable of maintaining sufficiently constant fields, provided they are carefully thermostatted[93] and placed well away from variable magnetic influences such as large moving ferrous objects. Field disturbances in the vicinity of permanent magnets can be minimised by mu-metal screening or by devices sensing flux changes. To achieve basic field stability with an electromagnet, a feedback system is required to stabilise the current passing through the magnet's coils. In this system the magnet current is passed through a small resistance and the resultant voltage obtained is then compared with a reference voltage. The difference between these voltages is amplified and used as error voltage for correction purposes.

High resolution n.m.r. spectrometers incorporating either type of magnet employ "flux-stabilising" coils[94] to detect any change in the total flux across the pole gap. The voltage induced in these coils is applied to a galvanometer and which provides an integrated correction signal that is passed through a pair of compensating coils. The field produced by these cancels the original flux change, restores

the galvanometer deflection to zero and hence the field to its original value.

3.A.3 THE MAGNETIC FIELD SWEEP

Theoretically either the strength of the main field, B_o, (field sweep method) or the frequency of the r.f. oscillator (frequency sweep method) may be varied whilst the other remains constant to bring the precessing magnetic nuclei into resonance with the rotating magnetic field B_1. In the early days of n.m.r. technology it was usually found more convenient to employ field sweeps due to the difficulties in providing a suitably stable and linear frequency sweep. However, modern spectrometers usually possess both sweep modes.

The sweeping or scanning of B_o can be accomplished in two ways, namely a recurrent sweep and a "non-recurrent" slow sweep. In the recurrent sweep the output of a sawtooth generator is amplified and the current fed to a pair of Helmholtz coils. Each of these coils has the same number of turns and the separation between them is equal to their radius, and is usually mounted on the outside of the probe body with its axis parallel to the direction of the main magnetic field. By varying the time base and the output of the generator it is possible to control both the rate of the sweep and the spectrum (field) amplitude. This sweep is employed when searching for the resonant field of a particular nucleus and when spectrometer adjustments, such as probe tuning for a line shape, are made.

The slow sweep unit is employed to record the signal, using a pen recorder, under slow passage conditions so that line distortion is minimised. Slow sweep can be achieved when a small dc voltage, acting as error signal, is applied to the flux stabiliser. This results

in a linearly varying false correction to the applied field. Therefore the change in B_o is brought about by a steady increase in current through the correction coils. The rate at which the small applied field is varied is controlled by the magnitude of the dc voltage. Alternatively, a slow sweep can be derived from a motor driven potentiometer linked to a recorder to produce a permanent record of the spectrum.

3.A.4 THE R.F. OSCILLATOR

In section 2.A.3 it has been shown that a nuclear transition is induced when one applies a rotating electromagnetic field, B_1, in a plane perpendicular to the direction of B_o. Usually a linearly oscillating field is employed for this purpose. An r.f. transmitter (r.f. oscillator) capable of generating a signal of constant frequency, the power of which can be varied if necessary, is used as a source of r.f. power. The signal is fed to a coil mounted in the pole gap of the magnet and wound with its axis perpendicular to the direction of the magnetic field, so as to produce a magnetic component of the electromagnetic field rotating in a plane at right angles to the main field direction. Hence a sample placed inside the coil is subjected to a rotating field suitably orientated for the induction of nuclear magnetic transitions.

The r.f. source usually has an automatic gain control amplifier as the final stage of the circuit and the output from this is fed to the probe via an attenuator system to achieve different r.f. levels.

3.A.5 THE DETECTION SYSTEM

The passage of r.f. radiation through the magnetised sample is

associated with two phenomena, namely absorption and dispersion. The line shapes associated with the absorption and dispersion modes are shown in Fig. 3.1 and 3.2. The resonance frequency can be determined from the observation of either of the two modes, but in practice it is easier to observe and interpret the absorption mode signals. The functions of the detector are to separate the absorption from the dispersion signal and also from that supplied by the r.f. oscillator. The latter function is necessary because, although the amplitude of the applied r.f. signal remains constant, only a small effect on it is produced by the absorption signal.

The sample holder, or probe, is the assembly containing the air turbine for sample spinning, the transmitter/receiver coil(s), the linear sweep coils (and a pre-amplifier). Its position may be varied to enable the best position in the field to be found. It can be divided into two principal types, corresponding to the methods of detection[95,96], which are the single coil and the double (crossed) coil probe. Only the latter type (and its corresponding method of detection) will be discussed in more detail later since one is used in the spectrometer employed for the present n.m.r. work.

3.A.6 THE VARIAN HA 100D SPECTROMETER

3.A.6.a THE ELECTROMAGNET

The magnetic field for the spectrometer is provided by an electromagnet, designed for optimum field homogeneity at a field intensity of 2.349 tesla. The magnet is equipped with a manually operated field trimmer to compensate for gradual changes in the field homogeneity along the y-axis. The magnet current can be adjusted from zero to a maximum value for various magnetic field requirements. The magnet has two water-cooled, low-impedance coils connected in series and mounted in a trunnion-

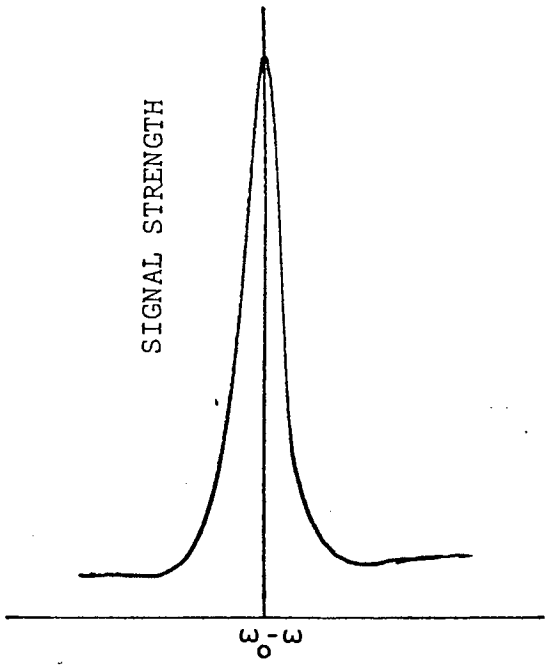

Fig. 3.1 ABSORPTION LINE SHAPE FOR N.M.R. RESONANCE

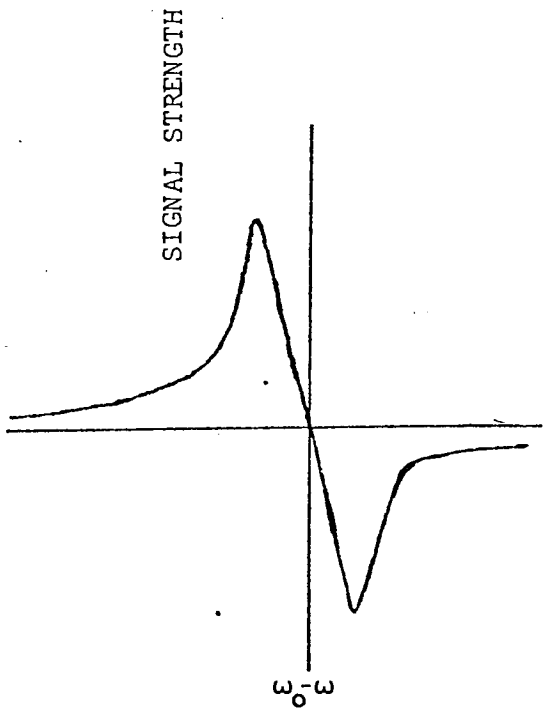

Fig. 3.2 DISPERSION LINE SHAPE FOR N.M.R RESONANCE

supported yoke. The pole cap covers, containing the homogeneity coils (Golay shims), and the yoke insulating jacket, insulate the pole pieces and yoke from the effects of ambient air temperature changes thus helping to maintain the magnetic field stability and homogeneity. The magnet temperature is controlled automatically by passing de-ionised water through the magnet cooling system via a heat exchanger. This helps in maintaining the stability and high resolution of the magnetic field.

3.A.6.b BASIC FIELD STABILISATION

A flux stabiliser unit provides a means for correcting magnetic field drifts and for producing slow sweep rates. Pairs of coils (pickup and buckout coils) are mounted over the pole pieces of the magnet to control the field. When a flux change occurs one coil detects this and the output from the flux stabiliser to the other coil corrects for the original change.

When a sweep is required, a dc voltage is supplied to one side of a galvanometer input coil at a point A. The change in current in the buckout coil induces a current in the pickup coil, and the resultant voltage appears at another point B. After this happens the field control system will adjust to a rate of current change in the buckout coil which equalises the voltages at the points A and B. This action provides a changing field or sweep.

Homogeneity of the magnetic field is controlled by the homogeneity control unit. This consists of Golay (shim) coils, mounted in pairs on the faces of the magnet. A rectified power supply in the control unit furnishes current to these coils. Adjustment of the dc current passing through the coils produces a field gradient in specific directions,

which can be used to counteract any inhomogeneity in the magnetic field.

3.A.6.c THE R.F. UNIT

The unit contains a highly stable fixed-frequency oscillator and a high-gain superheterodyne receiver. The transmitter section supplies a 100 MHz carrier to the probe, where the carrier is modulated. The resultant n.m.r. signal is then fed to the receiver section for amplification. A more detailed discussion of the function of the r.f. unit will be given later when considering the HR mode of operation.

3.A.6.d THE PROBE

The probe contains sweep coils for sweeping the magnetic field B_o, a transmitter coil for producing the rotating field B_1, a receiver coil for detecting the n.m.r. signal and two sets of paddles for adjusting any leakage between the transmitter and receiver coils. The receiver coil is wound on an inset so that its magnetic axis is parallel to the longitudinal axis of the sample. The transmitter coil is wound in two sections surrounding the receiver coil such that their axes are perpendicular. A Faraday shield is placed between the two coils to reduce the electrostatic coupling to a minimum. The sweep coils, located in the annular slots on the sides of the probe, are placed at a distance from the transmitter and receiver coils with their magnetic axes parallel to the transverse axis of the probe. The probe itself is milled from a single aluminium forging.

3.A.6.e THE DETECTION SYSTEM

The spectrometer employs the double coil or crossed coil method of detection, in what is sometimes called the nuclear induction method[96]. In this method, a separate receiver coil is wound around the sample with its axis perpendicular to both the axis of the transmitter coil

and the direction of B_o. With this arrangement the receiver will pick up the signal arising from the nuclear magnetisation vector corresponding to the absorption of energy by nuclei within the sample. Since the axes of the two coils are at right angles to one another, both coils should not be coupled and the transmitter signal is separated from the absorption and dispersion signals. Any departure from orthogonality between the coils results in a coupling between them, thus leading to the induction of a leakage voltage in the receiver coil. In fact, a small amount of leakage from the transmitter coil, being in-phase with the absorption signal, is needed to suppress the dispersion signal. Semi-circular metal sheets, or paddles, are mounted at the end of the transmitter coil to control the amount of leakage, since they can modify the lines of force due to the field and thus provide the variable degree of inductive coupling between the two coils.

The HA 100 D spectrometer can be operated in two modes, which are the HR and HA (field/frequency stabilised) mode. These two modes of operation will be discussed after describing the principles of the field/frequency control.

3.A.6.f THE FIELD-FREQUENCY LOCK SYSTEM

The spectrometer employs a field-frequency lock system which can be described as follows. Field-frequency control is a system in which the r.f. source and the magnetic field strength at the sample are held in constant proportion. To facilitate this, in an internal lock system, a reference compound is added to the sample to be studied so that n.m.r. experiments are performed on both the analytical and reference samples and the signal derived from the latter used to maintain the field/frequency porportionality.

All r.f. signals used are derived by magnetic field modulation, at audiofrequencies, of the carrier so that the latter and its upper and lower sidebands are transmitted to the sample. These signals can be separated from one another in synchronous (or phase-sensitive) detectors referenced to the relevant modulation frequency. The signal mode, absorption or dispersion, can be set by the audiofrequency reference phase applied to the synchronous detector. Nuclear magnetic responses are observed whenever one of the instrumental frequencies coincides with the nuclear precession frequency. One modulation sideband (control channel) is adjusted to be on resonance for the internal reference compound with the modulation index set to avoid saturation. The reference phase of the control channel synchronous detector is set to produce a dispersion mode signal which, because of its shape, is suitable for use to produce an error signal to pull the magnetic field back into resonance if thefield or the frequency tend to drift.

In the frequency sweep mode, the control channel operates at fixed B_o and constant modulation frequency whereas the analytical channel frequency is swept linearly through the spectrum (the frequency control is linked mechanically to the horizontal motion of the recorder arm). The movement of the recorder arm from left to right coresponds to a decrease in modulation frequency; thus the high frequency set of modulation sidebands is used to excite the resonance in order to obtain the spectra, so that the lines in the spectrum appear in the correct order of nuclear screening as if the field were swept from low to high field at fixed frequency.

In the field sweep mode, the analytical channel is kept at a constant modulation frequency obtained from a nominally fixed but manually variable oscillator and the control channel modulation frequency is swept linearly. In this case the low frequency set of modulation side-

bands is used and the modulation index of the analytical channel is kept constant throughout the sweep. When the recorder arm (governing the control channel) is stationary, the n.m.r. signal from the reference dispersion mode line is zero volts. As soon as the control frequency is changed, the r.f. field used to excite the internal reference line is swept and the reference line tends to move off resonance, thus generating a finite dc error signal which drives the main magnetic field in a linear fashion in order to hold the reference signal at resonance.

When a transfer from field sweep to frequency sweep mode is carried out, the functions of the two r.f. modulation controls are interchanged and their settings have to be modified to avoid saturation of the lock signal.

When the recorder arm reaches the indicator mark on the right hand side of the chart, the sweep oscillator is at 2500 Hz. If the manual oscillator is also at 2500 Hz, then the lock signal is at the same point on the chart. However, it may often be required /to examine, on one of five expansion scales, a portion of the spectrum far removed from the lock signal. This may be accomplished by off-setting the manual oscillator above or below 2500 Hz, thus displacing the lock signal to the left or right of the indicator mark.

3.A.6.g THE HR MODE OF OPERATION

In the HR mode , the r.f. unit (Fig. 3.3) is employed and the r.f. level at the probe, from the transmitter section, is controlled by a push-button switch attenuator and isolated by a buffer amplifier to eliminate frequency shift with load variations. A 2.5 KHz oscillator in the integrator/ decoupler unit energises the probe ac sweep coils to mod ulate the 100 MHz carrier. This accessory stabilises the base line

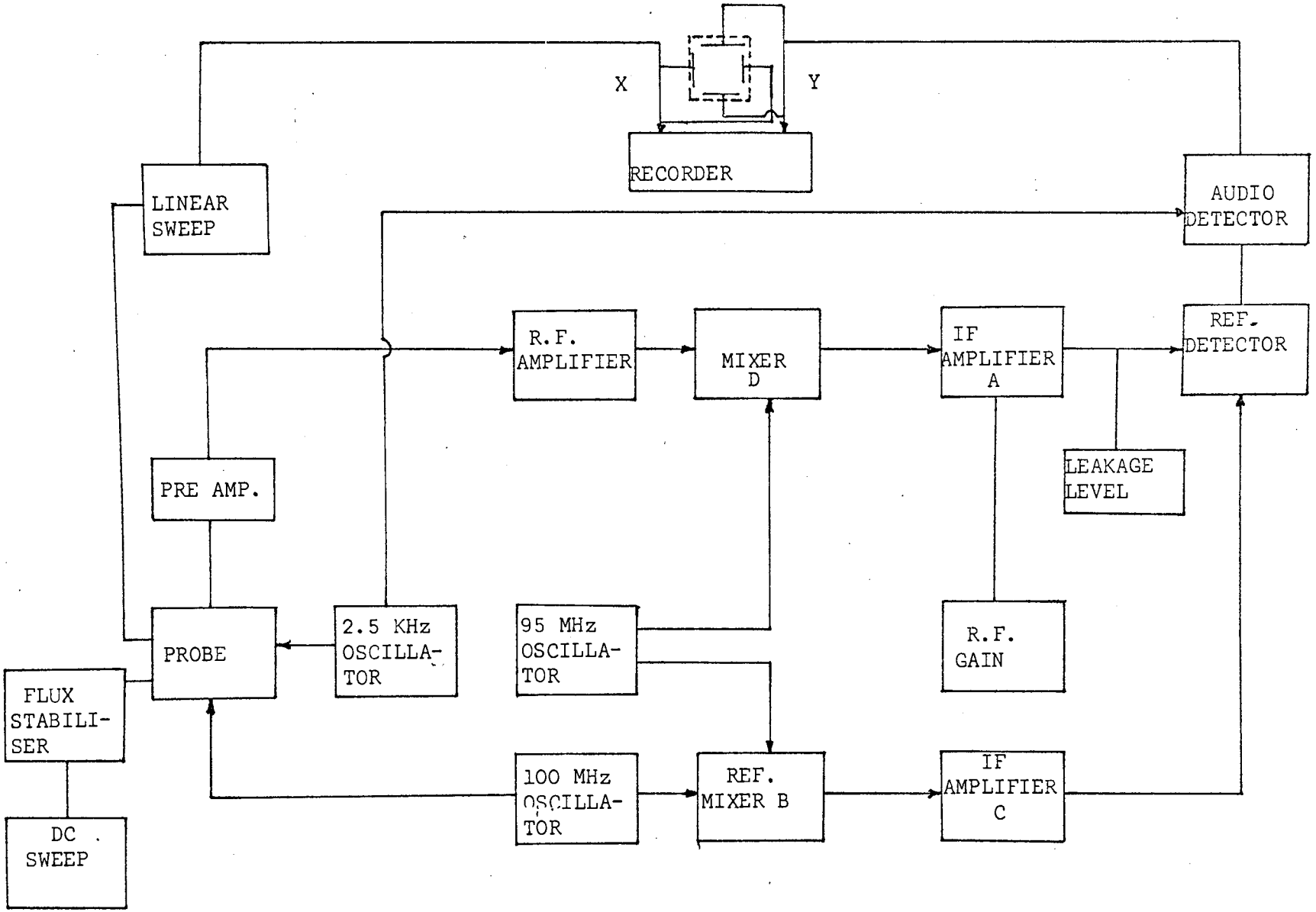

FIG. 3.3 SCHEMATIC DIAGRAM OF THE VARIAN HA 100D N.M.R. SPECTROMETER (HR MODE OF OPERATION)

of the spectrum output by means of field modul-ation and phase sensitive detection. The n.m.r signal at 99.975, 100 or 100.025 MHz is taken from the probe assembly via a low noise preamplifier to the first of two stages of r.f. amplification. The r.f. signal is then mixed with a local oscillator frequency (95 MHz) in the mixer D, resulting in $5\pm$ 0.025 MHz signals which are then passed to the first of two stages of IF amplification (IF amplifier A). Receiver gain is accomplished by varying the bias in the two stages with the receiver gain control. A 5MHz reference signal, derived from mixing the transmitter frequency from the 100 MHz oscillator and the local oscillator frequency in mixer B, is fed to the IF amplifier C. The IF amplifier output is applied to a diode detecting circuit, which includes the detector level meter, and to a phase detector circuit. The latter circuit mixes the 5 MHz reference output from the IF amplifier C and the n.m.r. signal from the IF amplifier A to produce a 2.5KHz signal which is phase sensitive detected relative to the reference 2.5KHz in the integrator/decoupler. The output signal is amplified and rectified for spectral or integral display on a recorder or oscilloscope.

3.A.6.h THE HA MODE OF OPERATION

In this mode of operation, the stability of the magnetic field is enhanced by the use of a field-frequency lock unit in the Internal Reference Proton Stabilisation Unit. This unit provides n.m.r. stabilisation by furnishing audio gain and phase detection in both signal and control channels between the r.f. unit, the recorder and the magnet stabilising circuits. The unit consists of a transmitter section and a receiver section contained on printed circuit cards (Fig. 3.4).

The transmitter section contains two audiofrequency oscillators, namely

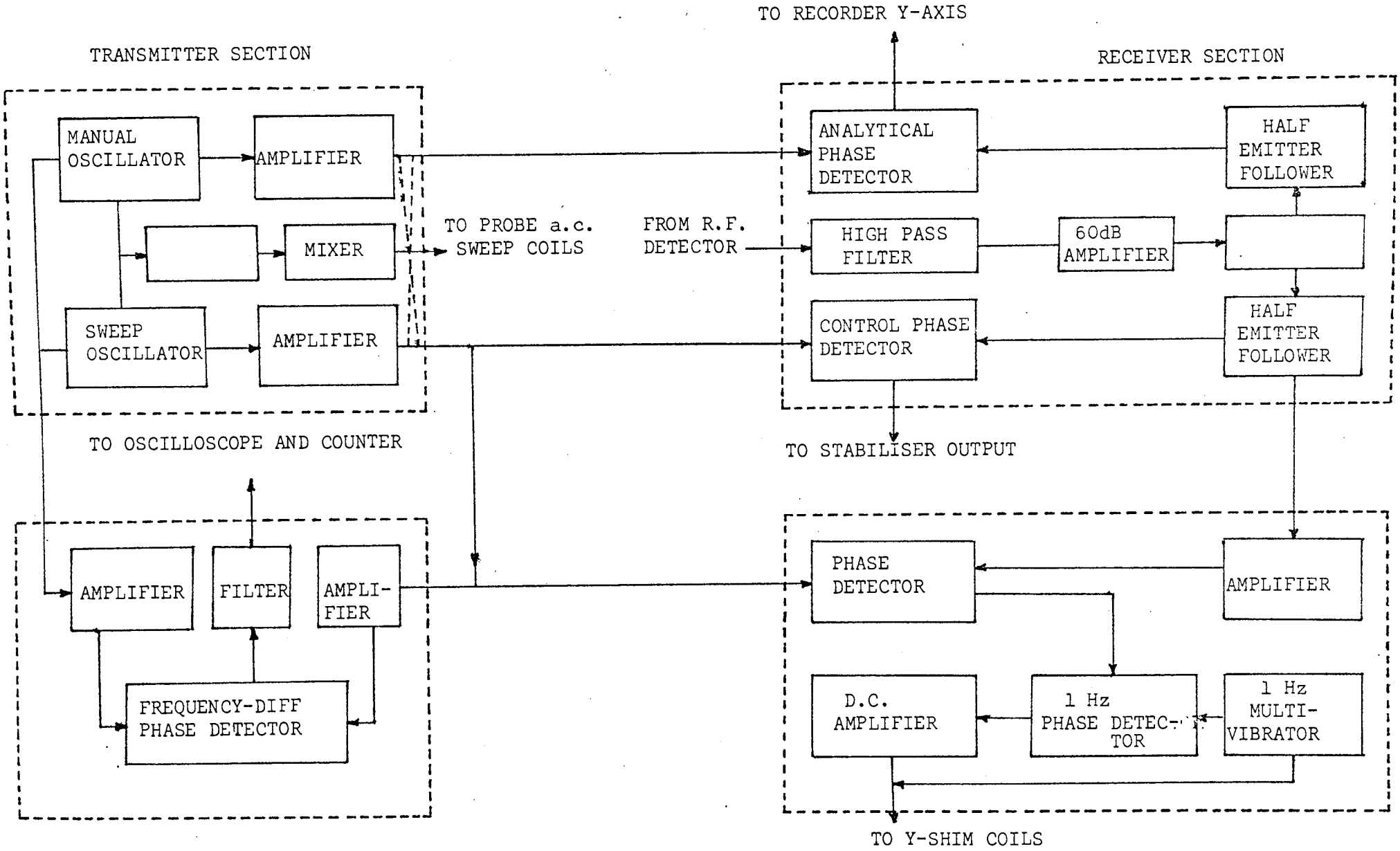

FIG. 3.4 SCHEMATIC DIAGRAM OF THE VARIAN HA-100 D NMR SPECTROMETER (HA MODE)

the sweep frequency and manual frequency oscillators. The sweep oscillator can be tuned for 50, 100, 250, 500 and 1000 Hz ranges whereas the manual oscillator has two frequency ranges, 1500 - 2500 Hz and 2500 - 3500 Hz.

The output frequencies from the sweep and manual oscillators are added and amplified and filtered, before being applied to the ac sweep coils of the probe. The audiosignals obtained modulate the 100 MHz carrier through the ac sweep coils and the resultant signals, which are the nuclear sideband resonances, are processed in the receiver section in a similar manner to that described in section 3.A.6.g.

The input signals to the receiver are applied to a 60 dB amplifier and high pass filter circuit which provides respectively signal amplification and high pass.filtering to reduce spinner noise. The signals are then separated into two channels: (1) the control channel, for providing audiogain, phase detection and filtering for the control resonance, and (2) the analytical channel which provides audiogain and phase detection for the analytical sample resonance. Impedance matching of the control and analytical signals to their respective amplifiers and phase detectors is provided by two separate emitter follower circuits.

The control signal is applied to the control amplifier and phase detector through the Field-Frequency switch. The reference frequency for phase detection is supplied by either the manual or sweep oscillator. The detected coherent sideband resonance is coupled through the Lock On switch to the stabilisation filter circuit card. The stabilisation filter provides low pass filtering for the dc control signal which is then applied to the flux stabiliser to complete

the control loop.

The analytical channel output from the emitter follower is applied to the audio-amplifier and phase detector. The reference frequency for phase detection is obtained either from the sweep or manual oscillator. The detected coherent sideband resonance is coupled to the integrator/decoupler unit where it is amplified and/ or integrated and then applied to the recorder circuits.

Both of the oscillator outputs may be switched to the frequency difference phase detector to enable the frequency difference between them to be determined. Depending upon the mode of operation, either one of these oscillator outputs is applied as reference voltage to this unit. The reference voltage is amplified and shaped into a square wave, then applied to the switching circuit. This circuit compares the phase of the reference and analytical signals to produce a differential frequency, which is coupled through a low-pass filter for application to a frequency counter or to an oscilloscope.

3.A.6.i THE AUTOSHIM HOMOGENEITY CONTROL

The main sources of transient inhomogeneity in the magnetic field are the gradients along the y-axis. The autoshim control maintains optimum homogeneity of the field by automatic adjustment of the y-axis shim coil current in response to an amplitude change in the control signal.

A 1 Hz square wave, generated in the autoshim control circuits, modulates the y-axis shim coil current and the shim coil field, in turn, modulates the n.m.r. signal. If the shim current is not at optimum

value, the modulation of the n.m.r. signal can be detected when the square wave sweeps the current beyond the optimum value. The signal modulation is phase detected to obtain a dc voltage which is then fed back to the shim coils so that the current of the latter is kept at optimum value.

3.A.6.j SPECTRAL CALIBRATION

A graphic record of the spectra is made at any one of the five selected sweep rates on a calibrated chart employing a flatbed recorder. Frequencies of the observed and lock signals can be obtained using a Varian 4315A frequency counter by putting the signal monitor switch to "Sweep" or "Manual oscillator frequency" and counting the two audio-modulation frequencies. Chemical shifts can then be determined by measuring and taking the difference between the sweep frequencies of the two absorptions involved. The accuracy of the shift measurements is normally ca. $\pm$ 0.1 Hz but with care $\pm$ 0.05 Hz can be achieved.

3.A.6.k THE XL 100 VARIABLE TEMPERATURE ACCESSORY

This accessory is used for controlling the sample temperature for analytical studies within the temperature range of 173.0 - 473.0K. The sample is placed in a temperature controlled nitrogen gas stream which then maintains the selected operating temperature of the sample. For operations below ambient temperature, the nitrogen gas is cooled at first by liquid nitrogen and then heated to the selected temperature by a heater in the probe. If experiments are made above ambient temperature, the gas flows directly into the probe and is heated to the required temperature. Once a temperature is selected, it is controlled through a bridge circuit containing a controller and sensor. As the heated gas flows past the sensor, the temperature sensitive element in the sensor changes a resistance in the bridge which is then

automatically balanced. Any change in the temperature control settings or in the sensor resistance alters the bridge balance, resulting in a change in the heater current. The nitrogen gas temperature is then increased or decreased correspondingly which effects a change in the sensor resistance. The bridge balance is regained and the heater current again resumes a steady value and the temperature is stabilised. The controller circuit maintains the dialled temperature within $\pm$ 1K for 5mm tubes at the sensor and $\pm$ 2K at the sample.

SECTION B

DIELECTRIC CONSTANT DETERMINATIONS

3.B.1 INTRODUCTION

Generally dielectric constants of liquids or solutions (which are of prime interest in the present work) are determined through direct measurements of capacitances. The approach adopted here for this purpose is the so-called heterodyne beat method. However, because no detailed description of the electronics of the particular apparatus employed in the present studies is available, only a general and brief discussion of the method will be offered.

3.B.2 THE HETERODYNE BEAT METHOD [69,129]

This method, which has been widely used, is suitable for liquids of negligible conductivity and especially for gases. It depends upon the control of the frequency of a vacuum tube (thermionic valve) oscillator by an adjustment of capacitances in a circuit, with the resistance and inductance kept constant. "Beats" can then be obtained between two such oscillators, the frequency of which represents the difference of

the two frequencies. A formation of beats is induced when two circuits are placed so close together as to contain a mutual inductance, i.e. the two circuits are coupled. The oscillations in one circuit (primary circuit) induce oscillations in the other (secondary) circuit. The secondary oscillations then react upon the primary oscillations, giving rise to a resultant oscillation having an amplitude which rises and falls periodically. Whenever oscillations in one circuit contain maximum amplitude, minimum or zero amplitude oscillations are obtained in the other circuit.

A heterodyne beat apparatus (Fig. 3.5) may contain two oscillators, one of which (generated by a quartz crystal) is usually held at constant frequency, while the other obtained similarly, is adjusted by varying a capacitance to give a controlled frequency, variable relative to that of the fixed oscillator. Alternatively a single oscillator could be used and the output split to provide reference and analytical frequency. When both oscillators are nearly in tune their frequencies produce beat frequencies equally spaced about the null point, at which the frequencies are equal.

Two separate condensers, each connected in parallel to one another, are connected to the oscillator circuit A through screen leads. One condenser, containing the substance the dielectric constant of which is to be measured, acts as a measuring cell whereas the other is a variable standard condenser. In this respect the frequency of the analytical signal coming from oscillator A can be adjusted over a range, corresponding to capacitance changes in the measuring cell induced by the dielectric properties of pure liquids or dilute solutions present in this, by using the standard condenser. The analytical signal is fed to a mixer, where it is combined with a reference signal from the fixed oscillator B. The resulting signal is then passed on to an oscilloscope

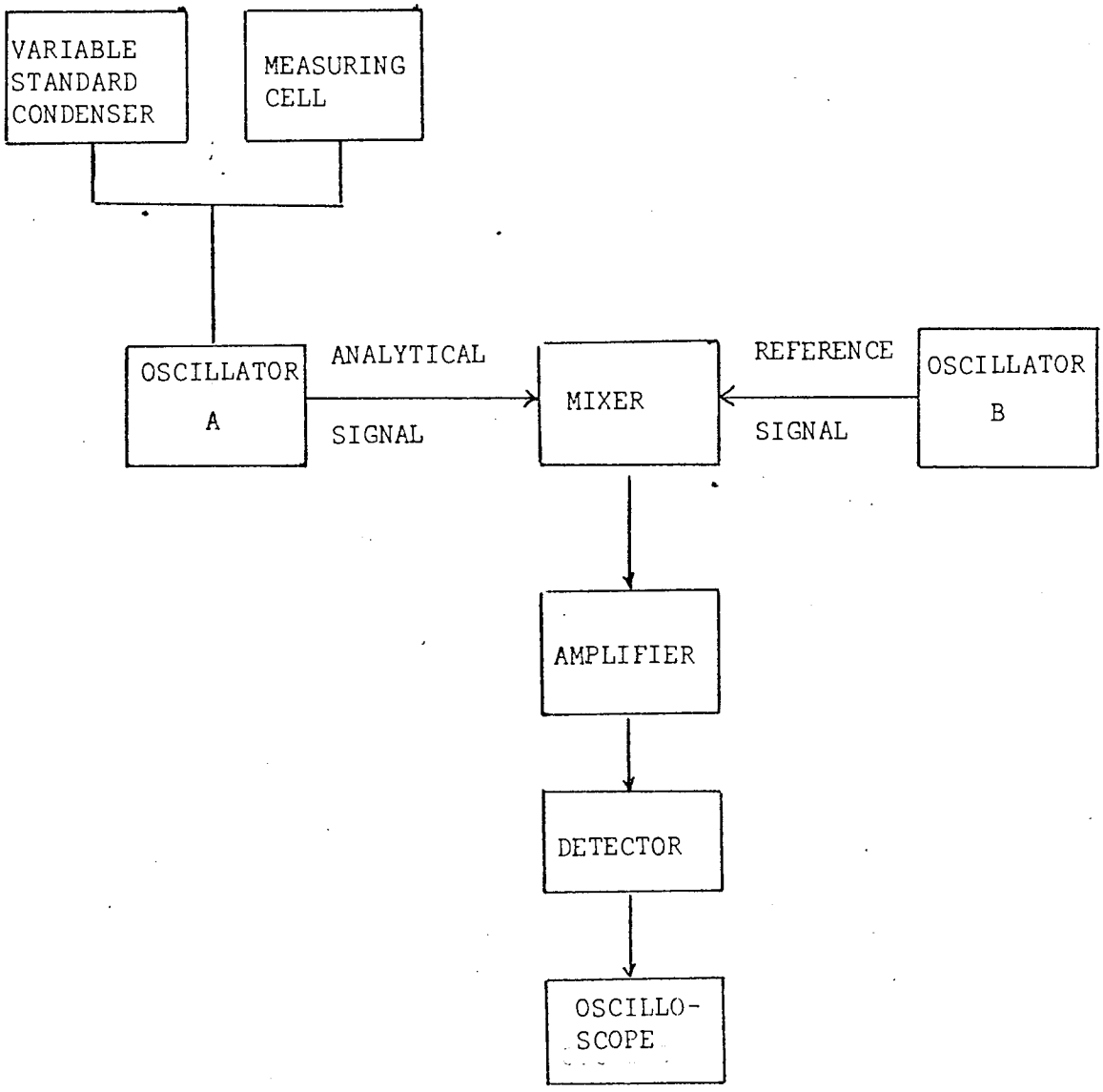

Fig. 3.5 SCHEMATIC DIAGRAM OF THE HETERODYNE BEAT APPARATUS

through a detector-amplifier circuit, for display.

3.B.3 THE APPARATUS EMPLOYED IN THE PRESENT WORK

The apparatus contains similar main components to that shown in Fig. 3.5 except that it has three condensers instead of two. The third (Sullivan) condenser, also connected in parallel with the other two, provides a coarse adjustment of the capacitance so as to bring the beats into the region detectable on the oscilloscope. The analytical frequency can then be tuned by the standard condenser to achieve the zero beat point on the oscilloscope. The reading on the standard condenser at this point, which corresponds to the capacitance of the measuring cell, can be taken through an eye-piece. The standard condenser has two reading scales fixed on it. The main scale is related to a range of capacitance from 300 - 720 pF and a vernier divided into 20 divisions, all of which corresponds to one division on the main scale.

The capacitance of the cell (thermostatted at 308.2K) essentially consists of two parts. The first is due to the cell itself and the leads and connections joining the various condensers and the oscillator unit, and the second part corresponds to the dielectric material present in the cell. The capacitance of the first part can be determined from the difference between the capacitances of the cell when filled with air and when filled with a liquid of known dielectric constant using equation (3.1). Having done this, the capacitance (C_x), and therefore the dielectric constant (ε_x), of the dielectric material in the cell can also be calculated from

$$\varepsilon_x = \frac{C_x - C_o}{C_{air} - C_o} \qquad (3.1)$$

where C_o is the capacitance due to the first part and C_{air} that when

the measuring cell is filled with air.

SECTION C

CRYOSCOPIC STUDIES

3.C.1 INTRODUCTION

The present cryoscopic studies involve the construction of phase diagrams for various binary systems from plots of temperature (freezing point) against composition of the mixture. Freezing points and other properties, such as eutectic and peritectic points, of mixtures can be obtained from their cooling curves, which are essentially plots of temperature against time. The commonly used apparatus for this purpose in most cases is based upon that originally devised by Beckmann[130], of which the main components are a cooling cell, a stirrer, a thermomemter and a cooling bath containing a freezing mixture.

It is generally found rather difficult to achieve accurate and reproducible results from cryoscopic studies. However, for the apparatus employed here, containing similar components to the Beckmann apparatus, reproducible results could be obtained within an accuracy of $\pm$ 0.5K for test samples.

3.C.2 THE CRYOSCOPIC APPARATUS

The various basic components of the apparatus used are listed below as

(a) A cooling cell, containing the sample under investigation

(b) A system for controlling the cooling rate of the sample

(c) A means of making accurate temperature measurements

(d) A component to record continuously the behaviour of the sample

under cooling.

These components will now be described briefly in turn.

3.C.2.a THE COOLING CELL

The cooling cell was constructed as a double-walled glass tube, in which the space between the two walls was connected directly to a vacuum system such that the rate of change in temperature of a sample could be adjusted by varying the pressure in the space (Fig. 3.6). The inner glass cell contained the sample being studied. A motor driven stainless steel rod having small paddles attached in different directions at one end was dipped into the sample and used to stir the latter. By using a variable speed motor the stirring rate could be kept constant or altered. The cell also contained a copper-constantan thermocouple. This thermocouple, with one junction in the sample and the other (reference junction) thermostatted at 298.2 $\pm$ 0.1K outside the cell, was connected to a recorder with a high input impedance.

Apart from the inlets for the stirrer and thermocouple, the upper part of the cooling cell was isolated from the atmosphere by a glass stopper.

3.C.2.b TEMPERATURE CONTROL

The rate of cooling of a sample during an experiment was achieved by the combined effect of changing the stirring rate (although this was normally kept constant) and the pressure inside the space between the two walls of the cooling cell. The cell was immersed in liquid nitrogen acting as the coolant for the present work. Normally the rate of stirring was constant, throughout the cooling process, and sufficiently fast to produce rapid equilibration within the sample. This was shown by a concave shape of the cooling curve after supercooling when the

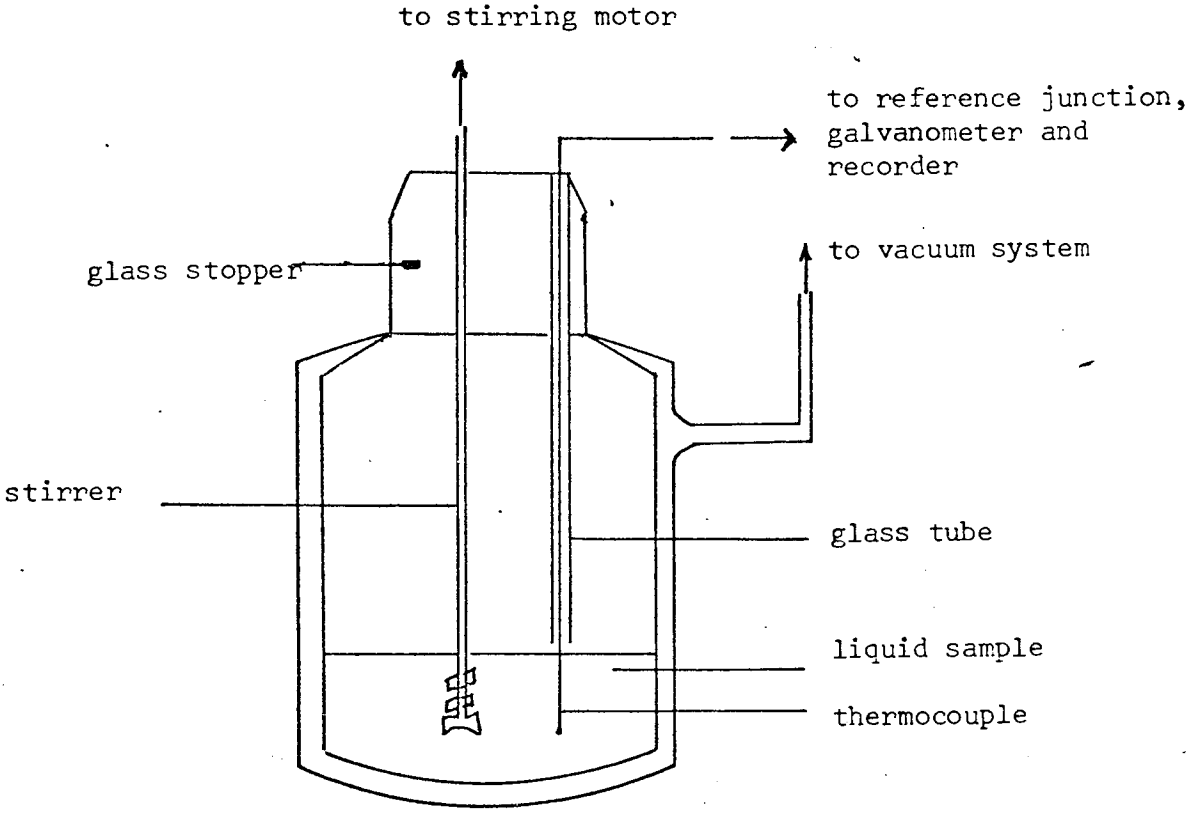

Fig. 3.6 DIAGRAM REPRESENTING THE DOUBLE-WALL COOLING CELL IN THE PRESENCE OF THE LIQUID SAMPLE AND VARIOUS COMPONENTS

freezing point of the sample had been reached.

The vacuum in the space between the walls of the cell was produced by a Genevac vacuum pump, with the maximum pressure inside the space being not more than 5.0×10^{-6} mHg. The cooling rate was kept around 0.2 - 0.3 K per minute by changing (as necessary) the pressure inside the space.

3.C.2.c TEMPERATURE MEASUREMENT AND CALIBRATION

This was achieved by employing a precalibrated scalamp galvanometer in connection with the thermocouple. The calibration of temperature with respect to the voltage reading on the galvanometer was conducted in the following manner.

Several organic liquids (analar grade) of differing freezing points were employed as references. They were cyclohexane (266.7K), cyclohexanone (256.8K), carbon tetrachloride (250.2K), m-xylene (225.3K) and toluene (178.2K).

For each substance the temperature at the start of the cooling experiment was read directly from a thermometer while the galvanometer voltage reading was set at zero. During the cooling process a graph was plotted between the galvanometer voltage readings and time. When the cooling was over, the cooling curve obtained was analysed for the freezing point. Taking the freezing point of each substance (from the curve) to be exactly at the same temperature as quoted above, the voltage change for 1K was calculated in each case. Each substance was cooled down three times and the average value recorded. It was found that a change of 1K corresponds to ca. 3.57 μV. Similar temperature calibration was also made on the recorder to check the

reliability of this value, and the result obtained was found to agree within $\pm$ 0.03 μV of the above value. The value so obtained was then used when a conversion from a galvanometer reading (or recorder pen deflection) to temperature was required.

3.C.2.d THE RECORDING FACILITY

A servoscribe recording potentiometer provided an automatic, continuous recording of the voltage change derived from the thermocouple for a sample upon cooling. The thermocouple was connected either to the galvanometer or the recorder (y-axis) by means of a two-way switch. Before cooling each sample, the voltage output from the thermocouple (as the voltage difference between that of the sample and that of the reference junction) was read on the galvanomter with the recorder pen set at a certain point. Using the conversion factor (section 3.C.2.c.), the temperature before cooling the sample was calculated for the chosen recorder pen position. When the cooling process was over, the cooling curve obtained via the recorder for the sample was analysed for the freezing, eutectic and/or peritectic points according to section 2.C.6.

CHAPTER 4

CRYOSCOPIC STUDIES OF SOME MOLECULAR INTERACTIONS TO ELUCIDATE THE STOICHIOMETRY OF THE COMPLEXES

4.1 INTRODUCTION

It has been stated in section 1.5 that the information obtained from studies of molecular interactions should be capable of elucidating the nature, strength, stoichiometry and geometry of the complexes formed. Furthermore, these studies have to be made in a manner such that each particular feature is elucidated properly and accurately. To achieve this any feature which, after its details are revealed, can facilitate the elucidation of the others should be considered first. Generally it is expected that once the stoichiometry of complexes has been deduced, the other features can be investigated more meaningfully. It is thus necessary to focus attention on complex stoichiometry at an early stage.

The presence of one or more complex species in a binary system can be studied and confirmed through cryoscopy[99-103], the theory and method of which has been previously discussed in section C, chapter 2. The technique involves the derivation of a phase diagram from a plot of the freezing points of solutions against the corresponding compositions. The presence of a complex species may then be deduced from any maximum existing on the diagram; the composition of the mixture at that maximum corresponds to the complex stoichiometry. It is intended to employ this technique to study at this stage the stoichiometry of complexes formed within various systems of interest in the present work.

4.2 EXPERIMENTAL

The chemicals employed in the studies were benzene (spectrosol), p-xylene (BDH), mesitylene (BDH), nitromethane (BDH), acetonitrile (spectrosol) and chloroform (analar), which were used without further purification. Examination of these chemicals by GLC revealed no impurities.

The various binary systems studied were chloroform-p-xylene, chloroform-mesitylene, nitromethane-benzene, nitromethane-p-xylene, acetonitrile-p-xylene, acetonitrile-benzene, nitromethane-mesitylene and acetonitrile-mesitylene.

For each system a series of solutions was prepared in such a way that the whole concentration range, from one pure component to the other, was covered. The cooling curve for each solution was obtained employing a servoscribe recorder connected to the cooling apparatus as described in section C chapter 3. The analysis of the cooling curves to obtain the freezing point, eutectic point and meritectic point was made according to the methods discussed in section 2.C.3. The aromatic concentrations (on the mole fraction scale) of the samples together with the corresponding freezing points (and eutectic or meritectic point) for each system are recorded in tables 4.1 - 4.8. The temperature measurements for the samples were accurate within $\bar{+}$ 0.5K. The cooling experiments were conducted on each sample twice and the average value recorded. The reproducibility and accuracy of the technique employed was checked by measurements on the chloroform-mesitylene system (Fig. 4.1) which has been studied earlier by the other workers[18]. It is found that the presence of 1:1 complexes is clearly shown on the diagram, the result of which agrees with that obtained from the previous cryoscopic studies referred to. The comparison of the results obtained from both studies is recorded in table 4.9.

TABLE 4.1

THE AROMATIC CONCENTRATION (REAL MOLE FRACTION) AND CORRESPONDING FREEZING POINT VALUES FOR THE CHLOROFORM-MESITYLENE SYSTEM

Sample	Mole fraction (mesitylene)	Freezing point/K	Eutectic point/K
A	1.0000	218.9	
B	0.9494	216.7	
C	0.9000	214.7	
D	0.7985	210.3	209.2
E	0.6999	214.0	
F	0.5979	219.3	
G	0.5061	224.1	
H	0.4002	217.9	
I	0.3119	211.6	
J	0.2005	202.8	200.5
K	0.1080	204.2	
L	0.0448	207.4	
M	0.0000	209.6	

TABLE 4.2

THE AROMATIC CONCENTRATION (REAL MOLE FRACTION) AND THE CORRESPONDING FREEZING POINT VALUES FOR THE CHLOROFORM-P-XYLENE SYSTEM

Sample	Mole fraction (p-xylene)	Freezing point/K	Eutectic point/K
A	1.0000	285.5	
B	0.9001	280.3	
C	0.7999	274.7	
D	0.7001	268.2	
E	0.6501	264.6	
F	0.6197	262.4	
G	0.6003	261.3	
H	0.5787	259.4	
I	0.5501	257.5	
J	0.4999	253.0	
K	0.3997	240.9	201.2
L	0.3002	224.6	
M	0.2002	205.4	
N	0.1001	204.9	
O	0.0501	207.6	
P	0.0000	209.6	

TABLE 4.3

THE AROMATIC CONCENTRATION (REAL MOLE FRACTION) AND CORRESPONDING FREEZING POINT VALUES FOR THE ACETONITRILE-BENZENE SYSTEM

Sample	Mole fraction (benzene)	Freezing point/K	Eutectic point/K
A	1.0000	278.8	
B	0.9517	275.8	
C	0.8929	272.3	
D	0.8543	270.3	
E	0.8035	267.5	
F	0.7599	265.3	
G	0.6963	262.1	
H	0.6596	260.0	
I	0.6450	259.6	
J	0.6061	257.5	
K	0.5535	255.4	
L	0.5005	252.6	
M	0.4432	250.0	
N	0.3991	249.0	248.8 (meritectic point)
O	0.3567	247.0	
P	0.3024	244.2	
Q	0.2531	241.9	
R	0.2031	238.0	
S	0.1480	233.3	
T	0.0987	225.2	224.4
U	0.0465	226.8	
V	0.0186	228.2	
W	0.0000	229.7	

TABLE 4.4

THE AROMATIC CONCENTRATION (REAL MOLE FRACTION) AND CORRESPONDING FREEZING POINT VALUES FOR THE NITROMETHANE-BENZENE SYSTEM

Sample	Mole fraction (benzene)	Freezing point/K	Eutectic point/K
A	1.0000	278.8	
B	0.9102	272.5	
C	0.8458	268.7	
D	0.8067	266.6	
E	0.7457	263.9	
F	0.7019	261.6	
G	0.6524	260.1	
H	0.6044	258.1	
I	0.5480	255.8	
J	0.5202	254.4	
K	0.4951	253.9	252.4 (meritectic point)
L	0.4612	253.0	
M	0.4463	252.7	
N	0.3993	251.7	
O	0.3500	249.4	
P	0.3036	247.0	
Q	0.2514	243.0	
R	0.2040	240.0	
S	0.1505	236.6	
T	0.1040	237.1	236.3
U	0.0514	238.7	
V	0.0000	240.6	

TABLE 4.5

THE AROMATIC CONCENTRATION (REAL MOLE FRACTION) AND CORRESPONDING FREEZING POINT VALUES FOR THE ACETONITRILE-P-XYLENE SYSTEM

Sample	Mole fraction (p-xylene)	Freezing point/K	Eutectic point/K
A	1.0000	285.5	
B	0.9437	283.6	
C	0.8977	282.3	
D	0.8539	281.0	
E	0.8014	280.1	
F	0.7481	278.3	
G	0.7029	277.4	
H	0.6562	276.5	
I	0.6015	275.2	
J	0.5464	274.2	
K	0.4976	273.5	
L	0.4489	272.3	
M	0.4008	271.1	
N	0.3492	269.1	
O	0.3030	268.4	
P	0.2523	266.6	
Q	0.2009	264.5	
R	0.1498	260.6	
S	0.0955	254.2	
T	0.0550	244.0	
U	0.0275	227.6	227.3
V	0.0083	228.6	
W	0.0000	229.7	

TABLE 4.6

THE AROMATIC CONCENTRATION (REAL MOLE FRACTION) AND CORRESPONDING FREEZING POINT VALUES FOR THE NITROMETHANE-P-XYLENE SYSTEM

Sample	Mole fraction (p-xylene)	Freezing point/K	Eutectic point/K
A	1.0000	285.5	
B	0.9498	283.9	
C	0.8964	281.5	
D	0.8489	280.4	
E	0.7785	278.2	
F	0.7489	276.9	
G	0.6996	276.2	
H	0.6494	275.1	
I	0.6049	274.2	
J	0.5499	273.3	
K	0.4979	272.6	
L	0.4495	271.9	
M	0.3995	270.8	
N	0.2986	268.6	
O	0.2488	267.7	
P	0.1944	265.8	
Q	0.1499	264.8	
R	0.1059	261.3	
S	0.0502	252.7	
T	0.0272	240.5	
U	0.0090	240.4	239.6
V	0.0186	240.3	
W	0.0000	240.6	

TABLE 4.7

THE AROMATIC CONCENTRATION (REAL MOLE FRACTION) AND CORRESPONDING FREEZING POINT VALUES FOR THE ACETONITRILE-MESITYLENE SYSTEM

Sample	Mole fraction (Mesitylene)	Freezing point/K	Eutectic point/K
A	1.0000	218.9	
B	0.9447	217.4	
C	0.9028	215.7	
D	0.8509	214.2	213.3
E	0.8045	214.2	
F	0.7534	217.0	
G	0.7016	219.9	
H	0.6547	221.0	
I	0.6043	221.9	
J	0.5460	223.0	
K	0.5037	223.7	
L	0.4475	223.8	
M	0.3992	223.7	
N	0.3499	223.8	
O	0.3036	223.7	
P	0.1966	224.3	
Q	0.1552	224.0	
R	0.1016	224.3	
S	0.0481	225.6	
T	0.0288	227.5	
U	0.0000	229.7	

TABLE 4.8

THE AROMATIC CONCENTRATION (REAL MOLE FRACTION) AND CORRESPONDING FREEZING POINT VALUES FOR THE NITROMETHANE-MESITYLENE SYSTEM

Sample	Mole fraction (mesitylene)	Freezing point/K	Eutectic point/K
A	1.0000	218.9	
B	0.9561	217.8	
C	0.8965	215.9	
D	0.8603	214.8	214.6
E	0.8099	218.0	
F	0.7598	222.1	
G	0.7033	225.7	
H	0.6501	228.9	
I	0.6024	232.2	
J	0.5620	234.0	
K	0.5016	236.4	
L	0.4541	236.6	
M	0.4002	236.5	
N	0.3476	236.3	
O	0.3062	236.8	
P	0.2521	236.8	
Q	0.2003	236.5	
R	0.1594	236.9	
S	0.1033	237.2	
T	0.0448	238.6	
U	0.0212	239.7	
V	0.0000	240.6	

TABLE 4.9 - COMPARISON OF THE RESULTS AS OBTAINED BY OTHER WORKERS AND FROM THE PRESENT STUDY FOR THE CHLOROFORM-MESITYLENE SYSTEM (CONT.)

	Eutectic point/K	Eutectic composition of mesitylene (mole fraction)	Freezing point of complex/K
Other work[18]	200.2	0.175	224.2
(± 0.5K)	208.7	0.775	
Present Work	200.0	0.173	223.2
(± 0.5K)	208.5	0.775	

4.3 RESULTS AND DISCUSSION

The freezing point-composition diagrams for all systems studied are shown in Fig 4.1 - 4.8. All of the eight binary systems considered involve three different solutes in various aromatic solvents (It has to be pointed out here that since the whole concentration range is employed in cryoscopic studies, either of the two components in a system can be considered as solute or solvent depending on the concentration of solution. In order not to cause confusion later on when the n.m.r. studies are discussed the aromatics are referred to as solvents and the others as solutes). To simplify the discussion, the behaviour of chloroform in various aromatics is considered first, followed by the other systems of interest.

4.3.a THE SYSTEMS OF CHLOROFORM WITH VARIOUS AROMATICS

The interactions between chloroform and various aromatics have been studied in detail by n.m.r. spectroscopy[104] and the stoichiometry of the complexes formed are indicated to be 1:1. This is also confirmed from the present cryoscopic studies in the case of chloroform-mesitylene

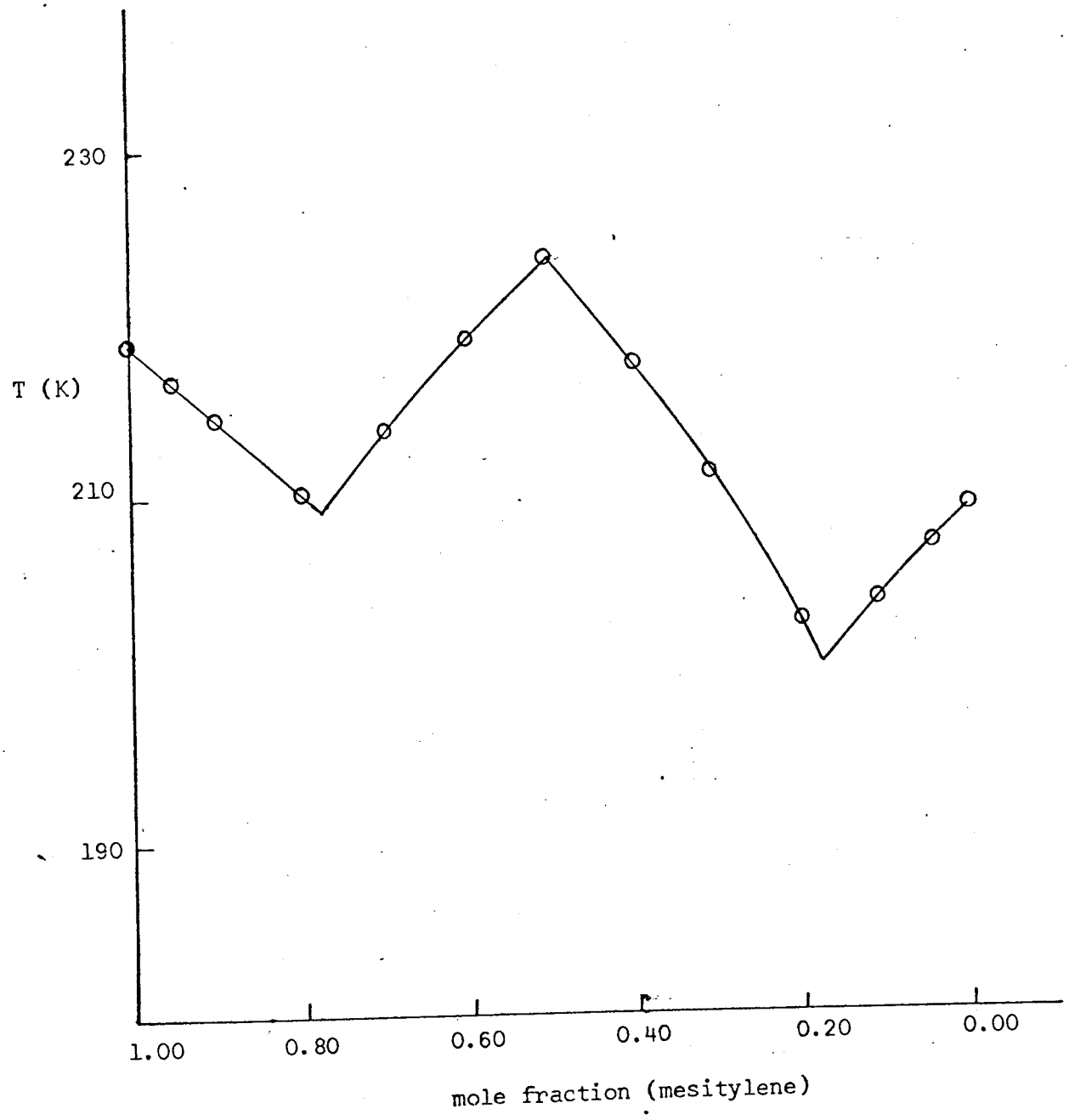

Fig. 4.1 SOLID-LIQUID PHASE DIAGRAM FOR THE CHLOROFORM-MESITYLENE SYSTEM

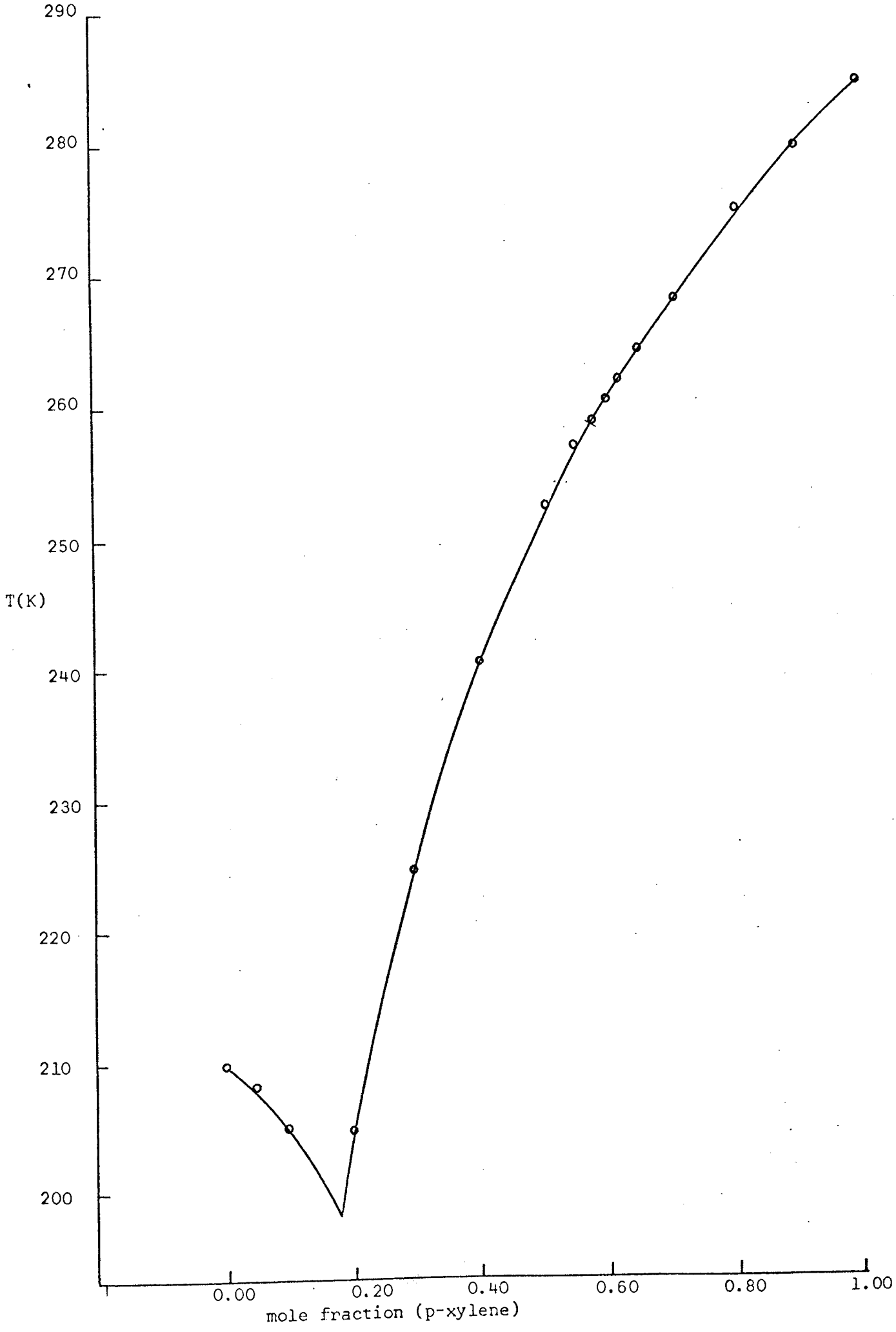

Fig. 4.2 SOLID-LIQUID PHASE DIAGRAM FOR THE CHLOROFORM-P-XYLENE SYSTEM

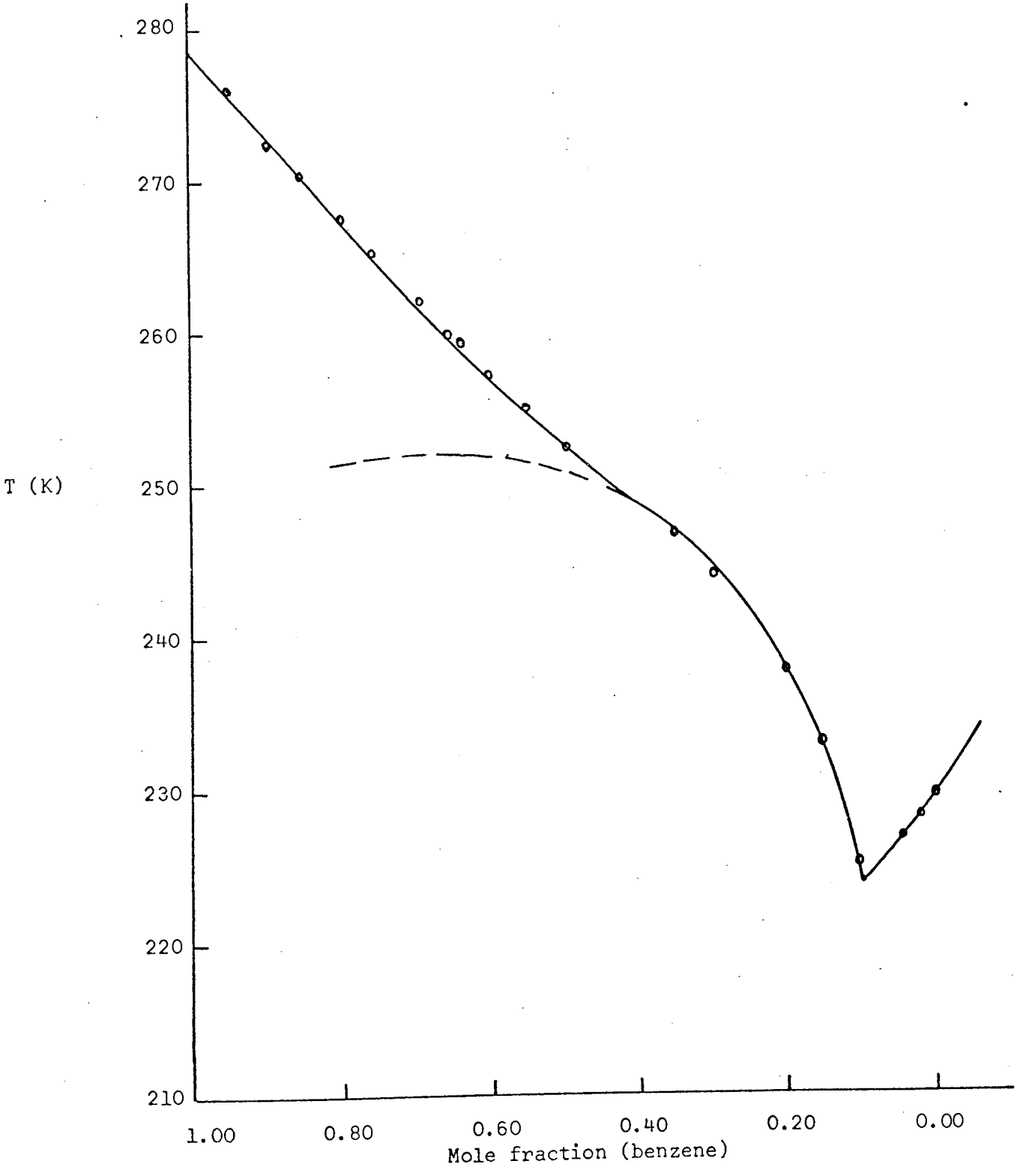

Fig. 4.3 SOLID-LIQUID PHASE DIAGRAM FOR THE ACETONITRILE-BENZENE SYSTEM.

THE MAXIMUM POINT ON THE DOTTED LINE REPRESENTS THE COMPOSITION OF THE UNSTABLE COMPLEX.

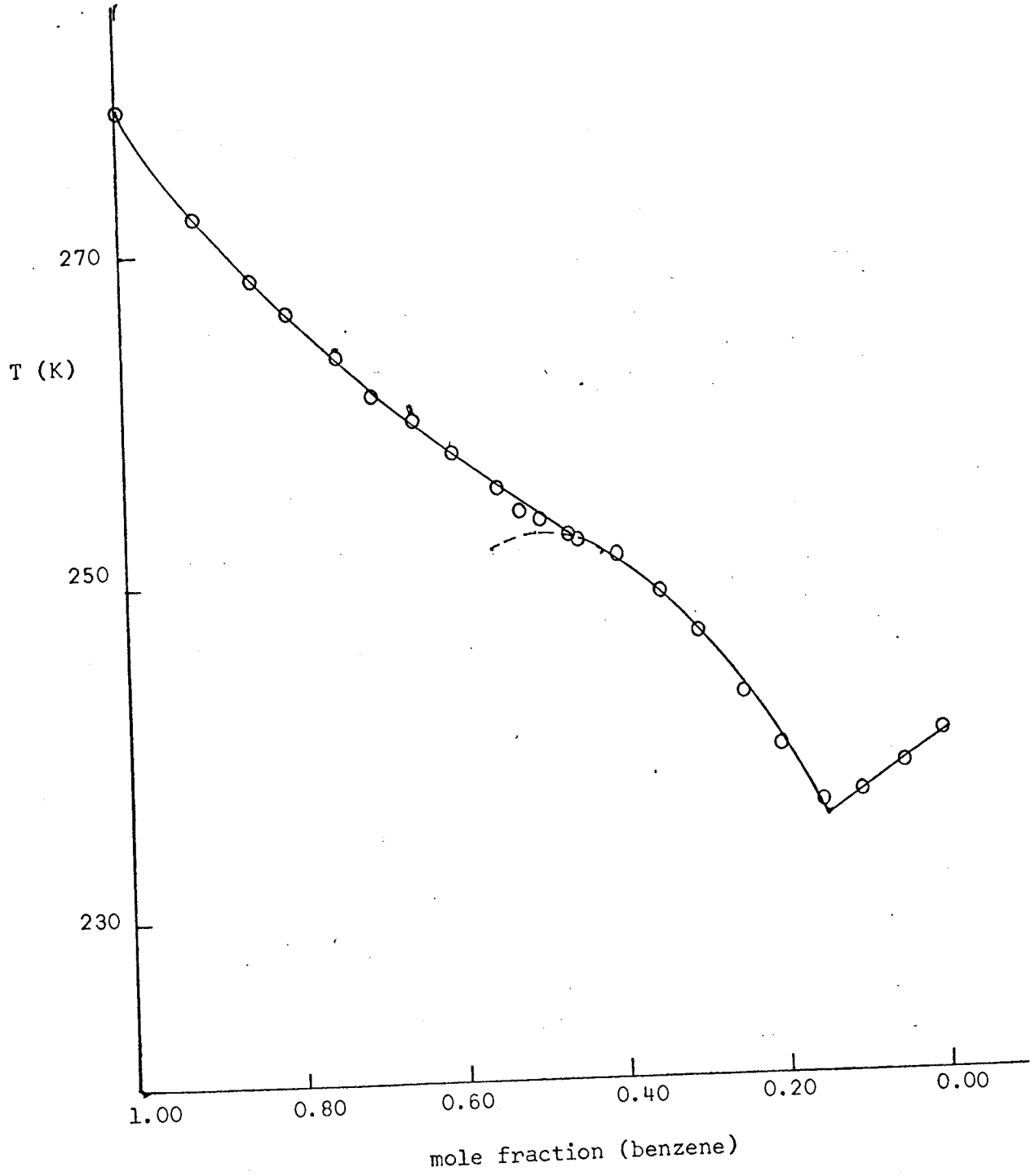

Fig. 4.4 SOLID-LIQUID PHASE DIAGRAM FOR THE NITROMETHANE-BENZENE SYSTEM. THE MAXIMUM POINT ON THE DOTTED LINE REPRESENTS THE COMPOSITION OF THE UNSTABLE COMPLEX.

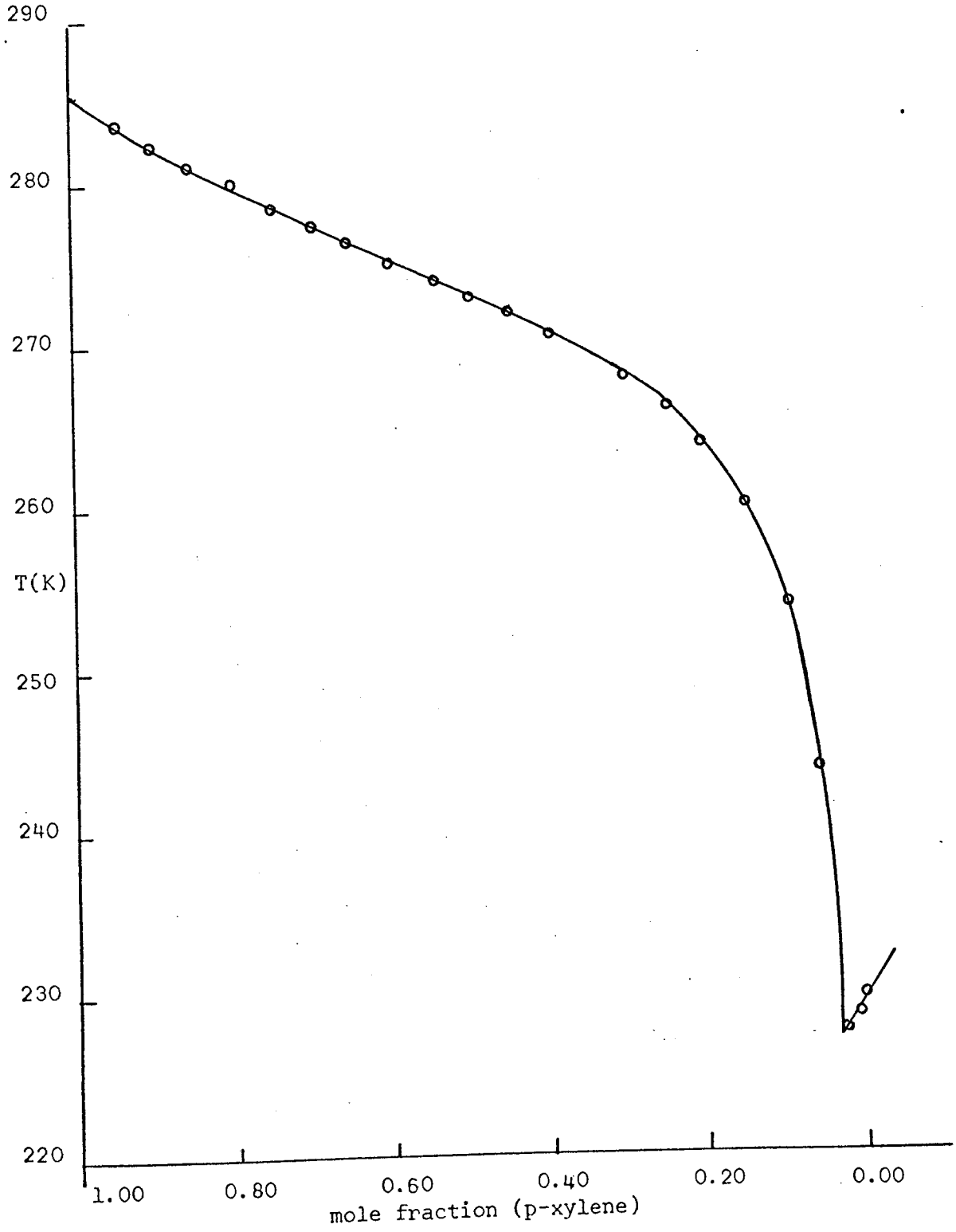

Fig. 4.5 SOLID-LIQUID PHASE DIAGRAM FOR THE ACETONITRILE-P-XYLENE SYSTEM

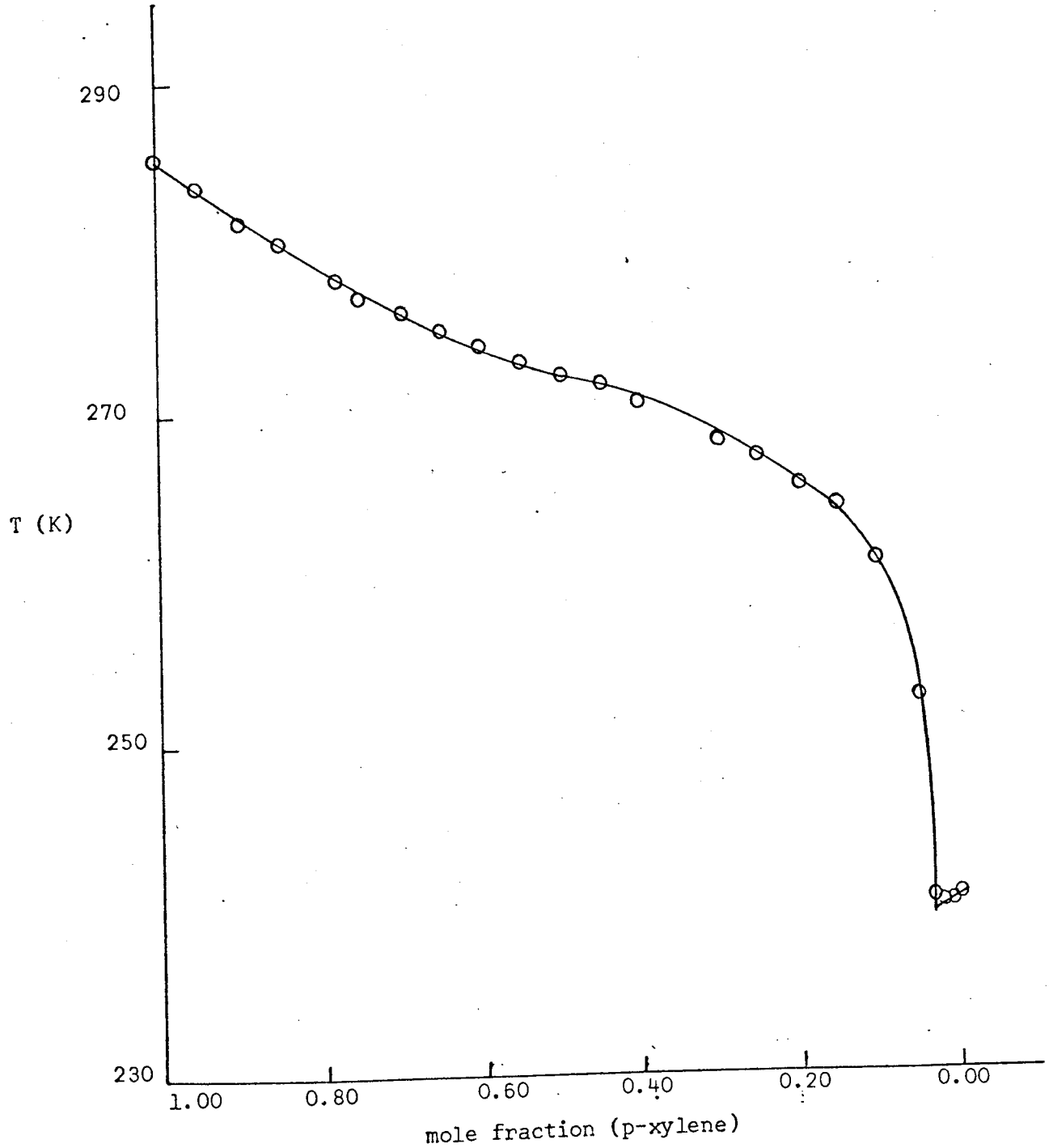

Fig. 4.6 SOLID-LIQUID PHASE DIAGRAM FOR THE NITROMETHANE-P-XYLENE SYSTEM

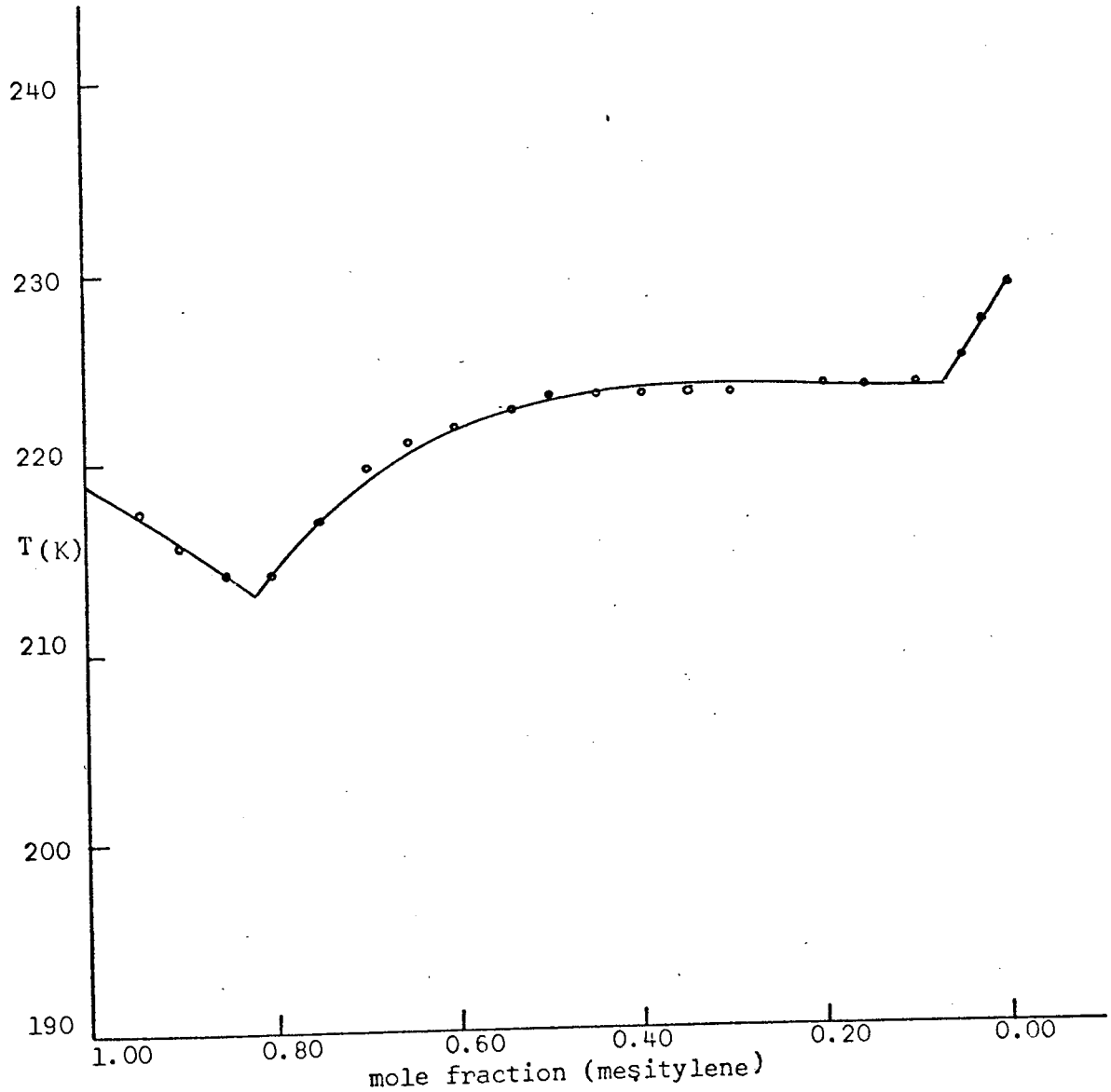

Fig. 4.7 SOLID-LIQUID PHASE DIAGFAM FOR THE ACETONITRILE-MESITYLENE SYSTEM

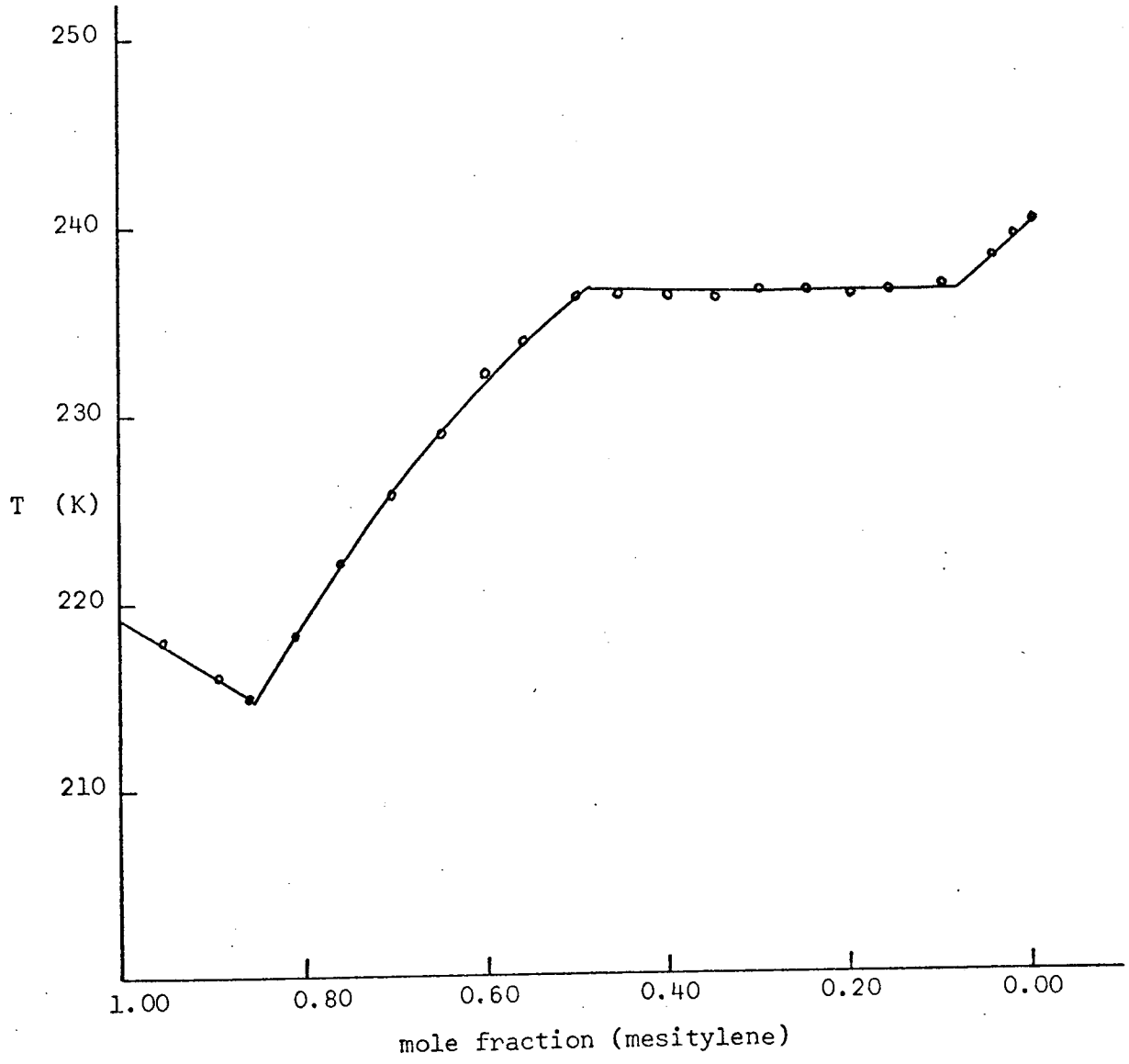

Fig. 4.8 SOLID-LIQUID PHASE DIAGRAM FOR THE NITROMETHANE-MESITYLENE SYSTEM

system. One would expect similar confirmation to be obtainable for the systems of chloroform with other aromatics, for example p-xylene. When the chloroform-p-xylene system was investigated to examine this point in the present work, it was found that no complex formation of any particular stoichiometry could be observed from Fig. 4.2. Superficially this is rather unexpected. However, Reeves and Schneider have investigated the systems of chloroform with benzene and mesitylene cryoscopically, and found that the presence of 1:1 complexes could be confirmed only in the chloroform-mesitylene system whereas in the other (chloroform-benzene) system no complex formation was observed. The absence of characteristics of 1:1 complexes in the latter case was explained in terms of two effects. The first is that owing to the high freezing point of benzene (278.8K) compared to that of chloroform (209.6K), large changes in freezing point with composition when more chloroform was added to the solution may obscure the curve showing characteristics of complex formation (obscuring effect) which should be seen on the diagram. The second is due to the weakness of the interactions between both components (weakness effect) such that they cannot be detected by cryoscopy. It would then appear that if these are the reasons, they may also be applicable to the chloroform-p-xylene system.

Considering the first effect, it is seen that mesitylene has a low freezing point of about 218.9K which is quite close to that for chloroform whereas p-xylene has even a higher freezing point (285.5K)than benzene. Therefore on the basis of the "obscuring effect", one would also not expect to observe the presence of 1:1 complexes in the chloroform-p-xylene system in the same way as in the case of chloroform with benzene. In the case of the second effect, referring to the weakness of complexes formed, this also appears to be justified. It has been found from previous n.m.r. investigations[104] that the strength of interactions between

chloroform and all three aromatics are of the order

mesitylene > p-xylene > benzene

in other words, mesitylene forms the strongest molecular complex with chloroform when compared with the other two aromatics. If is therefore possible that the existence of 1:1 complexes, which is normally detectable in the system of chloroform with mesitylene by cryscopy, cannot be detected in the chloroform-p-xylene (or benzene) system.

Having considered the two effects, it becomes apparent that both are operative in the chloroform-p-xylene system. It is therefore justified to conclude that the reason for not observing characteristics of complexes in this system is due to a combined influence of the effects discussed.

4.3.b THE ACETONITRILE/NITROMETHANE-BENZENE SYSTEMS

These two systems are discussed together since both exhibit a meritectic point upon cooling which indicates the presence of an unstable complex species within each system.

The diagram for the acetonitrile-benzene system (Fig. 4.3) represents one in which there is a formation of complexes with an incongruent freezing point. The cooling curves for this system, for which the concentration of benzene in the samples is from 0.50 upwards (table 4.10), confirm the presence of a meritectic halt at 248.8K on cooling in every sample. The longer the halt the closer is the composition of the sample to that corresponding to the complex. Using Tammann's method described previously in section 2.C.3 (Fig. 4.9), it is found that the meritectic and complex compositions are at 0.44 and 0.65 mole fractions of benzene respectively. The latter is approximately equal to an acetonitrile/benzene concentration ratio of 1/2. It is therefore evident that there

is a complex formed in this system which possesses a 1:2 stoichiometry, which agrees with the study made previously by Goates et al[17]. Since this 1:2 complex appears to be unstable and can dissociate either into other complexes of lower order (in this case the 1:1 complex is the only possibility) or into the pure components, it is of interest to compare both possibilities to find out which is the more likely. If the first possibility is correct, one should at least observe some evidence of 1:1 complex formation on the diagram (Fig. 4.3). In fact such an observation is not apparent. In the case of the second possibility, this is even less likely to happen than the first, since it is unlikely for a 1:2 complex to dissociate into its pure components without producing a 1:1 complex in the dissociation process. It would thus appear that if there is a 1:1 complex being formed, it is likely to be unstable and present in a small, negligible amount. Therefore it may be concluded that in this system only 1:2 complexes are formed.

The diagram obtained for the nitromethane-benzene system (Fig. 4.4) has a similar shape to that of the above system (Fig. 4.3). The system exhibits a meritectic point at 252.4K. When Tammann's method is applied to the results obtained, it is found that (table 4.11 and Fig 4.10) the meritectic and complex compositions are at approximately 0.43 and 0.50 mole fractions of benzene respectively, which indicates in the latter case that the unstable complex possesses 1:1 stoichiometry. Even though this complex is not stable, the only products obtained from its decomposition are the pure components and so it can be concluded that there is only 1:1 complex species present in the system.

4.3.C THE ACETONITRILE/NITROMETHANE-P-XYLENE SYSTEMS

The diagrams for both systems are shown in Fig. 4.5 and 4.6 respectively. The shape of the diagrams for both cases, apart from being similar to each other, are also similar to those of the systems

TABLE 4.10

THE AROMATIC CONCENTRATION AND CORRESPONDING MERITECTIC HALT LENGTHS FOR THE ACETONITRILE-BENZENE SYSTEM

Sample	Mole fraction (benzene)	halt length/10^2m
A	1.0000	-
B	0.9517	-
C	0.8929	2.7
D	0.8543	4.1
E	0.8035	5.2
F	0.7599	6.5
G	0.6963	8.2
H	0.6596	9.3
I	0.6450	9.3
J	0.6061	7.3
K	0.5535	5.0
L	0.5005	2.9
M	0.4432	-

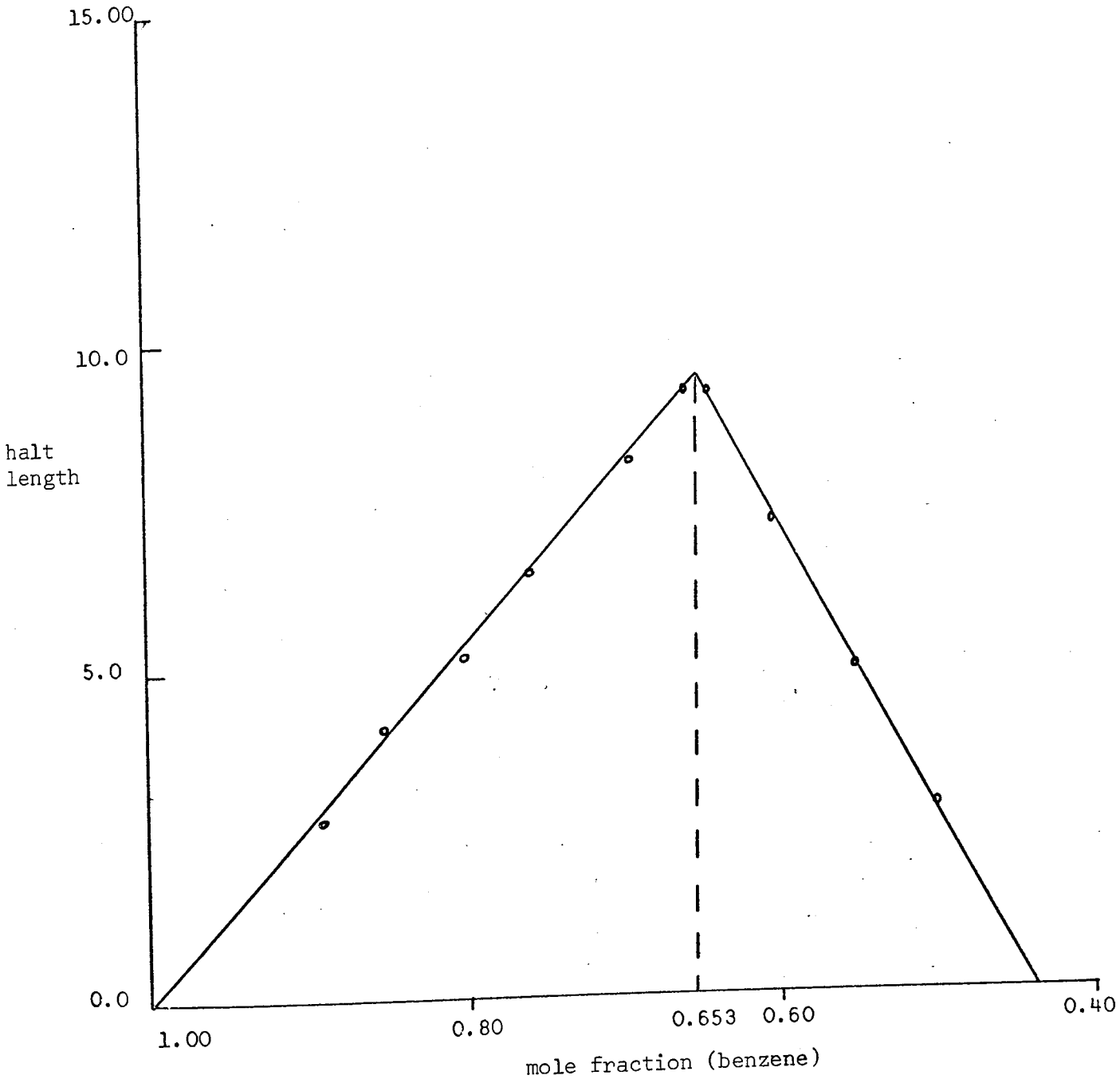

FIG. 4.9 TAMMANN'S PLOT FOR FINDING OUT THE COMPLEX STOICHIOMETRY FOR THE ACETONITRILE-BENZENE SYSTEM

TABLE 4.11

THE AROMATIC CONCENTRATION AND CORRESPONDING MERITECTIC HALT LENGTHS FOR THE NITROMETHANE-BENZENE SYSTEM

Sample	mole fraction (benzene)	halt length/10^2m
A	1.0000	-
B	0.9102	-
C	0.8458	1.7
D	0.8067	2.2
E	0.7457	2.8
F	0.7019	3.3
G	0.6524	3.8
H	0.6044	4.2
I	0.5480	4.9
J	0.5202	5.2
K	0.4951	5.0
L	0.4612	2.2
M	0.4463	1.0
N	0.3993	-

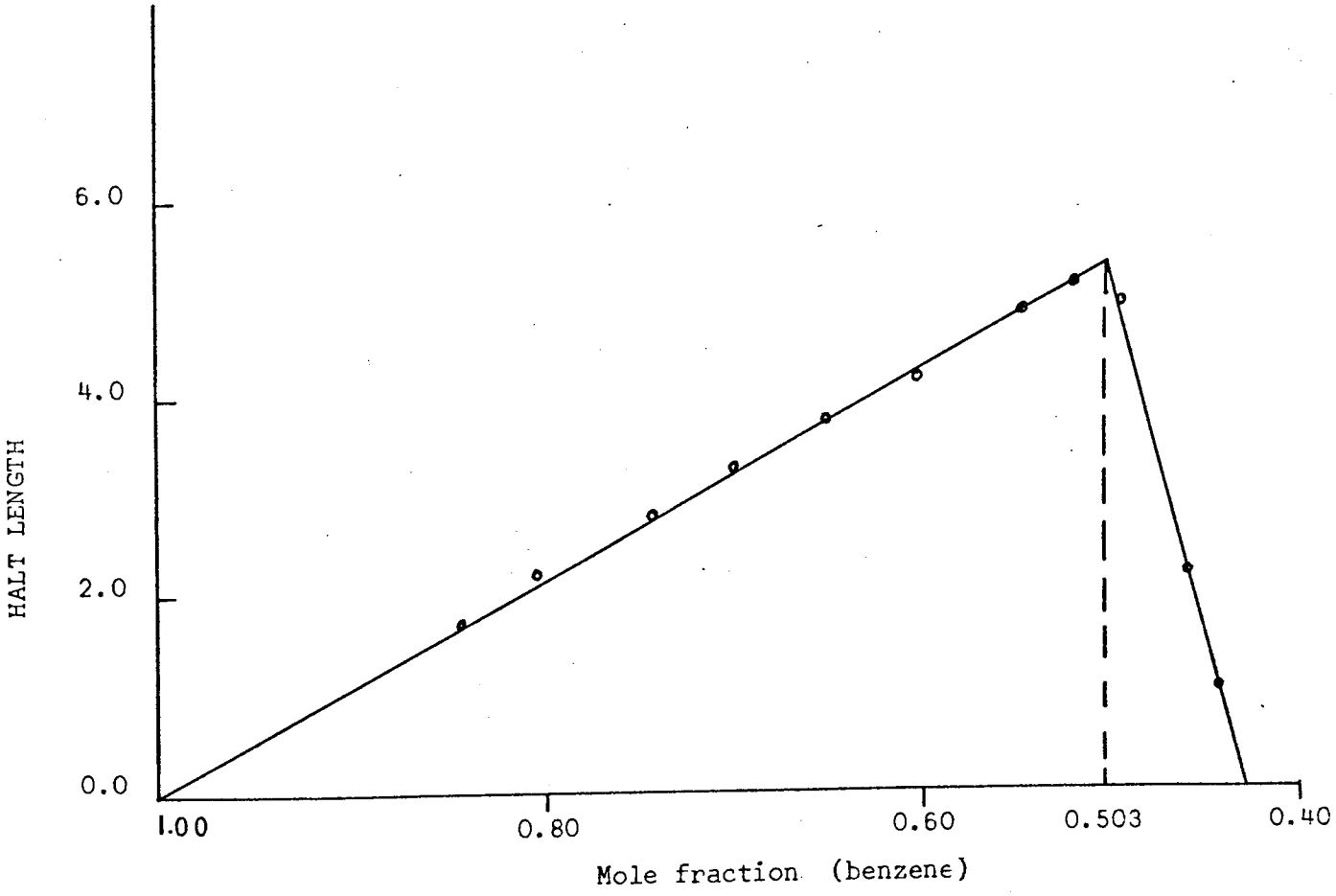

Fig. 4.10 TAMMANN'S PLOT FOR FINDING OUT THE COMPLEX STOICHIOMETRY FOR THE NITROMETHANE-BENZENE SYSTEM

discussed previously in section 4.3.b. The only difference is that no meritectic point could be observed when the analysis of the cooling curves was made. This observation also agrees with the previous study on the acetonitrile-p-xylene system made by Goates et al[17]. This makes it impossible for one to say whether there is any complex formation in both systems. However, judging from the appearance of discontinuity on the curves representing the variations of the freezing points with concentrations, it is likely that complexes are being formed. An attempt has been made to try to explain their absence from the diagrams in terms of the obscuring and weakness effects as discussed previously in section 4.3.a. It is found that the freezing point of solutions in both cases varies slowly with the composition, and so the obscuring effects (due to rapid change of freezing points) should be inoperative. In the case of weakness (of complex formation) effects, this also can be discounted since n.m.r. studies discussed in later chapters show that p-xylene forms a stronger complex with nitromethane or acetonitrile than benzene. Hence no explanation can be proposed for the time being for the absence of evidence for complexes and it has to be concluded that for these systems, the complex stoichiometry cannot be deduced from cryoscopic studies.

4.3.d. THE ACETONITRILE/NITROMETHANE-MESITYLENE SYSTEMS

The diagrams for these systems are shown in Fig. 4.7 and 4.8 respectively. In both cases it was observed during the cooling experiments that, for samples with a mole fraction range of mesitylene between 0.15 - 0.45, a heterogeneous mixture of two liquids was formed when the temperature of the solution was below 273.2K. This indicates that partial miscibility of the two components of these systems exists below the above stated temperature. Since the liquid phases were formed while the temperature of the mixture was decreasing and no halt or break could be observed on the cooling curve, it was impossible to find out the exact temperature at

this point for each sample. As soon as solid started to crystallise out from each liquid phase, the temperature remained constant which was found to be of the same value for every sample within the above specified concentration range of mesitylene. These temperatures were at 223.7K and 236.6K for the systems of mesitylene with acetonitrile and nitromethane respectively.

Judging from the discontinuity of the curves present on both diagrams (Fig. 4.7 and 4.8), it is evident that if the partial immiscibility did not occur it may be possible to observe a second eutectic point on each curve and therefore the characteristic behaviours of complex formation in these systems. So, like the other systems discussed in section 4.3.c, it is concluded that there are complexes formed in both systems, but the elucidation of the stoichiometry of these complexes is hindered by the immiscibility properties of the components.

The results from cryoscopic studies for various binary systems discussed so far in this chapter indicate a weak nature for complexes formed within these systems. This is confirmed by the evidence that their characteristic behaviours can only be observed in some systems, in which the complexes undergo dissociation. Hence it is justified to conclude that the cryoscopic studies have a limited scope when applied to weak molecular interactions in solutions.

CHAPTER 5

N.M.R. STUDIES OF COMPLEX FORMATION AT VARIOUS TEMPERATURES AND FURTHER CONSIDERATIONS ON COMPLEX STOICHIOMETRY

5.1 INTRODUCTION

When a solute is dissolved in an inert solvent such as cyclohexane the chemical shift of a nucleus in a simple solute such as $CHCl_3$ has a certain value which may be represented by δ_{free}. If the solute were dissolved and fully complexed in an active solvent it would be found that the shift would be changed to another value, δ_c. However, it is not possible to determine δ_c experimentally because usually there is a rapid exchange of the solute between the free and fully complexed states, and the only shift that can be measured, δ_{obs}, corresponds to an intermediate or time-averaged screening of the solute nucleus. Because of this the measured chemical shift is given as the time-averaged function[1]

$$\delta_{obs} = \Sigma P_i \delta_i \qquad (5.1)$$

where P_i is the fractional time the solute spends in the i^{th} state and δ_i is the chemical shift in the i^{th} state.

For an interaction, between a polar solute (A) and an aromatic solvent (B) in the presence of an inert solvent (S), of the type

$$A + B \rightleftharpoons A \ldots\ldots B \qquad (5.2)$$

equation (5.1), in terms of δ_{free} and δ_c, becomes

$$\delta_{obs} = P_A \delta_{free} + P_{AB} \delta_c \qquad (5.3)$$

or, in the form of the fractional populations of the solute in both states[105]

$$\delta_{obs} = \frac{(n_A - n_{AB})\,\delta_{free}}{n_A} + \frac{n_{AB}\,\delta_c}{n_A} \qquad (5.4)$$

where n_A is the initial number of moles of A and n_{AB} the number of moles of the complex formed at equilibrium.

Equation (5.4) may be rewritten as

$$\delta_{obs} = \frac{n_{AB}}{n_A} (\delta_c - \delta_{free}) + \delta_{free} \qquad (5.5)$$

or defining

$$\Delta_{obs} = \delta_{obs} - \delta_{free} \qquad (5.6)$$

and

$$\Delta_c = \delta_c - \delta_{free} \qquad (5.7)$$

Substitution of (5.6) and (5.7) into (5.5) gives

$$\Delta_{obs} = \frac{n_{AB}}{n_A} \cdot \Delta_c \qquad (5.8)$$

It can be seen that Δ_c, the total shift induced by B in A, can be evaluated once n_{AB} has been found. In principle the value of n_{AB}/n_A can be obtained from the value of the equilibrium constant, K, for the reaction which, if it is of the type specified by (5.2), is given by

$$K = \frac{[AB]}{[A][B]} \cdot \frac{\gamma_{AB}}{\gamma_A \gamma_B} \qquad (5.9)$$

where [AB] , [A] and [B] are the concentrations at equilibrium of the complex, free solute and free aromatic solvent respectively and γ_{AB}, γ_A and γ_B are the corresponding activity coefficients.

From (5.9) if the activity coefficients of all the interacting species in the system are considered self-cancelling , then

$$K = \frac{[AB]}{[A][B]} \qquad (5.10)$$

where K in this case is referred to as the equilibrium quotient. In practice the concentration of AB cannot be measured directly and neither can the value of K, even in the form of (5.10). However, by combining equations (5.8) and (5.9) in a suitable form the evaluation of both K and Δ_c is possible; the details of the procedures employed will be discussed later.

5.2 GENERAL CONSIDERATIONS OF THE EXPERIMENTAL CONDITIONS

The present n.m.r. studies have been focussed on interactions of the type, represented by (5.2), occurring in the presence of a third inert compound and the discussion henceforth will be confined to these. The presence of an inert third compound, such as cyclohexane (employed in the present work) in the system, in principle benefits the investigation in several ways. These are:

(a) the studies can be carried out on solid dipolar and solid aromatic materials

(b) cyclohexane is a suitable internal reference compound for shift measurements since it possesses a single and sharp resonance line which remains narrow down to its freezing point.

(c) the concentration of the solute can be maintained at a low value such that the effect of solute self-association is minimised.

(d) it is normally found that[1], as the ratio of the aromatic solvent to solute concentration in a series of samples of different compositions increases, the observed shift of a solute proton (δ_{obs}) tends to shift upfield due to an increase in the amount of complex being formed and the effectiveness of the aromatic anisotropic screening upon the solute. Thus different proportions of A and the aromatic (B) have to be used, and in view of (c) above cyclohexane (S) is used to facilitate this and hence the measurements of aromatic-induced shifts of the solute protons.

5.3 THE EVALUATION OF DATA

Because the variation of δ_{obs} is related to the proportion of solute complexed, through (5.5), it is possible to measure the shifts of a series of samples and use them to deduce values for K and Δ_c for the interaction.

In general this is achieved by employing two basic procedures, both of which are based on equation (5.5) or (5.8). The first is an iterative procedure suggested by Creswell and Allred[106] and the second is an extrapolation method modified from that originally proposed by Benesi and Hildebrand[107]. Both procedures will now be discussed briefly.

The method developed by Creswell and Allred makes use of equations (5.5) and (5.9) with K defined on a suitable concentration scale. Normally the activity coefficients of all the interacting species are neglected, and (5.9) is reduced to (5.10), so that an equilibrium quotient is used. For example, in terms of mole fractions, the equilibrium quotient is defined by

$$K_x = \frac{n_{AB}(n_S + n_A + n_B - n_{AB})}{(n_A - n_{AB})(n_B - n_{AB})} \qquad (5.11)$$

where n_S and n_B are the initial numbers of moles of the inert and aromatic solvent respectively. This method assumes that only 1:1 molecular complexes are formed. It is obvious from (5.5) that a plot of δ_{obs} versus n_{AB}/n_A, for a series of samples with a range of concentrations of solvent mixtures (B and S), should be linear with a gradient of Δ_c and an intercept of δ_{free}. Since n_{AB} cannot be determined directly, an iterative procedure must be employed in which different values of K_x are chosen and n_{AB}/n_A evaluated for each sample. When a value for K_x is found for which the dependent values of n_{AB}/n_A plotted against the corresponding δ_{obs} values give a straight line, then K_x is considered to be correct. In this way K_x and Δ_c can be evaluated. Because the whole process depends on a tedious search for the right value of K_x, it is normally achieved by the use of a computer.

The Benesi-Hildebrand method[108-110] is usually applied to data relating

to the formation of a 1:1 complex. As in the previous case the activity coefficients of the interacting species in the equilibrium expression are neglected. Another condition which is necessary for this method is that $[B]_o >> [A]_o$, where $[B]_o$ and $[A]_o$ are the initial concentration of B and A respectively, defined on any concentration scale, so that the amount of B used in forming a complex can be neglected. By applying these conditions, the original form of the Benesi-Hildebrand equation is obtained as

$$\frac{1}{\Delta_{obs}} = \frac{1}{K\,[B]_o\,\Delta_c} + \frac{1}{\Delta_c} \qquad (5.12)$$

Thus a plot of $1/\Delta_{obs}$ against $1/[B]_o$ should give a straight line, from which K and Δ_c values are obtainable from the slope and intercept of the line.

It has been a matter of considerable concern that, when evaluating data for any reaction employing the above procedures, apparent anomalies concerning the values of Δ_c and K have been found[110-112]. The most significant of these are

(a) when a particular set of experimental data is processed, the value of Δ_c obtained is found to depend on the concentration scale employed in the processing method and

(b) when a particular reaction is studied in different inert solvents, different values of Δ_c are obtained.

Homer et al[113] have critically studied the validity of both procedures and concluded that these anomalies arise from the facts that

(i) equation (5.5) is not strictly correct and is not interpreted correctly and

(ii) the concentration ranges over which the experimental data have

been obtained are such that the methods by which they are processed are unsound.

In addition to this, the authors have suggested a procedure to be adopted in processing the data in order to obtain reliable K and Δ_c values. In doing so certain conditions have to be fulfilled which are as follows:

a) Meaningful values of K and Δ_c can be obtained in terms of either mole fractions, molarities or molalities only when x_B approaches unity and K (and Δ_c) becomes independent of the concentration of B and activity coefficients of all species. This is found to be fulfilled when the concentration range of B varies approximately from 0.80 - 1.00 mole fraction and $x_A \rightarrow 0$;

b) In order to obtain K and Δ_c as in a), the Benesi-Hildebrand equation (5.12) must be used for data processing and the required parameters obtained from the tangent to the relevant curve at $x_S = 0$. Moreover, the equation should be modified to account for the variation of the chemical shifts of the "free" species with the composition of the mixture. However, because Jackson[14] has found for reactions similar to those studied here that making an allowance for this variation has little effect on the values of K and Δ_c obtained, it will be neglected in the present study;

c) When the mole fraction or molal concentration scale is employed, the size or volume of the inert solvent has to be taken into consideration in equation (5.5) and hence, in the equilibrium expression. This is made to account statistically for the chance the solute has of interacting with either an active or inert solvent molecule. To achieve this, the actual number of moles of the inert solvent, n_S, has to be converted into the appropriate number of moles of the aromatic solvent which have been replaced. Since one molecule of the inert solvent, to an approximation, behaves as V_S/V_B molecules of inert B, n_S should be replaced by $n_S V_S/V_B$

where V_S and V_B are the molar volumes of S and B respectively;

d) When the molar scale is employed, the correction for n_S is unnecessary since it is implicit in the scale;

e) The Creswell and Allred method is found to be unreliable for obtaining K and Δ_c when applied over the whole concentration range but values of ΔH° obtained by this method are still considered to be meaningful.

Jackson[14] has suggested that only a small portion, around 0.005 mole fraction of the total reaction mixture, can be considered as the actual solute and the rest as diluent solvent and thus converted into equivalent moles of the aromatic by multiplying it by the ratio V_A/V_B. Since the present work employs only about 0.005 mole fraction of the solute in each sample, this correction need not be considered further.

The present n.m.r. investigations have been designed to satisfy the experimental conditions described above including the conditions for processing the data on the mole fraction scale.

5.4 STUDIES AT VARIOUS TEMPERATURES

If the presence of any specific complex can be detected from a study of solvent-induced shifts as indicated in the previous sections, the shifts should be temperature dependent. This is expected because the equilibrium quotients which initially govern the shifts should also be temperature dependent. This has been found to be true in the past when n.m.r. investigations at various temperatures have been made[15,25]. It thus follows from section 1.5.3 that by performing n.m.r. measurements at different temperatures, and obtaining the corresponding values of K, the thermodynamic parameters ΔH°, ΔG°, and ΔS° for the interactions can be deduced. These parameters are useful in investigating the strength

of the complex and factors affecting its formation. ΔH° is of special interest because its constancy with temperature provides helpful evidence in establishing the presence of a single complex (or isomeric complexes) within the system of interest. The evaluation of ΔH°, ΔG° and ΔS° in the present work is made according to the relations given previously in section 1.5.3.

5.5 EXPERIMENTAL

The chemicals employed in the present work were benzene (spectrosol), cyclohexane (spectrosol), acetonitrile (spectrosol), p-xylene (BDH), mesitylene (BDH), nitromethane (BDH) and chloroform (analar). Examination by GLC of these chemicals revealed no impurities and they were used without further purification.

The various three-component systems studied were chloroform-mesitylene-cyclohexane, nitromethane-benzene-cyclohexane, nitromethane-p-xylene-cyclohexane, nitromethane-mesitylene-cyclohexane, acetonitrile-benzene-cyclohexane, acetonitrile-p-xylene-cyclohexane and acetonitrile-mesitylene-cyclohexane.

For each system a series of samples was prepared such that the mole fractions of the solutes were kept low and constant, i.e. about 0.005 for those involving chloroform and nitromethane and 0.006 for acetonitrile, with the mole fractions of the aromatics varying within the range 0.8 - 1.00. The sample compositions for each system are recorded in table 5.1 - 5.7.

All the ^{1}H spectra were obtained at 100 MHz using a Varian HA-100D spectrometer operating in field sweep mode with the frequencies of the chemical shifts measured by an electronic counter coupled with the

spectrometer. All systems were studied at five different temperatures within the range of 280 - 350K, except that of chloroform-mesitylene which has been studied similarly elsewhere. The measurements of temperatures higher and lower than 310K were made in the conventional way using standard ethylene glycol and methanol samples respectively. Both of these reference samples, together with the shift-temperature calibration charts, were supplied with the instrument. It was found that, once the temperature for each measurement was set, the temperature variation from sample to sample was normally less than $\pm$ 0.5K.

The data were processed on an ICL 1905 computer to obtain K_x and Δ_c values for each system. The program employed called BHCURVEFIT is based on the Benesi-Hildebrand equation, which is as discussed previously in section 5.3, given on mole fraction scale by

$$\frac{1}{\Delta_{obs}} = \frac{1}{x_B K_x \Delta_c} + \frac{1}{\Delta_c} \qquad (5.13)$$

The gradient and intercept were taken at $x_B = 1.0$ to yield K_x and Δ_c. The corrected aromatic mole fractions were calculated using the equation

$$x_B = \frac{n_B}{n_A + n_B + n_S(V_S/V_B)} \qquad (5.14)$$

These corrected values, together with the corresponding values of observed solvent-induced shift, required as computer input data, are recorded in tables 5.8 - 5.14. The densities of the various species needed for the bulk corrections in (5.14) are recorded in table 5.15 and the values required at the different temperatures, at which measurements of samples were made, were obtained from linear plots of the data given elsewhere[114].

TABLE 5.1

SAMPLE COMPOSITION FOR THE NITROMETHANE-BENZENE-CYCLOHEXANE SYSTEM

Sample	Moles of nitro-methane/10^{-5}	Moles of benzene/10^{-3}	Moles of cyclohexane/10^{-3}
A	6.2909	0.0000	16.5613
B	7.4377	13.3701	3.2475
C	7.0282	14.2184	2.4506
D	7.5524	14.6921	1.8925
E	8.2405	15.1211	1.5928
F	9.2398	15.3314	1.2603
G	9.2398	15.7816	1.0166
H	7.3231	15.9808	0.6012
I	8.0767	16.1473	0.4248
J	9.0432	16.3734	0.2489
K	7.4377	16.5049	0.0876

TABLE 5.2

SAMPLE COMPOSITION FOR THE NITROMETHANE-P-XYLENE-CYCLOHEXANE SYSTEM

Sample	Moles of nitromethane/10^{-5}	Moles of p-xylene/10^{-3}	Moles of cyclo-hexane/10^{-3}
A	6.2909	0.0000	16.5613
B	9.8460	13.3783	3.2284
C	7.8636	14.1567	2.4734
D	8.7319	15.0617	1.6062
E	9.4364	15.3968	1.2705
F	7.4049	15.6767	0.9206
G	10.2391	16.0524	0.6660
H	9.0104	16.3163	0.2395
I	9.4364	16.5583	0.1299

TABLE 5.3

SAMPLE COMPOSITION FOR THE NITROMETHANE-MESITYLENE-CYCLOHEXANE SYSTEM

Sample	Moles of nitromethane/10^{-5}	Moles of mesitylene/10^{-3}	Moles of cyclohexane/10^{-3}
A	6.2909	0.0000	16.5613
B	8.3715	13.3263	3.2398
C	7.4377	14.3735	2.2654
D	7.1101	14.5078	2.1163
E	8.6828	14.6688	1.9261
F	10.0426	15.0479	1.5690
G	8.0603	15.3454	1.2265
H	7.7326	15.6897	0.9251
I	7.8473	16.0056	0.5945
J	7.3394	16.1413	0.4256
K	8.2405	16.3200	0.2419
L	7.3558	16.4799	0.0826

TABLE 5.4

SAMPLE COMPOSITION FOR THE CHLOROFORM-MESITYLENE-CYCLOHEXANE SYSTEM

Sample	Moles of chloroform/10^{-5}	Moles of mesitylene/10^{-3}	Moles of cyclohexane/10^{-3}
A	7.9912	0.0000	16.6179
B	6.1735	13.3343	3.2862
C	6.4918	14.1611	2.4743
D	6.0060	15.0051	1.6207
E	6.5253	15.3658	1.3455
F	6.5421	15.6926	0.9936
G	6.1233	15.9885	0.5942
H	6.8688	16.2833	0.3016
I	8.3598	16.4931	0.1343

TABLE 5.5

SAMPLE COMPOSITION FOR THE ACETONITRILE-BENZENE-CYCLOHEXANE SYSTEM

Sample	Moles of acetonitrile/10^{-5}	Moles of benzene/10^{-3}	Moles of cyclohexane/10^{-3}
A	9.9630	0.0000	16.5767
B	11.1079	13.2800	3.2269
C	10.6694	14.1612	2.4195
D	14.5425	14.7185	1.8954
E	11.4976	15.0191	1.5600
F	13.3976	15.3174	1.2210
G	12.4496	15.6977	1.0183
H	12.0822	16.1029	0.6613
I	12.2284	16.1703	0.4293
J	10.6450	16.3467	0.2968
K	11.1566	16.6054	0.0876

TABLE 5.6

SAMPLE COMPOSITION FOR THE ACETONITRILE-P-XYLENE-CYCLOHEXANE SYSTEM

Sample	Moles of acetonitrile/10^{-5}	Moles of p-xylene/10^{-3}	Moles of cyclohexane/10^{-3}
A	9.9630	0.0000	16.5767
B	9.8168	13.2989	3.2520
C	10.9617	14.1710	2.4181
D	11.1809	14.7707	1.9153
E	10.7425	15.0285	1.5447
F	13.3002	15.4127	1.1983
G	11.5950	15.6386	0.9229
H	10.3527	15.9822	0.6032
I	11.1809	16.1408	0.4045
J	13.3732	16.3281	0.2584
K	9.8168	16.5184	0.1321

TABLE 5.7

SAMPLE COMPOSITION FOR THE ACETONITRILE-MESITYLENE-CYCLOHEXANE SYSTEM

Sample	Moles of acetonitrile/10^{-5}	Moles of mesitylene/10^{-3}	Moles of cyclohexane/10^{-3}
A	9.9630	0.0000	16.5767
B	9.5245	13.5720	3.5926
C	15.2733	14.3611	2.4765
D	10.8886	14.6790	1.9826
E	11.6681	14.9912	1.6464
F	10.4014	15.2934	1.4847
G	12.0335	15.6373	0.9117
H	9.7681	16.0193	0.6332
I	10.5476	16.1788	0.3809
J	11.2053	16.3427	0.2547
K	10.8399	16.5382	0.0863

TABLE 5.8

THE CORRECTED AROMATIC MOLE FRACTION (x_B), δ_{obs} AND Δ_{obs} VALUES AT 100 MHz AND VARIOUS TEMPERATURES FOR THE NITROMETHANE-BENZENE CYCLOHEXANE SYSTEM

Temperature/ K	Sample	x_B	δ_{obs}/Hz	Δ_{obs}/Hz
291.0	B	0.7719	-161.52	100.53
	C	0.8266	-159.17	102.88
	E	0.8864	-156.85	105.20
	F	0.9091	-156.15	105.90
	G	0.9273	-155.66	106.39
	H	0.9562	-154.99	107.06
	I	0.9690	-154.55	107.50
	J	0.9818	-154.21	107.84
	K	0.9936	-153.89	108.16
306.4	B	0.7719	-167.20	95.03
	C	0.8266	-164.91	97.32
	D	0.8645	-163.70	98.53
	E	0.8864	-162.59	99.64
	F	0.9091	-162.07	100.16
	G	0.9273	-161.48	100.75
	H	0.9562	-160.39	101.84
	I	0.9690	-160.01	102.22
	J	0.9818	-159.80	102.43
	K	0.9936	-159.22	103.01
318.7	B	0.7719	-173.46	86.72
	C	0.8266	-171.21	88.97
	D	0.8645	-169.79	90.39
	E	0.8864	-169.02	91.16
	F	0.9091	-168.14	92.04
	G	0.9273	-167.57	92.61

TABLE 5.8 (Cont.)

Temperature/ K	Sample	x_B	δ_{obs}/Hz	Δ_{obs}/Hz
	H	0.9562	-166.47	93.71
	I	0.9690	-166.16	94.02
	J	0.9818	-165.71	94.47
	K	0.9936	-165.28	94.90
326.5	B	0.7719	-175.74	84.69
	C	0.8266	-173.16	87.27
	D	0.8645	-171.06	89.37
	E	0.8864	-170.22	90.21
	F	0.9091	-169.66	90.77
	G	0.9273	-168.68	91.75
	H	0.9562	-168.30	92.13
	J	0.9818	-167.95	92.48
	K	0.9936	-167.56	92.87
354.2	B	0.7719	-184.58	75.28
	C	0.8266	-182.36	77.50
	D	0.8645	-180.91	78.95
	E	0.8864	-179.98	79.88
	F	0.9091	-179.16	80.70
	G	0.9273	-178.61	81.25
	H	0.9562	-177.53	82.33
	J	0.9818	-176.76	83.10
	K	0.9936	-176.33	83.53

TABLE 5.9

THE CORRECTED AROMATIC MOLE FRACTION (x_B), δ_{obs} and Δ_{obs} VALUES AT 100MHz AND VARIOUS TEMPERATURES FOR THE NITROMETHANE-P-XYLENE-CYCLOHEXANE SYSTEM

Temperature/ K	Sample	x_B	δ_{obs}/Hz	Δ_{obs}/Hz
295.9	C	0.8671	-168.30	93.65
	D	0.9144	-166.48	95.47
	E	0.9325	-165.87	96.08
	F	0.9510	-165.26	96.69
	G	0.9649	-164.85	97.10
	H	0.9873	-164.24	97.71
	I	0.9932	-163.95	98.00
304.3	B	0.8250	-172.87	88.90
	C	0.8668	-171.28	90.49
	D	0.9143	-169.37	92.40
	E	0.9323	-168.83	92.94
	F	0.9509	-168.15	93.62
	G	0.9648	-167.56	94.21
	H	0.9873	-166.91	94.86
321.5	C	0.8664	-178.57	83.10
	D	0.9140	-176.66	85.01
	E	0.9321	-176.08	85.59
	F	0.9507	-175.36	86.31
	G	0.9647	-175.01	86.66
	H	0.9872	-174.35	87.22
	I	0.9931	-174.14	87.53

TABLE 5.9 (Cont.)

Temperature/ K.	Sample	x_B	δ_{obs}/Hz	Δ_{obs}/Hz
330.9	C	0.8662	-182.10	78.95
	D	0.9138	-180.41	80.64
	E	0.9320	-179.60	81.45
	F	0.9506	-179.10	81.95
	G	0.9646	-178.59	82.46
	H	0.9872	-177.94	83.11
	I	0.9931	-177.78	83.27
341.1	C	0.8659	-185.35	75.74
	D	0.9136	-183.47	77.62
	E	0.9318	-182.82	78.27
	F	0.9505	-182.18	78.91
	G	0.9645	-181.85	79.24
	H	0.9871	-181.14	79.95
	I	0.9931	-180.98	80.11

TABLE 5.10

THE CORRECTED AROMATIC MOLE FRACTION(x_B), δ_{obs} AND Δ_{obs} VALUES AT 100MHz AND VARIOUS TEMPERATURES FOR THE NITROMETHANE-MESITYLENE-CYCLOHEXANE SYSTEMS

Temperature/ K	Sample	x_B	δ_{obs}/ Hz	Δ_{obs}/ Hz
295.4	B	0.8408	-170.32	91.63
	C	0.8907	-168.42	93.53
	E	0.9072	-167.68	94.27
	G	0.9414	-166.42	95.53
	H	0.9561	-165.76	96.19
	I	0.9719	-165.24	96.71
	J	0.9799	-164.91	97.04
	K	0.9886	-164.57	97.38
	L	0.9961	-164.37	97.58
307.8	B	0.8402	-175.11	86.82
	C	0.8903	-172.88	89.05
	E	0.9069	-172.46	89.47
	G	0.9412	-170.94	90.99
	I	0.9718	-169.74	92.19
	J	0.9798	-169.51	92.42
	K	0.9885	-169.26	92.67
	L	0.9961	-169.01	92.92
321.1	B	0.8398	-182.11	79.41
	C	0.8900	-180.06	81.46
	E	0.9066	-179.30	82.22
	G	0.9410	-178.25	83.27
	H	0.9558	-177.70	83.82
	I	0.9717	-177.01	84.51
	J	0.9797	-176.76	84.76
	K	0.9885	-176.52	85.00
	L	0.9961	-176.31	85.21

TABLE 5.10 (Cont.)

Temperature/ K	Sample	x_B	δ_{obs}/ Hz	Δ_{obs}/ Hz
331.4	B	0.8394	-185.68	75.23
	C	0.8896	-183.76	77.15
	G	0.9408	-181.92	78.99
	H	0.9556	-181.36	79.55
	I	0.9716	-180.73	80.18
	J	0.9797	-180.37	80.54
	K	0.9885	-180.14	80.77
	L	0.9961	-179.92	80.99
341.3	B	0.8388	-189.05	71.68
	C	0.8892	-187.04	73.69
	F	0.9239	-185.82	74.91
	G	0.9406	-185.28	75.45
	H	0.9555	-184.73	76.00
	I	0.9715	-184.01	76.72
	J	0.9796	-183.72	77.01
	K	0.9884	-183.46	77.27
	L	0.9960	-183.19	77.54

TABLE 5.11

THE CORRECTED AROMATIC MOLE FRACTION (x_B), δ_{obs} AND Δ_{obs} VALUES AT 100MHz AND VARIOUS TEMPERATURES FOR THE ACETONITRILE-BENZENE-CYCLOHEXANE SYSTEM

Temperature/ K	Sample	x_B	δ_{obs}/ Hz	Δ_{obs}/ Hz
281.4	B	0.7718	73.79	103.87
	C	0.8279	76.48	106.56
	D	0.8645	77.70	107.78
	E	0.8878	78.99	109.07
	F	0.9116	79.23	109.31
	G	0.9268	80.01	110.09
	H	0.9524	80.96	111.04
	I	0.9687	81.27	111.35
	J	0.9784	81.59	111.67
	K	0.9936	82.19	112.27
305.8	B	0.7718	65.36	91.78
	C	0.8279	68.30	94.72
	D	0.8645	69.62	96.04
	E	0.8878	70.99	97.41
	F	0.9116	71.56	97.98
	G	0.9268	72.15	98.57
	I	0.9687	73.73	100.15
	J	0.9784	74.20	100.62
	K	0.9936	74.82	101.24
319.7	B	0.7718	59.31	86.13
	D	0.8645	63.17	89.99
	E	0.8878	64.50	91.32
	F	0.9116	65.26	92.08
	G	0.9268	65.84	92.66
	H	0.9524	67.15	93.97

TABLE 5.11 (Cont.)

Temperature/ K	Sample	x_B	δ_{obs}/ Hz	Δ_{obs}/ Hz
	I	0.9687	67.63	94.45
	J	0.9784	68.14	94.96
	K	0.9936	68.73	95.55
326.8	B	0.7718	57.07	83.35
	C	0.8279	59.83	86.11
	D	0.8645	61.08	87.36
	E	0.8878	62.31	88.59
	F	0.9116	63.02	89.30
	G	0.9268	63.68	89.96
	H	0.9524	64.81	91.09
	I	0.9687	65.55	91.83
	J	0.9784	65.92	92.20
	K	0.9936	66.49	92.77
341.3	B	0.7718	52.50	78.24
	C	0.8279	55.26	81.00
	E	0.8878	57.78	83.52
	F	0.9116	58.57	84.31
	G	0.9268	59.17	84.91
	H	0.9524	60.38	86.12
	I	0.9687	61.04	86.78
	J	0.9784	61.50	87.24
	K	0.9936	61.93	87.67

TABLE 5.12

THE CORRECTED AROMATIC MOLE FRACTION (x_B), δ_{obs} and Δ_{obs} VALUES AT 100MHz AND VARIOUS TEMPERATURES FOR THE ACETONITRILE-P-XYLENE-CYCLOHEXANE SYSTEM

Temperature/ K	Sample	x_B	δ_{obs}/ Hz	Δ_{obs}/ Hz
290.4	B	0.8235	59.06	87.14
	C	0.8699	61.05	89.13
	D	0.8980	62.14	90.22
	E	0.9174	62.96	91.04
	F	0.9362	63.47	91.55
	G	0.9508	64.11	92.19
	H	0.9680	65.05	93.13
	I	0.9785	65.31	93.39
	J	0.9863	65.53	93.61
305.6	B	0.8230	55.79	82.39
	C	0.8695	57.95	84.55
	D	0.8976	59.03	85.63
	F	0.9360	60.69	87.29
	G	0.9507	61.28	87.88
	H	0.9679	61.94	88.54
	I	0.9784	62.22	88.82
	J	0.9836	62.51	89.11
318.6	B	0.8227	50.58	77.35
	C	0.8692	52.59	79.36
	D	0.8974	53.64	80.41
	E	0.9169	54.43	81.20
	F	0.9358	55.00	81.77
	G	0.9506	55.67	82.44
	H	0.9678	56.53	83.30

TABLE 5.12 (Cont.)

Temperature/ K	Sample	x_B	δ_{obs}/ Hz	Δ_{obs}/ Hz
	I	0.9784	56.81	83.58
	J	0.9862	56.93	83.70
326.8	B	0.8224	48.14	74.46
	C	0.8690	49.97	76.29
	D	0.8972	51.05	77.37
	E	0.9168	51.93	78.25
	F	0.9357	52.39	78.71
	G	0.9504	53.16	79.48
	H	0.9677	53.89	80.21
	I	0.9783	54.21	80.53
	J	0.9862	54.36	80.68
341.7	B	0.8218	43.63	69.47
	C	0.8686	45.60	71.44
	D	0.8969	46.81	72.65
	E	0.9165	47.70	73.54
	F	0.9355	48.15	73.99
	G	0.9503	48.88	74.72
	H	0.9676	49.50	75.34
	I	0.9783	49.78	75.62
	J	0.9862	49.97	75.81

TABLE 5.13

THE CORRECTED AROMATIC MOLE FRACTION (x_B), δ_{obs} AND Δ_{obs} VALUES AT 100 MHz AND VARIOUS TEMPERATURES FOR THE ACETONITRILE-MESITYLENE-CYCLOHEXANE SYSTEM

Temperature/ K	Sample	x_B	δ_{obs}/ Hz	Δ_{obs}/ Hz
293.3	B	0.8292	56.29	85.36
	D	0.9049	59.70	88.77
	E	0.9213	60.22	89.29
	F	0.9297	60.75	89.82
	G	0.9566	61.80	90.87
	H	0.9702	62.48	91.55
	I	0.9820	63.05	92.12
	J	0.9880	63.30	92.37
	K	0.9959	63.56	92.63
304.7	B	0.8288	51.90	78.54
	C	0.8814	54.50	81.14
	D	0.9046	55.56	82.20
	E	0.9211	56.21	82.85
	F	0.9296	56.60	83.24
	G	0.9565	57.44	84.08
	H	0.9701	58.03	84.67
	I	0.9819	58.44	85.08
	J	0.9880	58.70	85.34
	K	0.9959	58.80	85.44
319.3	B	0.8282	45.95	72.16
	D	0.9043	49.27	75.48
	E	0.9207	49.82	76.03
	F	0.9293	50.42	76.63
	G	0.9563	51.21	77.42

TABLE 5.13 (Cont.)

Temperature/K	Sample	x_B	δ_{obs}/Hz	Δ_{obs}/Hz
	H	0.9699	52.01	78.22
	I	0.9819	52.42	78.63
	J	0.9879	52.55	78.76
	K	0.9959	52.91	79.12
326.7	B	0.8278	43.39	69.72
	D	0.9040	46.89	73.32
	E	0.9205	47.69	74.02
	F	0.9291	48.13	74.46
	G	0.9562	49.06	75.39
	H	0.9699	49.69	76.02
	I	0.9818	50.04	76.37
	J	0.9879	50.23	76.56
	K	0.9959	50.55	76.88
337.9	B	0.8272	40.57	66.50
	D	0.9037	43.75	69.68
	E	0.9202	44.32	70.25
	F	0.9288	44.90	70.83
	G	0.9560	45.54	71.47
	H	0.9697	46.37	72.30
	I	0.9817	46.76	72.69
	J	0.9878	46.86	72.79
	K	0.9959	47.21	73.14

TABLE 5.14

THE CORRECTED AROMATIC MOLE FRACTION (x_B), δ_{obs} and Δ_{obs} VALUES AT 100MHz AND 308.1 K FOR THE CHLOROFORM-MESITYLENE-CYCLOHEXANE SYSTEM

Sample	x_B	δ_{obs}/Hz	Δ_{obs}/Hz
B	0.8384	-465.28	99.13
C	0.8798	-463.38	101.03
D	0.9221	-461.43	102.98
E	0.9359	-460.74	103.67
F	0.9528	-460.20	104.21
G	0.9718	-459.10	105.31
H	0.9857	-458.49	105.92
I	0.9937	-458.31	106.10

TABLE 5.15

DENSITIES OF VARIOUS SUBSTANCES AT DIFFERENT TEMPERATURES

Substance	Density/10^{-3} kgm^{-3}		
	293.2K	303.2K	313.2K
Cyclohexane	0.7785	0.7691	0.7594
Benzene	0.8791	0.8685	0.8575
p-Xylene	0.8609	0.8525	0.8437
Mesitylene	0.8653	0.8569	0.8485

5.6 RESULTS AND DISCUSSION

It is generally accepted that the parameters required for the investigations of complex structures are the additional screening (Δ_c) of the solute protons in the complex relative to that in the non-complexed state and the various thermodynamic parameters[15,25] for the reaction. However, it is not possible to obtain values for these until the solute/solvent ratio in each complex studied, and thus the stoichiometry of this, has been established. Even though the latter point has already been investigated through cryoscopy (chapter 4), there are still some systems needing further clarification because the results obtained from those studies are not conclusive.

5.6.a THE STOICHIOMETRY OF THE COMPLEX

Apart from cryoscopy, n.m.r. studies at various temperatures can also provide some information on the stoichiometry of a complex. It has been pointed out earlier[11] that the constancy of ΔH with temperature indicates the presence of a single complex species. In other words a plot of $\ln K_x$, calculated on the basis of 1:1 stoichiometry, versus 1/T (section 1.5.3) which gives a straight line (with a slope equal to $-\Delta H/R$) indicates the presence of a single (or a series of isomeric) 1:1 complex species, since their enthalpies of formation should be identical. For a system in which several complex species are present the plot should not be linear unless all the enthalpies are identical or similarly temperature independent, an unlikely possibility.

The other evidence which can be employed in conjunction with the above conclusion comes from the values of Δ_c. It is found[22,25,104,106] for those systems in which the formation of 1:1 complexes alone is well established, that there is little change in the values of Δ_c obtained

over a temperature range of 280-350K.

So far the only information about complex stoichiometries obtainable from cryscopy for systems of current interest is that both the chloroform-mesitylene and nitromethane-benzene systems result in a formation of 1:1 complex whereas a 1:2 acetonitrile:benzene complex is formed. It is evident that the other systems of interest require further consideration which may be possible through n.m.r. studies.

It has been shown recently from the latter studies[115] that the interactions between various methyl halides and benzene can be interpreted in terms of the formation of 1:1 complexes. Since the present investigations are focussed upon complexes formed between various methyl-substituted benzenes and nitromethane or acetonitrile (as solutes), which possess to some extent similar molecular structures to those of methyl halides, one would expect superficially that these complexes might also to possess 1:1 stoichiometry. Bearing this in mind, all the data in tables 5.8 - 5.14 were processed using the program BHCURVEFIT. The values of K_x and Δ_c obtained are recorded in table 5.16. It has to be pointed out that owing to the high sensitivity of K_x to experimental errors, the figures after the first decimal place for the values shown in the table are considered to be insignificant but they are quoted here as the original computer results obtained. To simplify the discussion, the results for the acetonitrile-benzene system will be discussed separately later on.

A perusal of table 5.16 shows that the values of Δ_c obtained for all the systems at various temperatures (within the range of 280-350K) do not show any regular or significant variation with temperature. On the contrary, they may be considered as constant for each particular system, with the maximum variation not exceeding $\pm$ 0.06 ppm. This, apart from

TABLE 5.16

THE K_x AND Δ_c VALUES FOR VARIOUS SOLUTE-AROMATIC SOLVENT SYSTEMS AT DIFFERENT TEMPERATURES

System	Temperature/K	K_x	Δ_c/ppm
Nitromethane-benzene	291.0	2.8102	1.469
	306.4	1.9455	1.563
	318.7	1.5769	1.555
	326.5	1.5026	1.571
	354.2	1.2239	1.522
Nitromethane-p-xylene	295.9	2.4621	1.401
	304.3	1.9499	1.441
	321.5	1.6993	1.420
	330.9	1.6530	1.344
	341.1	1.4927	1.376
Nitromethane-mesitylene	295.4	2.6988	1.364
	307.8	2.2963	1.335
	321.1	1.7482	1.342
	331.4	1.4331	1.377
	341.3	1.2684	1.389
Acetonitrile-benzene	281.4	1.9720	1.696
	305.8	1.3057	1.792
	319.7	1.1115	1.821
	326.8	0.9399	1.927
	341.3	0.8537	1.918
Acetonitrile-p-xylene	290.4	1.6982	1.494
	305.6	1.5720	1.466
	318.6	1.4190	1.436
	326.8	1.3583	1.410
	341.7	1.1574	1.426

TABLE 5.16 (CONT.)

System	Temperature/K	K_x	Δ_c/ppm
Acetonitrile-mesitylene	293.3	1.9464	1.382
	304.7	1.8593	1.316
	319.3	1.5921	1.289
	326.7	1.4101	1.335
	337.9	1.0655	1.421
Chloroform-mesitylene	308.1	2.1887	1.549
Chloroform-mesitylene[104]	277.1	3.522	1.691
	288.4	2.807	1.661
	304.8	2.272	1.595
	311.7	2.135	1.551
	322.1	1.782	1.554

confirming the cryoscopic result found for the nitromethane-benzene system, also supports the original assumption that the other systems possess 1:1 complex species.

The system chloroform-mesitylene, in which complexes of 1:1 stoichiometry have been well established[14,104], was studied only at ambient temperature simply to establish the accuracy of the present work by reference to that of other workers (see table 5.16). The values of K_x and Δ_c obtained by Whitney[104] at various temperatures for this system are included in table 5.16 for this purpose. These additionally show the constancy of Δ_c with temperature (the maximum variation is within $\pm$0.07ppm) for a system with well established 1:1 stoichiometry. In view of the fact that an extensive study and discussion of this system has already been reported by Whitney, further reference to it will not be made here.

In order to find out if the systems recorded in table 5.16 contain one or more comlex species, plots of $\ln K_x$ against the reciprocal of absolute temperature were made. It is found that all the plots show linearity (a typical diagram is shown in Fig. 5.1), indicating the constancy of ΔH with temperature and thus the presence of a single 1:1 complex species. This evidence, together with the other deduced from the constancy of Δ_c with temperature, enables the circumstantial conclusion to be drawn that for all systems studied, excluding that of acetonitrile-benzene for which the variation in Δ_c is c.a. 0.2 ppm, only complexes of 1:1 stoichiometry are formed.

THE ACETONITIRLE-BENZENE SYSTEM

The values of Δ_c, evaluated on the basis of 1:1 stoichiometry, obtained at various temperatures for the acetonitrile-benzene system appear to be anomalous and vary within the temperature range of the investigations by $\pm$ 0.12 ppm (table 5.16). This seems to be too large to be accounted for

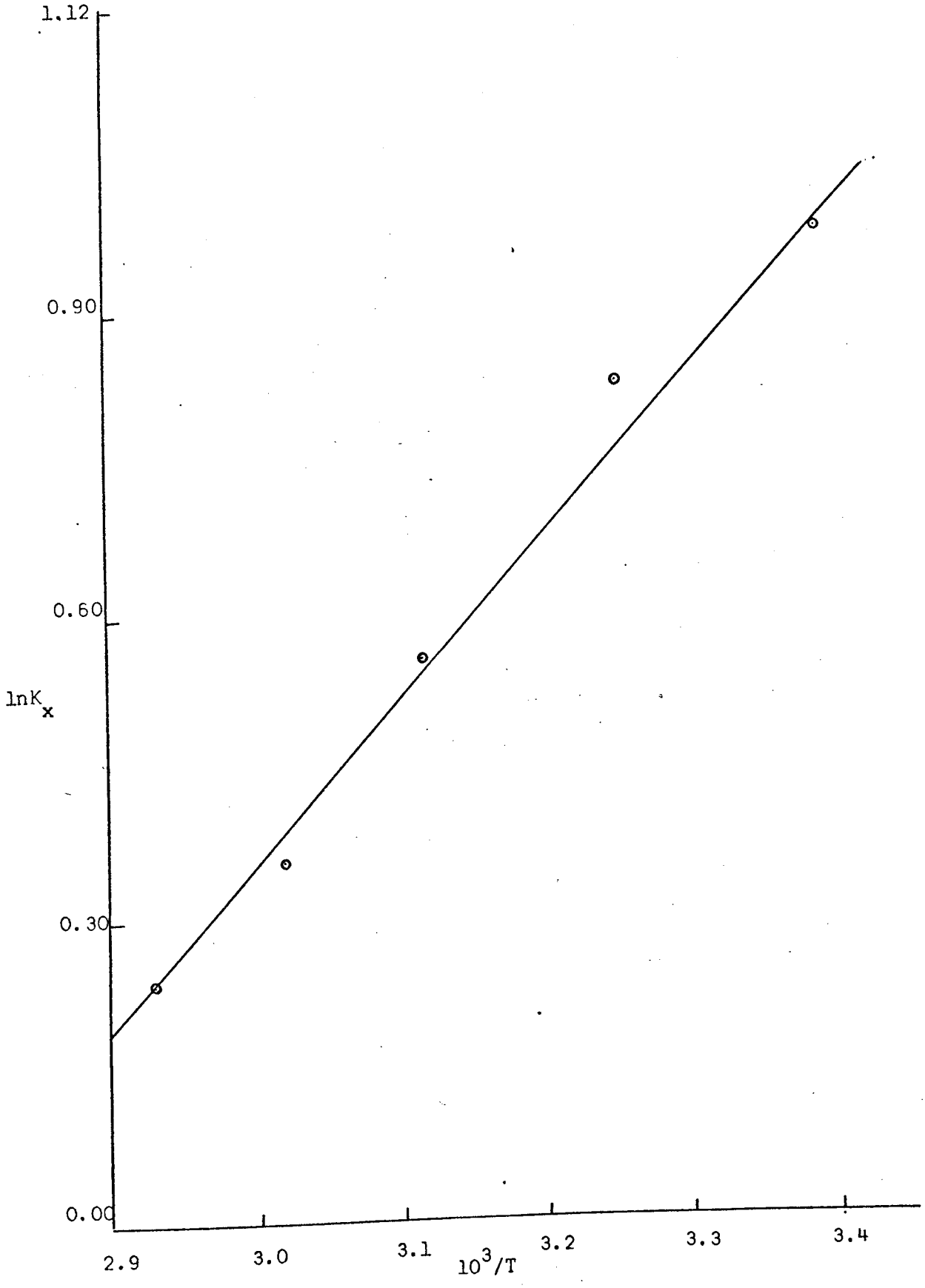

FIG. 5.1 RELATIONSHIP BETWEEN $\ln K_x$ AND RECIPROCAL OF ABSOLUTE TEMPERATURE FOR COMPLEXES OF NITROMETHANE-MESITYLENE SYSTEM

as experimental error so it may concluded that the interaction may result in the formation of complex species other than one of 1:1 stoichiometry. Certainly the results already obtained from cryoscopic studies of this system indicate that only 1:2 complexes are formed in the system. Further support for this conclusion comes from the plot of $\ln K_x$ (for 1:1 complex) against 1/T, which is found to be better fitted by a curve than a straight line (Fig.5.2). Further insight to this point is forthcoming from values of K_x and Δ_c calculated on the basis of 1:2 stoichiometry. To obtain these, some modifications of equations (5.10) and (5.14) have to be made, as follows:

For any system containing a single complex species of the type

$$A + nB \rightleftharpoons A.....B_n \qquad (5.15)$$

i.e. the complex possesses 1:n stoichiometry, (5.10) has to be changed to

$$K = \frac{[AB_n]}{[A]\ [B]^n} \qquad (5.16)$$

and on adopting the same conditions as in the basic Benesi-Hildebrand method, a similar expression to (5.14) can be deduced as

$$\frac{1}{\Delta_{obs}} = \frac{1}{K_x x_B^n \Delta_c} + \frac{1}{\Delta_c} \qquad (5.17)$$

It is evident that (5.17) is inapplicable for a system with a subsequent reaction represented by

$$A + B \rightleftharpoons AB \overset{B}{\rightleftharpoons} AB_2 \cdots \overset{B}{\rightleftharpoons} AB_n \qquad (5.18)$$

in other words, when several complex species are present in the same system. However, for a system containing only complexes of 1:2 stoichiometry (n=2), (5.17) can be written as

$$\frac{1}{\Delta_{obs}} = \frac{1}{K_x x_B^2 \Delta_c} + \frac{1}{\Delta_c} \qquad (5.19)$$

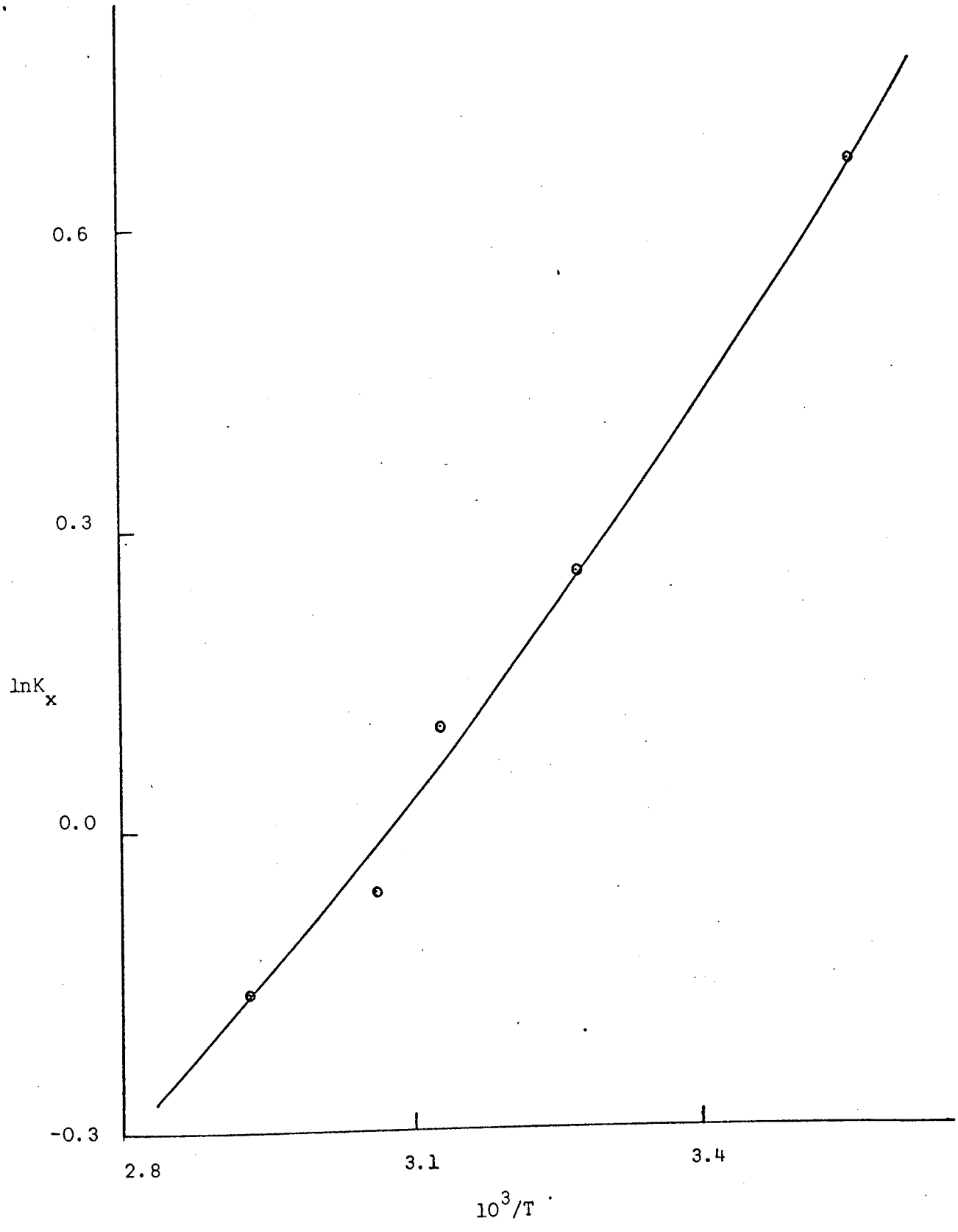

Fig. 5.2 RELATIONSHIP BETWEEN lnK$_x$ AND RECIPROCAL OF ABSOLUTE TEMPERATURE FOR COMPLEXES OF ACETONITRILE-BENZENE SYSTEM (K$_x$ CALCULATED ON THE BASIS OF 1:1 STOICHIOMETRY)

Equation (5.19) therefore was employed in the evaluation of the K_x and Δ_c values for this system with the criteria proposed by Homer et al[113] still applicable (c.f. equation (5.13)). Bearing this in mind all the data in table 5.12 were processed employing the program BHCURVEFIT (with x_B^2 values fed as input data instead of x_B values). The values of K_x and Δ_c so obtained are recorded in table 5.17.

A perusal of table 5.17 shows that the values of Δ_c obtained at different temperatures appear to be constant with maximum variation not more than $\pm$ 0.04 ppm. It is therefore likely from this evidence that the experimental observation regarding the constancy of Δ_c with temperature, previously adopted in systems with 1:1 complexes, can be extended to this

TABLE 5.17

K_x and Δ_c VALUES AT DIFFERENT TEMPERATURES FOR THE ACETONITRILE-BENZENE SYSTEM

Temperature/K	K_x	Δ_c/ppm
281.4	7.3636	1.276
305.8	5.1064	1.211
319.7	3.9215	1.202
326.8	3.5817	1.190
341.3	3.0080	1.221

case to confirm the existence of 1:2 complexes, provided values of Δ_c are evaluated on the latter basis. A plot of $\ln K_x$ (table 5.17) against 1/T for this system is shown in Fig. 5.3, from which it is seen that a straighter line is obtained than in Fig. 5.2, indicating the independence of ΔH of temperature. This evidence further supports the original results

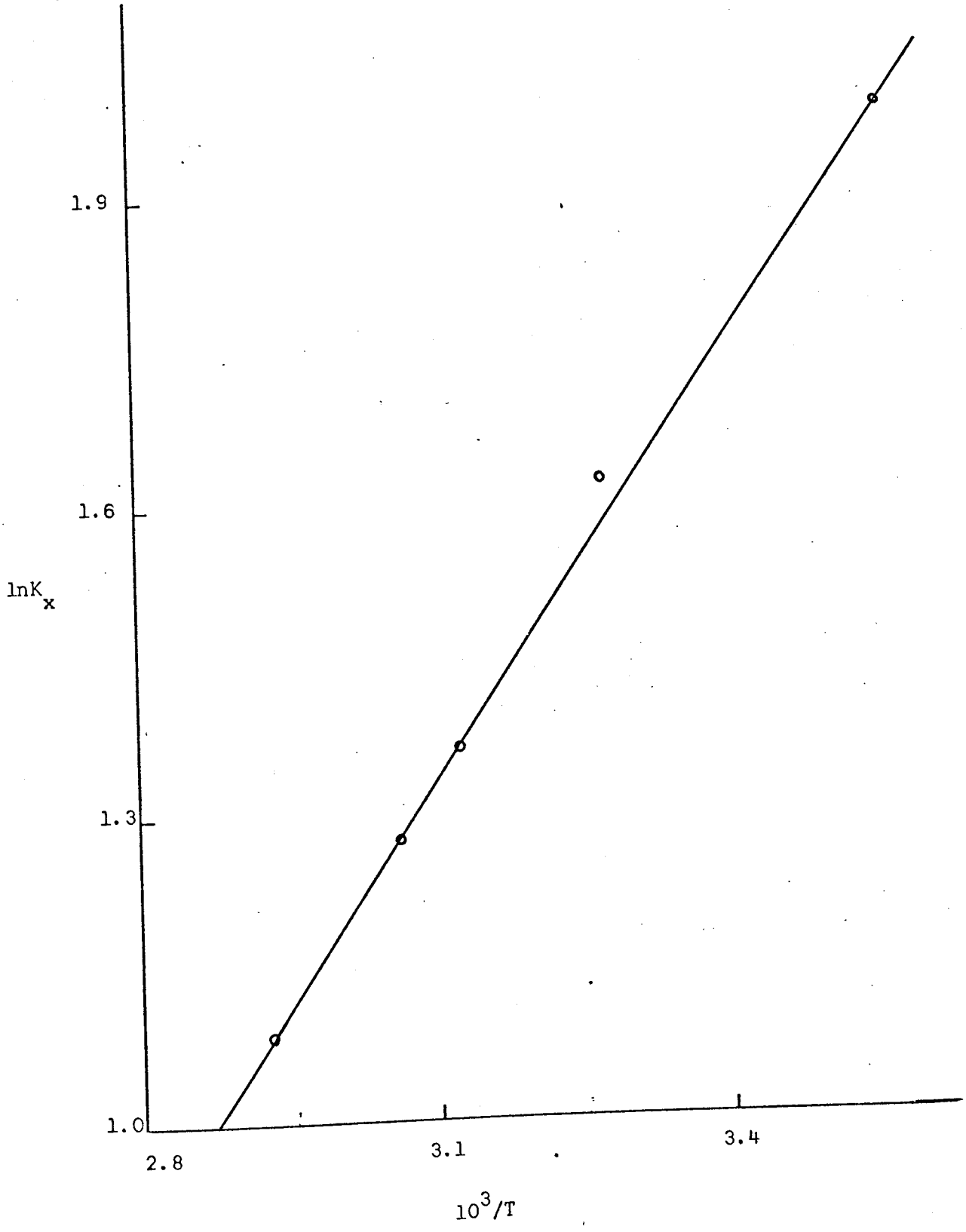

Fig.5.3 RELATIONSHIP BETWEEN lnK$_x$ AND RECIPROCAL OF ABSOLUTE TEMPERATURE FOR COMPLEXES OF ACETONITRILE-BENZENE SYSTEM (K$_x$ CALCULATED ON THE BASIS OF 1:2 STOICHIOMETRY)

interpreted from cryoscopic studies that only 1:2 complexes are formed in the acetonitrile-benzene system.

So far it is evident that by employing both cryoscopic and n.m.r. studies the stoichiometries of the interactions for all systems of interest in the present work can be established; these are recorded in table 5.18, together with the average corresponding Δ_c values. However, it is apparent from the above n.m.r. results that, to determine the stoichiometry of any complex without previous knowledge of cryoscopic studies, is in general difficult. Only by assuming the stoichiometry and interpreting the values of K_x and Δ_c evaluated on this basis can an indication be obtained as to whether or not this assumption is correct. In an attempt to obviate this speculative approach, a new method was proposed.

TABLE 5.18

STOICHIOMETRIES OF THE INTERACTIONS AND AVERAGE Δ_c VALUES FOR VARIOUS SOLUTE-AROMATIC SOLVENT SYSTEMS

System	Stoichiometry	Δ_c/ppm
Nitromethane-benzene	1:1	1.536
Nitromethane-p-xylene	1:1	1.396
Nitromethane-mesitylene	1:1	1.341
Acetonitrile-benzene	1:2	1.220
Acetonitrile-p-xylene	1:1	1.446
Acetonitrile-mesitylene	1:1	1.349

5.6.b A PROPOSAL FOR ELUCIDATING DIRECTLY THE STOICHIOMETRY OF A COMPLEX

It is seen from (5.17) that for a single complex species possessing 1:n

stoichiometry, one obtained a similar relation to that of the basic Benesi-Hildebrand equation viz:-

$$\frac{1}{\Delta_{obs}} = \frac{1}{K_x X_B^n \Delta_c} + \frac{1}{\Delta_c} \qquad (5.17)$$

If Δ_{max} represents that value of Δ_{obs} at $x_B = 1$, (5.17) reduces to

$$\frac{1}{\Delta_{max}} = \frac{1}{K_x \Delta_c} + \frac{1}{\Delta_c} = \frac{1}{\Delta_c}\left(\frac{1 + K_x}{K_x}\right)$$

or

$$\frac{1}{\Delta_c} = \frac{K_x}{(1 + K_x)\Delta_{max}} \qquad (5.20)$$

Combination of (5.17) and (5.20) gives

$$\frac{1}{\Delta_{obs}} = \frac{1}{x_B^n (1 + K_x)\Delta_{max}} + \frac{K_x}{(1 + K_x)\Delta_{max}}$$

which can be rearranged as

$$\frac{\Delta_{max}}{\Delta_{obs}} = \frac{1}{x_B^n(1 + K_x)} + \frac{K_x}{(1 + K_x)} \qquad (5.21)$$

Differentiation of (5.21) with respect to x_B leads to

$$\frac{\partial(\Delta_{max}/\Delta_{obs})}{\partial x_B} = \frac{+n}{x_B^{n-1}(1 + K_x)} \qquad (5.22)$$

Hence

$$\log\left(-\partial(\Delta_{max}/\Delta_{obs})/\partial x_B\right) = \log n - (n-1)\log x_B - \log(1 + K_x) \qquad (5.23)$$

It is evident from (5.22) and (5.23) that by plotting $\Delta_{max}/\Delta_{obs}$ versus x_B, the gradients of the curve at various values of x_B can be evaluated. If the log of these values is then plotted against corresponding log x_B the slope of the new curve at $x_B = 1$ yields n - 1, and hence the stoichiometry of the complex. The value of K_x can also be deduced from the

intercept. However, if a value of K_x is obtained in this case from a log function (equation (5.23)), any slight variation of the intercept (which is found to be small) can cause such a large discrepancy in K_x that it is unreliable.and so it should be deduced instead from (5.17).

Adopting this new approach, four sets of data (table 5.8 - 5.13) at different temperatures for each system were processed by a program MODCURVEFIT to obtain gradients at various x_B values from the plot of $\Delta_{max} / \Delta_{obs}$ against x_B, which were then used finally to evaluate n in the same way as described above. The results obtained are recorded in table 5.19.

A perusal of table 5.19 shows that for each system only two sets of data out of four processed yield correct values of n (c.f. table 5.18). The other two either give lower or much higher values of n than expected (in one case up to n = 8) which indicate that the results still cannot be considered conclusive.

TABLE 5.19

STOICHIOMETRIES OF THE INTERACTIONS DEDUCED BY THE NEW APPROACH FOR VARIOUS SOLUTE-AROMATIC SOLVENT SYSTEMS AT DIFFERENT TEMPERATURES

System	Stoichiometry (1:n)			
	281-296.0K	304.0-308.0K	318.0 - 321.5K	326.5-331.5K
Nitromethane-benzene	1:1	1:1	1:6	1:8
Nitromethane-p-xylene	1:4	1:1	1:2	1:1
Nitromethane-mesitylene	1:2	1:1	1:5	1:1
Acetonitrile-benzene	1:1	1:2	1:2	1:3
Acetonitrile-p-xylene	1:1	1:1	1:4	1:5
Acetonitrile-mesitylene	1:4	1:1	1:1	1:6

The approach appears to be highly sensitive to the data processed such that a wide range of values forn is obtained. Although it is encouraging in view of the fact that some correct results are obtained, it has to be concluded under the present circumstances that the approach cannot be adapted for the required purpose. It thus follows that, to produce conclusive results, further (and significant) improvements are required mainly in the accuracy of the experimental measurements. Due to a paucity of time, no further investigations of this method were made.

According to section 5.4 n.m.r. studies at various temperatures, apart from giving support to the deduction of complex stoichiometries from cryoscopic studies, can also be used in the evaluation of various thermodynamic parameters (ΔH°, ΔS° and ΔG°) for the interactions. These are essential in elucidating the nature and "strength" of complexes. However, it seems more appropriate to consider the strength after the nature of the interactions has been well established. For this reason the presentation (including the discussion) of the values for these thermodynamic parameters is postponed for the time being.

CHAPTER 6

DIELECTRIC STUDIES OF MOLECULAR COMPLEXES

INTRODUCTION

The studies described so far were directed towards elucidating the stoichiometries of some molecular complexes. The aim of the work reported in the present chapter is to establish the nature of the interactions by studies of the dielectric constants of mixtures containing the active species. Also, at the same time, an attempt is made to evaluate the equilibrium quotients for various interactions to see if they are compatible with those obtained from n.m.r. studies.

PART A: THE DETERMINATION OF THE EQUILIBRIUM QUOTIENTS FOR VARIOUS INTERACTIONS THROUGH DIELECTRIC POLARISATION STUDIES

6.1 INTRODUCTION

Several workers have earlier employed dielectric studies as a potential means not only for detecting the formation of weak complexes in solutions, but also for determining the extent to which such complexes are formed. Earp and Glasstone[116] have studied an interaction between two substances A and B which yield a complex AB (of 1:1 stoichiometry) by dielectric polarisation calculations. They have made the assumption in their method that, when a solute (A) is infinitely dilute in an active solvent (B), all of the solute is in the form of the complex and thence calculated the amount of solute taking part in the interaction and also the equilibrium constant for the system. However, their assumption is obviously misleading and the method was criticised by Hammick et al[117] who, in turn, have proposed several alternative methods, one of which was applied by Few and Smith[118]. The method involved the determinations of the apparent molecular polarisations at infinite

dilutions of A in B, in an inert solvent S and in mixtures of B and S, which were finally used to calculate the equilibrium constants. It was later employed by several groups of workers[119,120] in studies of interactions between various alcohols and pyridine.

The purpose of the studies in the present section is to apply, through polarisation determinations, a new approach to the evaluation of equilibrium quotients (K) for various molecular interactions studied previously by n.m.r. By employing the criteria described in section 5.3, it is expected that both studies should give compatible results. An advantage gained in adopting this approach is that no polarisations at infinite dilutions of any interacting species are needed, since they require extrapolations of the curves (plotted between polarisations and concentrations) which can introduce some uncertainties to the values obtained.

6.2 THE APPROACH ADOPTED IN THE DETERMINATION OF EQUILIBRIUM QUOTIENTS

According to the discussion in section B, Chapter 2, the molar polarisation of a substance is given by

$$P = \frac{\varepsilon - 1}{\varepsilon + 2} \cdot \frac{M}{\rho} \qquad (6.1)$$

where ε is the dielectric constant, M the molecular weight and ρ the density of the substance.

The polarisation of a binary mixture, i.e. a dilute solution of a polar solute A in an aromatic solvent B, is then given as

$$P_{A,B} = x_A P_A + x_B P_B = \frac{\varepsilon_{A,B} - 1}{\varepsilon_{A,B} + 2} \cdot \frac{(x_A M_A + x_B M_B)}{\rho_{A,B}} \qquad (6.2)$$

where x_A and x_B, P_A and P_B, and M_A and M_B are, respectively, the mole fractions, the molar polarisations, and the molecular weights of A and B, while $\varepsilon_{A,B}$ and $\rho_{A,B}$ are the dielectric constant and density of the solution.

Since

$$x_A = 1 - x_B \tag{6.3}$$

Substitution of (6.3) into (6.2) gives

$$P_A = \frac{P_{A,B} - P_B}{x_A} + P_B \tag{6.4}$$

If P_B is assumed to be constant and unaffected by the amount of solute present in the solution (an approximation), the polarisation P_A of the solute for that solution may be calculated from the dielectric constant and density of the solution through Equation (6.2). It is found in most cases that P_A increases with decreasing concentration of A, and the rate of increase tends to be greater the lower the concentration. The relation (6.2) also holds for the other dilute (binary) solutions in general. If the additivity rule for polarisations represented by (6.2) is assumed to hold for a three-component system composed of a dilute solution of A in B (of upper mole fraction range within c.a. 0.90 - 1.00, which is similar to that of n.m.r. work) with cyclohexane (S) as the third component and molecular interactions between A and B of the type

$$A + B \rightleftharpoons A.....B \tag{6.5}$$

exist within the solution, the relation

$$P_{A,B,S} = P_A(x_A - x_{AB}) + P_B(x_B - x_{AB}) + P_S x_S + P_{AB} x_{AB} \tag{6.6}$$

is expected to hold[117]. For (6.6) P_S and x_S are the polarisation and mole fraction of cyclohexane respectively, $P_{A,B,S}$ the polarisation of

the mixture, P_{AB} that of the complex formed and x_{AB} the mole fraction of complex at equilibrium. When the conditions that x_A is low and constant and $x_B \gg x_A$ are applied, it follows that

$$P_B (x_B - x_{AB}) \simeq P_B x_B \tag{6.7}$$

Combination of (6.6) and (6.7) gives

$$P_{A,B,S} = P_A x_A + P_B x_B + P_S x_S + x_{AB}(P_{AB} - P_A)$$

or defining P_T as

$$P_T = P_{A,B,S} - P_B x_B - P_S x_S = P_A x_A + x_{AB}(P_{AB} - P_A) \tag{6.8}$$

let

$$x_{AB} = \alpha x_A \tag{6.9}$$

where α is the fraction of solute taking part in complex formation. It is evident from (6.8) and (6.9) that

$$P_T/x_A = \alpha(P_{AB} - P_A) + P_A \tag{6.10}$$

Equation (6.10) possesses the same form as (5.5) derived from n.m.r. studies in previous chapter.

According to equation (5.11), K_x for a system can be evaluated from

$$K_x = \frac{n_{AB}(n_A + n_B + n_S - n_{AB})}{(n_A - n_{AB})(n_B - n_{AB})} \tag{6.11}$$

where n_i represents the number of moles of the i^{th} component. In other words

$$K_x = \frac{x_{AB}}{(x_A - x_{AB})(x_B - x_{AB})} \simeq \frac{x_{AB}}{(x_A - x_{AB})x_B} \tag{6.12}$$

Substitution of (6.9) into (6.12) results in the expression

$$K_x = \frac{\alpha}{(1 - \alpha)x_B} \tag{6.13}$$

i.e. $$\frac{1}{\alpha} = \frac{1}{K_x x_B} + 1 \qquad (6.13)$$

Combination of (6.10) and (6.13) leads to

$$\frac{x_A}{P_T - P_A x_A} = \frac{1}{K_x x_B (P_{AB} - P_A)} + \frac{1}{P_{AB} - P_A} \qquad (6.14)$$

If a quantity P_{NETT} is defined as

$$P_{NETT} = \frac{P_T - P_A x_A}{x_A}$$

then, from (6.14)

$$\frac{1}{P_{NETT}} = \frac{1}{K_x x_B (P_{AB} - P_A)} + \frac{1}{P_{AB} - P_A} \qquad (6.14a)$$

Hence a plot of $1/P_{NETT}$ against $1/x_B$ should be linear with K_x and P_{AB} obtainable from its gradient and intercept respectively. Equation (6.14a) also has the same form as that of the Benesi-Hildebrand equation (5.14), and so the whole process of evaluating K_x and P_{AB} can still be carried out in the manner described in Chapter 5.

It can be seen from the above discussion that by studying various binary solutions of A with S and B with S, the values of P_A&P_B for each solution can be determined through (6.2) (with P_S taken to be of the same value in every solution). These values were employed in the studies of various three-component solutions (A + B + S) through (6.8) to obtain P_{NETT} for each solution, which was then used to evaluate K_x and P_{AB} as described above.

Furthermore, as stated earlier, since it was found that P_A and P_B vary with the concentrations of A and B in the binary mixtures, the concentration ranges of A and B employed in sample preparations were kept

the same in both the two- and three-component systems. These were made to minimise the error that might be introduced when the values of P_A and P_B were used to calculate P_{NETT}.

6.3 EXPERIMENTAL

The chemicals employed were the same as those in the previous chapter. The systems studied were benzene-cyclohexane, p-xylene-cyclohexane, mesitylene-cyclohexane, nitromethane-cyclohexane, acetonitrile-cyclohexane, nitromethane-benzene-cyclohexane, nitromethane-p-xylene-cyclohexane, nitromethane-mesitylene-cyclohexane, acetonitrile-benzene-cyclohexane, acetonitrile-p-xylene-cyclohexane and acetonitrile-mesitylene-cyclohexane.

For binary systems of nitromethane or acetonitrile with cyclohexane, the concentrations of the solute in the samples were kept within 0.00 - 0.03 mole fraction. In the case of the various aromatic-cyclohexane systems the concentrations of the aromatics in the samples were kept within the mole fraction range of 0.90 - 1.00. The samples for three-component systems were prepared in a manner similar to those for the n.m.r. investigations described in section 5.4. The sample compositions for the various three-component systems are recorded in tables 6.1 - 6.6.

The solution dielectric constants were determined as follows: By using a heterodyne beat apparatus, described previously in section B Chapter 3, the capacitances of the solutions were measured. The corresponding values of dielectric constant were then calculated from the relation

$$\varepsilon_X = \frac{C_X - C_0}{C_{air} - C_0} \qquad (6.15)$$

where ε_X is the dielectric constant of a pure substance or solution, C_X the corresponding capacitance, C_{air} the capacitance when only air is present in the measurement cell and C_0 the capacitance created by the electrical leads joining between various condensers. Using cyclohexane as a standard substance, for which ε at 308.2K is equal to 2.0006, C_0 was calculated. The value of C_0 obtained was then used in determining ε for the other samples. All measurements of solution capacitances were made at 308.2 $\pm$ 0.1K with an accuracy of $\pm$ 0.01pF.

Due to the paucity of time, the densities of solutions required for the polarisation calculations (equation 6.2) were not measured directly. On the contrary, the polarisations were calculated from an approximation described as follows:

From (6.2), to an approximation, it would be justified (on the basis of negligible volume changes on mixing for dilute solutions e.g. chloroform and acetone[121]) to assume that for a two-component solution

$$\rho_{A,B} = \frac{w_A + w_B}{v_A + v_B} \qquad (6.16)$$

where w_A and w_B and v_A and v_B are the real weight and volume of solute and solvent present in the solution respectively. Since

$$w/M = n \text{ and } v/n = V \qquad (6.17)$$

where V is the molar volume, it follows from (6.16) and (6.17) that

$$\rho_{A,B} = \frac{n_A M_A + n_B M_B}{n_A V_A + n_B V_B} \qquad (6.18)$$

or

$$\rho_{A,B} = \frac{x_A M_A + x_B M_B}{x_A V_A + x_B V_B}$$

Substitution of (6.18) into (6.2) gives

$$P_{A,B} = \frac{\varepsilon_{A,B} - 1}{\varepsilon_{A,B} + 2} \cdot (x_A V_A + x_B V_B) \qquad (6.19)$$

If the same assumption is applied to a three-component solution (A+B+S) in which an AB complex species is formed, a similar expression to (6.18) can be obtained as

$$\rho_{A'B,S} = \frac{M_A(x_A - x_{AB}) + M_B(x_B - x_{AB}) + M_S x_S + M_{AB} x_{AB}}{V_A(x_A - x_{AB}) + V_B(x_B - x_{AB}) + V_S x_S + V_{AB} x_{AB}} \qquad (6.20)$$

Furthermore, if (6.2) is also assumed to be applicable in this case, it would appear that

$$P_{A,B,S} = \frac{\varepsilon_{A,B,S} - 1}{\varepsilon_{A,B,S} + 2} \cdot \frac{(M_A(x_A - x_{AB}) + M_B(x_B - x_{AB}) + M_S x_S + M_{AB} x_{AB})}{\rho_{A,B,S}} \qquad (6.21)$$

Combination of (6.20) and (6.21) results in

$$P_{A,B,S} = \frac{\varepsilon_{A,B,S} - 1}{\varepsilon_{A,B,S} + 2} \cdot (V_A(x_A - x_{AB}) + V_B(x_B - x_{AB}) + V_S x_S + V_{AB} x_{AB}) \qquad (6.22)$$

But

$$V_{AB} = V_A + V_B \qquad (6.23)$$

Hence it is evident that

$$P_{A,B,S} = \frac{\varepsilon_{A,B,S} - 1}{\varepsilon_{A,B,S} + 2} \cdot (x_A V_A + x_B V_B + x_S V_S) \qquad (6.24)$$

Equations (6.19) and (6.24) were used in the calculations of the polarisations of two- and three- component solutions respectively. The values obtained are recorded in table 6.7 - 6.17 together with the corresponding values of dielectric constants.

The accuracy of the solution dielectric constants is about $\pm$ 0.0005. This consequently results in the accuracy of the values of polarisations being around $\pm$ 0.01 x 10^{-6} $m^3 mol^{-1}$.

The data were processed on the ICL 1905 computer using the program BHCURVEFIT with K_x and P_{AB} obtained from the slope and intercept (at $x_B = 1$) of the plot (see equation (6.14a)) between $1/x_B$ and $1/P_{NETT}$. The values of x_B and P_{NETT} required as computer input data are recorded in table 6.12 - 6.17.

TABLE 6.1

COMPOSITIONS OF VARIOUS SAMPLES FOR THE NITROMETHANE-BENZENE - CYCLOHEXANE SYSTEM

Sample	Moles of solute/10^3	Moles of benzene/10	Moles of cyclo-hexane/10^2
A	1.7246	3.0111	3.0933
B	1.6769	3.0646	2.4921
C	1.6933	3.1351	1.8323
D	1.8689	3.1984	1.1461
E	1.8280	3.2329	0.8119
F	1.7513	3.2682	0.4953
G	1.7315	3.2954	0.1453

TABLE 6.2

COMPOSITIONS OF VARIOUS SAMPLES FOR THE NITROMETHANE-P-XYLENE-CYCLOHEXANE SYSTEM

Sample	Moles of solute/10^3	Moles of p-xylene/10	Moles of cyclohexane/10^2
A	1.1214	2.3515	1.3607
B	1.0722	2.4008	0.8342
C	1.0894	2.4248	0.5946
D	1.1129	2.4458	0.3530
E	1.1908	2.4725	0.1083

TABLE 6.3

COMPOSITIONS OF VARIOUS SAMPLES FOR THE NITROMETHANE-MESITYLENE-CYCLOHEXANE SYSTEM

Sample	Moles of solute/10^3	Moles of mesitylene/10	Moles of cyclohexane/10^2
A	1.0588	1.9999	1.6211
B	1.1456	2.0982	0.6478
C	1.0785	2.1206	0.4259
D	1.0208	2.1407	0.2134
E	1.0699	2.1530	0.0937

TABLE 6.4

COMPOSITIONS OF VARIOUS SAMPLES FOR THE ACETONITRILE-BENZENE-CYCLOHEXANE SYSTEM

Sample	Moles of solute/10^3	Moles of benzene/10	Moles of cyclohexane/10^2
A	1.6701	3.0049	3.1519
B	1.6589	3.0652	2.5137
C	1.4823	3.1349	1.7779
D	1.5088	3.1987	1.1354
E	1.7030	3.2384	0.8151
F	1.5363	3.2661	0.5229
G	1.5317	3.2967	0.1421

TABLE 6.5

COMPOSITIONS OF VARIOUS SAMPLES FOR THE ACETONITRILE-P-XYLENE-CYCLOHEXANE SYSTEM

Sample	Moles of solute/10^3	Moles of p-xylene/10	Moles of cyclohexane/10^2
A	1.2231	2.3549	1.4004
B	1.3417	2.3937	0.7841
C	1.3015	2.4231	0.6238
D	1.3424	2.4556	0.3462
E	1.3273	2.4746	0.1065

TABLE 6.6

COMPOSITIONS OF VARIOUS SAMPLES FOR THE ACETONITRILE-MESITYLENE-CYCLOHEXANE SYSTEM

Sample	Moles of solute/10^3	Moles of mesitylene/10	Moles of cyclohexane/10^2
A	1.1907	2.0525	1.6081
B	1.1778	2.0900	1.1738
C	1.0971	2.1548	0.5210
D	1.0869	2.1839	0.2988
E	1.1030	2.1934	0.1031

TABLE 6.7

THE REAL AROMATIC MOLE FRACTIONS (x_B), THE SOLUTION DIELECTRIC CONSTANTS ($\varepsilon_{B,S}$) AND SOLUTION POLARISATIONS ($P_{B,S}$) OF VARIOUS SAMPLES FOR THE BENZENE-CYCLOHEXANE SYSTEM AT 308.2K

Sample	x_B	$\varepsilon_{B,S}$	$P_{B,S}/10^6 m^3 mol^{-1}$
A	0.8978	2.2340	26.957
B	0.9269	2.2413	26.903
C	0.9460	2.2461	26.867
D	0.9656	2.2510	26.828
E	0.9754	2.2536	26.810
F	0.9866	2.2562	26.785
G	0.9957	2.2586	26.768
H	1.0000	2.2596	26.758

TABLE 6.8

THE REAL AROMATIC MOLE FRACTIONS (x_B), THE SOLUTION DIELECTRIC CONSTANTS ($\varepsilon_{B,S}$) AND SOLUTION POLARISATIONS ($P_{B,S}$) OF VARIOUS SAMPLES FOR THE P-XYLENE-CYCLOHEXANE SYSTEM AT 308.2K

Sample	x_B	$\varepsilon_{B,S}$	$P_{B,S}/10^6 m^3 mol^{-1}$
A	0.9004	2.2324	36.008
B	0.9240	2.2378	36.223
C	0.9480	2.2415	36.404
D	0.9605	2.2428	36.487
E	0.9757	2.2442	36.583
F	0.9861	2.2449	36.642
G	0.9951	2.2453	36.692
H	1.0000	2.2456	36.720

TABLE 6.9

THE REAL AROMATIC MOLE FRACTIONS (x_B), THE SOLUTION DIELECTRIC CONSTANTS ($\varepsilon_{B,S}$) AND SOLUTION POLARISATIONS ($P_{B,S}$) OF VARIOUS SAMPLES FOR THE MESITYLENE-CYCLOHEXANE SYSTEM AT 308.2K.

Sample	x_B	$\varepsilon_{B,S}$	$P_{B,S}/10^6 m^3 mol^{-1}$
A	0.9253	2.2382	40.514
B	0.9709	2.2499	41.198
C	0.9807	2.2524	41.344
D	0.9911	2.2551	41.502
E	0.9962	2.2564	41.579
F	1.0000	2.2583	41.636

TABLE 6.10

THE REAL MOLE FRACTIONS OF THE SOLUTE (x_A), THE SOLUTION DIELECTRIC CONSTANTS ($\varepsilon_{A,S}$) AND SOLUTION POLARISATIONS ($P_{A,S}$) OF VARIOUS SAMPLES FOR THE NITROMETHANE-CYCLOHEXANE SYSTEM AT 308.2K

Sample	x_A	$\varepsilon_{A,S}$	$P_{A,S}/10^6 m^3 mol^{-1}$
A	0.0054	2.0429	28.326
B	0.0070	2.0575	28.597
C	0.0088	2.0704	28.828
D	0.0111	2.0908	29.198
E	0.0132	2.1024	29.393
F	0.0150	2.1179	29.667
G	0.0169	2.1359	29.984
H	0.0190	2.1529	30.276

TABLE 6.11

THE REAL MOLE FRACTIONS OF THE SOLUTE (x_A), THE SOLUTION DIELECTRIC CONSTANTS ($\varepsilon_{A,S}$) AND SOLUTION POLARISATIONS ($P_{A,S}$) OF VARIOUS SAMPLES FOR THE ACETONITRILE-CYCLOHEXANE SYSTEM AT 308.2K

Sample	x_A	$\varepsilon_{A,S}$	$P_{A,S}/10^6 m^3 mol^{-1}$
A	0.0043	2.0407	28.297
B	0.0086	2.0797	29.013
C	0.0167	2.1510	30.270
D	0.0202	2.1866	30.886
E	0.0241	2.2249	31.530
F	0.0301	2.2780	32.388
G	0.0343	2.3174	33.007
H	0.0389	2.3673	33.784

TABLE 6.12

THE REAL AROMATIC MOLE FRACTIONS (x_B), THE SOLUTION DIELECTRIC CONSTANTS ($\varepsilon_{A,B,S}$), THE SOLUTION POLARISATIONS ($P_{A,B,S}$) AND THE NETT POLARISATIONS (P_{NETT}) OF VARIOUS SAMPLES OF THE NITROMETHANE-BENZENE-CYCLOHEXANE SYSTEM AT 308.2K

Sample	x_B	$\varepsilon_{A,B,S}$	$P_{A,B,S}/10^6 m^3 mol^{-1}$	$P_{NETT}/10^6 m^3 mol^{-1}$
A	0.9022	2.3057	27.96	50.58
B	0.9201	2.3118	27.92	53.68
C	0.9400	2.3185	27.89	57.24
D	0.9600	2.3252	27.87	60.78
E	0.9701	2.3287	27.86	62.58
F	0.9799	2.3319	27.85	64.24
G	0.9904	2.3354	27.84	66.04

TABLE 6.13

THE REAL AROMATIC MOLE FRACTIONS (x_B), THE SOLUTION DIELECTRIC CONSTANTS ($\varepsilon_{A,B,S}$), THE SOLUTION POLARISATIONS ($P_{A,B,S}$) AND THE NETT POLARISATIONS (P_{NETT}) OF VARIOUS SAMPLES FOR THE NITROMETHANE-P-XYLENE-CYCLOHEXANE SYSTEM AT 308.2K

Sample	x_B	$\varepsilon_{A,B,S}$	$P_{A,B,S}/10^6 m^3 mol^{-1}$	$P_{NETT}/10^6 m^3 mol^{-1}$
A	0.9410	2.2872	37.24	54.74
B	0.9623	2.2896	37.38	57.14
C	0.9718	2.2910	37.45	58.94
D	0.9814	2.2921	37.51	60.34
E	0.9909	2.2930	37.58	61.14

TABLE 6.14

THE REAL AROMATIC MOLE FRACTIONS (x_B), THE SOLUTION DIELECTRIC CONSTANTS ($\varepsilon_{A,B,S}$), THE SOLUTION POLARISATIONS ($P_{A,B,S}$) AND THE NETT POLARISATIONS (P_{NETT}) OF VARIOUS SAMPLES FOR THE NITROMETHANE-MESITYLENE- CYCLOHEXANE SYSTEM AT 308.2K

Sample	x_B	$\varepsilon_{A,B,S}$	$P_{A,B,S}/10^6 m^3 mol^{-1}$	$P_{NETT}/10^6 m^3 mol^{-1}$
A	0.9205	2.3001	41.80	79.62
B	0.9649	2.3112	42.46	91.50
C	0.9754	2.3138	42.62	93.86
D	0.9855	2.3162	42.77	96.56
E	0.9908	2.3175	42.85	97.56

TABLE 6.15

THE REAL AROMATIC MOLE FRACTIONS (x_B), THE SOLUTION DIELECTRIC CONSTANTS ($\varepsilon_{A,B,S}$) THE SOLUTION POLARISATIONS($P_{A,B,S}$) AND THE NETT POLARISATIONS (P_{NETT}) OF VARIOUS SAMPLES FOR THE ACETONITRILE-BENZENE-CYCLOHEXANE SYSTEM AT 308.2K

Sample	x_B	$\varepsilon_{A,B,S}$	$P_{A,B,S}/10^6 m^3 mol^{-1}$	$P_{NETT}/10^6 m^3 mol^{-1}$
A	0.9005	2.3150	28.03	10.80
B	0.9196	2.3191	27.99	11.10
C	0.9421	2.3237	27.95	11.80
D	0.9613	2.3279	27.92	12.00
E	0.9705	2.3297	27.90	12.20
F	0.9797	2.3317	27.88	12.56
G	0.9911	2.3341	27.86	12.70

TABLE 6.16

THE REAL AROMATIC MOLE FRACTIONS (x_B), THE SOLUTION DIELECTRIC CONSTANTS ($\varepsilon_{A,B,S}$) THE SOLUTION POLARISATIONS ($P_{A,B,S}$) AND THE NETT POLARISATIONS (P_{NETT}) OF VARIOUS SAMPLES FOR THE ACETONITRILE-P-XYLENE- CYCLOHEXANE SYSTEM AT 308.2K

Sample	x_B	$\varepsilon_{A,B,S}$	$P_{A,B,S}$, $/10^6 m^3 mol^{-1}$	$P_{NETT}/10^6 m^3 mol^{-1}$
A	0.9393	2.3042	37.56	15.96
B	0.9631	2.3106	37.79	32.36
C	0.9698	2.3124	37.86	38.04
D	0.9808	2.3155	37.97	46.04
E	0.9904	2.3181	38.07	54.20

TABLE 6.17

THE REAL AROMATIC MOLE FRACTIONS (x_B), THE SOLUTION DIELECTRIC CONSTANTS ($\varepsilon_{A,B,S}$), THE SOLUTION POLARISATIONS ($P_{A,B,S}$) AND THE NETT POLARISATIONS (P_{NETT}) OF VARIOUS SAMPLES FOR THE ACETONITRILE-MESITYLENE-CYCLOHEXANE SYSTEM AT 308.2K

Sample	x_B	$\varepsilon_{A,B,S}$	$P_{A,B,S}$, $/10^6 m^3 mol^{-1}$	$P_{NETT}/10^6 m^3 mol^{-1}$
A	0.9224	2.3052	41.82	48.86
B	0.9418	2.3079	42.10	52.52
C	0.9715	2.3123	42.53	56.38
D	0.9817	2.3138	42.68	57.52
E	0.9904	2.3151	42.80	59.82

6.4 RESULTS AND DISCUSSION

The values of K_x and P_{AB} obtained for various systems are recorded in table 6.18 A perusal of the table shows that values of K_x for these systems, except that of the acetonitrile-benzene which is evaluated on the basis of 1:2 stoichiometry (c.f. equation (5.19)), lie within the range of 0.05 - 0.65 and appear to be rather low. In the case of nitromethane acting as a common solute, no regular (or significant) change can be observed when one aromatic is replaced by another. A similar situation for the regular change also arises for the values of P_{AB}.

Judging from the criteria adopted in sample preparations for the present study, which are the same as those for n.m.r. study, it would be expected that the values of K_x deduced from both studies should be compatible. When these are compared (table 6.19) it is apparent that there is a significant difference between them. The values of K_x from n.m.r. work are much higher by up to three or four times in most cases. Considering the generally recognised reliability of the n.m.r. results, it must be concluded that the results obtained from the polarisation study are meaningless. The reasons for not obtaining compatible results with those from n.m.r. study may be due to the unsoundness of the approach and/or the data obtained. Since the present approach adopted as a whole appears to be theoretically justified, it is likely that the present failure originates from the fact that the required experimental accuracy of the data was not achieved.

However, it is a matter of the author's opinion that several factors may be recognised which affect the calculations in the present approach

TABLE 6.18

THE EQUILIBRIUM QUOTIENTS (K_x) AND COMPLEX POLARISATIONS (P_{AB}) FOR VARIOUS SOLUTE-AROMATIC SOLVENT SYSTEMS AT 308.2K

System	K_x	$P_{AB}/10^6 m^3 mol^{-1}$
nitromethane-benzene	0.50	284.75
nitromethane-p-xylene	0.64	251.90
nitromethane-mesitylene	0.40	274.30
acetonitrile-benzene	1.29	216.77
acetonitrile-p-xylene	0.05	269.36
acetonitrile-mesitylene	0.48	263.88

TABLE 6.19

COMPARISON OF THE EQUILIBRIUM QUOTIENTS OBTAINED FROM N.M.R. AND POLARISATION STUDIES

System	K_x(n.m.r.)	K_x(polarisation)	Difference
nitromethane-benzene	1.94	0.50	1.44
nitromethane-p-xylene	1.95	0.64	1.31
nitromethane-mesitylene	2.29	0.40	1.89
acetonitrile-benzene	5.11	1.29	3.82
acetonitrile-p-xylene	1.57	0.05	1.52
acetonitrile-mesitylene	1.86	0.48	1.38

to such an extent that the results obtained are far from expected. It may be worthwhile to discuss these factors briefly as a guide for future investigations employing similar approaches to the present one. They are:

(a) The contribution to the polarisations of solutions from various species. It can be seen from (6.8) and (6.14a) that, to obtain P_{NETT}, the contributions to $P_{A,B,S}$ from various species in the solutions (i.e. the quantity $P_B x_B + P_S x_S$) have to be subtracted from $P_{A,B,S}$. These contributions are originally evaluated from two-component solutions and vary from sample to sample depending on the amount of B and S present in the sample, and may be changed (by a small amount) in the presence of the third component A. When these are used to calculate P_{NETT} they may introduce some uncertainties to the calculations.

(b) The polarisations of solutes employed in the calculations, i.e. P_A. In previous studies[117,120] these values were taken as those at infinite dilution in an inert solvent whereas here they are taken as the values when the whole amount of the solute (around 0.005 mole fraction)is present in solution. It still remains to be proved which is the correct approach .

(c) The aromatic concentration range employed. The equations governing the calculations, (6.10) and (6.14a), are expected to hold only for dilute solutions and so a narrow aromatic concentration range (0.90 - 1.00) is employed. It is possible, within this concentration range, that the change in polarisations for the interactions from one sample to another is so small that the required experimental accuracy cannot be achieved.

(d) If the errors do arise as described in (c), it is apparent that the small changes in volume on mixing of two or more substances cannot be neglected in the calculations of the densities of solutions as in (6.16). Neglecting these can also provide some error and so the densities of mixtures must be determined directly in this case.

On average, each factor separately should not introduce a large error to the calculations and therefore the discrepancy of the results may arise from a combined effect of these factors.

PART B : CONSIDERATIONS OF THE NATURE OF THE INTERACTIONS

6.5 INTRODUCTION

It has been observed that[77] many polar solute molecules, when dissolved in various solvents, possess different dipole moments (μ) depending on the solvents employed. In other words, a solute dipole moment obtained in the presence of an inert solvent (μ_{inert}) is different from that obtained when using an active solvent (μ_{sol}). It follows that molecular interactions between the solute and solvent must therefore contribute to changes in the solute dipole moments. These are such that generally μ_{sol} is found to be larger than μ_{inert}. It is possible to write a relation for these values as

$$\mu_{sol} = \mu_{inert} + \mu_{ind} \qquad (6.25)$$

where μ_{ind} is the induced dipole moment. The size of μ_{ind} normally depends on the nature of the interactions (chapter 1). Hence it is likely, from the studies on solution dipole moments of a solute, that the nature of various interactions can be elucidated.

6.6 EXPERIMENTAL

The systems studied were chloroform-cyclohexane, chloroform-p-xylene, chloroform-mesitylene, nitromethane-cyclohexane, nitromethane-benzene, nitromethane-p-xylene, nitromethane-mesitylene, acetonitrile-p-xylene, acetonitrile-cyclohexane, acetonitrile-benzene and acetonitrile-mesitylene.

For each system studied a series of solutions, with the weight fractions of the solute kept within the range 0.00 - 0.03, was prepared. The refractive indices of solutions were measured employing an Abbe refractometer with an accuracy of $\pm$ 0.0001 The determinations of the dielectric constants of solutions were made in the same manner as discussed in section 6.3. All the measurements were made at 308.2$\pm$ 0.1K. The values of dielectric constants and refractive indices obtained for various systems are recorded in tables 6.20 - 6.30.

The solution dipole moments of various solutes were calculated by Guggenheim's method as described in section 2.B.4, employing equation (2.97) or (2.100). The values of physical constants of properties required for such calculations are recorded in tables 6.31 - 6.32.

6.7 RESULTS AND DISCUSSION

In Guggenheim's method, the limiting slopes at $w_2 = 0$ of the plots between the dielectric constants and separately the refractive indices of solutions and the weight fractions of solute (w_2), are employed in the calculation of a solute dipole moment (equation 2.97). This implies that the plots could either be in the form of curves or straight lines. When these plots were made in the present study it was found that almost in every case a straight line was obtained. This observation agrees with that found earlier for other dilute solutions[74]. Two typical examples for these plots are shown in Fig. 6.1 and 6.2.

The solution (infinite dilution) dipole moments (μ_{SOL}) of different solutes in various solvents obtained from the calculations are recorded in table 6.33. Since cyclohexane is employed as an inert solvent in the present work, the values of μ_{SOL} obtained for the various solute-

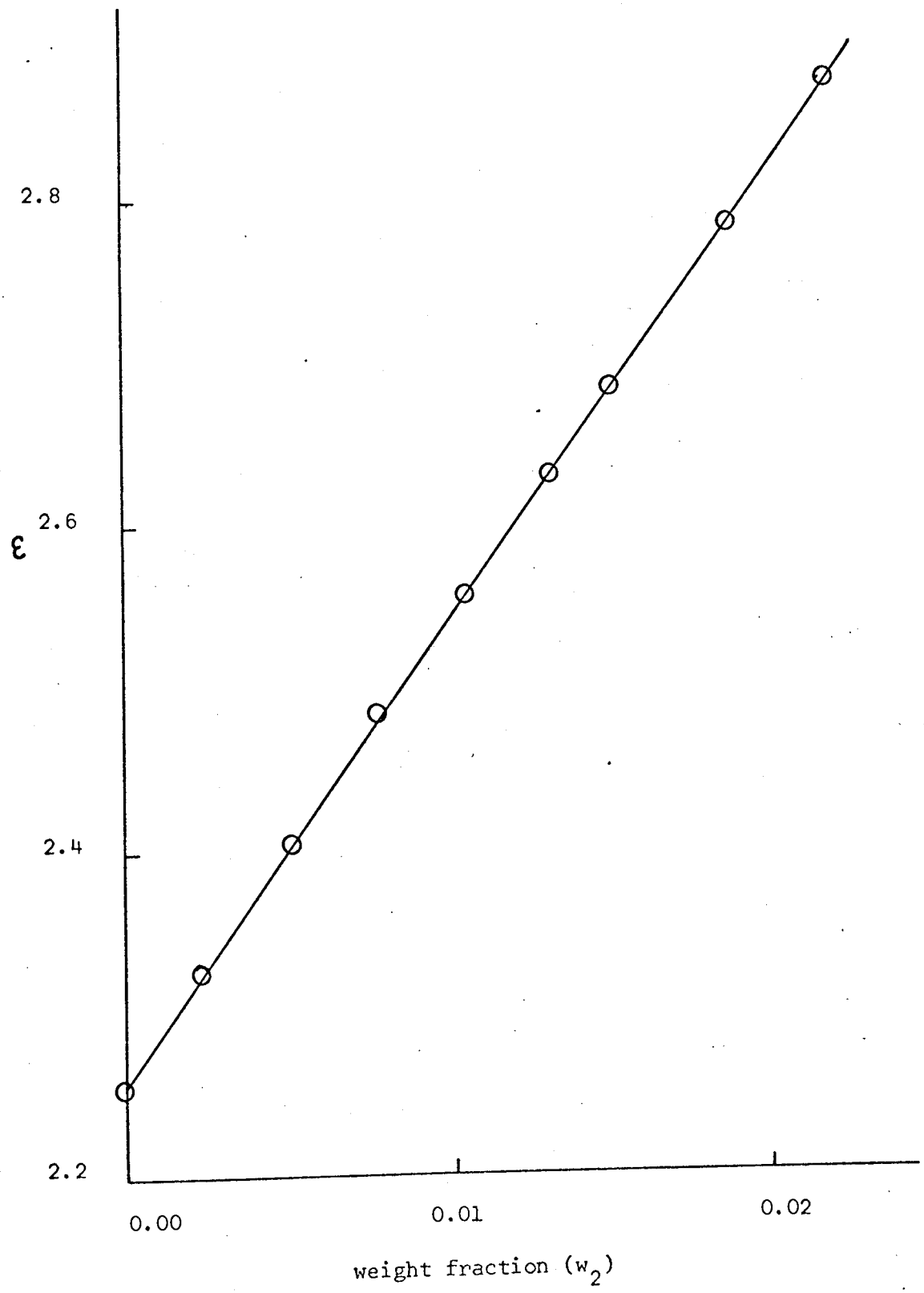

FIG. 6.1 RELATIONSHIP BETWEEN WEIGHT FRACTIONS OF THE SOLUTE (w_2) AND DIELECTRIC CONSTANTS (ε) OF SOLUTIONS FOR THE ACETONITRILE-BENZENE SYSTEM

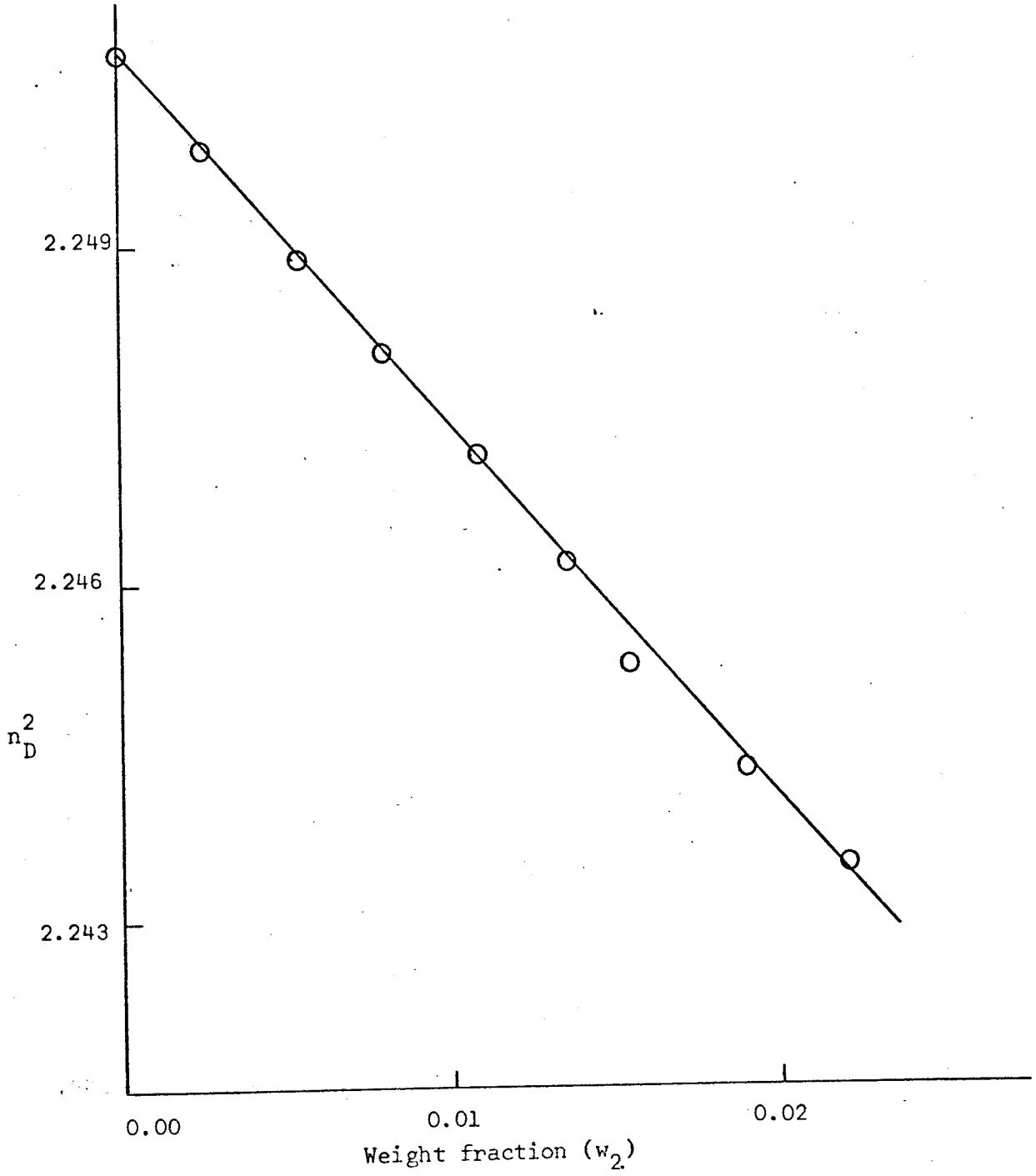

FIG. 6.2 RELATIONSHIP BETWEEN WEIGHT FRACTIONS OF THE SOLUTE (w_2) AND SQUARES OF REFRACTIVE INDICES OF SOLUTIONS (n_D^2) FOR THE ACETONITRILE-BENZENE SYSTEM

TABLE 6.20

THE WEIGHT FRACTIONS OF THE SOLUTE (w_2), THE DIELECTRIC CONSTANTS (ε) AND SQUARES OF REFRACTIVE INDICES (n_D^2) OF VARIOUS SAMPLES FOR THE CHLOROFORM-CYCLOHEXANE SYSTEM AT 308.2K.

Sample	w_2	ε	n_D^2
A	0.00000	2.0006	2.03149
B	0.00722	2.0070	2.03167
C	0.00997	2.0104	2.03174
D	0.01471	2.0157	2.03185
E	0.01569	2.0172	-
F	0.01929	2.0211	2.03197
G	0.02096	2.0228	-
H	0.02379	2.0262	2.03207
I	0.02665	2.0287	2.03215
J	0.03105	2.0336	2.03224
K	0.03263	2.0370	2.03231

TABLE 6.21

THE WEIGHT FRACTIONS OF THE SOLUTE (w_2), THE DIELECTRIC CONSTANTS (ε) AND SQUARES OF REFRACTIVE INDICES (n_D^2) OF VARIOUS SAMPLES FOR THE CHLOROFORM-P-XYLENE SYSTEM AT 308.2K.

Sample	w_2	ε	n_D^2
A	0.00000	2.2526	2.23607
B	0.00504	2.2590	2.23543
C	0.00751	2.2622	2.23516
D	0.01094	2.2675	2.23488
E	0.01252	2.2699	2.23460
F	0.01580	2.2740	2.23413
G	0.01659	2.2769	2.23386

TABLE 6.22

THE WEIGHT FRACTIONS OF THE SOLUTE (w_2), THE DIELECTRIC CONSTANTS (ε) AND SQUARES OF REFRACTIVE INDICES (n_D^2) OF VARIOUS SAMPLES FOR THE CHLOROFORM-MESITYLENE SYSTEM AT 308.2K

Sample	w_2	ε	n_D^2
A	0.00000	2.2613	2.22045
B	0.00536	2.2683	2.21985
C	0.00667	2.2708	2.21954
D	0.00955	2.2740	2.21923
E	0.01160	2.2776	2.21893
F	0.01412	2.2803	2.21863
G	0.01634	2.2838	2.21835
H	0.01695	2.2852	2.21805
I	0.01893	2.2870	2.21777
J	0.02090	2.2891	2.21744
K	0.02312	2.2928	2.21716

TABLE 6.23

THE WEIGHT FRACTIONS OF THE SOLUTE (w_2), THE DIELECTRIC CONSTANTS (ε) AND SQUARES OF REFRACTIVE INDICES (n_D^2) OF VARIOUS SAMPLES FOR THE ACETONITRILE-CYCLOHEXANE SYSTEM AT 308.2K.

Sample	w_2	ε	n_D^2
A	0.00000	2.0006	2.04447
B	0.00214	2.0407	2.04378
C	0.00424	2.0797	2.04290
D	0.00823	2.1510	2.04178
E	0.00996	2.1866	2.04127
F	0.01189	2.2249	2.04075
G	0.01489	2.2780	2.03987
H	0.01705	2.3174	2.03930
I	0.01938	2.3673	2.03867

TABLE 6.24

THE WEIGHT FRACTIONS OF THE SOLUTE (w_2), THE DIELECTRIC CONSTANTS (ε) AND SQUARES OF REFRACTIVE INDICES (n_D^2) OF VARIOUS SAMPLES FOR THE ACETONITRILE -BENZENE SYSTEM AT 308.2K.

Sample	w_2	ε	n_D^2
A	0.00000	2.2553	2.25075
B	0.00246	2.3257	2.24985
C	0.00534	2.4058	2.24892
D	0.00812	2.4867	2.24808
E	0.01079	2.5602	2.24718
F	0.01346	2.6355	2.24622
G	0.01543	2.6899	2.24532
H	0.01899	2.7898	2.24436
I	0.02221	2.8778	2.24349

TABLE 6.25

THE WEIGHT FRACTIONS OF THE SOLUTE (w_2), THE DIELECTRIC CONSTANTS (ε) AND SQUARES OF REFRACTIVE INDICES (n_D^2) OF VARIOUS SAMPLES FOR THE ACETONITRILE-P-XYLENE SYSTEM AT 308.2K.

Sample	w_2	ε	n_D^2
A	0.00000	2.2491	2.24134
B	0.00205	2.3077	2.24059
C	0.00486	2.3840	2.23984
D	0.00582	2.4078	2.23957
E	0.00770	2.4579	2.23897
F	0.00989	2.5161	2.23834
G	0.01216	2.5744	2.23772
H	0.01359	2.6103	2.23718
I	0.01601	2.6733	2.23625

TABLE 6.26

THE WEIGHT FRACTIONS OF THE SOLUTE (w_2), THE DIELECTRIC CONSTANTS (ε) AND SQUARES OF REFRACTIVE INDICES (n_D^2) OF VARIOUS SAMPLES FOR THE ACETONITRILE-MESITYLENE SYSTEM AT 308.2K.

Sample	w_2	ε	n_D^2
A	0.00000	2.2618	2.24520
B	0.00171	2.3086	2.24466
C	0.00348	2.3550	2.24403
D	0.00506	2.3996	2.24343
E	0.00689	2.4451	2.24286
F	0.00872	2.4931	2.24227
G	0.01050	2.5384	2.24161
H	0.01236	2.5862	2.24104
I	0.01620	2.6776	2.23981

TABLE 6.27

THE WEIGHT FRACTIONS OF THE SOLUTE (w_2), THE DIELECTRIC CONSTANTS (ε) SQUARES OF REFRACTIVE INDICES (n_D^2) OF VARIOUS SAMPLES FOR THE NITROMETHANE -CYCLOHEXANE SYSTEM AT 308.2K.

Sample	w_2	ε	n_D^2
A	0.00000	2.0006	2.02002
B	0.00394	2.0429	2.01955
C	0.00513	2.0575	2.01935
D	0.00642	2.0704	2.01920
E	0.00807	2.0908	2.01905
F	0.00961	2.1024	2.01888
G	0.01095	2.1179	2.01870
H	0.01238	2.1359	2.01856
I	0.01390	2.1529	2.01836

TABLE 6.28

THE WEIGHT FRACTIONS OF THE SOLUTE (w_2), THE DIELECTRIC CONSTANTS (ε) AND SQUARES OF REFRACTIVE INDICES (n_D^2) OF VARIOUS SAMPLES FOR THE NITRO-METHANE-BENZENE SYSTEM AT 308.2K.

Sample	w_2	ε	n_D^2
A	0.00000	2.2605	2.26447
B	0.00398	2.3272	2.26355
C	0.00547	2.3534	2.26308
D	0.00743	2.3881	2.26270
E	0.00884	2.4124	2.26231
F	0.01047	2.4386	2.26187
G	0.01128	2.4535	2.26156
H	0.01542	2.5166	2.26097

TABLE 6.29

THE WEIGHT FRACTIONS OF THE SOLUTE (w_2), THE DIELECTRIC CONSTANTS (ε) AND SQUARES OF REFRACTIVE INDICES (n_D^2) OF VARIOUS SAMPLES FOR THE NITRO-METHANE -P-XYLENE SYSTEM AT 308.2K.

Sample	w_2	ε	n_D^2
A	0.00000	2.2476	2.24776
B	0.00221	2.2875	2.24718
C	0.00585	2.3461	2.24646
D	0.00800	2.3798	2.24582
E	0.01071	2.4238	2.24499
F	0.01461	2.4894	2.24405
G	0.01788	2.5412	2.24328
H	0.02029	2.5800	2.24257

TABLE 6.30

THE WEIGHT FRACTIONS OF THE SOLUTE (w_2), THE DIELECTRIC CONSTANTS (ε) AND SQUARES OF REFRACTIVE INDICES (n_D^2) OF VARIOUS SAMPLES FOR THE NITROMETHANE-MESITYLENE SYSTEM AT 308.2K.

Sample	w_2	ε	n_D^2
A	0.00000	2.2694	2.23207
B	0.00307	2.3163	2.23124
C	0.00393	2.3286	2.23099
D	0.00469	2.3408	2.23075
E	0.00563	2.3551	2.23040
F	0.00708	2.3790	2.23014
G	0.00800	2.3942	2.22982
H	0.00972	2.4218	2.22928

TABLE 6.31

THE VALUES OF PHYSICAL CONSTANTSUSED IN THE CALCULATIONS

Avogadro constant (N_A)	=	6.023×10^{23} mol^{-1}
Boltzmann constant (k)	=	1.380×10^{-23} JK^{-1}

TABLE 6.32 THE MOLECULAR WEIGHTS (M) DENSITIES (ρ) AT 308.2K AND DIPOLE MOMENTS IN THE GASEOUS STATES (μ) FOR VARIOUS SUBSTANCES

Substance	$M/10^3 kg$	$\rho^{114}/10^{-3} kgm^{-3}$	$\mu^{122}/(3.335 \times 10^{30})Cm$
Cyclohexane	84.162	0.7643	0.00
Benzene	78.114	0.8632	0.00
p-Xylene	106.168	0.8483	0.00
Mesitylene	120.195	0.8527	0.00
Chloroform	119.378	1.4615	1.01
Nitromethane	61.040	1.1178	3.50
Acetonitrile	41.052	0.7661	3.90

cyclohexane systems are referred to as μ_{INERT}. Originally no study was made on the chloroform-benzene system but, for comparison with others, the value of μ_{SOL} for this system reported elsewhere[97] is also included in the table.

A perusal of the table shows that in the presence of an aromatic solvent, μ_{SOL} of the solutes are higher than the corresponding values

TABLE 6.33

THE SOLUTION DIPOLE MOMENTS FOR DIFFERENT SOLUTES IN VARIOUS SOLVENTS AT 308.2K (ACCURACY $\pm$ 0.067 x 10^{-30}Cm)

Solute	$\mu_{SOL}/(3.335 \times 10^{30})$Cm			
	Cyclohexane	Benzene	p-Xylene	Mesitylene
Chloroform	1.17	1.22[97]	1.26	1.33
Acetonitrile	3.08	3.37	3.36	3.32
Nitromethane	2.90	3.20	3.17	3.06

of μ_{INERT}. The difference between μ_{SOL} and μ_{INERT} (referred to as μ_{IND} as in (6.25)) for various solutes, when p-xylene or benzene is a common solvent, follows the order (table 6.34).

Chloroform < nitromethane $\simeq$ acetonitrile

This to some extent, according to table 6.32, follows the same trend as the increase in dipole moments in the gaseous state of the solutes.

Since it has already been found that these solutes interact with the aromatics, this evidence may be related to the nature of the interactions. However, although interactions are taking place within the systems of present interest, the values of μ_{SOL} obtained do not as a whole represent those of the solutes in the fully complexed state

($\mu_{COMPLEX}$). μ_{SOL} can be equal to $\mu_{COMPLEX}$ only when all the solute molecules are complexed whereas in fact only some are[22]. In order to compare these results with those obtained previously from n.m.r. studies, the determination of $\mu_{COMPLEX}$ for each system is required.

TABLE 6.34

VALUES OF INDUCED MOMENTS (μ_{IND}) FOR VARIOUS SOLUTE-AROMATIC SOLVENT SYSTEMS

System	$\mu_{IND}/(3.335 \times 10^{30})$Cm
Chloroform-benzene	0.05
Chloroform-p-xylene	0.09
Chloroform-mesitylene	0.16
Acetonitrile-benzene	0.29
Acetonitrile-p-xylene	0.28
Acetonitrile-mesitylene	0.24
Nitromethane-bezene	0.30
Nitromethane-p-xylene	0.27
Nitromethane-mesitylene	0.16

A METHOD FOR DETERMINING THE DIPOLE MOMENTS OF COMPLEXES

Huck[22] has developed a method for determining the dipole moment of any complex from a knowledge of μ_{SOL} and μ_{INERT}. The method was applied satisfactorily in the studies of interactions between several polar solutes and various aromatics and can be described in the following manner.

For a binary system (A + B), as employed in the present dipole moment studies, in which there is an interaction of the type specified by (6.5), the expression for K_x relevant to the interaction is given as (c.f. (6.11))

$$K_x = \frac{n_{AB}(n_A + n_B - n_{AB})}{(n_A - n_{AB})(n_B - n_{AB})} \tag{6.26}$$

with $n_S = 0$. If the fraction of the solute (A) complexed is represented by α, i.e. $n_{AB} = \alpha n_A$, then

$$K_x = \frac{\alpha n_A(n_A + n_B - \alpha n_A)}{(n_A - \alpha n_A)(n_B - \alpha n_A)} \tag{6.27}$$

At an infinite dilution of A in B, $n_B \gg n_A$ and (6.27) becomes

$$K_x \approx \frac{\alpha}{1 - \alpha} \tag{6.28}$$

Consequently, it would appear reasonable to interpret the infinite dilution situation such that the solute can be considered to spend part of its time free, with dipole moment μ_{INERT}, and the rest complexed, with dipole moment $\mu_{INERT} + \mu_{ARO}$, in the proportion of $(1-\alpha):\alpha$. In other words.

$$\mu_{COMPLEX} = \mu_{INERT} + \mu_{ARO} \tag{6.29}$$

where μ_{ARO} is the dipole moment induced in the aromatic by the solute in the complex. The total orientation polarisation of the solute ($P_{o,TOTAL}$) can therefore be regarded as arising from two components in the manner indicated by equation (6.2) as

$$P_{o,TOTAL} = \alpha P_{o,COMPLEX} + (1 - \alpha)P_{o,INERT} \tag{6.30}$$

Because it has already been shown in section 2.B.4 that

$$P_o = \frac{4}{9}\pi N_A \frac{\mu^2}{kT} \tag{6.31}$$

combination of (6.30) and (6.31) leads to

$$\mu^2_{SOL} = \alpha\mu^2_{COMPLEX} + (1-\alpha)\mu^2_{INERT}$$

or

$$\mu_{COMPLEX} = \left(\frac{\mu^2_{SOL} - (1-\alpha)\mu^2_{INERT}}{\alpha}\right)^{\frac{1}{2}} \qquad (6.32)$$

It is thus evident that by assuming the applicability of the relevant K_x, obtained from n.m.r. studies, to two-component systems, the proportion of the solute considered in the complex state at infinite dilution can be found from (6.28). The value obtained is then employed in (6.32) to calculate $\mu_{COMPLEX}$.

Adopting this method, using the value of K_x recorded in table 6.35 and those of μ_{SOL} and μ_{INERT} in table 6.33, $\mu_{COMPLEX}$ for various systems studied were determined. These are shown in table 6.35 together with the values of μ_{ARO} deduced through (6.29).

An examination of table 6.35 shows that the values of $\mu_{COMPLEX}$ and μ_{ARO} for every system are in fact higher than the corresponding values of μ_{SOL} and μ_{IND}. It has to be pointed out that since the acetonitrile-benzene complex possesses a different stoichiometry (1:2) from other complexes (1:1), one would expect a different orientation of the solute with respect to the aromatic in this complex. To compare $\mu_{COMPLEX}$ for this system with others would therefore seem inappropriate at this stage. Hence it is excluded from the present general discussion and will be referred to again in the next chapter.

The fact that the induced moments can be measured may be explained as follows. Although the aromatic molecules themselves are non-polar, they possess π-electrons which, in turn, enable them to be easily polaris-ed by

neighbouring polar solutes. If the interactions are such that the solutes polarise the aromatics, this results in dipole moments being induced in the latter. The process is then followed by electrostatic attractions between both interacting species. At the same time the solutes experience the resultant dipole moments (of their own and those induced in the aromatics) leading to an increase to $\mu_{COMPLEX}$ It is seen from table 6.35 that μ_{ARO} for all the solutes, with p-xylene as a solvent, still follow the same order of increase as μ_{IND} already discussed and it might be considered generally that the more polar are the solutes, the larger is the expected increase in μ_{ARO}. In this way acetonitrile or nitromethane produces larger μ_{ARO} with p-xylene than chloroform. Hence it is possible to conclude initially that, for all these systems, the interactions are taking place through dipole-induced dipole mechanism (section 1.3.2).

TABLE 6.35

THE ESTIMATED VALUES OF DIPOLE MOMENTS OF COMPLEXES ($\mu_{COMPLEX}$) AND OF THOSE INDUCED IN THE AROMATICS BY THE SOLUTES(μ_{ARO}) AT 308.2K, TOGETHER WITH THE AVERAGE COMPLEX LIMITING SHIFT VALUES (Δ_c) AND K_x AS OBTAINED PREVIOUSLY FROM THE N.M.R. STUDIES FOR THE VARIOUS SOLUTE-AROMATIC SOLVENT SYSTEMS (THE ARROWS SHOWN IN THE TABLE INDICATE THE ORDER OF INCREASE OF μ_{ARO}, Δ_c, K_x FOR INTERACTIONS OF A PARTICULAR SOLUTE WITH DIFFERENT AROMATICS).

System	$\mu_{COMPLEX}$ / (3.335×10^{30})Cm	μ_{ARO} / (3.335×10^{30})Cm	Δ_c / ppm	K_x
Chloroform-benzene	1.24	0.07 ↓	1.313^{104} ↓	2.00^{104} ↓
Chloroform-p-xylene	1.30	0.13 ↓	1.521^{104} ↓	2.02^{104} ↓
Chloroform-mesitylene	1.39	0.22 ↓	1.610^{104} ↓	2.19^{104} ↓

cont.

TABLE 6.35 (Cont.)

System	$\mu_{COMPLEX}$ / (3.335×10^{30})Cm	μ_{ARO} / (3.335×10^{30})Cm	Δ_c / ppm	K_x
Acetonitrile-benzene	3.42	0.34	1.220	5.11
Acetonitrile -p-xylene	3.53	0.45 ↑	1.446 ↑	1.57 ↓
			1.349	
Acetonitrile-mesitylene	3.44	0.36		1.86 ↓
Nitromethane-benzene	3.34	0.44 ↑	1.536 ↑	1.94 ↓
Nitromethane-p-xylene	3.30	0.40	1.396	1.95
Nitromethane-mesitylene	3.13	0.23	1.341	2.30 ↓

However, the order of change of μ_{ARO} for the solutes, when benzene or mesitylene is a common solvent, is not the same as in the case of p-xylene. Neglecting the case when benzene is present, because its interaction with acetonitrile results in a different type of complex from those with other solutes, the trend for an increase in μ_{ARO} of chloroform with various aromatics is clearly in an opposite direction to those of the other two solutes (table 6.35).

Whitney[104] and Yadava[25] have found that there are two main factors governing the formation of a dipole-induced dipole complex, namely electrostatic attraction and steric effects. The electrostatic factor depends on the polarising and polarisability properties of the solute and aromatic molecules. Because the polarisability increases (in the present cases) from benzene to mesitylene, the interactions between a common

solute and these aromatics should result in an increase in this factor on going up the aromatic series. This consequently should lead to a closer approach of the solute to the aromatic, and therefore an increase in K_x (which through ΔG governs the feasibility of a reaction occuring), μ_{ARO} and Δ_c (the last two[80,24] varying inversely with the cube of the distance between the interacting species). The steric factor consists of two contributions, first a negative contribution due to, for a common solute, methyl groups on the aromatic blocking the approach of the solute thus reducing the values of K_x, μ_{ARO} and Δ_c and, second, a positive contribution due to the solute being trapped by the aromatic methyl groups. The latter contribution has the same effect as the electrostatic factor but for the aromatics employed here it is assumed negligible. Both electrostatic and steric factors (or steric repulsion for the present interactions) compete with each other in the formation of a complex.

It is apparent from table 6.35 that the interactions between chloroform and various aromatics result in the same order of increase for K_x, μ_{ARO} and Δ_c. This evidence indicates the predominating effect of the electrostatic factor and therefore the increasing dipole-induced-dipole interactions, which agrees with n.m.r. studies made earlier by Whitney[104]. However, a perusal of the interactions of both acetonitrile and nitromethane with the aromatics from table 6.35 shows that, although the solutes appear to be moving away from the aromatics due to steric repulsion from the latter, the feasibility of the reactions is increasing. This is superficially unexpected and no attempt can be made to explain it for the time being. The matter will be postponed until the next chapter.

CHAPTER 7

OBSERVATIONS ON THE GEOMETRIES AND STRENGTHS OF SOME MOLECULAR COMPLEXES

INTRODUCTION

It was stated in Chapter 1 that the main purpose of the present work is to establish the general features of molecular complexes formed by various compounds employing three different physical techniques, namely n.m.r. spectroscopy, dielectric constant and cryoscopy. So far the stoichiometries of the complexes have been elucidated from the cryoscopic and n.m.r. studies, and the nature of the complexes from the dielectric studies. There still remain two features to be established namely the geometries and strengths of the interactions. The work reported in this chapter attempts to achieve these objectives, using all the results and information obtainable from the various studies reported above.

PART A: THE DETERMINATION OF THE TIME-AVERAGED GEOMETRIES OF MOLECULAR COMPLEXES

7.1 INTRODUCTION

The determination of the geometries of molecular complexes in the past has been made using mainly a single method of study. Few attempts have been made to combine several techniques such as (in the present work) n.m.r., dielectric and cryoscopic methods together so that a more complete understanding of the problem can be obtained.

Of all the three physical methods mentioned, it is realised that the cryoscopic study has to be excluded from the present considerations since it can only give information about the stoichiometries of complexes. This leaves only the other two to be employed. Earlier workers[23,25] have shown that information obtainable from n.m.r. studies can provide reasonably conclusive evidence for complex configurations in many cases. It would therefore appear logical here to attempt to establish these initially through the n.m.r. results and then through

the dielectric results.

7.2 A PROCEDURE ADOPTED FOR THE DETERMINATION OF COMPLEX CONFIGURATIONS THROUGH N.M.R. STUDIES

A list of the screenings at various points surrounding a benzene molecule, based on the work of Johnson and Bovey[24], is given in a recent publication[33]. Employing the list, Cooke[23] has developed a method for determining the geometries of several complexes formed from various solutes and aromatics. The method has been applied successfully by Yadava[25] and Whitney[104] and will now be discussed in some detail.

In this method the co-ordinates of any point relative to the aromatic ring are defined with reference to three axes, the first of which (the p-axis) lies along the plane of the ring and a second (the z axis) is along the aromatic six-fold axis. The third axis is at right angles to these two axes. For symmetrical complexes formed with molecules like benzene and other aromatics employed in the present work only the first two axes (p and z) are required to define any structural co-ordinate as the third becomes the same as on the p-axis. After the additional shieldings of one or more hydrogen atoms of the solute (Δ_c) due to complex formation have been determined through the procedure described previously in Chapter 5, it is possible to fix their positions with respect to the ring and consequently the geometry of complex. However, in most cases there are several different co-ordinate (z,p) points corresponding to each particular value of Δ_c. The procedure then adopted is to locate the correct positions of the solute hydrogen atoms in the complexes studied by plotting the appropriate screening contributions listed in the table referred to above, for selected

values of z, against p values. By using the experimentally determined Δ_c value, the co-ordinates of all the points about the ring having an equivalent value of the experimental and theoretical screenings can be obtained. From the knowledge of these co-ordinates a graph can be plotted between the various p and z values to obtain an isomagnetic screening diagram. One or more isoshielding lines, depending on the numbers of type of proton present in the solute, can be drawn. Some examples of the diagrams will be shown later on. For a solute containing more than one type (i.e. magnetically unequivalent) of proton, its position in the complex can be fixed directly since only one particular group of co-ordinate points will fit the structure of the solute. If the solute contains only one type of proton (as those employed here), this cannot be done and conditions concerning p in the complex haveto be imposed to obtain a corresponding z value (the solute hydrogen atom-aromatic ring separation distance).

However, it has to be pointed out that, in the Johnson-Bovey approach, the chemical shift is estimated for aromatic hydrogens by measuring the difference in shielding between aromatic protons and closely related olefinic protons such as those of cyclohexadiene (in which no ring current exists). It has been suggested recently[98] that about 17% of the observed shift difference between benzene and cyclohexadiene is due to electric and anisotropic screening differences other than the presence of a π-cloud. Thus the inferences from the approach, which are based on the ring current effects, have to be treated with caution. Furthermore, when considering methylated benzenes in place of benzene it becomes apparent that a correction has to be made to the screenings for the effects of the anisotropy in the magnetic susceptibility of the various bonds of the methyl groups. However, Whitney[104] has recently found (in complexes of the type studied here) that the methyl substituent

bond anisotropy effects contribute only ca.0.007 ppm to the shieldings and can be considered negligible. It would therefore appear that the screenings, listed previously for various points around a benzene molecule, can also be applied to the other methylated benzene molecules. The determination of the complex configurations in the present work will be made on this basis.

Because the results obtained previously from cryoscopic and n.m.r. studies in chapter 4 and 5 have shown that the complex formed between benzene and acetonitrile possesses a different stoichiometry from the others, this will be discussed separately.

7.2.a THE TIME-AVERAGED GEOMETRIES OF SOME SOLUTE-AROMATIC COMPLEXES

It has been suggested recently by Homer and Cooke[123] that the general complex structures, which may be best described as time-averaged, are those that allow maximum interaction energy between the participating species which is compatible with the steric and electronic interactions between the solute and aromatic molecules. Although the aromatics are twice as polarisable in the plane of the ring as along the six-fold axis, it was shown that the interaction energy for a dipole acting along the six-fold axis of the aromatic is about twice that when acting in the plane of the ring. Because of this, several investigators[15,104] have shown that there is normally one type of structure most favoured for dipole-induced dipole complexes. This is the one in which the most electropositive end of the solute (usually its hydrogen atom or atoms) tends to be located above the plane of the ring adjacent to the axis of symmetry, and with its dipolar axis coincident, or nearly so, with the six-fold axis.

In order to evaluate the geometries of the complexes of present interest,

the average values of Δ_c at different temperatures for various sytems as recorded intable 6.35 are employed. It can be seen from the table that these Δ_c values, for the interactions of chloroform, nitromethane and acetonitrile separately with the aromatics, in general are close to each other. In addition to this, it is also known that the relevant complexes formed are of the same stoichiometry (1:1) except that of acetonitrile-benzene. This evidence, together with the knowledge that both acetonitrile and nitromethane possess to some extent similar dipole moments (Chapter 6) and molecular structures, leads to a strong possibility that all three solutes may adopt a similar orientation with respect to the aromatics in the complexes, similar to that suggested[104] for chloroform with benzene.

Considering the values of Δ_c for the interactions of various solute-aromatic systems in the present work, it is apparent that the solute protons lie in a shielded region[24]. Assuming that all the complexes of these systems possess a similar geometry due to reasons mentioned above, there are two possible principal arrangements of the solutes relative to the aromatics in the complexes as shown in Fig. 7.1. One of these should represent the real time-averaged geometry of the complexes. When these structures are considered on the basis of interaction energies, it appears that structure (a) (which has in fact been suggested for the chloroform-benzene complex) is the one more likely to take place.

If structure (a), on time average, represents the correct geometry of the complexes, then the solute would lie symmetrically about the six-fold axis of the aromatic molecules with their hydrogen atoms nearest to the ring.

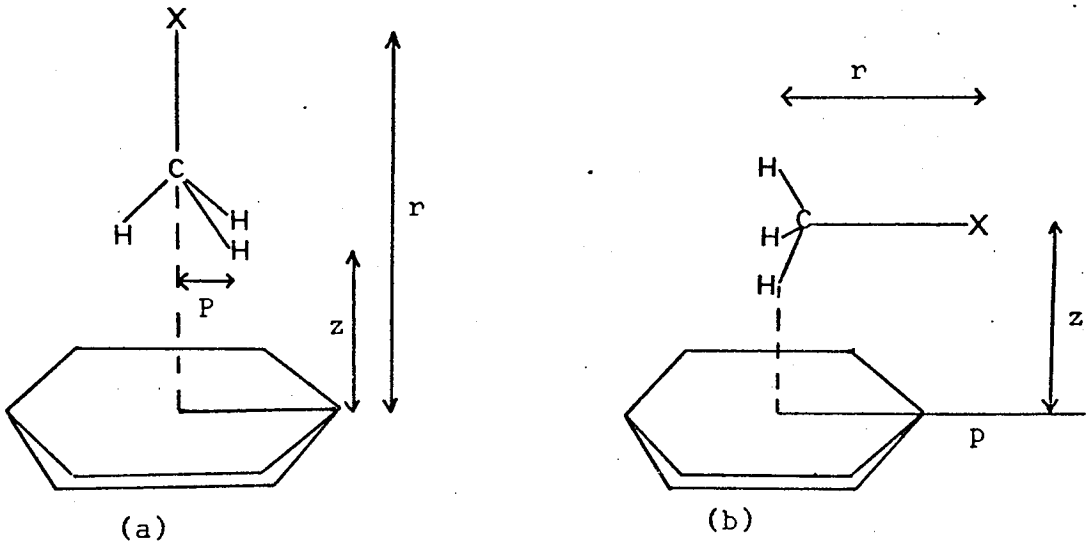

FIG. 7.1 POSSIBLE ARRANGEMENTS OF THE COMPLEXES AND THE DEFINITIONS OF THE DISTANCES r,p,z. (X = NO_2, CN, Cl_3 GROUP) FOR $CHCl_3$ ONLY ONE H ATOM IS PRESENT

It has been found that for this type of complex configuration the participating species are effectively in direct contact with each other, i.e. the z value estimated from the sum of the van der Waals radii should be about 3.05 Å. This value is equal to a combination of the radius of a hydrogen atom (1.20 Å) and the half thickness of an aromatic molecule (1.85 Å).

Adopting the approach discussed in section 7.2, different isoshielding diagrams were drawn employing the values of p and z (obtained from the Johnson and Bovey table referred to earlier) corresponding to the values of Δ_c shown in table 6.35. A typical diagram is shown in Fig. 7.2. As mentioned earlier, conditions concerning p have to be imposed for these solutes to evaluate the z values for the complexes. Using the molecular parameters quoted in table 7.1, the theoretical p values for this type of arrangement of solutesin the complexes were found to be 0.00 ring radii (0.00 Å) for chloroform, 0.640 ring radii (0.890Å) for nitromethane and 0.649 ring radii (0.902Å) for acetonitrile; one ring radius (r.r.) is equal to 1.390Å. Employing these p values the values of z were obtained from the isoshielding diagrams for all the complexes studied. The results are recorded in table 7.2.

An examination of the table shows that the values of z for these complexes can be compared favourably with the sum of the van der Waals radii (3.05Å). This consequently indicates that the complexes are more likely to possess configuration (a). A circumstantial conclusion is therefore drawn upon this basis. The complex structure is shown in Fig. 7.3. It can also be seen from the table that, as more methyl groups are substituted into the aromatic ring, chloroform appears to move closer to the ring along the aromatic six-fold axis whereas nitromethane and acetonitrile behave in an opposite manner; the evidence .. agrees with that found earlier in Chapter 6.

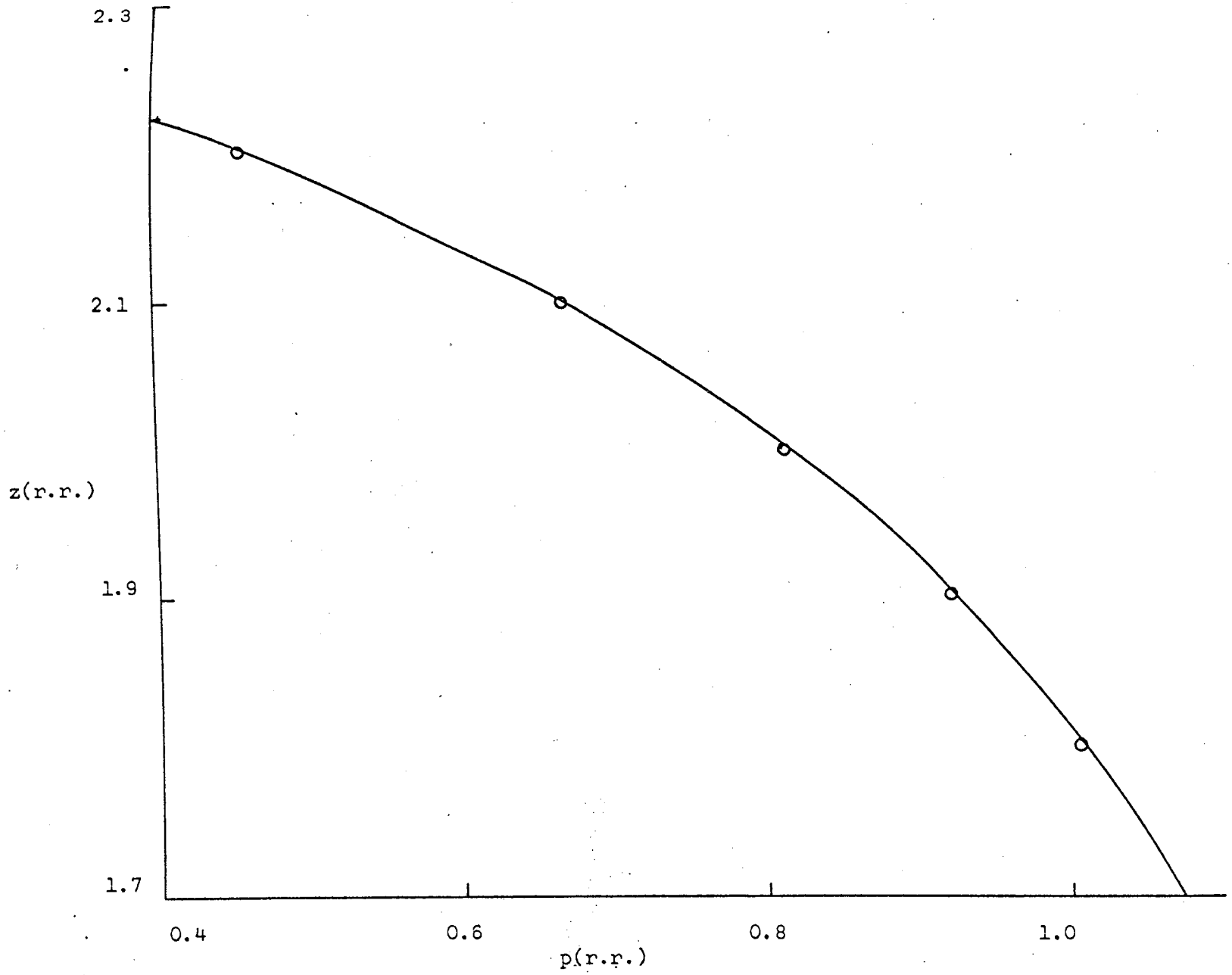

FIG. 7.2 ISOSHIELDING LINE FOR THE NITROMETHANE-BENZENE SYSTEM

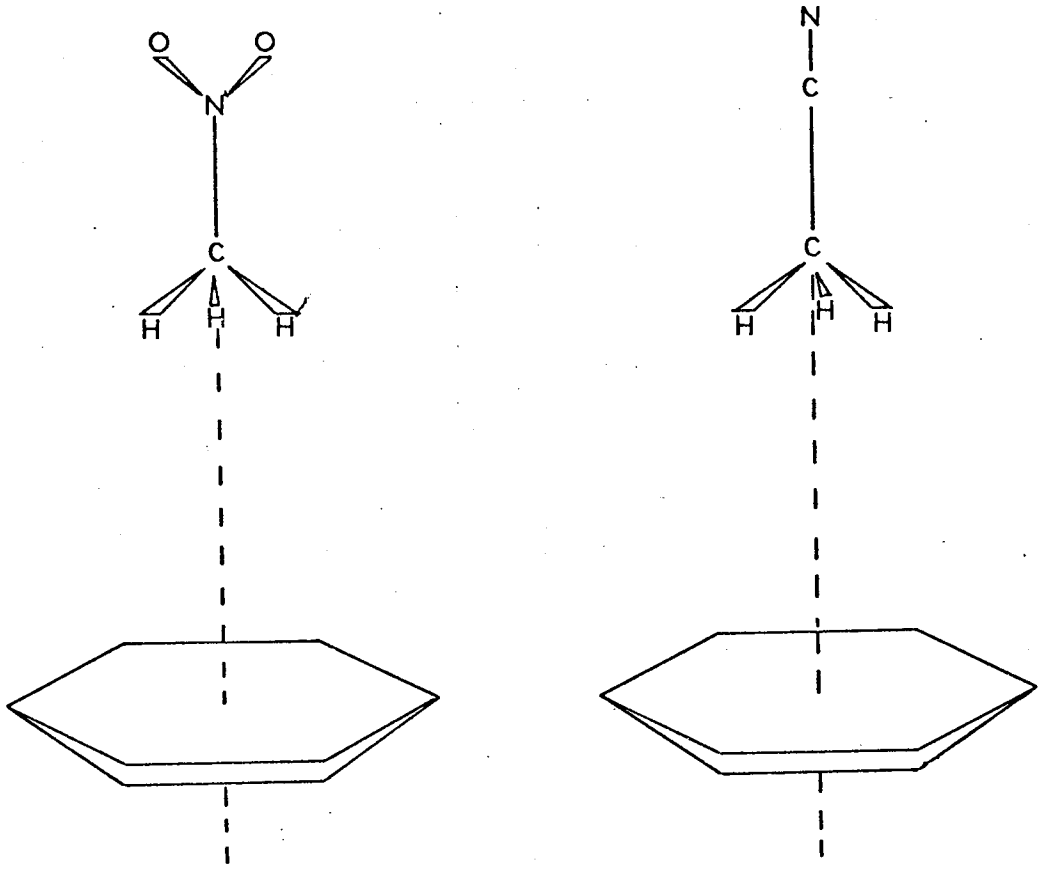

FIG. 7.3 PROPOSED STRUCTURE FOR THE NITROMETHANE-AROMATIC, ACETONITRILE-AROMATIC AND CHLOROFORM-AROMATIC COMPLEXES

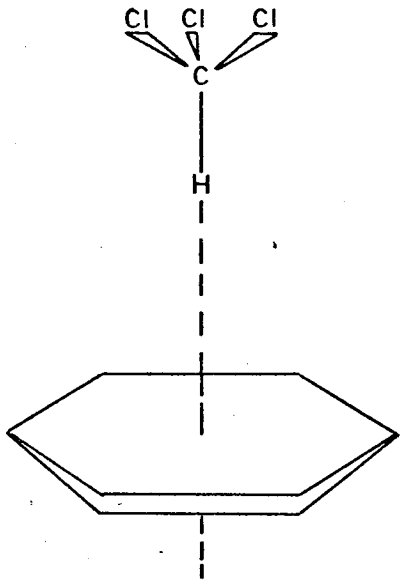

FIG. 7.3 (cont.)

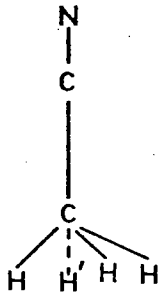

FIG. 7.4 THE POSITION OF THE EQUIVALENT PROTON (H') FOR ACETONITRILE

TABLE 7.1

MOLECULAR PARAMETERS FOR NITROMETHANE, ACETONITRILE AND CHLOROFORM[124]

Molecule	Bond length/ Å						Bond angle/radian		
	C-H	C-C	C≡N	N=O	C-N	C-Cl	∠HCH	∠ONO	∠HCCl
Nitro-methane	1.09	-	-	1.22	1.47	-	1.911	2.269	-
Aceton-itrile	1.105	1.46	1.15	-	-	-	1.911	-	-
Chloro-form	1.07	-	-	-	-	1.77	-	-	1.894

TABLE 7.2

THE PARAMETERS FOR THE VARIOUS SOLUTE-AROMATIC COMPLEXES

Complex	Δ_c/ppm	P/Å	z/Å
Chloroform-benzene	1.313	0.000	3.366
Chloroform-p-xylene	1.521	0.000	3.257
Chloroform-mesitylene	1.610	0.000	3.179
Nitromethane-benzene	1.536	0.890	2.943
Nitromethane-p-xylene	1.396	0.890	3.055
Nitromethane-mesitylene	1.341	0.890	3.109
Acetonitrile-p-xylene	1.446	0.902	3.006
Acetonitrile-mesitylene	1.349	0.902	3.094

Although the complex structure as shown in Fig. 7.3 appears to be correct at the time being, only the general conclusion that the solute protons lie symmetrically about the six-fold axis of the aromatic is obtained from the present studies. However the electronegative ends (CN, NO_2 and Cl_3

groups) of the solutes cannot be fixed exactly. It is still possible that these groups may not lie on but somewhere off the six-fold axis, a modification of the present structure. Further considerations later on should clarify the matter.

7.2.b TIME-AVERAGED GEOMETRY OF THE ACETONITRILE-BENZENE COMPLEX

Since the correct solute/solvent ratio for the complex is found to be 1:2, the evaluation of its geometry has to be made in relation to one acetonitrile being surrounded by two benzene molecules. Having considered this and also the fact that both benzene molecules must experience equal electronegativity effect from the CN group, the only reasonable complex structure is that of a sandwiched one. In this structure the solute lies in the middle of and equidistant from both benzene rings. The main molecular axis of the solute is parallel to the planes of the rings with its electronegative and lying beyond the vicinity of the rings owing to the repulsion from the π- cloud. However, with this arrangement of the solute, each of its three protons of the methyl group experiences a different shielding (which is inversely proportional to the cube of the distance from the methyl proton to the centre of the benzene ring). Because the experimental value of Δ_c obtained for this complex represents the average shielding on these protons, an approximation was then made to simplify the problem. In this approximation the shielding of the three protons is considered to be identical to that of an equivalent proton lying at the intersection of the extrapolated C-X bond and the plane containing the protons (Fig. 7.4). Any determinations of the structural (z,p) co-ordinates of the solute in the complex were therefore referred to the equivalent proton.

Using the molecular parameters for acetonitrile given earlier in table

7.1, the theoretical p value for the solute was assumed to be 0.00 r.r (0.00 Å). Upon imposing this value of p on the isoshielding line corresponding to the Δ_c value of 1.220 ppm (Fig. 7.5), an experimental value for z was obtained as 2.547 r.r. (3.540 Å). The results are tabulated in table 7.3 and the complex structure shown in Fig. 7.6. The theoretical z value calculated from the sum of van der Waals radii for the system was equal to 3.70 Å. Comparison of both z values gives credence to the assumed structure and indicates again that the solute and benzene are in direct contact with each other in the complex.

The discussion of the complex geometries so far is based upon the n.m.r. results obtained previously in Chapter 5. To throw more light upon these, the results from dielectric studies reported in Chapter 6 will now be considered.

TABLE 7.3

THE PARAMETERS FOR THE ACETONITRILE-BENZENE COMPLEX

Δ_c/ppm	p/Å	z/Å
1.220	0.000	3.540

7.3 FURTHER CONSIDERATIONS OF COMPLEX CONFIGURATIONS THROUGH DIELECTRIC STUDIES

It has already been suggested in the previous chapter that for all the systems in the present work the interactions are dipole-induced dipole, and the dipole moments induced in various aromatics (μ_{ARO}) by the solutes were calculated. Frank[80] has shown that in general μ_{ARO} is

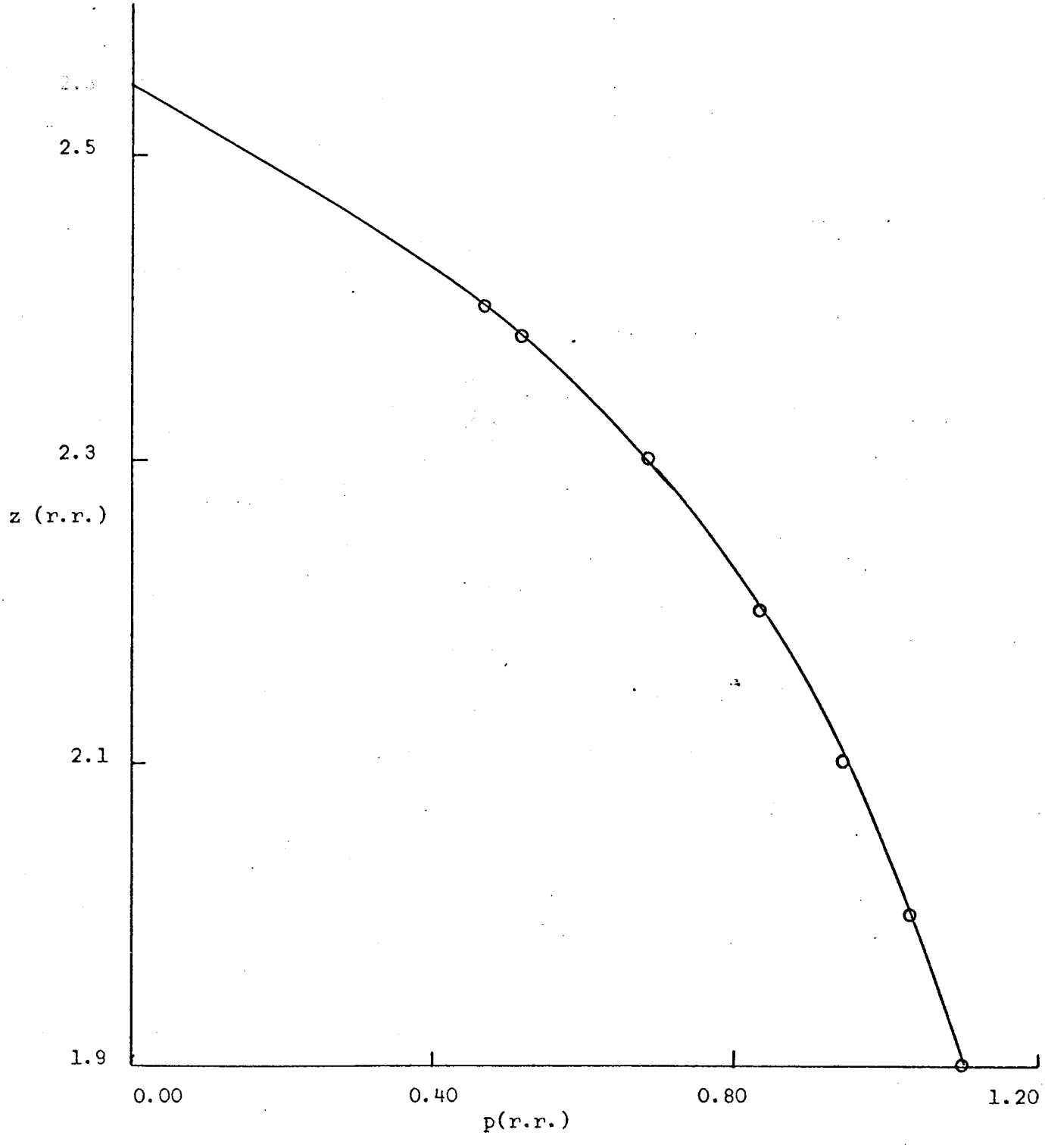

FIG. 7.5 ISOSHIELDING LINE FOR THE ACETONITRILE-BENZENE SYSTEM

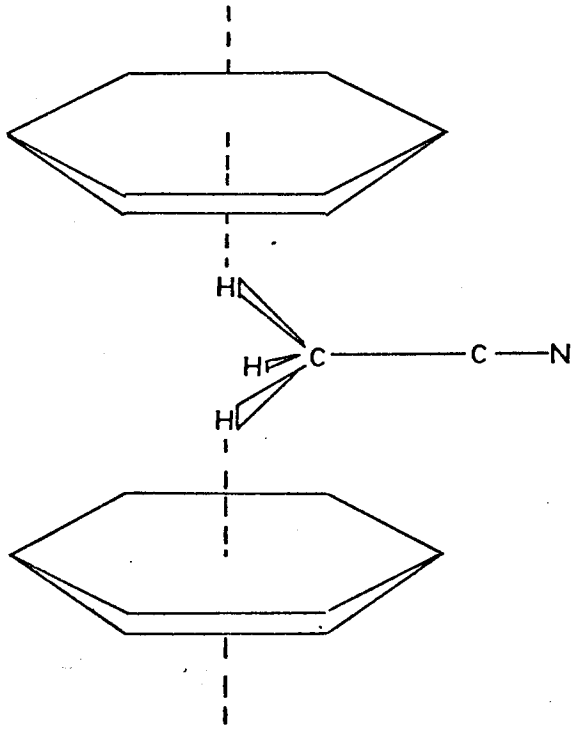

FIG. 7.6 PROPOSED STRUCTURE FOR THE ACETONITRILE-BENZENE COMPLEX

related to the distance from the point dipole in the solute to the point at which it induces a dipole, r. This relation can be described in the following way.

When a polar solute of moment (when present in an inert solvent) μ_{INERT} is placed in an aromatic medium of polarisability α, it induces a moment μ_{ARO} in the medium. The magnitude of μ_{ARO} is given by

$$\mu_{ARO} = \alpha F \qquad (7.1)$$

where F is the intensity of the electric field acting on the aromatic molecule and[125]

$$F = \frac{E(\varepsilon + 2)}{3} \qquad (7.2)$$

where E is the total electric field in the medium and ε the dielectric constant of the medium. It is a matter of contention what the significance of ε in (7.2) is. As E is considered to arise from a point dipole in the solute, ε therefore may have contributions from both the solute and aromatic. However, for the present work the assumption that ε refers to the aromatic alone, as made by Frank, is still adopted. For symmetrical aromatic molecules employed in the present studies, E can be resolved into two components, namely E_x and E_y. E_x is the component of the field in the direction of the dipole axis of the solute whereas E_y is that at right angles to this direction. The relations of these field components to r are given as

$$E_x = \mu_{INERT} (3 \cos^2\theta - 1) / \varepsilon r^3 \qquad (7.3)$$

and

$$E_y = 3 \mu_{INERT} \cos\theta \sin\theta / \varepsilon r^3 \qquad (7.4)$$

where θ is the angle between the solute dipole axis and the radial vector subtended from the solute point dipole to the point at which the dipole is induced.

Combination of equations (7.1) - (7.4) gives finally

$$(\mu_{ARO})_x = \frac{a\mu_{INERT}(\varepsilon + 2)(3\cos^2\theta - 1)}{3\varepsilon r^3} \qquad (7.5)$$

$$(\mu_{ARO})_y = \frac{a\mu_{INERT}(\varepsilon + 2)\cos\theta\sin\theta}{\varepsilon r^3} \qquad (7.6)$$

It is therefore evident that by employing equations (7.5) and (7.6), the distance r can be calculated for each complex studied. To simplify the matter for discussion, the acetonitrile-benzene complex will be considered separately later on.

For the arrangement of a solute in a complex shown in Fig. 7.3, the solute dipole axis is along the six-fold axis of the aromatic and $\theta = 0$ radian. Thus from (7.6)

$$(\mu_{ARO})_x = \frac{2a_\perp\mu_{INERT}(\varepsilon + 2)}{3\varepsilon r^3} \qquad (7.7)$$

$$(\mu_{ARO})_y = 0$$

where $a_\perp$ is the perpendicular polarisability of the aromatic. It is apparent that in this case μ_{ARO} (table 6.35) is in fact the same as $(\mu_{ARO})_x$. Using the values of μ_{ARO} and μ_{INERT} reported earlier in tables 6.35 and 6.33 and the various parameters recorded in table 7.4, the values of r (assuming the solute point dipole is acting at the ring centre) for various complexes were evaluated through (7.7). From these values the distances (from the equivalent proton) of the effective dipolar centres for the solutes in the complexes (r-z) were calculated (Fig. 7.1a). The results obtained are given in table 7.5. It is evident that to define the accuracy of these results would be difficult

because of the number of steps and approximations in the approach (see also section 6.7) and no attempt will be made to do so here.

A perusal of table 7.5 shows that on moving up the aromatic series the value of r-z, which is in fact the distance from the centre of the hydrogen atoms of the solute to the point where its molecular point dipole is located, appears to decrease for chloroform and increase for nitromethane or acetonitrile. Generally it is expected that the position of this point dipole should be constant and lie well towards the electronegative end of the molecule[15,22]. When comparing these r-z distances with the molecular dimensions of the solutes shown in Fig. 7.7[124,127], it is found that only chloroform results appear rational. The values of r-z for other solutes indicate that their point dipoles do not lie towards their negative ends, which is a rather unexpected result. The discrepancy of these results obtained appears to suggest that the present approach adopted in the determination of r is incorrect at some point. To investigate this possibility, the implications of the Johnson-Bovey approach (which is employed in the evaluation of z) is considered in more detail.

TABLE 7.4

DIELECTRIC CONSTANTS AT 308.2K (FROM THE PRESENT WORK) AND THE POLARISABILITIES[126] (PERPENDICULAR $a_\perp$ AND PARALLEL $a_{/\!/}$) FOR VARIOUS AROMATICS

Aromatic	ε	$a_\perp/10^{30}m^3$	$a_{/\!/}/10^{30}m^3$
Benzene	2.2553	7.33	11.14
p-Xylene	2.2491	10.75	13.40
Mesitylene	2.2618	12.47	17.10

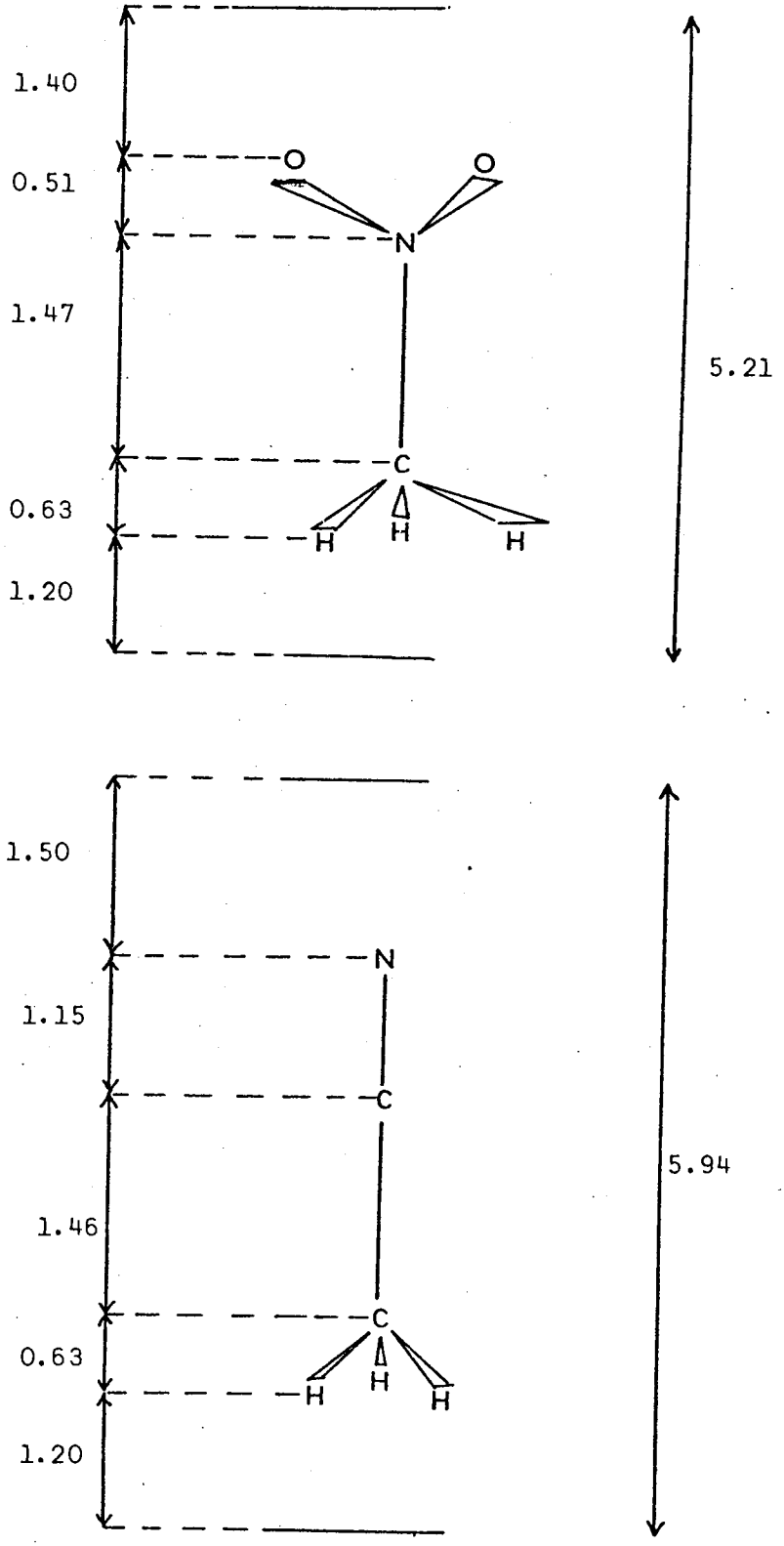

FIG. 7.7 SOME DIMENSIONS OF THE SOLUTE STUDIED (ALL DISTANCES ARE IN $\mathring{A}$)

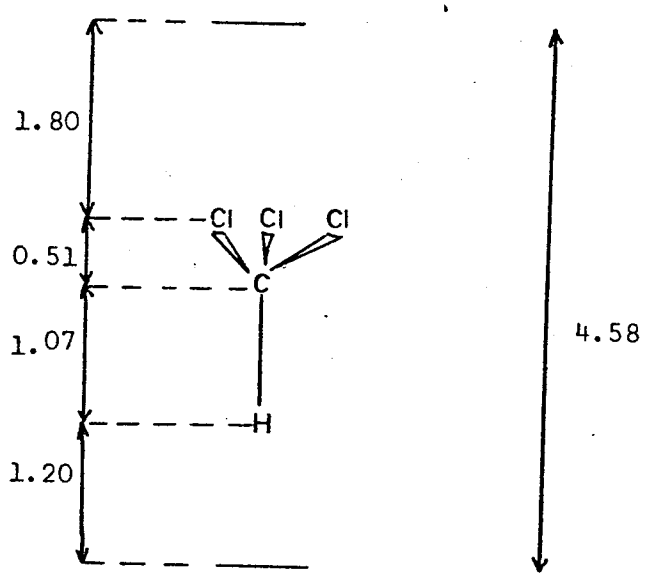

FIG. 7.7 (cont.)

TABLE 7.5

THE DIPOLE MOMENTS INDUCED IN THE AROMATICS BY THE SOLUTE (μ_{ARO}), THE DISTANCES BETWEEN THE SOLUTES POINT DIPOLES AND THE RING CENTRES (r) AND THE DISTANCES OF THE EFFECTIVE DIPOLAR CENTRES (r-z) FOR VARIOUS COMPLEXES.

Complex	$\mu_{ARO}/(3.335 \times 10^{30})$ Cm	r/Å	(r-z)/Å
Chloroform-benzene	0.07	5.36	1.99
Chloroform-p-xylene	0.13	4.96	1.70
Chloroform-mesitylene	0.22	4.37	1.19
Nitromethane-benzene	0.44	3.93	0.99
Nitromethane-p-xylene	0.40	4.61	1.56
Nitromethane-mesitylene	0.23	5.82	2.71
Acetonitrile-p-xylene	0.45	4.52	1.52
Acetonitrile-mesitylene	0.36	5.12	2.02

A PSEUDO-JOHNSON-BOVEY APPROACH

In the treatment of Johnson and Bovey of the anisotropic screening by a benzene molecule (or in the present cases an aromatic molecule due to the reasons stated earlier[104]), the π-electrons were considered to be precessing in two circular paths (loops), one on each side of and equidistant from the carbon-carbon (C-C) plane containing the ring centre, with the radii of the loops equal to the C-C distance in the aromatic ring. The separation of these loops was taken to be 1.28Å. Fig. 7.8 represents this two-loop model of an aromatic molecule in the presence of a solute molecule, with A and B as the loops above and below the C-C plane respectively. The distance z corresponds to that obtained previously from n.m.r. studies using the model whereas the distance

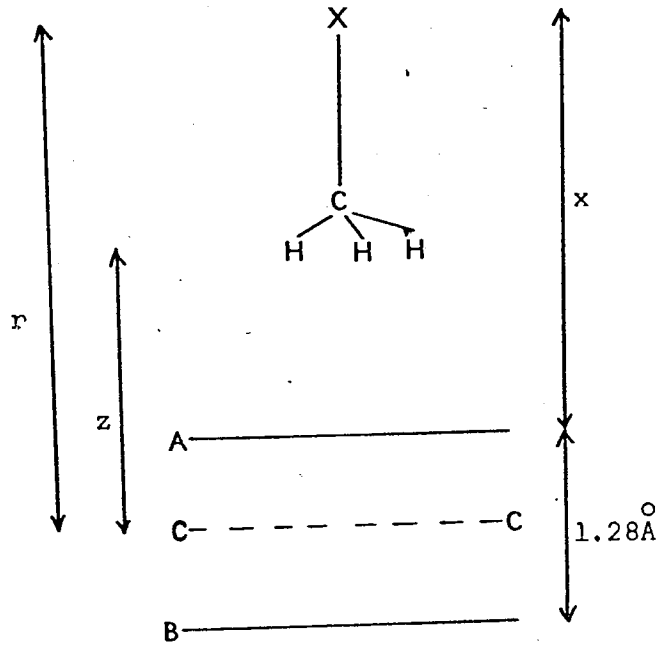

FIG. 7.8 DIAGRAM REPRESENTING THE TWO-LOOP MODEL OF AN AROMATIC MOLECULE AND VARIOUS DISTANCES CORRESPONDING TO THE SOLUTE (X = Cl_3, NO_2, CN GROUP)

r is deduced from dielectric studies. This value of r is calculated originally from a consideration that the point dipole on the solute operates at the ring centre such that the total induced moment originates from the latter.

A closer look at the two-loop model for n.m.r. screening suggests no reason why, when moments are induced in the aromatic, these cannot be considered to arise from perturbations of the distributions of the π-electrons in the two loops separately. Thus it may be justified to assume that the solute point dipole is in fact operating at the centres of loops A and B, not at the ring centre as originally considered. Moreover, it is evident through (7.7) that the magnitude of the moment induced by the point dipole varies inversely with the cube of distance from it to the point of operation. Therefore the magnitudes of the former at both loops should differ considerably. Taking x as the distance from the point dipole to loop A, the moments induced at A can be written as

$$\left(\mu^{A}_{ARO} \right)_x = \frac{2 a_{\perp} \mu_{INERT} \, (\varepsilon + 2)}{3 \varepsilon x^3} \qquad (7.8)$$

and that at loop B as

$$\left(\mu^{B}_{ARO} \right)_x = \frac{2 a_{\perp} \mu_{INERT} (\varepsilon + 2)}{3 \varepsilon (x + 1.28)^3} \qquad (7.9)$$

It is seen from (7.7) and (7.8) that $\left(\mu^{A}_{ARO} \right)_x$ is always greater than $\left(\mu^{B}_{ARO} \right)_x$ and their sum is different from (7.7). $\left(\mu^{A}_{ARO} \right)_x + \left(\mu^{B}_{ARO} \right)_x$ can be the same as that of (7.7) only when $\left(\mu^{A}_{ARO} \right)_x = \left(\mu^{B}_{ARO} \right)_x$, which is impossible for the present complex configuration.

The total induced moment in the aromatic is then given as

$$(\mu_{ARO})_x = (\mu^{A}_{ARO})_x + (\mu^{B}_{ARO})_x = \frac{2a_1\mu_{INERT}(\varepsilon+2)}{3\varepsilon}\left(\frac{1}{x^3} + \frac{1}{(x+1.28)^3}\right) \quad (7.10)$$

According to Fig. 7.8, r is equal to x + 0.64. It is evident that by adopting the two-loop model approach (and employing (7.10)) the values of x, and therefore r, can be calculated for each complex studied. Using (7.10), the values of x and r were calculated. The results obtained are given in Table 7.6 together with the corrected values of r-z. An examination of the corrected values of r-z shows that the solute point dipoles in most cases lie well towards the electronegative ends of the solutes (Fig. 7.7). There are one or two isolated cases when the point dipoles lie just beyond the molecular dimensions of the solutes but this may arise from experimental errors. This consequently confirms that the present approach, based upon a consideration of the point dipoles acting at both electron loops and not at the ring centres of the aromatics, is justified.

TABLE 7.6

THE DISTANCES FROM THE SOLUTE POINT DIPOLES TO THE FIRST ELECTRON LOOP (x), THE CORRECTED DISTANCES BETWEEN THE SOLUTE POINT DIPOLES AND RING CENTRES OF THE AROMATICS (r) AND THE CORRECTED DISTANCES OF THE EFFECTIVE DIPOLAR CENTRES (r-z) FOR VARIOUS COMPLEXES (THE ARROWS INDICATE THE DIRECTION OF INCREASE OF r AND r-z)

Complex	x/Å	r/Å	(r-z)/Å
Chloroform-benzene	6.22	↑6.86	↑3.49
Chloroform-p-xylene	5.73	6.37	3.11
Chloroform-mesitylene	4.99	5.63	2.45
Nitromethane-benzene	4.67	5.31	2.37
Nitromethane-p-xylene	5.41	6.05	2.99
Nitromethane-mesitylene	6.53	↓7.17	↓4.06
Acetonitrile-p-xylene	5.18	5.82	2.81
Acetonitrile-mesitylene	5.93	↓6.57	↓3.48

Evidently from table 7.6 the distances r and r-z for a particular solute with various aromatics show considerably either an increase or a decrease on moving up the aromatic series. In fact the distances r-z of a solute should be close to each other if its interactions with different aromatics result in a similar, rigid complex structure. An apparent change in these distances indicates that there must be some otherwise hidden process taking place in the complexes. It has already been suggested[104], for complexes of chloroform with various methyl-substituted benzenes, that chloroform undergoes a wobbling motion about the aromatic six-fold axis (Fig. 7.9). Other evidence to support this wobbling model will be seen from the consideration of the entropies of complex formation. The extent of the motion can be represented by the angle α . It is evident that the substitution of methyl groups into the ring seems to increase this motion for chloroform, (larger α) resulting in, on time average, a smaller value for r and z (table 7.2). If both acetonitrile and nitromethane also adopt the wobbling motion in the complexes, it would appear that their motion is more restricted by the presence of methyl groups in the aromatic ring (smaller α)hence leading to an increase in r and z.

EVIDENCE FOR NON-RIGID STRUCTURES OF MOLECULAR COMPLEXES

Up to this point it is seen that the geometry of all the complexes have been evaluated initially, through n.m.r. results, by making one or two assumptions beforehand. The correct geometry appears to agree with that of Fig. 7.1a. It is logical to bring in more evidence to support (or otherwise) this conclusion by considering the dielectric data in the context of the complex structure represented by Fig. 7.1b, because if it is not the one adopted in the complexes, then μ_{ARO} calculated for this structure will be different from those shown in table 7.5.

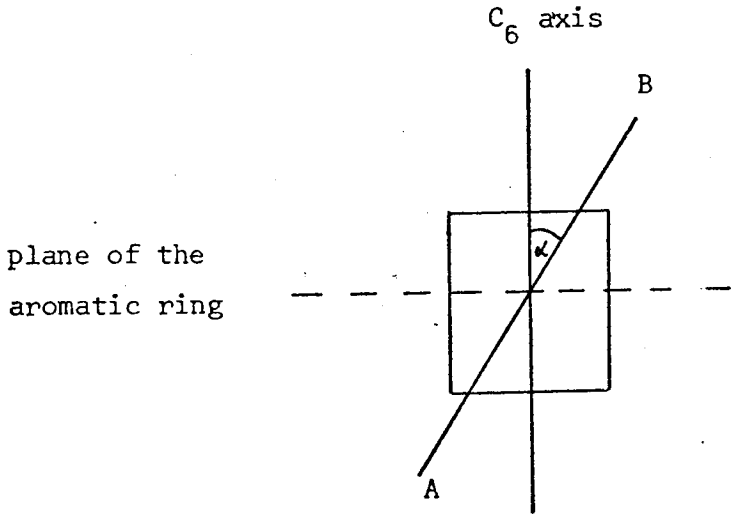

FIG. 7.9 DIAGRAM REPRESENTING THE WOBBLING MOTION OF THE SOLUTE ABOUT THE SIX-FOLD AXIS (AB REPRESENTS THE SOLUTE MOLECULAR AXIS)

This alternative arrangement of the solute relative to the aromatic depicted on the basis of the two-loop model is shown in Fig. 7.10. In this case A and B represent the centres of the two electron loops in the aromatic where the solute point dipole (at O) is operating. θ and ϕ are the angles between the solute dipole axis (along OH′) and the radial vectors (r_A and r_B) subtended from the point dipole to A and B. H′ represents the equivalent proton of the solute as discussed earlier (or just the (ordinary) proton as in the case of chloroform) and OH′ therefore corresponds to the distance of effective dipolar centres from these points. The components of the induced moments along the x and y directions at A and B are respectively $(\mu^A_{ARO})_x$, $(\mu^A_{ARO})_y$, $(\mu^B_{ARO})_x$ and $(\mu^B_{ARO})_y$. It is evident that for this arrangement of the participating species of the complex, the x and y-axes become automatically the same as the p and z-axes.

Assuming the solute is in direct contact with the outer plane of the ring, the distances z of its proton (calculated from the sum of van der Waals radii) were found to be 3.95Å for acetonitrile, 4.36Å for nitromethane and 5.34Å for chloroform. From (7.5) and (7.6) it is found that

$$
\begin{aligned}
(\mu^A_{ARO})_x &= \frac{\alpha_{/\!/}\mu_{INERT}(\varepsilon+2)(3\cos^2\theta - 1)}{3\varepsilon r_A^3} \\
(\mu^B_{ARO})_x &= \frac{\alpha_{/\!/}\mu_{INERT}(\varepsilon+2)(3\cos^2\phi - 1)}{3\varepsilon r_B^3} \qquad (7.11) \\
(\mu^A_{ARO})_y &= \frac{\alpha_{\perp}\mu_{INERT}(\varepsilon+2)\cos\theta\sin\theta}{\varepsilon r_A^3} \\
(\mu^B_{ARO})_y &= \frac{\alpha_{\perp}\mu_{INERT}(\varepsilon+2)\cos\phi\sin\phi}{\varepsilon r_B^3}
\end{aligned}
$$

where $\alpha_{/\!/}$ is the parallel polarisability of the aromatic. The total

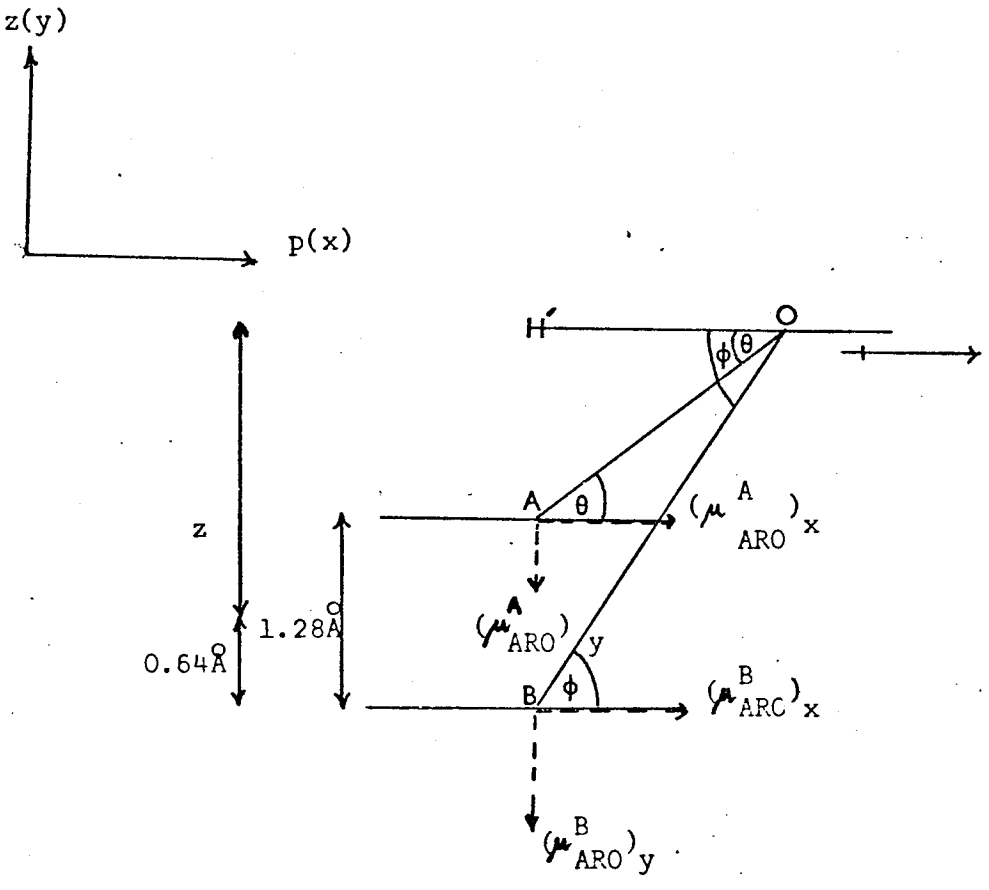

FIG. 7.10 DIAGRAM REPRESENTING THE COMPONENTS OF MOMENTS INDUCED IN THE AROMATIC BY THE SOLUTE POINT DIPOLE (ON THE ASSUMPTION THAT THE COMPLEX POSSESSES THIS STRUCTURE)

induced moment in the aromatic is therefore

$$\mu_{ARO}\ (\text{total}) = \left[\left(\left(\mu^{A}_{ARO}\right)_x + \left(\mu^{B}_{ARO}\right)_x\right)^2 + \left(\left(\mu^{A}_{ARO}\right)_y + \left(\mu^{B}_{ARO}\right)_y\right)^2\right]^{\frac{1}{2}} \qquad (7.12)$$

Also it is seen from Fig. 7.10 that

$$r_A^2 = (z-0.64)^2 + (OH')^2 \qquad (7.13)$$

and

$$r_B^2 = (z + 0.64)^2 + (OH')^2$$

It is thus evident that by adopting a reasonable value for the distance OH', the total induced moment in the aromatic can be calculated for each complex studied through (7.11) -(7.13).

Taking OH' as 3.00Å, such that the solute point dipole lies well towards the electronegative end of each solute studied, μ_{ARO}(total) was calculated for each complex. The results obtained are given in table 7.7 together with the experimental values of μ_{ARO} deduced earlier from dielectric studies (table 7.5).

A perusal of table 7.7 shows that the values of μ_{ARO} (calculated) do not show overall a significant difference from the corresponding values of μ_{ARO} (experimental). In most cases the differences are within 0.33×10^{-30} Cm. To investigate the effect of the distance OH' on the calculations this was varied by $\pm$ 0.5Å. This only resulted in a change of μ_{ARO} (calculated) by less than $\pm 0.067 \times 10^{-30}$ Cm which does not alter the results in table 7.7 significantly. It would therefore appear from this evidence that there is little energetic difference between the two extreme structures assumed and that there is almost an equal chance for these complexes to adopt either configurations shown in Fig. 7.1. Having considered this, it is of importance to reconsider the structural

co-ordinates for both complex structures from n.m.r. studies to find out if there is any correlation between them.

TABLE 7.7

THE CALCULATED TOTAL INDUCED MOMENTS, μ_{ARO} (calc.), FOR VARIOUS COMPLEXES ON THE ASSUMPTION THAT THE COMPLEX STRUCTURE IS THE SAME AS FIG. 7.1.b (THE DISTANCE OH´ TAKEN AS 3.0Å) AND THE CORRESPONDING EXPERIMENTAL VALUES OF INDUCED MOMENTS, μ_{ARO} (exp.), FROM DIELECTRIC STUDIES

Complex	μ_{ARO}(calc.)/3.335 x 10^{30} Cm	μ_{ARO}(exp)/3.335 x 10^{30} Cm
Chloroform-benzene	0.07	0.07
Chloroform-p-xylene	0.10	0.13
Chloroform-mesitylene	0.11	0.22
Nitromethane-benzene	0.27	0.44
Nitromethane-p-xylene	0.39	0.40
Nitromethane-mesitylene	0.46	0.23
Acetonitrile-p-xylene	0.53	0.45
Acetonitrile-mesitylene	0.61	0.36

From section 7.2, for any solute to adopt an orientation as in Fig.7.1b, the p value for the equivalent proton would have to be taken as 0.00Å. Using this p value / the corresponding value for z for each complex studied was obtained from the relevant isoshielding diagram (section 7.2.a). The results are given in table 7.8 together with those obtained earlier for a complex structure represented by Fig. 7.1.a.

An examination of table 7.8 shows that the systems of chloroform with various aromatics give the same values for z in both cases. This is

because, for either complex structure, their p values remained unchanged (0.00Å). For complexes of the other solutes, it is seen that their hydrogen atoms appear to approach the ring more closely than that predicted on the basis of the extreme configuration 7.1.b, whereas in configuration 7.1.a they appear to be in direct contact with the ring.

TABLE 7.8

THE THEORETICAL (ASSUMING THE INTERACTING SPECIES ARE IN DIRECT CONTACT REGARDLESS OF THE SIZE OF THE SOLUTE.NEGATIVE END) AND OBSERVED z VALUES FOR BOTH COMPLEX STRUCTURES, SHOWN IN FIG. 7.1, IF ADOPTED BY THE VARIOUS COMPLEXES

Complex	Structure 7.1a		Structure 7.1b	
	z(obs)/Å	z(theor.)/Å	z(obs)/Å	z(theor.)/Å
Chloroform-benzene	3.366	3.050	3.366	3.050
Chloroform-p-xylene	3.257	3.050	3.257	3.050
Chloroform-mesitylene	3.179	3.050	3.179	3.050
Nitromethane-benzene	2.943	3.050	3.241	3.940
Nitromethane-p-xylene	3.055	3.050	3.368	3.940
Nitromethane-mesitylene	3.109	3.050	3.525	3.940
Acetonitrile-p-xylene	3.066	3.050	3.378	3.950
Acetonitrile-mesitylene	3.094	3.050	3.451	3.950

It would seem, therefore, that a reasonable description of the structure of the complexes is one in which the solute adopts any of the variety of orientations ranging from 7.1.a and tending to 7.1.b.

Because no definite conclusion can be drawn upon the exact complex configuration, an energetic compromise must be recognised (Fig.7.11) and the solutes assumed to be "wobbling" about the six-fold axis (which

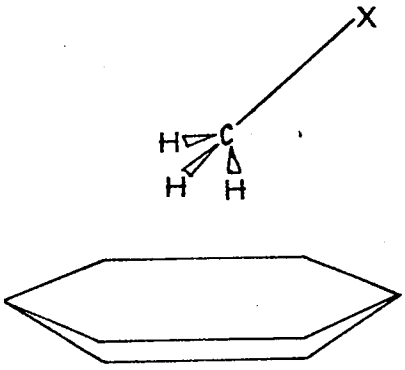

Fig. 7.11 ANOTHER POSSIBLE STRUCTURE FOR 1:1 COMPLEXES (X = CN, NO_2, Cl_3 GROUP)

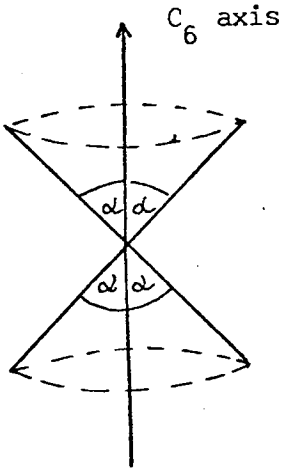

Fig. 7.12 THE CONE STRUCTURE REPRESENTING THE WOBBLING MOTION OF A SOLUTE

agrees with the conclusion made earlier) leading to a cone structure as shown in Fig 7.12. In other words whenever a complex is formed the structures between 7.1.a and 7.11 are adopted and that on time average the complex appears superficially as if only one (eg. 7.1.a) exists.

THE ACETONITRILE-BENZENE COMPLEX

According to Fig. 7.6, the structure of this complex is to some extent similar to that of Fig 7.1.b except that it involves two aromatic molecules. The determination of the distance of effective dipolar centres of the system therefore involves a similar consideration to that in Fig. 7.10. Fig. 7.13 represents the various components of moments induced by the solute at different electron loops with A and B and A' and B' as two sets of loop centres in the two aromatic molecules. The other symbols still carry their usual meanings as in Fig. 7.10. The distance z is already found from n.m.r. studies to be 3.54Å.

Because of the symmetrical arrangement of both benzene molecules with respect to the solute in the complex, it is seen that the sums of the induced moments along the y (z) - axis in both aromatics, which are $(\mu^{A}_{ARO})_y + (\mu^{B}_{ARO})_y$ and $(\mu^{A'}_{ARO})_y + (\mu^{B'}_{ARO})_y$, cancel each other out. This leaves only the sums of components of induced moments along the x (p) - axis in the aromatics, $(\mu^{A}_{ARO})_x + (\mu^{B}_{ARO})_x$ and $(\mu^{A'}_{ARO})_x + (\mu^{B'}_{ARO})_x$ (which are also equivalent to one another), to be considered. The total sum of the latter is in fact equal to μ_{ARO} for the interactions quoted earlier in table 6.35 as they all are in the same direction as μ_{INERT} of the solute. In other words.

$$(\mu^{A}_{ARO})_x + (\mu^{B}_{ARO})_x = (\mu^{A'}_{ARO})_x + (\mu^{B'}_{ARO})_x = 1.134 \times 10^{-30} \text{ Cm} \quad (7.14)$$

or

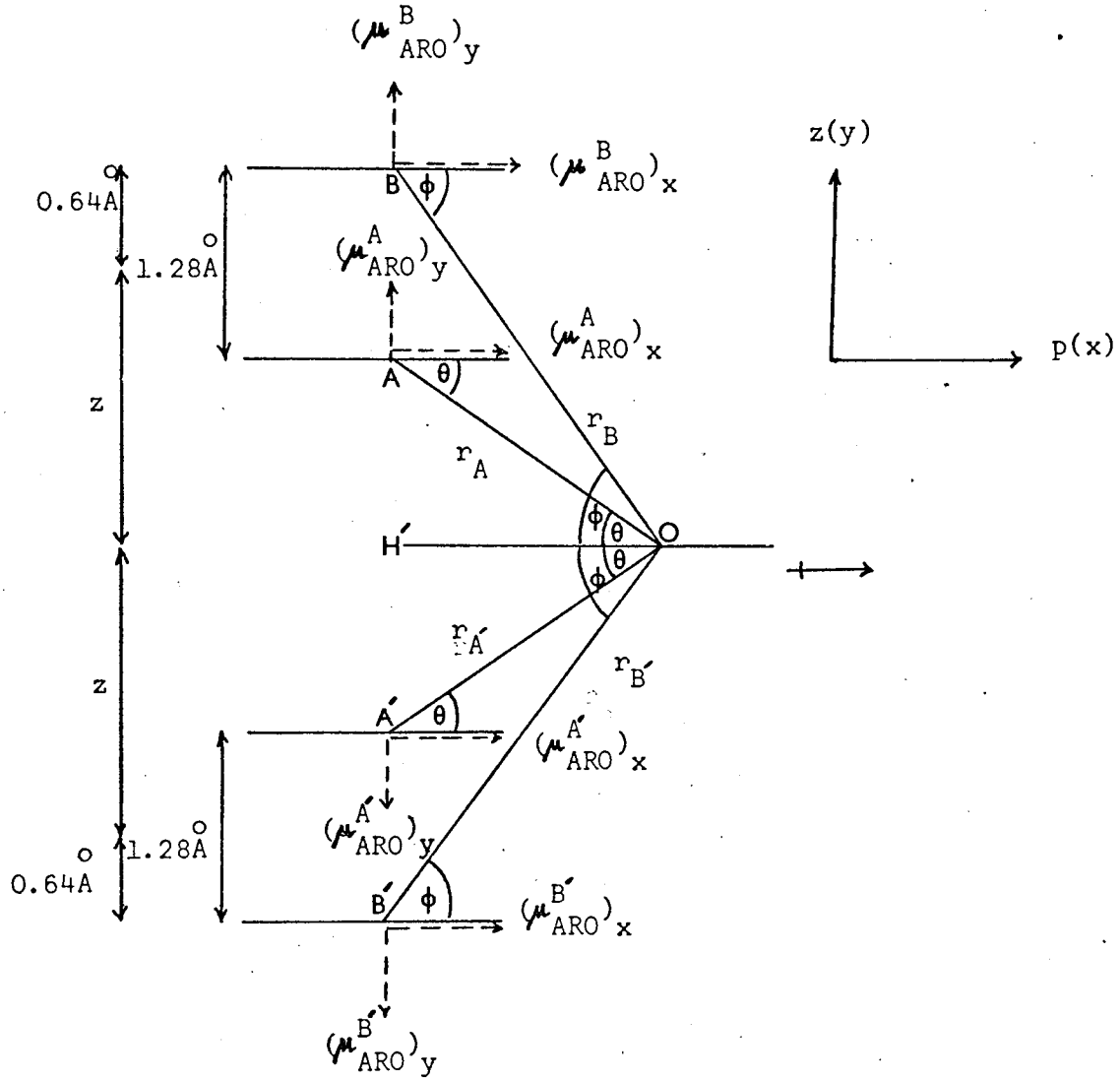

FIG. 7.13 DIAGRAM REPRESENTING THE COMPONENTS OF MOMENTS INDUCED IN THE AROMATICS BY THE SOLUTE POINT DIPOLE FOR THE ACETONITRILE-BENZENE COMPLEX.

$$(\mu^{A}_{ARO})_x + (\mu^{B}_{ARO})_x = (\mu^{A'}_{ARO})_x + (\mu^{B'}_{ARO})_x = 0.567 \times 10^{-30} \text{ Cm} \quad (7.15)$$

Since both benzene molecules experience equal induced moments, the consideration from now on will be confined to only one of them.

Considering the aromatic molecule containing A and B with the total moments induced in it represented by equation (7.15). It is evident that there are four unknown parameters, r_A, r_B, θ and ϕ, required to find the distance OH'. This cannot be done directly. An indirect method was employed by assuming different values for OH' and calculating the sum $(\mu^{A}_{ARO})_x + (\mu^{B}_{ARO})_x$ for each value of OH' using equation (7.11) and (7.13). A graph was then plotted between the distance OH' and $(\mu^{A}_{ARO})_x + (\mu^{B}_{ARO})_x$ (Fig. 7.14). By imposing the value of $(\mu^{A}_{ARO})_x + (\mu^{B}_{ARO})_x$ as 0.567×10^{-30} cm, the distance OH' (the distance of effective dipolar centres) for this complex is found to be 5.780Å.

Comparison of the distance with the dimension of acetonitrile in Fig.7.7 shows that in this case the point dipole lies beyond the electronegative end of acetonitrile. Bearing in mind the approximations implicit in the approach, this location is not unreasonable.

It is possible that for this arrangement of the solute relative to the aromatic, its point dipole may be perturbing electron circulations throughout the loops and not only at the loop centres as for other cases. If this possibility is considered in detail it may produce some improvement to the location of the point dipole.

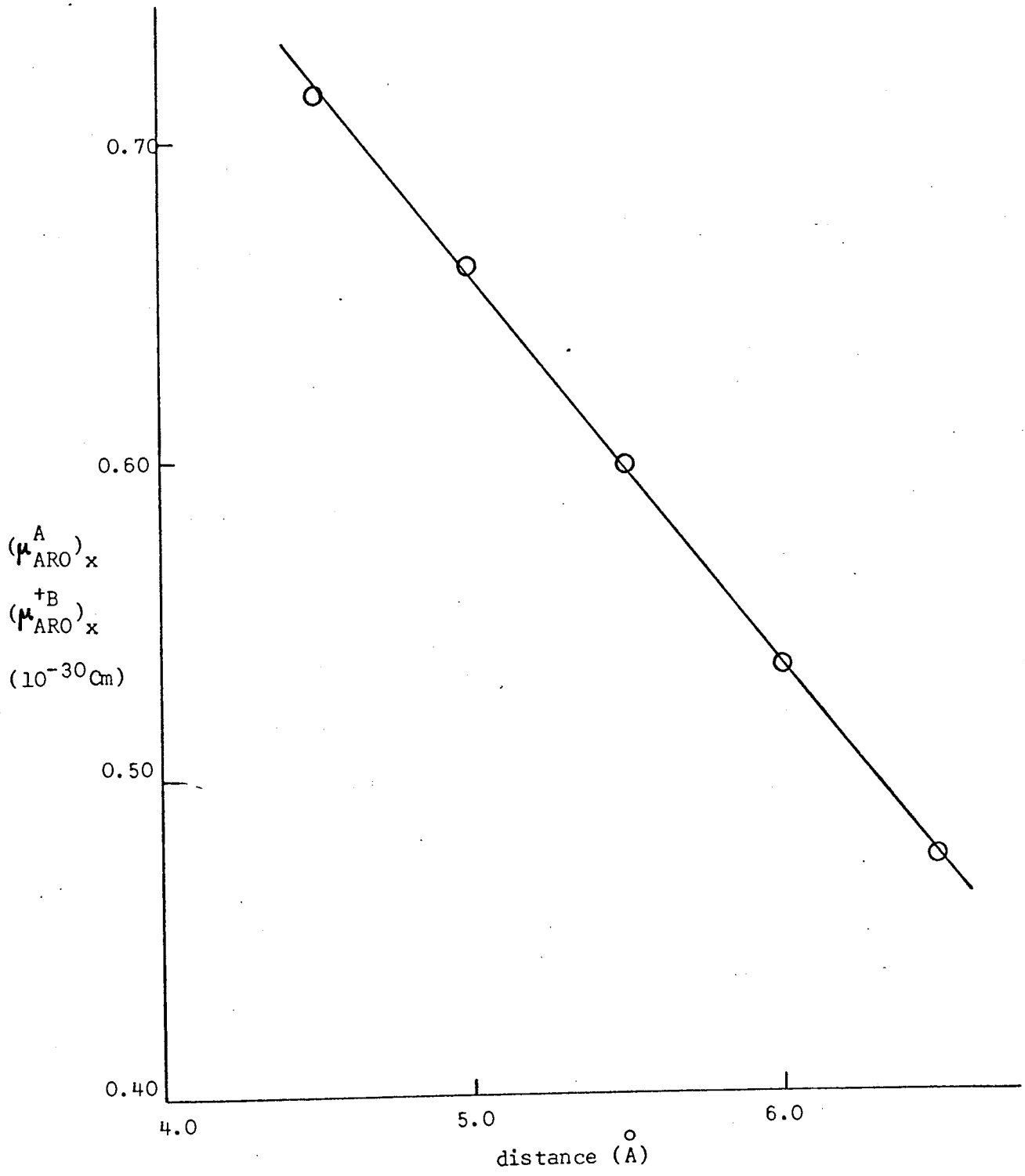

FIG. 7.14 RELATIONSHIP BETWEEN THE DISTANCE OF EFFECTIVE DIPOLAR CENTRES AND THE SUM $(\mu^{A}_{ARO})_x + (\mu^{B}_{ARO})_x$ FOR THE ACETONITRILE-BENZENE COMPLEX

PART B: CONSIDERATIONS ON THE STRENGTHS OF THE INTERACTIONS

7.4 INTRODUCTION

Having obtained information about the geometries of the various interactions studied, their strengths can be fully considered. The basic requirements for this purpose are the values of the thermodynamic parameters ΔH°, ΔS° and ΔG° which for the present work can be evaluated through n.m.r. studies at different temperatures using the relations

$$\Delta G^{\circ} = -RT\ln K_x$$

$$\frac{\partial \ln K_x}{\partial (1/T)} = -\Delta H/R \qquad (7.16)$$

and

$$\Delta G = \Delta H - T\Delta S$$

where all the symbols carry their usual meanings defined earlier in section 1.5.3. So far, apart from the values of K_x already evaluated in Chapter 5, the other parameters have not yet been determined. These will now be deduced; the values obtained by Whitney[104] for the interactions of chloroform with various aromatics will be merely quoted.

7.5 THE VARIOUS THERMODYNAMIC PARAMETERS

Using the values of K_x at different temperatures reported in Table 5.16, the values of ΔH°, ΔG° and ΔS° at 298.2K for all the systems of nitromethane and acetonitrile with various aromatics studied were evaluated through a least squares computer program called PARATHERM. This program fits the best straight line for a plot of $\ln K_x$ against 1/T with the various parameters obtainable from those relations in equation (7.16). The values so obtained, together with the corresponding values for chloroform-aromatic systems, are recorded in table 7.9.

A perusal of the table shows that the values of ΔH°, ΔG° and ΔS° are of the order of magnitude normally expected for the formation of weak complexes. Since the complexes of acetonitrile with benzene possess a different stoichiometry from the rest, it is illogical to compare them initially with those of the other complexes and so they are excluded from the present discussion. However, the magnitude of their thermodynamic parameters also shows their weak nature.

TABLE 7.9

THERMODYNAMIC PARAMETERS AND K_x VALUES AT 298.2K FOR VARIOUS SOLUTE-AROMATIC SOLVENT SYSTEMS

System	$-\Delta H^{\circ}$/kJ mole^{-1}	$-\Delta G^{\circ}$/kJ mole^{-1}	$-\Delta S^{\circ}$/JK^{-1} mole^{-1}	$K_x^{298.2}$
Chloroform-benzene[104]	13.363	2.155	37.584	2.388
Chloroform-p-xylene[104]	10.334	1.925	28.196	2.176
Chloroform-mesitylene[104]	10.748	2.263	28.455	2.493
Nitromethane-benzene	8.368	1.774	22.117	2.046
Nitromethane-p-xylene	8.343	2.004	21.268	2.245
Nitromethane-mesitylene	12.234	2.201	33.511	2.429
Acetonitrile-benezene	12.151	4.251	26.494	5.559
Acetonitrile-p-xylene	4.955	1.197	12.594	1.622
Acetonitrile-mesitylene;	7.619	1.599	20.192	1.906

It is evident that the changes of ΔH° and ΔS° from system to system, with nitromethane (or acetonitrile) acting as a common solute, follow the same pattern, i.e. on going from benzene to mesitylene the trend is

benzene > p-xylene < mesitylene

The ΔG° values for the same systems show a different pattern of

benzene < p-xylene < mesitylene

This evidence appears to demonstrate the difference in employing either ΔH° or ΔG° as a measure of the strength of a complex as discussed earlier in section 1.5.3 (this is not clear for the interactions of chloroform with various aromatics because ΔG° and ΔH° for these systems exhibit a similar pattern of change). It has already been shown in Chapter 5 that ΔH is independent of temperature. Since the feasibility of a reaction occurring (and the strength of the complex) should vary with the change in temperature, it must be measured directly through ΔG°, which is temperature dependent, and not ΔH.

Another point to support this can be seen from the values of ΔG° directly. These values in most cases are of a similar magnitude, except that for the acetonitrile-benzene system, which is about two or three times greater than the rest, indicating an existence of a different type of complex (1:2). At the same time the ΔH° value for this system does not differ significantly from those of the other systems (which have already been proved to contain only 1:1 complex species)

If ΔG° is considered for the purpose of indicating the strength of the complexes, it would appear that for the systems of present interest the strength of the interactions does not correlate systematically as a whole with the substitution of methyl groups on benzene.

7.6 THE ANALYSIS OF K_x VALUES

It has been discussed earlier in section 6.7 that the extent of complex formation depends mainly on some certain factors owing to the structures

and physical properties of both the solute and aromatic molecules. For a dipole-induced dipole interaction it is dependent on the polarisability of the aromatic, dipole moment of the solute and the steric environments for both species. For a common solute any change in the above factors is then related to the aromatic. This change is due to three different factors, namely the polarisation, steric blocking and trapping factors. It would therefore appear justified to regard the contribution to K_x for various solute-methyl substituted aromatic systems of present interest as arising from three separate terms as follows[128]:

a) A polarisation term, defined as the product of a polarising term x (characteristic of the solute) and a polarisability term for the aromatic compounds, which provides a positive contribution. Because, for the aromatic molecules studied here, a linear relation between six-fold axis polarisability and molar volume exists, this term can be weighted by the aromatic molar volume;

b) A steric trapping term (y) which gives either a negative or a positive contribution;

c) A steric blocking term (z) which gives a negative contribution.

Assuming benzene exerts negligible trapping or blocking effects, both y and z terms for other aromatics may be weighted by the differences in their molar volumes and that of benzene $(V_A - V_B)$. The term y is expected to be operative only when the substituents on the aromatic, if any, project appreciably above the ring. Thus K_x for any system studied can be described as

$$K_x = V_A x + (V_A - V_B)(\delta_i y - z) \qquad (7.17)$$

where δ_i is a factor regarding the size of the substituent groups on

the aromatic and is equal to +1 if their radii are greater than half the aromatic thickness; otherwise this factor is zero.

Adopting the relevant values of aromatic molar volumes shown in table 7.10, it is seen that for a solute-benzene system

$$K_x = 0.894x \qquad (7.18)$$

In the cases of p-xylene and mesitylene it is expected that their methyl groups do not project significantly above the ring and $\delta_i = 0$. The corresponding K_x for these sytems are then

$$K_x = 1.240x - (1.240 - 0.894)z \qquad (7.19)$$

and

$$K_x = 1.396x - (1.396 - 0.894)z \qquad (7.20)$$

It is therefore evident that by employing equations (7.18) - (7.20), the x, and z terms can be calculated for each solute. From these values different contributions to K_x may be deduced for all the solute-aromatic systems.

Following this, the values of K_x for each system recorded in table 7.9 were analysed. The results obtained are given in tables 7.11 and 7.12, together with those obtained by Whitney[104] for the various chloroform-aromatic systems. It has to be pointed out that the acetonitrile-benzene system is excluded from the present consideration due to the obvious reason that it contains a different type of complex, and cannot be compared properly with the other systems.

An examination of table 7.12 shows that there is a reasonable correlation between the calculated and experimental K_x values. The results obtained for the acetonitrile-aromatic systems must be treated with caution as

the x value is evaluated employing only equations (7.19) and (7.20) and not (7.18)

TABLE 7.10

VALUES OF DENSITIES[116] AND MOLAR VOLUMES FOR VARIOUS AROMATICS AT 298.2K

Aromatic	Density/10^{3}kgm^{-3}	Molar volume/10^{4}m^{3}mol^{-1}
Benzene	0.8735	0.894
p-Xylene	0.8565	1.240
Mesitylene	0.8610	1.396

TABLE 7.11

THE POLARISING (x), AND THE STERIC BLOCKING (z) TERMS FOR VARIOUS SOLUTES (THE TRAPPING TERM, y, =0) AT 298.2K

Solute	x/10^{-4} molm^{-3}	z/10^{-4} mol m^{-3}
Chloroform[104]	2.586	2.474
Nitromethane	2.289	1.621
Acetonitrile	1.109	-0.713

This could be the reason why the z value (and therefore the blocking factor) contains an opposite sign to the other solutes. For nitromethane, upon moving up the aromatic series, the contribution from the polarisation factor appears to predominate that from the blocking effect, resulting in an increase in K_x (and thus ΔG°). This evidence indicates that the methyl groups on the aromatic, apart from restricting the wobbling motion of the solute in the complex which leads to a

decrease in r and z, do not push the solute away from the aromatic to such an extent that the strength of the interaction is decreased. The results for the chloroform-aromatic systems, which exhibit the same change pattern, support the evidence already found from dielectric studies (section 7.3).

TABLE 7.12

VARIOUS CONTRIBUTIONS TO K_x VALUES FOR THE VARIOUS SOLUTE-AROMATIC SOLVENT SYSTEMS AT 298.2K

System	Polarisation Factor	Steric Blocking Factor	Calculated K_x	Experimental K_x
Chloroform-benzene[104]	2.313	0	2.313	2.388
Chloroform-p-xylene[104]	3.205	-0.853	2.352	2.176
Chloroform-mesitylene[104]	3.610	-1.241	2.369	2.493
Nitromethane-benzene	2.046	0	2.046	2.046
Nitromethane-p-xylene	2.838	-0.561	2.277	2.245
Nitromethane-mesitylene	3.195	-0.814	2.381	2.429
Acetonitrile-p-xylene	1.375	0.247	1.622	1.622
Acetonitrile-mesitylene	1.548	0.358	1.906	1.906

7.7 THE ANALYSIS OF ΔS VALUES

According to section 7.3, it is expected that the solute is undergoing a wobbling motion about the aromatic six-fold axis, except in the case of acetonitrile with benzene. If this motion is really taking place,

it should be sensitive to the change in temperature. Further support for this may be obtained from a consideration of the entropy effects with temperature. This is so since, with an increase in temperature, the possibility of the motion should be increased and therefore the entropy of the complex, S_{AB}, also would be expected to increase. If S_A and S_B (positive) represent respectively the entropies of the free solute and solvent, it follows that[121]

$$\Delta S = S_{AB} - S_A - S_B \qquad (7.26)$$

Assuming that all the entropies increase at the same rate as temperature increases, S_{AB} of a complex undergoing the motion should increase more rapdily than S_A and S_B, and ΔS becomes negative more slowly or less negative. For a complex with a rigid structure ΔS would become more negative. To test this point, ΔS at different temperatures for all the complexes (of nitromethane and acetonitrile with various aromatics) studied were evaluted employing the relations of (7.16) and the relevant data in tables 5.16 and 7.9. The results are given in table 7.13 together with those of chloroform-aromatic complexes obtained by Whitney. A perusal of the table shows that for each particular complex, within the range of temperature employed, no regular (or significant) change for ΔS is observed. In fact ΔS only changes by not more than $2 JK^{-1}mole^{-1}$ and any attempt to interpret this cannot be made possible. On average it appears that, within the narrow temperature range of n.m.r. studies in the present work (280 - 360K), ΔS is almost independent of temperature.

It can be seen that for a particular solute ΔS (excluding that of acetonitrile-benzene) tends to increase on moving up the aromatic series. Consequently, from above, if it is accepted that the formation of a more

TABLE 7.13

VARIATION OF ΔS WITH TEMPERATURE FOR THE COMPLEXES OF NITROMETHANE, CHLOROFORM AND SEPARATELY ACETONITRILE WITH VARIOUS AROMATICS

Complex	Temperature/K	$-\Delta S/JK^{-1}mole^{-1}$
Nitromethane-benzene	291.0	20.165
	306.4	21.798
	318.7	22.139
	326.5	22.257
	354.2	21.971
Nitromethane-p-xylene	295.9	20.713
	304.3	21.863
	321.5	21.506
	330.9	21.049
	341.1	21.143
Nitromethane-mesitylene	295.4	33.125
	307.8	32.823
	321.1	33.759
	331.4	33.940
	341.3	33.823
Acetonitrile-benzene	281.4	26.585
	305.8	26.141
	319.7	26.650
	326.8	26.581
	341.3	26.443
Acetonitrile-p-xylene	290.4	12.652
	305.6	12.461
	318.6	12.637
	326.8	12.606
	341.7	13.267

TABLE 7.13 (cont.)

Complex	Temperature/K	$-\Delta S/JK^{-1}mole^{-1}$
Acetonitrile-mesitylene	293.3	20.423
	304.7	19.849
	319.3	20.006
	326.7	20.465
	337.9	22.063
Chloroform-benzene[104]	281.8	37.877
	292.3	37.529
	302.0	37.046
	309.1	38.819
	319.3	37.990
Chloroform-p-xylene[104]	286.9	28.241
	292.9	27.970
	302.6	28.278
	311.4	27.814
	321.8	28.352
Chloroform-mesitylene[104]	277.1	28.288
	288.4	28.668
	304.8	28.480
	311.7	28.162
	322.1	28.555

rigid complex is followed by a greater ΔS, this trend implies that, if the solutes are in fact wobbling about in the complexes as proposed originally, their motion would be more restricted as more methyl groups are substituted into the aromatic ring; the result agrees with that interpreted from dielectric studies.

The above discussion as a whole can also be applied for complexes of chloroform. The only difference is that in the latter cases ΔS shows a decrease with the substitution of methyl groups on the ring, indicating a less rigid complex structure. This is somewhat surprising but does support the dielectric results in section 7.3.

7.8 CONCLUSIONS CONCERNING THE STRUCTURES OF THE 1:1 COMPLEXES

It is concluded earlier in section 7.4 that a solute appears to adopt a variety of orientations with respect to the aromatic in the complex ranging from structure 7.1.a to 7.11. From a colloquial standpoint the complex structure has been described as one in which the solute quoted "wobbles" in a cone of permitted orientations. In view of the short lifetime of a complex this should not be interpreted to mean extensive motion of the solute relative to the aromatic throughout the lifetime of the complex, but some limited motion may be possible. It is envisaged that as different complexes are formed they do so within one of the permitted orientations bounded by the cone. The n.m.r. evidence indicates that overall the relative perpendicular orientation (Fig. 7.1.a) may be the more energetically favoured. In any event, because most physical properties of the characteristics of the complexes have a time-averaged self-cancelling component in the p axis, the structure deduced from these parameters appears to be as shown in Fig. 7.1.a. Further evidence from the analysis of ΔS values and dielectric data also indicates that the extent of the

permitted orientations may become either more (for nitromethane and acetonitrile) or less restricted (for chloroform) by the presence of methyl groups on the aromatic. Judging from this behaviour, it is reasonable to offer an explanation for it. To do so, an insight into the dimensions of the solutes and the aromatics has to be obtained. These are given in Fig. 7.15 for all the relevant solutes.

In Fig. 7.15 AOB represents the plane at the top of the aromatic ring closest to the solute with the distances OA and OB equal to the radii of the ring. The carbon-carbon plane at the centre of the ring is denoted by the C-C-C line. To simplify each diagram, the hydrogen atoms of the aromatic are neglected and only methyl groups substituted on the C-C plane are shown. The circle around each atom in the diagram represents the van der Waal's radius of that atom as this has to be taken into account. The positive or negative character of an atom is represented by δ^+ or δ^-.

In the case of nitromethane, when the aromatic contains no methyl groups, it can adopt freely a variety of orientations with respect to the ring (Fig.7.11). When methyl groups are present on the ring, it can be seen that, for each particular orientation of the solute, the methyl group on one side of the aromatic is expected to repel the solute hydrogen atoms away whereas the other methyl group tries to pull the solute negative end (oxygen atoms) closer to the ring. Because on time average the hydrogen atoms of the solute spend most of their time closer to the ring than the oxygen atoms, the repulsive effect should be more pronounced. This overall results in the orientation of nitromethane being more restricted and the complex becomes relatively rigid.

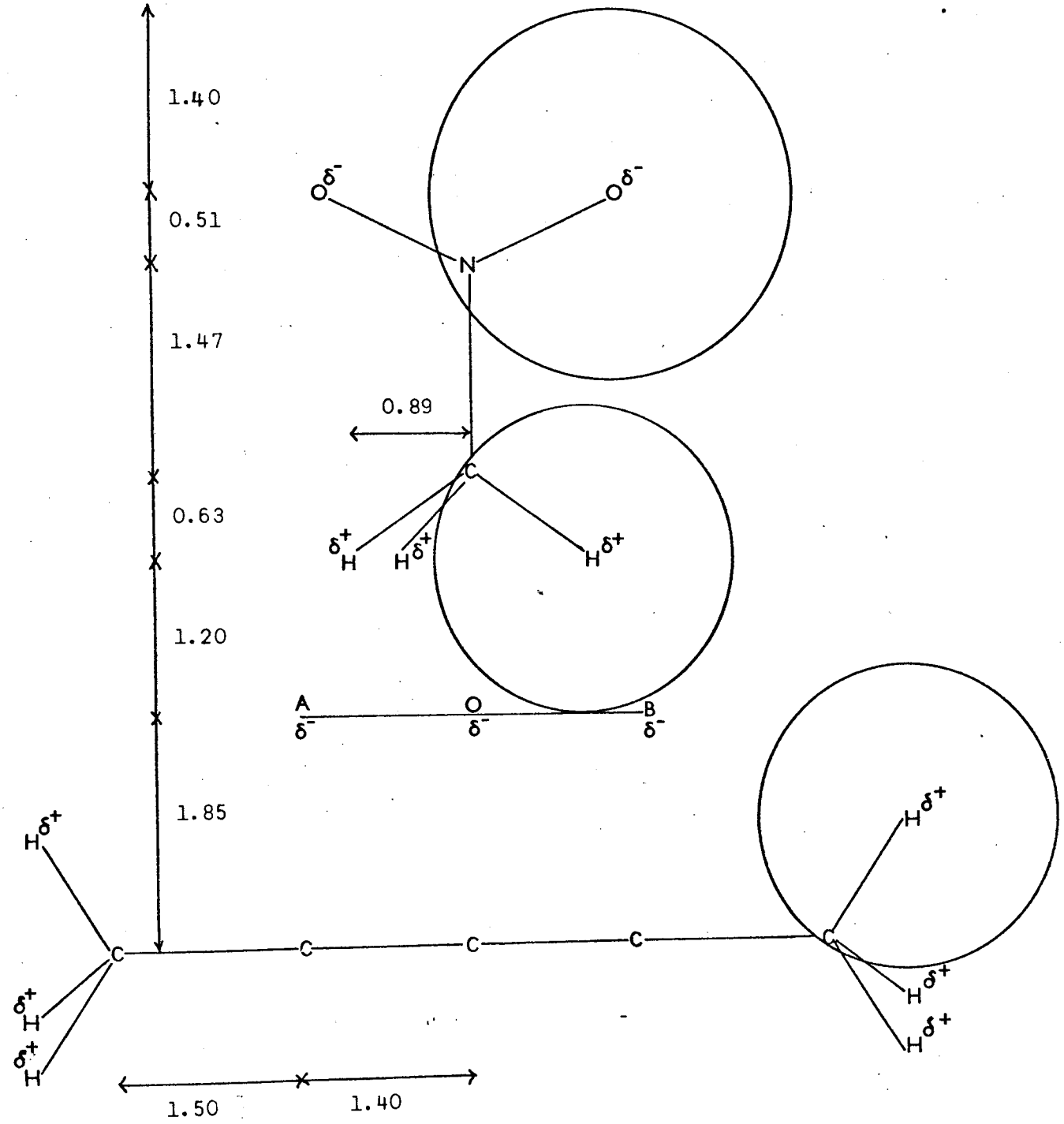

Fig. 7.15 DIMENSIONS OF SOME SOLUTESWITH RESPECT TO THE AROMATIC RING (ALL DISTANCES ARE TO SCALE AND IN Å)

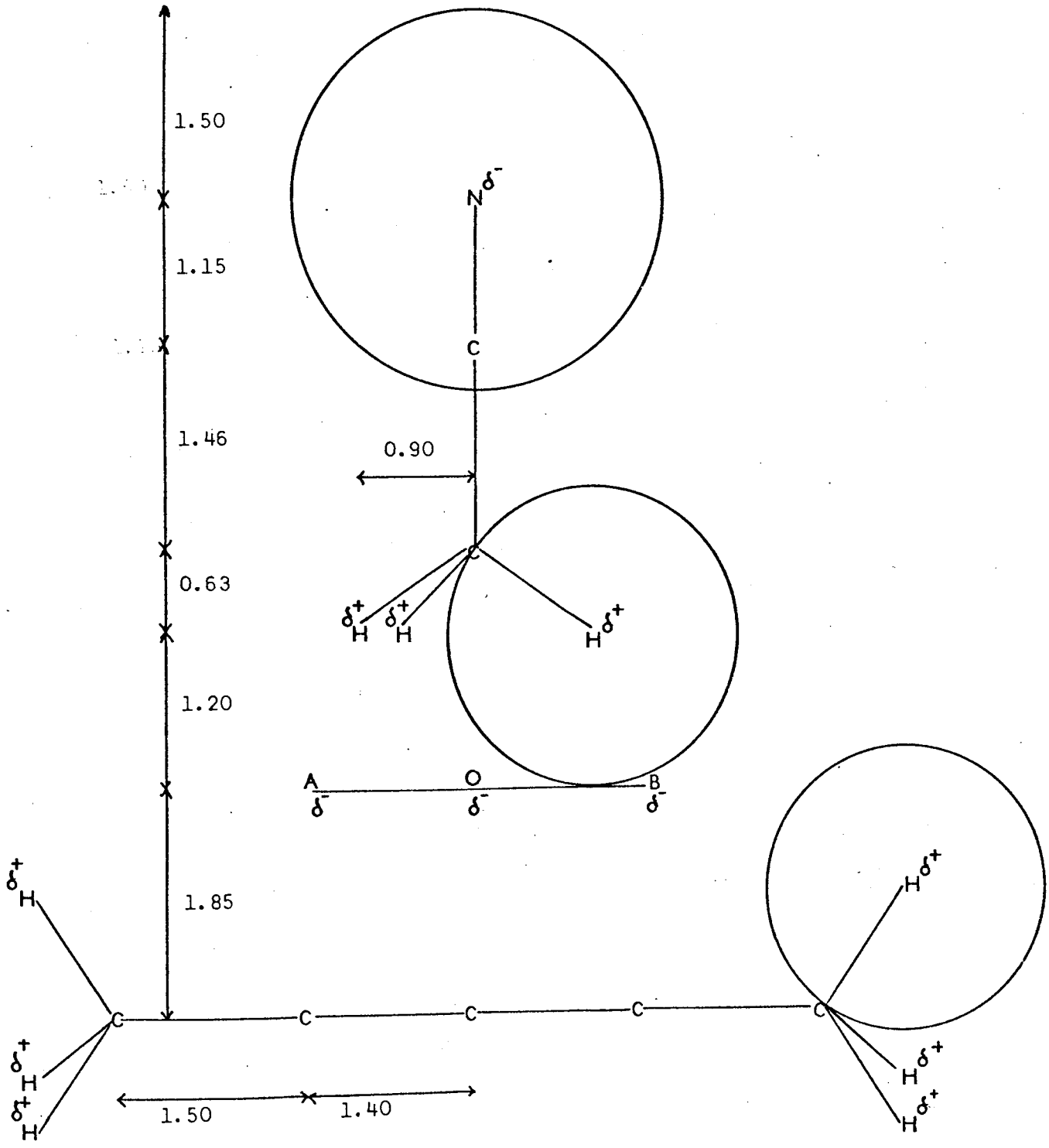
1.50
1.15
1.46
0.63
1.20
1.85
N δ-
C
0.90
C
δ+ H
δ+ H
H δ+
A
O
B
δ-
δ-
δ-
δ+ H
δ+ H
δ+ H
C
C
C
C
C
H δ+
H δ+
H δ+
1.50
1.40

Fig. 7.15 (CONT.)

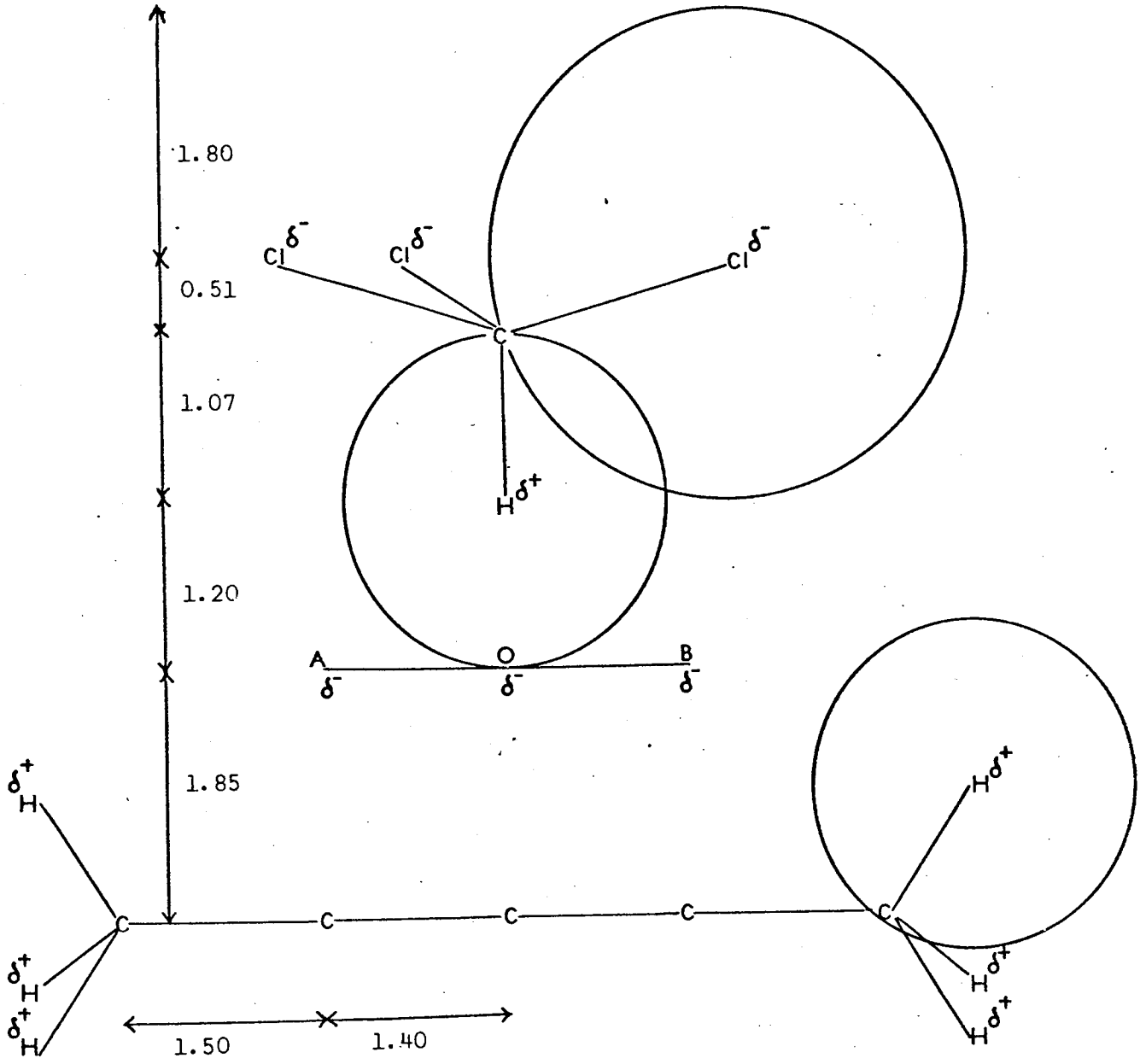
1.80
0.51
1.07
1.20
1.85
Cl δ⁻
Cl δ⁻
Cl δ⁻
C
H δ⁺
A
O
B
δ⁻
δ⁻
δ⁻
δ⁺ H
δ⁺ H
δ⁺ H
C
C
C
C
C
H δ⁺
H δ⁺
H δ⁺
1.50
1.40

Fig. 7.15 (CONT.)

For the various orientations of acetonitrile with respect to the aromatic, the significance of this repulsion is more evident as its negative end (nitrogen atom) lies further away from the ring when compared to that of nitromethane, and thus any of its orientation is expected also to be more restricted by the methyl groups on the ring for the reasons given above.

Turning to the case of chloroform, it is apparent that this is different from the other solutes. The negative end of chloroform (chlorine atoms) lies rather close to the ring which implies that its attraction with either of the methyl groups on the ring could be significant. It would appear therefore for this solute, during its "wobbling" motion, that for each of its particular orientations relative to the ring the attraction is more pronounced than the corresponding repulsion from the methyl groups. Consequently this leads to a less rigid complex structure as the aromatic nucleus is methylated.

CHAPTER 8

GENERAL CONCLUSIONS

GENERAL CONCLUSIONS

Studies of molecular interactions between chloroform, nitromethane and acetonitrile separately (as solutes) with benzene and some methyl-substituted aromatic solvents have been conducted employing three different physical techniques, namely n.m.r. spectroscopy, dielectric constant studies and cryoscopy. From these studies an attempt has been made to elucidate the nature, stoichiometry, strength and geometry of the complexes formed and the factors affecting their formation.

A preliminary attempt has been made to establish directly through n.m.r. studies the stoichiometries of the complexes without making the usual assumptions. However, the approach has been found to give unsatisfactory results mainly because of the difficulty in achieving the experimental accuracy demanded by the method. Similarly, the results obtained from cryoscopic studies indicate that this technique alone has a limited range of applicability. Therefore to obtain unambiguously the stoichiometries of the complexes a combination of the techniques was found to be necessary. N.m.r. studies made in conjunction with cryoscopic studies have been used therefore in an attempt to determine the stoichiometry of the complexes. It is found that only in the acetonitrile-benzene system is a 1:2 complex formed and that the other solute-aromatic complexes possess solely 1:1 stoichiometry.

The values for K_x, obtained at different temperatures from n.m.r. studies, for all the systems studied are low and indicative of the formation of weak complexes. The independence of ΔH of temperature for each system confirms the presence of a single (or several isomeric) complex species in the system.

of deducing K_x

A new method through dielectric studies has been attempted employing the same experimental conditions as those in n.m.r. work, so that the relevant values of K_x deduced from both techniques would be expected to be compatible to each other . It is found that this purpose is not achieved because of the difficulty in obtaining sufficiently accurate results from the dielectric studies. Various factors which could contribute to this discrepancy have been suggested. However, data obtained by an alternative dielectric approach indicate that a dipole-induced-dipole interaction is basically responsible for complex formation, with the solutes polarising the aromatics to permit electrostatic attraction between both interacting species. The extent of complex formation (and therefore the strength of the complexes) appears to be governed, for a common solute, not only by the electrostatic effect but also by the steric effects. The analysis of K_x values also gives some evidence to support this.

The values of Δ_c and moments induced in the aromatics by the solutes upon complex formation (μ_{ARO}), obtained respectively from n.m.r. and dielectric studies, have been used to elucidate the structures of the complexes. A time-averaged geometry of a 1:2 complex for acetonitrile-benzene is proposed in which the solute molecule is sandwiched between two aromatic molecules, with its electronegative end lying beyond the vicinity of the ring owing to the repulsion from the π-cloud. For this arrangement the solute and the aromatic are in direct contact with each other. In the case of the remaining 1:1 complexes the solute has been described as adopting a variety of orientations relative to the aromatic ring, and from a colloquial standpoint it is quoted as "wobbling" in a cone of permitted orientations. In this respect different complexes formed during the process are confined within one of the permitted orientations bounded by the cone. Because on time average most physical properties of the characteristics of the complexes have

their components in the p axis self-cancelled, the complex structure deduced from these parameters would appear to be one in which the solute lies symmetrically about the aromatic six-fold axis with its electropositive end in contact with the aromatic ring.

Some evidence has been obtained from the analysis of ΔS values and Δ_c and dielectric data indicating that the various orientations of the solutes, in the presence of methyl groups on the aromatic ring, become less restricted in the case of chloroform and more restricted for the other two solutes. An explanation has been offered for this behaviour in terms of the attraction and repulsion exerted on these solutes by the aromatic methyl groups.

REFERENCES

1. R.Foster, "Organic Charge-Transfer Complexes", Academic Press, London and New York (1969)
2. Y.K.Syrkin and M.E.Dyatkina, "Structure of Molecules and the Chemical Bond", Dover Publications, Inc., New York (1964)
3. F.London, Trans. Faraday Soc., 33, 8 (1937)
4. R.S.Mulliken, J. Phys. Chem., 56, 801 (1952)
5. K.E.Schuler, J.Chem. Phys., 21, 765 (1953)
6. M.Tamres, S.Searles, E.M.Leighly and D.W.Mohrman, J.Am.Chem . Soc. 76, 3983 (1954)
7. M.Tamres, J.Am.Chem. Soc., 74, 3375 (1952)
8. J.Homer and M.C.Cooke, J.Chem. Soc. Faraday Trans I, 69 1990 (1973)
9. W.G.Schneider, J.Phys.Chem., 66, 2653 (1962)
10. R.E.Klinck and J.B.Stothers, Can. J. Chem., 40, 2329 (1962)
11. L.E.Orgel and R.S.Mulliken, J.Am.Chem.Soc., 79, 4839 (1957)
12. P.Lazlo and D.H.Williams, J.Am.Chem.Soc., 88, 2799 (1966)
13. J.H.Bowie, J.Ronayne and D.H.Williams, J.Chem.Soc. (B), 785 (1966)
14. C.J.Jackson, Ph.D Thesis, University of Aston in Birmingham (1971)
15. M.C.Cooke, Ph.D Thesis, University of Aston in Birmingham (1970)
16. J.Homer and M.C.Cooke, J.Chem.Soc. (A), 777 (1969)
17. J.R.Goates, J.B.Ott and A.H.Budge, J.Phys.Chem., 65, 2162 (1961)
18. L.W.Reeves and W.G.Schneider, Can.J.Chem., 35, 251 (1957)
19. G.J.Korinek and W.G.Schneider, Can.J.Chem., 35, 1157 (1957)
20. G.D.Johnson and R.E.Bowen, J.Am.Chem.Soc., 87, 1655 (1965)
21. J.V.Hatton and R.E.Richards, Mol. Phys., 5, 139 (1962)
22. P.J.Huck, PhD Thesis, University of Aston in Birmingham (1968)
23. J.Homer and M.C.Cooke, J.Chem.Soc. (A), 773 (1969)
24. C.E.Johnson and F.A.Bovey, J.Chem.Phys., 29, 1012 (1958)

25. R.R.Yadava, PhD Thesis, University of Aston in Birmingham (1972)

26. S.Tolansky, "High Resolution Spectroscopy", Methuen, London (1947)

27. W.Pauli, Naturwisschaften, 12, 741 (1924)

28. N.F.Ramsey, "Molecular Beams", Oxford University Press (1956)

29. O.Stern, Z.Phys., 7, 249 (1921); W.Gerlach and O.Stern, Ann. Phys. Leipzig, 74, 673 (1924)

30. F.Bloch, W.W.Hansen and M.Packard, Phys. Rev., 69, 127 (1946)

31. E.M.Purcell, H.C.Torrey and R.V.Pound, Phys. Rev., 69, 37 (1946)

32. J.A.Pople, W.G.Schneider and H.J.Bernstein, "High Resolution Nuclear Magnetic Resonance", McGraw-Hill, New York (1959)

33. J.W.Emsley, J.Feeney and L.H.Sutcliffe, "High Resolution Nuclear Magnetic Resonance Spectroscopy", Vol.I, Pergamon Press, New York (1965)

34. E.V.Condon and G.H.Shortley, "Theory of Atomic Spectra", Cambridge University Press (1953)

35. S.G.Starling and A.J.Woodall, "Physics", Longmans, London (1957)

36. A.Abragam, "The Principles of Nuclear Magnetism", Clarendon Press, Oxford (1961)

37. J. Schwinger, Phys. Rev., 51, 648 (1937)

38. W.A.Anderson, Phys. Rev., 104, 850 (1956)

39. F.Bloch, Phys. Rev., 70, 460 (1946)

40. G.V.D.Tiers, J.Phys. Chem., 65, 1916 (1961)

41. R.Kubo and K.Tomita, J.Phys. Soc. Japan, 9, 888 (1954)

42. W.D.Knight, Phys. Rev., 76, 1259 (1949)

43. W.G.Proctor and F.C.Yu, Phys. Rev., 77, 717 (1950)

44. W.C.Dickinson, Phys. Rev., 77, 736 (1950)

45. G.V.D.Tiers, J.Phys. Chem., 63, 1379 (1959)

46. A.Saika and C.P.Slichter, J.Chem. Phys, 22, 26 (1954)

47. A.D.Buckingham, T.Schaeffer and W.G.Schneider, J.Chem. Phys., 32, 1227 (1960)

48. T.P. Das and R.Bersohn, Phys. Rev., 104, 476 (1956)

49. C.P. Slichter, "Principles of Magnetic Resonance", Harper and Row, New York (1963)

50. B.R.McGarvey, J.Chem. Phys., 27, 68 (1957)

51. J.A.Pople, J.Chem. Phys. 24, 1111 (1956)

52. A.A.Bothner-By and R.E.Glick, J.Chem. Phys., 26, 1651 (1957)

53. B.B.Howard, B.Linder and M.T.Emerson, J.Chem. Phys., 36, 485 (1962)

54. A.A.Bothner-By, J. Mol.Spect., 5, 52 (1960)

55. T.W.Marshall and J.A.Pople, Mol. Phys., 3, 339 (1960)

56. J. Homer and P.J.Huck, J.Chem. Soc. (A), 277 (1968)

57. L.Onsager, J.Am.Chem.Soc., 58, 1486 (1936)

58. A.D.Buckingham, Can.J.Chem., 38, 300 (1960)

59. P.Diehl and R. Freeman, Mol. Phys., 4, 39 (1961)

60. I.G.Ross and R.A.Sack, Proc. Phys. Soc., B63, 893 (1950)

61. W.C.Dickinson, Phys. Rev., 81, 717 (1951)

62. A.A.Bothner-By and R.E.Glick, J.Chem.Phys., 26, 1647 (1957)

63. R.J.Abraham, Mol.Phys., 4, 369 (1961)

64. J. Homer and D.L.Redhead, J.Chem.Soc. Faraday Trans.II, 68,793 (1972)

65. M.N.Hughes, A.M.James and N.R.Silvester, "SI Units and Conversion Tables", The Machinery Publishing Co.Ltd., London (1970)

66. T.M.Yarwood and F.Castle, "Physical and Mathematical Tables", Macmillan Education Ltd., London (1972)

67. N.Hill, W.E.Vaughan, A.H.Price and M.Davies, "Dielectric Properties and Molecular Behaviour", Van Nostrand Co., London (1969)

68. C.P. Smyth, "Dielectric Behaviour and Structure", McGraw-Hill, New York (1955)

69. J.R.Partington, "An Advanced Treatise on Physical Chemistry", Vol.V, Longmans, Green and Co., London (1954)

70. J.C.Maxwell, "Treatise on Electricity", Oxford University Press, London (1892)

71. P. Debye, "Polar Molecules", Dover Publications Inc., New York (1929)

72. I.J.W Williams and I.J.Krchma, J.Am.Chem.Soc., 49, 1676 (1927)

73. I.F. Halverstadt and W.D.Kumler, J.Am.Chem.Soc., 64, 2988 (1942)

74. L.Onsager, J.Am.Chem.Soc., 58, 1486 (1936)

75. W.M.Heston, Jr., A.D.Franklin, E.J.Hennelly and C.P. Smyth, J. Am.Chem.Soc., 72, 3443 (1950)

76. E.A.Guggenheim, Trans. Faraday Soc., 45, 714 (1949)

77. F.H.Müller, Trans. Faraday Soc., 30, 729 (1934)

78. J. Weigle, Helv. Phys. Acta, 6, 68 (1933)

79. K.Higasi, Sci. Papers Inst. Phys. Chem. Research(Tokyo), 28, 284 (1936)

80. F.C.Frank, Proc. Roy. Soc., 152, 171 (1935)

81. J.W.Smith and L.B.Witten, Trans. Faraday Soc., 47, 1304 (1951)

82. A.D.Buckingham, J.Y.H Chau, H.C.Freeman, R.J.W.Le Fèvre, D.A.A.S.N. Rao and J.Tardif, J.Chem.Soc., 1405 (1956)

83. A.Findlay, "The Phase Rule and Its Applications", Dover Publications Inc., New York (1951)

84. S.Glasstone, "Physical Chemistry", Macmillan & Co., London (1951)

85. H.A.C.McKay and B.Higman, Phil. Mag., 19, 367 (1935)

86. D.Cook, Y.Lupien and W.G.Schneider, Can.J.Chem., 34, 957 (1956)

87. B.J. Mair, A.R.Glasgow,Jr. and F.D.Rossini, J.Research NBS, 26, 591 (1941)

88. G.Tammann, Z.Anor.Chem., 37, 303 (1903)

89. A.N. Sharpe and S.Walker, J.Chem.Soc., 2974 (1961)

90. A.L.Bloom and M.E.Packard, Science, 122, 738 (1955)

91. W.A.Anderson, Rev. Sci. Inst., 32, 241 (1961)

92. F.Bloch, Phys. Rev., 94, 496 (1954)

93. B.A.Evans and R.E.Richards, J.Sci.Inst., 37, 353 (1960)

94. H.Primas and H.H.Günthard, Rev.Sci.Inst., 28, 510 (1957)

95. N.Bloembergen, E.M.Purcell and R.V.Pound, Phys.Rev., 73, 679 (1948)

96. F.Bloch, W.W.Hansen and M.Packard, Phys. Rev., 70, 474 (1946)

97. A.L.McClellan, "Table of Experimental Dipole Moments", W.H. Freeman & Co, London (1963)

98. J.A.Pople, Proc.Roy. Soc., 239A, 541 (1957)

99. R.P.Rastogi and H.L.Girdhar, J.Chem. and Eng.Data, 7, 176 (1962)

100. M.L.McGlashan and R.P.Rastogi, Trans. Faraday Soc., 54, 496 (1958)

101. J.B.Ott, J.R.Goates and A.H.Budge, J. Phys.Chem., 66,1387 (1962)

102. J.R.Goates, R.J.Sullivan and J.B.Ott, J.Phys. Chem.,63,589 (1959)

103. R.P.Rastogi and R.K.Nigam, Trans. Faraday Soc., 55,2005 (1959)

104. P.M.Whitney, PhD.Thesis, University of Aston in Birmingham. (1973)

105. H.S.Gutowsky and A.Saika, J.Chem.Phys., 21, 1688 (1953)

106. C.J.Creswell and A.L.Allred, J.Phys.Chem., 66, 1469 (1962)

107. H.A.Benesi and J.H.Hildebrand, J.Am.Chem.Soc., 71, 2703 (1949)

108. F.Takahashi and N.C.Li, J.Am.Chem.Soc., 88, 1117 (1966)

109. P.J.Berkeley, Jr. and M.W.Hanna, J.Phys.Chem., 67, 846 (1963)

110. M.W.Hanna and A.L.Ashbaugh, J.Phys.Chem., 68, 811 (1964)

111. R.L.Scott, Rec.Trav.Chim., 75, 787 (1956)

112. P.J.Trotter and M.W.Hanna, J.Am.Chem.Soc., 88, 3724 (1966)

113. J.Homer, M.H.Everdell, C.J.Jackson and P.M.Whitney, J.Chem.Soc. Faraday Trans II, 68, 874 (1972)

114. J.Timmermans, "Physico-Chemical Constants of Pure Organic Compounts", Elsevier Publishing Co. (1950)

115. B.W.Tempest, BSc Project Thesis, University of Aston in Birmingham (1968)

116. D.P.Earp and S.Glasstone, J.Chem.Soc., 1709 (1935)

117. D.Ll.Hammick, A.Norris and L.E.Sutton, J.Chem.Soc., 1755 (1938)

118. A.V.Few and J.W.Smith, J.Chem.Soc., 2781 (1949)

119. D.Cleverdon, G.B.Collins and J.W.Smith, J.Chem.Soc., 4499 (1956)

120. R.J. Bishop and L.E. Sutton, J.Chem.Soc., 6100 (1964)

121. E.A. Moelwyn-Hughes, "Physical Chemistry", Pergamon Press, London (1964)

122 A.A. Maryott and F. Buckley, "Table of Dielectric Constants and Electric Dipole Moments of Substances in the Gaseous States", NBS Circular 537, Washington D.C. (1953)

123. J. Homer and M.C. Cooke, J.Chem.Soc. (A), 1984 (1969)

124. "Tables of Interatomic Distances and Configurations of Molecules and Ions", Special Publication No. 11, Chem.Soc., London (1958)

125. H. Fröhlich, "Theory of Dielectrics", Oxford University Press, London (1949)

126. C.G. LeFèvre and R J W Le Fèvre, Rev.Pure and Applied Chem., 5, 261 (1955)

127. "Handbook of Chemistry and Physics", The Chemical Rubber Publishing Co., Cleveland, U.S.A. (1968)

128. J. Homer and R.R. Yadava, J.Chem.Soc. Faraday Trans.I, 70, 609(1974)

129. A. Weissberger and B.W. Rossiter, "Physical Methods of Chemistry", Vol. I, Wiley-Interscience, New York (1972)

130. D.P. Shoemaker and C.W. Garland, "Experiments in Physical Chemistry", McGraw-Hill, New York (1967)